University of Strathclyde Engineering

Investigation of 405-nm Light as a Pathogen Reduction Technology for Human Blood Plasma: Evaluation of Antimicrobial Action & Protein Compatibility

A thesis presented in fulfilment of the requirement for the degree of

Doctor of Philosophy

2024

Caitlin Fiona Stewart (BEng Hons)

Department of Electronic and Electrical Engineering

University of Strathclyde Glasgow, UK

Declaration of Author's Rights

Funding Support

This work was supported by a UK Engineering and Physical Sciences Research Council (EPSRC) Doctoral Training Grant to Caitlin Stewart (Reference EP/R513349/1), and an EPSRC Impact Acceleration Account—University of Strathclyde 2017 (EP/R51178X/1) to Dr M. Maclean, and Professor S.J. MacGregor.

Acknowledgements

The author would firstly like to thank her supervisors Dr M. Maclean, Professor J. Anderson and Professor S.J. MacGregor, for their dedicated support, guidance and encouragement throughout the course of this study. Without their invaluable input and expertise, this research would not have been possible.

The author would like to acknowledge Dr C.D. Atreya and the research team at the Office of Blood Research and Review, Center for Biologics Evaluation and Research (CBER), in the Food and Drug Administration (Silver Spring, USA) for their support and collaboration throughout this research endeavour. Their commitment, expertise, and shared passion for advancing this technology has strengthened the findings of this study.

Thanks are due to S. Doak and A. Carlin for their technical expertise and support with the construction of the light unit, the Scottish National Blood Transfusion Service (SNBTS) for provision of blood components, and Grifols (UK) for providing blood bags for research purposes. The author would also like to thank her family, friends and fiancé, Cameron Quinn, for their patience, love and encouragement throughout the duration of this PhD study.

This Thesis is dedicated to the authors parents, Fiona Russell and Andrew Stewart, whose love and belief have been a constant source of motivation.

Abstract

Despite significant advancements in blood transfusion safety, the risk of infectious agents entering the blood supply remains. Pathogen reduction technologies (PRTs) have been developed to improve blood product safety by proactively treating to remove infectious agents. Whilst these existing PRTs provide broad-spectrum antimicrobial activity, treatments fall short in preserving the quality and functionality of the transfusion products, and are typically limited by the need for photosensitizers and bag transfers which can lead to extensive processing times. Violet-blue 405-nm light recently showed potential to be developed as an alternative, antimicrobial tool for *in situ* treatment of *ex vivo* stored blood products, without the need for photosensitizers.

The overarching aim of this study was to gain an understanding of the operational factors required to ensure the reliable, repeatable, and effective use of 405-nm light for microbial reduction of prebagged plasma. The first objective investigated the broad-spectrum antimicrobial efficacy and compatibility of 405-nm light using low volume (250 µL) plasma samples. These small-scale tests showed that a 360 Jcm^{-2} dose achieved >95% inactivation for all pathogens investigated across all seeding densities, while displaying compatibility with the plasma itself. The second objective examined whether changing the dose delivery method influenced the antibacterial efficiency and compatibility of the treatment, and demonstrated that use of lower irradiances provided both greater antibacterial efficiency and treatment compatibility compared to higher irradiances when applying a fixed light dose. These small-scale studies supported the development of a large-scale light unit for treatment of larger volume, prebagged plasma. Initial testing using 100 mL prebagged plasma, as a proof-of-concept to assess the pathogen reduction efficacy and compatibility of 405-nm light, determined that a dose of 115 Jcm^{-2} was capable of broad-spectrum microbial inactivation whilst preserving plasma protein integrity and functionality. Testing advanced to more clinically relevant, 300 mL volumes of prebagged plasma, and identified a 405-nm light dose of 288 Jcm^{-2} as an optimal treatment sufficient to reduce microbial contamination (>96% microbial reductions), whilst not compromising the quality of the plasma.

Overall, this study presents 405-nm light as an alternative, potentially less damaging PRT for treatment of plasma, compared to existing PRTs which require the use of UV-light and/or addition of photosensitizers, and supports further development of the technology for broader use in transfusion medicine.

Table of Contents

List of Figures

List of Tables

List of Abbreviations

APTT I Activated Partial Thromboplastin Time

ARC I American Red Cross

BTPs I Blood Transfusion Products

CJD I Creutzfeldt-Jakob disease

CMV I Cytomegalovirus

CYRO I Cryoprecipitate

DNA I Deoxyribonucleic Acid

FCV I Feline Calicivirus

FDA I Food and Drug Administration

FFP I Fresh Frozen Plasma (frozen within 8-hrs from donation)

FP24 I Frozen Plasma (frozen between 8 to 24-hrs from donation)

HAV I Hepatitis A Virus

HBV I Hepatitis B Virus

HCV I Hepatitis C Virus

HIV I Human Immunodeficiency Virus

HTLV-1/2 I Human T-cell Lymphotropic Virus-1/2

IG I Immunoglobulin

JPAC I Joint United Kingdom Blood Transfusion and Tissue Transplantation Services Professional Advisory Committee

MB I Methylene-blue

MB-FFP I Methylene-blue Fresh Frozen Plasma

NAT I Nucleic Acid Testing

NHS I National Health Service

NHSBT I National Health Service Blood and Transplant

NIBTS I Northern Ireland Blood Transfusion Service

PCs l Platelet Concentrates

PRT l Pathogen Reduction Technology

PTT l Prothrombin Time

RBCs l Red Blood Cells

RNA l Ribonucleic Acid

SAG-M solution l Saline-adenine-glucose-mannitol solution

SD l Solvent-detergent

SNBTS l Scottish National Blood Transfusion Service

TMA l Thrombotic Microangiopathies

TRALI l Transfusion-related Acute Lung Injury

TTIs l Transfusion Transmitted Infections

TTP l Thrombotic Thrombocytopenic Purpura

UV l Ultraviolet

vWF l von Willebrand Factor

WBS l Welsh Blood Service

WHO l World Health Organisation

Chapter One I Thesis Introduction

1.0 I Overview

Since the implementation of clinical safety measures including donor screening, sample diversion and nucleic acid amplification testing (NAT), the risk of viral transmission from blood transfusion products has significantly reduced [Brecher and Hay, 2005]. Nevertheless, the low but known risk of bacterial contamination remains the second leading cause of death – after clerical errors – from blood transfusion [Hillyer *et al,* 2003; FDA Center for Biologics Evaluation and Research, 2018]. In response to this, three main areas of avoidance, detection and elimination have been explored with the common goal of providing a near zero-risk blood supply. Conventional viral reduction techniques for treatment of human plasma, including the use of solvent-detergent (SD), dry heat treatment (100°C for 30-min), methylene-blue in combination with visible light have been employed throughout Europe and North America for decades. Whilst these techniques significantly reduce the risk of transmitting enveloped viruses, they are much less effective against non-enveloped viruses, bacteria, yeast, fungi, parasites and protozoa [Klein, 2005; Klein and Bryant, 2009]. Additionally, the impact on blood product quality has been indicated through a major loss of protein activity and more concerningly, the increased risk of adverse transfusion reactions [Burnouf and Radosevich, 2000; Klein, 2005; Seltsam, 2017; Gehrie *et al*, 2019]. Due to the harsh chemical and/or physical inactivation mechanism, such treatments are not suitable for cellular components including platelet concentrates (PCs) and red blood cells (RBCs).

In light of this, continued research led to development of novel, light-based pathogen reduction technologies (PRTs) that are compatible for treatment of both human plasma and cellular blood products [Klein, 2005; Klein and Bryant, 2009]. These technologies aim to improve blood safety by treating to inactivate a wide range of infectious agents. Studies have shown that PRTs can significantly reduce the incidence of transfusion-transmitted infections (TTIs) and improve overall blood transfusion safety [Klein and Bryant, 2009; Fournier-Wirth *et al*, 2010; Dodd, 2012]. With infection reactivity responsible for approximately one-third of all discarded blood donations, PRTs may also provide an opportunity to reduce wastage of valuable blood products.

The most established PRTs include the Intercept (Cereus Corporation, USA) and Mirasol (TerumoBCT, USA) systems, which use ultra-violet (UV) light in combination

with photosensitizers to achieve antimicrobial effects. Whilst these UV-light based technologies promise high antimicrobial efficacy and have shown to be clinically safe, several studies have reported significant reductions in post-treatment blood product quality and functionality, with emphasis on the loss of coagulation factors in human plasma [Klein, 2005; Seltsam, 2017; Gehrie *et al*, 2019]. Further, UV-light based systems have operational limitations as the requirement for bag transfers and various processing stages are associated with increased treatment times and introduces an opportunity for contamination [Solheim and Seghatchian, 2006].

Violet-blue light, with a peak wavelength of 405-nm, is being investigated as a novel, alternative approach for pathogen reduction of blood transfusion products. Proof-of-concept studies have established the antimicrobial efficacy of 405-nm light for pathogen reduction of plasma and PCs using a small selection of bacteria, yeast and most recently a blood-borne parasite *Trypanosoma cruzi* and an enveloped virus, human immunodeficiency virus-1 [Maclean *et al,* 2016, 2020; Jankowska *et al*, 2020; Lu *et al,* 2020; Ragupathy *et al*, 2022]. In addition to the non-requirement for photosensitive additives, studies have demonstrated that pathogen reduction can be achieved *in situ* in the blood bag itself; an operational advantage made possible due to the penetrability of these visible light wavelengths [Maclean *et al*, 2016, 2020; Jankowska *et al*, 2020]. These initial studies also provided an insight to the potential compatibility of 405-nm light with PCs, with the successful recovery and survival of the treated-platelets demonstrated in a murine model [Maclean *et al*, 2020; Lu *et al*, 2020].

The work of this thesis significantly expands existing knowledge to gain a deeper understanding of the suitability of 405-nm light technology for pathogen reduction treatment of prebagged plasma – an important blood transfusion product in its own right, but also the suspending fluid for platelet concentrates, and whole blood components. As a wide variety of pathogens have been detected in blood transfusion products, it is essential to investigate the broad-spectrum antimicrobial efficacy, but also critically, the compatibility of antimicrobial doses of 405-nm light with the human plasma itself. Also, little is known about the optimal treatment regime with regards to antimicrobial efficacy and protein stability. Investigating the impact of the method of dose delivery will provide an insight to the optimal treatment regime, i.e a high-intensity rapid treatment *versus* a low-intensity continuous treatment.

A major advancement in the work of this thesis is the development and testing of a large-scale 405-nm light system for treatment of prebagged human plasma. The antimicrobial efficacy and compatibility potential of 405-nm light for treatment of prebagged plasma will then be assessed. Proof-of-concept studies will use small, 100-mL prebagged plasma to investigate the broad-spectrum antimicrobial efficacy and protein compatibility of 405-nm light treatment. A scaled-up study, using large 300-mL prebagged human plasma, will then be performed to assess the efficacy and compatibility of 405-nm light as a PRT for clinically-relevant volumes, with results compared to those of existing, clinically-used, PRTs.

An overview of the contents of each chapter of this Thesis is listed below:

Chapter 2 I *Background & Literature Review:* Provides information on key blood products, their clinical indication and prevalence of transfusion. This chapter focuses on the issue of TTIs, and details existing clinical safety measures that are implemented to avoid, detect and eliminate potential contamination. This will include an overview of newly developed pathogen reduction technologies for blood transfusion products and an introduction to the potential use of violet-blue 405-nm light.

Chapter 3 I *General Methodology & Materials:* Provides information on the storage, preparation and handling of human plasma, microorganisms and general media used throughout the study. This chapter will also provide general information on the light arrays used throughout the study.

Chapter 4 I *Broad-Spectrum Antimicrobial Efficacy of 405-nm Light for Plasma Treatment: Small-Scale Testing:* Identifies a 405-nm light dose capable of inactivating selected bacteria without causing visible damage to plasma proteins. Further protein analysis was conducted to determine upper dose levels at which major protein damage is observed. This dose was then evaluated against a range of bacteria at various contamination levels, in order to assess the broad-spectrum antibacterial efficacy of the technology.

Chapter 5 I *Assessing the Influence of 405-nm Light Dose Delivery on Antibacterial Efficiency and Protein Compatibility: Small-Scale Testing:* Investigates the impact of different 405-nm light dose delivery regimes on antibacterial efficiency, and protein compatibility to gain an insight to the optimal treatment conditions for the pathogen reduction of plasma.

Chapter 6 I *Broad-Spectrum Antimicrobial Efficacy and Compatibility of 405-nm Light for the Treatment of 100-mL Prebagged Plasma:* Provides information on the design, development and characterisation of a large-scale 405-nm light system for treatment of prebagged plasma. Results demonstrate the broad-spectrum inactivation efficacy of a 405-nm light treatment for 100-mL plasma bags, seeded with a range of bacteria and a yeast commonly implicated in TTIs. This chapter also evaluates the compatibility of effective antimicrobial doses with 100-mL prebagged plasma using a panel of protein analysis techniques.

Chapter 7 I *405-nm Light as a PRT for the Treatment of 300 mL Prebagged Plasma:* This Chapter was designed to investigate the antimicrobial efficacy (using three key organisms commonly implicated in TTIs) and compatibility of 405-nm light as a pathogen reduction treatment for 300-mL prebagged plasma, as a representation of the most clinically relevant scenario.

Chapter 8 I *Conclusions and Future Work:* Concludes the key findings from each chapter and, highlights the 405-nm light dose recommended for an effective and compatible treatment of low volume plasma samples and prebagged plasma. Recommendations for further research, that expands on the antimicrobial and protein compatibility results found in this study, as well as the areas of opportunity to optimise the 405-nm light treatment, are covered.

Investigating these areas will provide essential insights to the operational requirements to ensure the reliable, repeatable and effective use of violet-blue, 405-nm light for novel decontamination of prebagged plasma. Further, the results will support the development of the technology for treatment of other clinically-relevant blood transfusion products, including PCs and RBCs. Future implementation of 405-nm light as PRT technology for blood transfusion products has the potential to reduce the incidence of TTIs, reduce the wastage of valuable blood products and most importantly, reduce transfusion-related mortality.

Chapter Two I Background & Literature Review

2.0 I Overview

Bacterial contamination remains the most prevalent infectious complication of blood transfusion in the developed world [Brecher and Hay, 2005; FDA Center for Biologics Evaluation and Research, 2018]. Introduction of donor screening and advancements in infectious marker testing have significantly improved blood safety however the risk of bacterial contamination remains and a variety of other infectious agents including newly emerging viruses, parasites and yeast continue to threaten blood transfusion safety. Pathogen reduction technologies (PRTs), that employ ultraviolet (UV) light, have been developed to improve blood product safety by treating to inactivate infectious agents. Whilst these UV-light based PRTs promise high inactivation efficacy and are shown to be clinically safe, several studies have reported reductions in post-treatment blood product quality and functionality, with emphasis on the loss of coagulation factors in plasma [Klein, 2005; Seltsam, 2017; Gehrie *et al*, 2019]. Further, use of UV-light wavelengths and requirement for photosensitizers have operational disadvantages as treatments require bag transfers and/or additive removal stages which increases processing times.

Visible violet-blue light, with a peak wavelength of 405-nm, has demonstrated the potential to reduce the risk of infection from plasma and platelet transfusion products, without the need for additional photosensitizers or bag transfers. A proof-of-concept study by Maclean *et al* (2016), demonstrated the bactericidal effects of 405-nm light for prebagged plasma for the first time [Maclean *et al*, 2016]. From this discovery, collaborative research between The Robertson Trust Laboratory for Electronic Sterilisation Technologies (ROLEST) at the University of Strathclyde (Glasgow, UK) and the Office of Blood Research and Review, Center for Biologics Evaluation and Research (CBER), in the Food and Drug Administration (Silver Spring, USA) has focused on the development of violet-blue 405-nm light as a PRT for blood transfusion products. This present study focuses on expanding existing knowledge of 405-nm light to evaluate its suitability as a PRT for treatment of plasma.

This chapter provides an overview of the blood transfusion service in the UK, covers key blood transfusion products (BTPs) and introduces the issue of transfusion transmitted infections (TTIs) with a focus on the source and incidence of bacterial contamination. This chapter will then review existing clinical safety measures implemented to avoid, detect and eliminate potential contamination, including viral

reduction techniques and newly developed and commercialised PRTs. Finally, this chapter will introduce the potential use of visible, violet-blue 405-nm light as an alternative, potentially less damaging antimicrobial approach, to existing PRTs for blood transfusion products.

2.1 I Blood Transfusions

This section will review the organisational structure of the Blood Transfusion Services in the UK, the blood supply chain and key BTPs. It will also review the prevalence of blood component transfusions and report on the global threat of TTIs.

2.1.1 National Guidance for Blood Transfusion Services

The World Health Organisation (WHO) recommend countries to establish a nationally coordinated blood transfusion service to provide safety policies and quality assurance systems. In the United Kingdom (UK), The Joint UK Blood Transfusion and Tissue Transplantation Services Professional Advisory Committee (JPAC) are responsible for providing safe practice guidelines to the UK Blood Transfusion Services. The national guidance sets the safety standards outlined in the Blood Safety and Quality Regulations 2005 Act which are legally enforced by European Directives. Within the UK National Health Service (NHS), there are 4 health authorities that manage blood and transfusion services; The NHS Blood and Transplant England, The Scottish National Blood Transfusion Service (SNBTS) managed by NHS National Services Scotland, The Northern Ireland Blood Transfusion Service (NIBTS) managed by the Northern Ireland Blood Transfusion Special Agency and The Welsh Blood Service (WBS) managed by Velindre NHS Trust (Figure 2.1).

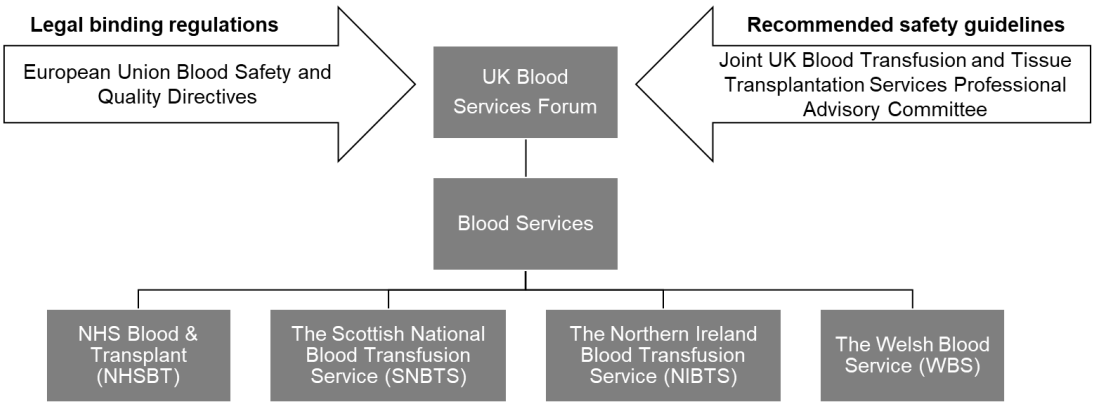

Figure 2.1. Organisational Structure of the UK Blood Services. Information collected from the Guidelines from the JPAC (JPAC, 2014).

2.1.2 Whole Blood to Blood Components

Whole blood is rarely transfused directly to patients, instead blood component therapy is used to optimise the dose delivery of individual blood products depending on the patients' clinical indication. As shown in Figure 2.2, whole blood is composed of plasma (~54%), red blood cells (RBCs, ~45%), and platelets and white blood cells (<1%) [Chargé and Hodgkinson, 2022]. Blood fractionation is typically performed within 8-hrs from blood collection, after which, individual blood components are transferred to their optimal storage conditions to maintain functional efficacy [Basu and Kulkarni, 2014]. All blood components are filtered to remove residual white blood cells, otherwise known as leukocytes. This leukoreduction process has shown to reduce the risk of adverse reactions, including the risk of alloimmunization to donor antigens, in patients receiving the blood transfusion [Salyer, 2007].

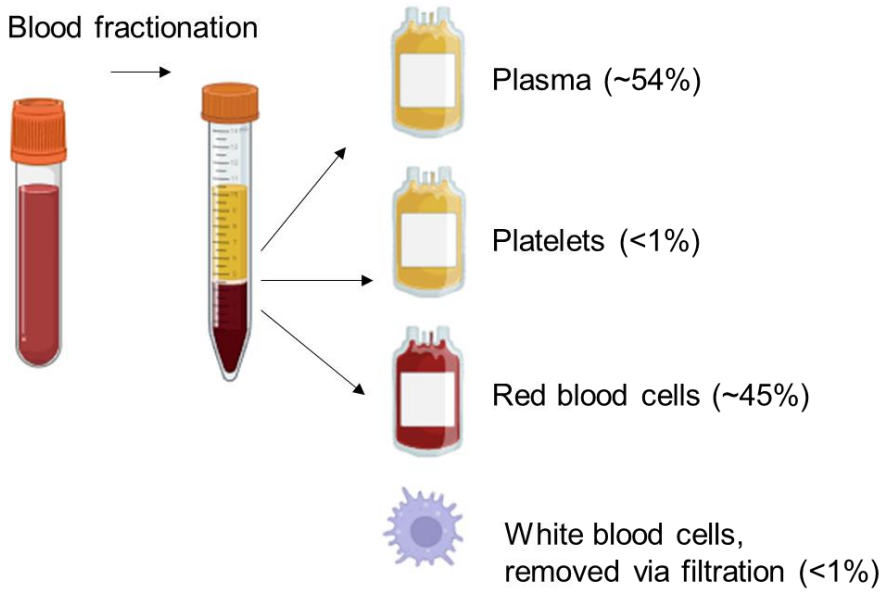

Figure 2.2. Key blood transfusion products. Adapted from Chargé and Hodgkinson (2022), and created with BioRender.com.

The most commonly used blood transfusion products include RBC concentrates, plasma and PCs. Other valuable products such as cryoprecipitate (CYRO) and cryo-reduced precipitate are yielded from plasma for therapeutic applications [JPAC, 2014]. An overview of blood product processing and storage protocols followed in the UK is provided in Figure 2.3.

The following sections will provide an overview of the most frequently transfused blood products, including their composition, optimal storage conditions and clinical indication for transfusion.

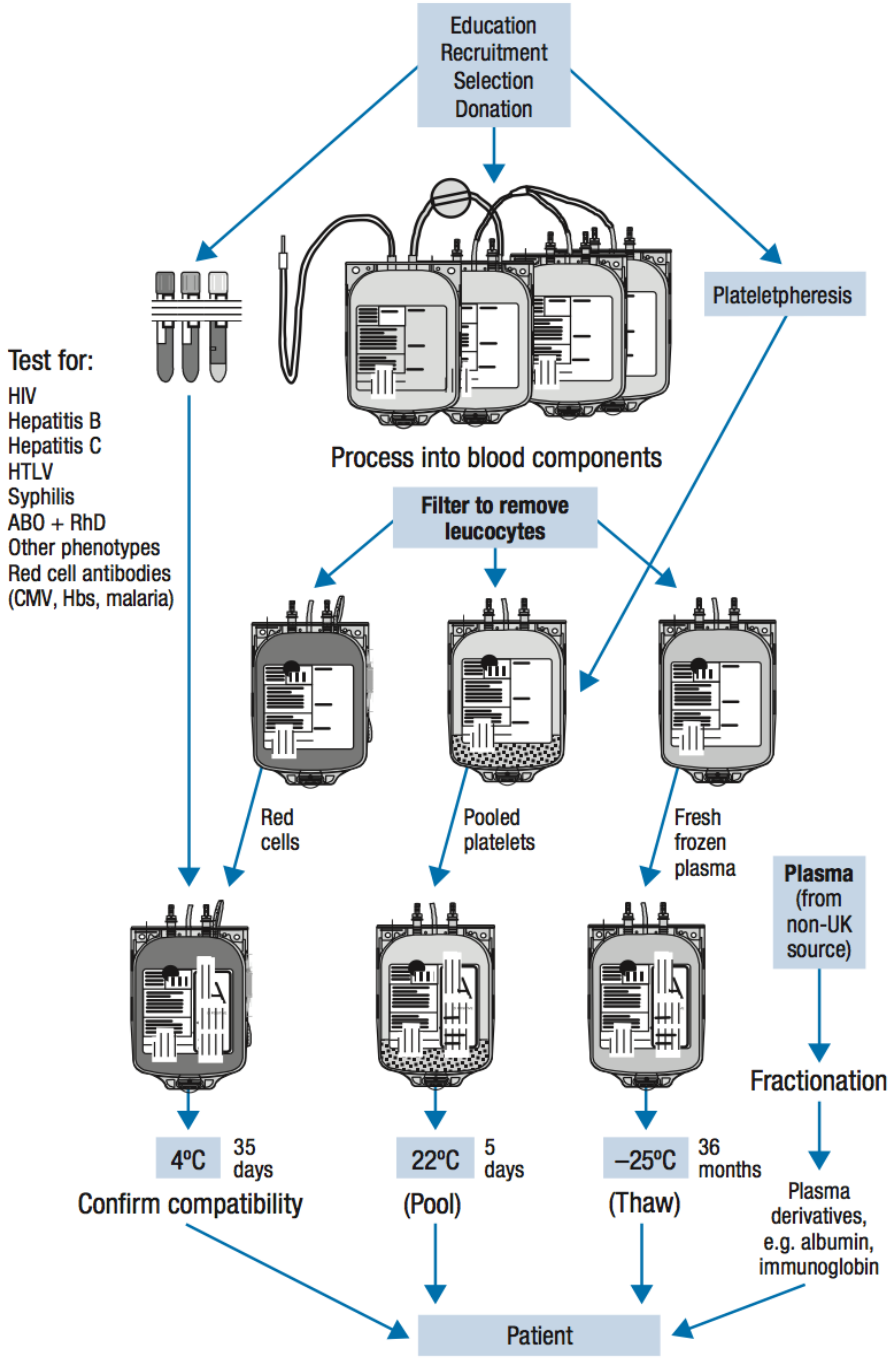

Figure 2.3. Processing of whole blood to blood components, recommended by the JPAC. Adapted from the JPAC, 2014.

2.1.2.1 Red Blood Cell Concentrates

Composition: RBCs, also known as erythrocytes, account for approximately 45% of the total blood volume and are key in the transportation of oxygen using the iron-containing, metalloprotein haemoglobin [Basu and Kulkarni, 2014].

Storage: RBCs are suspended in additive solution containing saline, adenine, glucose and mannitol (SAG-M) and stored under refrigerated conditions at 2-6℃ for up to 42 days [JPAC, 2014].

Clinical Indications: RBC transfusions are required to mitigate the signs and symptoms of anaemia by restoring the oxygen-carrying capacity in patients, and are commonly used during cardiovascular surgery and trauma cases. RBC transfusions are also a first-line therapy for patients suffering from sickle cell disease [Basu and Kulkarni, 2014].

2.1.2.2 Platelet Concentrates

Composition: Platelets, also termed thrombocytes, are essential mediators that trigger the coagulation cascade and assist in blood clotting at the site of injury. They are small cell fragments, released from larger Megakaryocyte cells, that account for approximately 1% of total blood volume [Rumbaut and Thiagarajan, 2010].

Storage: For transfusion, PCs are suspended in plasma, and must be stored at 20–24°*C* with continuous gentle agitation (to prevent platelet aggregation) in oxygen-permeable containers. Typically, PCs are stored for up to 5 days, however in the case of a negative bacterial culture, some blood banks allow storage for up to 7 days [JPAC, 2014]. Platelets are extremely sensitive blood cells, with research showing that slight changes in pH or oxygen levels can shift platelet metabolism to the anaerobic pathway which can lead to lactic acid production, acidosis and platelet death [Escort *et al*, 2017].

Clinical Indication: Platelets are an essential component of haemostasis therefore patients with a low platelet count (thrombocytopenia) or platelet dysfunction may require a PC transfusion to prevent or treat a haemorrhage. Regular PC transfusions are a mainstay treatment for patients with chronic conditions known to affect either the production of platelets and/or platelet function such as cirrhosis, multiple myeloma or kidney disease [Escort *et al*, 2017].

2.1.2.3 Plasma

Composition: Plasma is the non-cellular, fluid component of blood accounting for approximately 55% of total blood volume and consists of water (~90%), nutrients, hormones and vitamins (~3%) and proteins (~7%) including fibrinogen, albumin, haptoglobin, transferrin [Karafin and Hillyer, 2013].

Storage: Plasma can be stored at -25°C for up to 3 years or below -65°C for 7 years. If frozen within 8-hr of collection, the majority of clotting factors are preserved and the plasma product can be referred to as fresh frozen plasma (FFP) [Karafin and Hillyer, 2013]. If, due to transportation or processing delays, the plasma product is unable to be frozen within the first 8-hr, it is referred to as 24-hr frozen plasma (FP24). Whilst FP24 contains protein levels comparable to FFP, the storage delay has shown to reduce coagulation activity of specific clotting proteins, Factors V and VIII [Karafin and Hillyer, 2013; JPAC, 2014].

To prepare plasma for transfusion, following JPAC guidelines, frozen plasma can either thaw in a water bath at 37°C for approximately 45-min and be stored at 1-6°C for up to 24-hr, or thaw at 1-6°C, and be stored for up to 5 days. Due to the demand for readily available plasma in trauma cases, it is common practice for Accident and Emergency hospital departments to have an inventory of thawed plasma stored in refrigerated conditions (1-6°C) [Karafin and Hillyer, 2013].

Clinical Indication: Transfusion of plasma is given primarily for 3 indications: to prevent bleeding, stop bleeding or to correct deficiencies of clotting factors [Adam and Fischer, 2020]. It is a common treatment for critically ill patients with severe infections, burns, or liver failure in Accident and Emergency units [Patel and Josephson, 2018]. FFP is also used for therapeutic purposes, with plasma exchanges considered the first-line therapy for all thrombotic microangiopathies (TMA), a clinical condition defined by haemolytic anaemia, low platelet count and organ damage due to the formation of microscopic blood clots in small blood vessels [Winters, 2017].

2.1.2.4 Plasma Products

Cryoprecipitate (CRYO) is made by thawing FFP between 1-6°C and recovering the insoluble component that is rich in essential blood clotting proteins such as fibrinogen and Factor VIII. Patients with a deficiency in clotting proteins are at an increased risk of haemorrhaging following minimal trauma, surgery or dental procedures. Replacement of the deficient clotting factor is the primary treatment to either alleviate

symptoms or to treat excessive bleeding for example the clotting factor may be infused ‘on demand’ during a bleeding episode or, in severe cases, patients may receive ‘prophylactic’ therapy as a preventative measure. CRYO transfusions are indicated for the treatment of fibrinogen deficiency in cases of clinical bleeding and trauma [Karafin and Hillyer, 2013; JPAC, 2014].

The supernatant expressed during the manufacture of CRYO, referred to as the cryo-reduced precipitate, is also used during plasma exchange therapy for patients with thrombotic thrombocytopenic purpura (TTP), a blood disorder characterised by excessive blood clot formation. This plasma product is preferred for patients with TTP, as it provides a high concentration of non-clotting but otherwise essential plasma proteins including human albumin, nutrients and vitamins [Karafin and Hillyer, 2013].

Haemophilia is major coagulation disorder, characterised by the absence or reduced function of clotting factor VIII (Haemophilia-A) or IX (Haemophilia-B) which results in impaired clot formation. Of the 400,000 patients suffering from this coagulation disorder worldwide, 80% of the cases are a result of a Factor VIII deficiency (Haemophilia-A) [Barton and Bierman, 2018]. In recent years, the treatment for severe haemophilia has evolved in developed countries, from the use of FFP or clotting factor concentrate transfusions to plasma-derived or recombinant Factor VIII clotting factor injections [Marwaha, 2013]. In the UK, patients with severe Haemophilia-A must follow a preventative treatment plan that involves injecting a clotting factor medicine called Octocog Alfa every 48-hrs. Patients with mild to moderate cases of haemophilia can be treated on-demand, whereby a medicine called desmopressin is injected at the time of bleeding to stimulate the production of clotting factor VIII [NHS Haemophilia, 2020].

In the developing world, the lack of health care infrastructure, funding and resources, limits the availability of clotting factor. Under these circumstances, hospitals must rely on the availability of fresh whole blood, FFP and cryoprecipitate to manage and treat haemophilia [Ghosh, 2016].

Fresh plasma is also used to manufacture a range of plasma-based medicines. Immunoglobulin (IG) products are made from pooled plasma (collected from 3,000-10,000 blood donors) which is then fractionated and purified to a concentrate of more than 90% antibodies. Intravenous IG is used to treat patients with weak immune systems or primary immune deficiency disorders [NHS Blood and Transplant (a), 2022]. The NHS Blood and Transplant service (UK) report that plasma based IG

products are currently used to treat over 17,000 people in England [NHS Blood and Transplant (b), 2022]. Human albumin is another valuable plasma-based medicine that is used to correct hypoalbuminemia (low levels of human albumin) and/or treat shock following major bleeding, burns, or infection, by increasing the volume of plasma [NHS Blood and Transplant (c), 2022]. As a safety precaution following the outbreak of mad cow disease (covered in Section 2.2.3), the UK banned the use of UK-donated plasma to manufacture plasma-derived medicinal products, and relied upon imported plasma-derived products, primarily from the US. In 2020, the ban was lifted, which means that critically important medicines, such as immunoglobulin and human albumin can now be derived from UK plasma donors [NHS Blood and Transplant (c), 2022].

2.1.3 Prevalence of Blood Transfusions

Blood transfusions are one of the most commonly performed, life-saving clinical procedures [Ackfeld *et al*, 2022]. As detailed in Section 2.1.2, individual blood components are transfused to optimise the delivery depending on the clinical indication. Key blood transfusion products include RBCs, PCs and plasma. In the US, approximately 21 million units of blood are transfused every year. RBC concentrates are the most frequently transfused blood product accounting for 72% of total transfusions. Plasma (including plasma products) and PCs are also frequently transfused, accounting for 16% and 12% of all transfusions respectively [American Red Cross, 2023].

The WHO report that the clinical use of blood varies significantly between low- and high-income countries. In high-income countries, blood transfusions are most commonly required in emergency trauma cases and cardiovascular and transplant surgery for patients over the age of 65. In low- to mid-income countries, the majority of transfusions are used to manage pregnancy-associated complications and severe childhood anaemia, with 52% of reported transfusions treating children under the age of 5 [World Health Organization, 2023].

2.2 I Transfusion Transmitted Infections

This section will cover the issue of TTIs, defined as ‘a pathogen that is known to be fatal, to be life-threatening, or to cause severe impairment and that is potentially transmissible through the blood supply’ [Dean *et al,* 2018]. The main organisms

responsible for TTIs and routes of contamination will be detailed [Domanović *et al*, 2017; Fred *et al*, 2018].

2.2.1 Viral agents

A wide variety of viral agents have shown to be capable of being transmitted through blood transfusion [Brecher and Hay, 2005]. Since the early 1960s, the implementation of infection control strategies including specific surface antigen testing, significantly reduced the overall risk and prevalence of viral TTIs, in the developed world. Nevertheless, viral transmission continues to compromise patient safety with reports that viruses are responsible for 32% of TTIs [Domanović *et al*, 2017]. Viral agents most commonly associated with TTIs will be covered in this section.

2.2.1.1 Human Immunodeficiency Virus

Blood-borne transmission of human immunodeficiency virus (HIV) emerged as a global health threat in the early 1980s, with the virus being identified as the causative agent in 1985. By this point, over 28,000 patients had contracted HIV via transfusion in the US alone. As the infection went undetected and, at this point, was untreatable, many victims developed Acquired Immunodeficiency Syndrome (AIDS). Since then, significant research has focused on the transmission mechanisms of HIV in attempt to reduce the spread of infection. In the UK, the current risk of a HIV-positive blood donation entering the blood supply is low at 1 in 7 million [JPAC, 2014]. However, in low-income countries the risk of infection is significantly higher with 1 in every 150 donations testing positive for HIV [American Red Cross, 2023]. Transfusion transmitted HIV is also found to carry the highest risk of all other routes of transmission, with over 90% of recipients transfused with infected blood found to be positive in follow-up testing [Scott and Wu, 2019].

2.2.1.2 Hepatitis Virus

All hepatitis viruses (A-E) are capable of being transmitted by blood transfusion. The hepatitis B and C virus (HBV and HCV) are known to carry the greatest risk to patient safety with high incidences of liver cirrhosis and hepatocellular cancer reported in recipients receiving contaminated blood. While the incidence of hepatitis infectivity in donations in the UK is low at 1 in 1.2 million, outbreaks of transfusion transmitted viral hepatitis continue to be reported globally [Grubyte *et al*, 2021].

2.2.1.3 Human T-cell lymphotropic virus

Human T-cell lymphotropic viruses I and II (HTLV-I and HTLV-II) are T-cell-associated ribonucleic acid retroviruses endemic in Japan, the Caribbean region, and parts of South America. Whilst studies have shown that HTLV blood donation infectivity is low, at <0.02% [Stigum *et al*, 2000], the UK blood services enforce mandatory antibody screening as transfusion transmitted HTLV infections are reported to have severe clinical outcomes [Dean *et al*, 2018].

2.2.1.4 Human Parvovirus B19

The most common transmission of human parvovirus B19 (B19) infection occurs via the respiratory route however, it can be transmitted through blood and plasma derivatives. As transfusion transmission is rare, screening of blood donors for B19 infection is not standard practice. However, some countries including Japan, Germany, and the Netherlands, have implemented B19 screening tests for blood donations as an additional safety measure [Jia *et al*, 2019]. This may, in part, be due to the fact that the B19 viral particle is extremely small and lacks an envelope, which limits the inactivation efficacy of conventional antiviral methods used to treat plasma (detergent, extreme pH, heat) [The Food and Drug Administration, 2009].

2.2.1.5 The Contaminated Blood Scandal

In the 1970s, major blood donation shortages led to the UK NHS sourcing around 50% of its supply of factor concentrate (a vital BTP used to manage bleeding disorders, covered in Section 2.1.2.4) from the US [The Infected Blood Inquiry, 2020]. Unlike the UK, during this period US donors were being paid to donate blood. Compensation schemes often attracted donors from high-risk groups for HIV and hepatitis C, with reports showing that the US blood banks were accepting blood donations from prisoners and drug addicts. In 1982, the Lancet and WHO published statements urging to stop the use of blood imported from countries collected from paid donors, including the US, especially for the treatment for haemophilia patients who received frequent clotting factor transfusions. Unfortunately, these serious health warnings were ignored by the NHS and the UK government, and no immediate action was taken to end the use of high-risk, US imported blood [Grayson, 2007].

It wasn't until the UK introduced blood screening for HIV and Hepatitis C in 1986 and 1991, respectively, that contaminated blood, imported from the US, would have been detected and discarded. Between the time that the UK accepted factor concentrate

from the US and the introduction of blood screening, approximately 26,800 patients received blood contaminated with HIV or hepatitis C. Many patients, unaware of their infection before diagnosis, will have unknowingly sexually transmitted the infection to their partners. This crisis, now publicly referred to as 'The Contaminated Blood Scandal', resulted in over 2,400 patient deaths [Grayson, 2007; The Infected Blood Inquiry, 2000].

Only recently has the extent of The Contaminated Blood Scandal come to light. The Infected Blood Inquiry was initiated by the UK Government in July 2018 to investigate the malpractice that led to so many patients receiving contaminated blood, the impact on their families, and how all involved authorities responded to the crisis. An interim report was published in Spring 2023, that recommended that a compensation scheme should be setup to support those who received infected blood or to their bereaved partners. The Inquiry's final report is due to be published in May 2024 [The Infected Blood Inquiry, 2020].

2.2.2 Parasites

Blood-borne parasitic diseases are responsible for approximately 3% of TTIs [Singh and Sehgal, 2010; Domanović *et al*, 2017]. Malaria (*Plasmodium* spp.) and leishmaniasis (*Leishmania donovani*), endemic in Africa and South Asia, as well as Chagas disease (*Trypanosoma cruzi*), endemic in Central and South America, are among the most reported transfusion transmitted parasitic infections [Singh and Sehgal, 2010].

2.2.3 Prions

A prion is an infectious misfolded protein that can trigger normal proteins in the brain to fold abnormally. The accumulation of prion plaques in the brain are known to cause irreversible damage to nerve cells. Creutzfeldt-Jakob disease (CJD) is an untreatable, fatal prion disease. Human variant CJD was first reported in the UK in 1996, and was thought to have occurred via ingestion of cattle products contaminated with bovine spongiform encephalopathy (BSE, 'mad cow disease'). After this discovery, strict control measures were put in place to prevent BSE entering the food chain. Whilst these measures reduced the risk of infection transmission, it has not yet been eliminated in the UK with 178 variant CJD cases been reported since [The National CJD Research & Surveillance Unit, 2020].

There have been 5 known cases of human variant CJD being transmitted by transfusion [NHS (a), 2021]. As a precaution against the transmission of variant CJD, a ban was introduced in 1998 to stop the use UK-sourced plasma. Similar restrictions were implemented in the US, with the US FDA imposing a ban on blood donations from anyone who had spent more than six months in the UK from 1980 to 1997 [Gottlieb, 1999].

During this time, the UK depended on imported plasma and plasma products primarily from the US. The Government recently changed the legislation to permit the use of plasma from UK donors. This meant that plasma from UK donors could be used to manufacture medicines, including immunoglobulins (from 2012) and albumin (from 2020) for the NHS, reducing the reliance on imports [NHS Blood and Transplant (c), 2023; NHS Blood and Transplant (d), 2023]. One year later, the FDA released new guidance that removed the donor eligibility restriction [FDA Center for Biologics Evaluation and Research, 2022]. Following this, many American blood banks, including the American Red Cross, have lifted the restriction [American Red Cross, 2022].

2.2.4 Yeast and Fungi

Yeast and fungal infections continue to be transmitted through blood transfusions [Harrison *et al*, 2010; Burghi *et al*, 2011]. *Candida* is the leading cause of fungal infections worldwide [Kotthoff-Burrell, 2019]. Whilst *Candida* species are commonly isolated from the oral and gastrointestinal tracts of healthy individuals, if organisms gain access to the blood stream, the commensal organisms can develop into a potentially fatal blood infection, referred to as Candidemia. In the case of immunocompromised patients, Candidemia is known to have an associated mortality rate of 30-60% [Hirano *et al*, 2015].

2.2.5 Bacteria

Bacterial contamination of blood products is an on-going challenge in transfusion medicine as it remains the most prevalent infectious complication of blood transfusion in the developed world [Wagner *et al*, 1994; Brecher and Hay, 2005; Domanović *et al*, 2017; FDA Center for Biologics Evaluation and Research, 2018]. The high level of infectivity is in part, due to the ability of bacteria to readily proliferate in a nutrient-rich blood product during storage at ambient room temperatures. Whilst the bacterial concentration, at time of donation, may be low at 1–10 colony forming units per mililitre

(CFUmL^{-1}), reports have shown that bacterial loads in PCs can proliferate to reach bacterial densities >10^6 CFUmL^{-1} during time in storage at 20-24°*C*. In the UK, *Treponema pallidum* (the bacteria which causes Syphilis), is currently the only bacterial species that undergoes detection testing during blood donation screening. More information on this will be provided in Section 2.2.6.

In cases where >10 units of blood are being transfused, The Massive Transfusion Protocol recommends that blood products should be warmed to 37℃ immediately before transfusion, to reduce the risk of hypothermia [Meißner and Schlenke *et al,* 2012]. For many microorganisms, this is the optimal temperature for microbial growth. Therefore, this warming practice potentially introduces an opportunity for contaminants to re-establish their natural logarithmic growth pattern [Hillyer *et al,* 2003]. Hillyer *et al* (2003) reports that these conditions can enable bacterial contaminants to reach high loads which increases the risk of a severe septic reaction post-transfusion that has a high mortality rate of 20-30% [Hillyer *et al*, 2003].

The clinical severity of transfusion transmitted bacterial sepsis depends on a combination of various factors:

- The dose i.e. the number of bacteria infused
- The replication rate of the organisms
- The species of bacteria present in the blood product
- The recipients general health status

The following sections will cover the common sources of contamination implicated in bacterial infections associated with individual blood products. Data reviewed in the following section has been collected from the French Haemovigilance (BACTHEM, 2001), the United States Bacterial Contamination Associated with Transfusion Reaction (BACON, 2001) and the British Serious Hazards of Transmission (SHOT, 2002) clinical studies which reported transfusion transmitted bacterial infections between 1998 to 2001. Brecher and Hay (2005) reviewed these clinical studies to assess the threat of bacterial contamination of blood components [Brecher and Hay, 2005].

2.2.5.1 Sources of Bacterial Contamination

Bacterial skin commensals are the most commonly recovered organisms from infected blood donations [Brecher and Hay, 2005]. In this case, it is expected that contamination occurred at time of blood collection as a result of incomplete skin disinfection and/or the removal of a skin core during phlebotomy. Brecher and Hay (2005) report that asymptomatic donors with transient bacteraemia are responsible for the majority of contamination cases associated with Gram-negative bacteria [Brecher and Hay, 2005]. Defects in the blood collection pack such as leaky seals and micro-punctures, have also been linked to cases of transfusion-associated bacterial sepsis, especially in cases where blood products have been in thawed in water baths [Hillyer *et al*, 2003].

2.2.5.2 Bacterial TTI's from Platelet Concentrates

Transfusion of PCs carry the highest risk for transfusion-associated bacterial sepsis with approximately 1 in every 1000 - 2000 transfused units later found to have been contaminated with bacteria. With around 4 million PCs transfused in the USA, it is projected that up to 4,000 units of bacterially contaminated PCs are transfused every year. Haemovigilance data indicates that approximately 10% of patients transfused with bacterially contaminated PCs develop sepsis [Brecher and Hay, 2005]. Figure 2.4 highlights key organisms implicated in bacterial infections associated with platelet transfusions. Clinical observations show that Gram-positive organisms including *Staphylococcus* and *Bacillus* species are the most common contaminants responsible for more than half of reported TTIs. Whilst Gram-negative TTIs are not as frequent, they are responsible for the majority of transfusion-associated bacterial sepsis fatalities [Brecher and Hay, 2005].

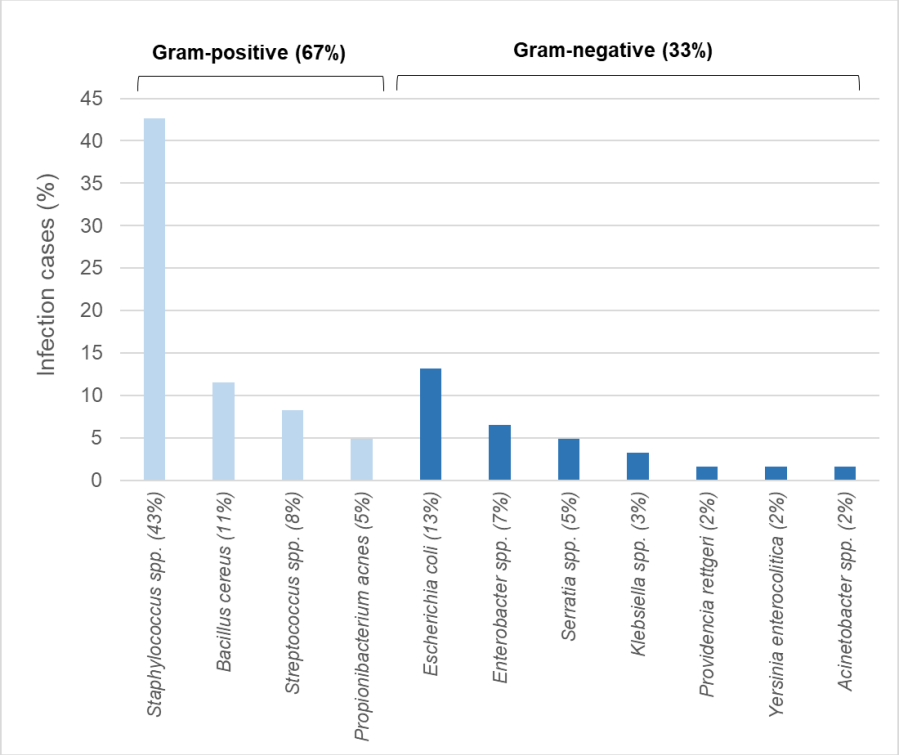

Figure 2.4. Organisms implicated in bacterial infections associated with platelet transfusions, reported in the BACTHEM (French), BACON (USA) and SHOT (UK) surveillance studies. Adapted from Brecher and Hay (2005).

2.2.5.3 Bacterial TTI's from Red Blood Cell Concentrates

The prevalence of bacterial contamination in RBCs is significantly less than PCs with approximately 1 in 40,000 RBC units contaminated [Hillyer *et al*, 2003]. However, as RBCs are the most frequently transfused blood product the overall risk of bacterial infectivity should not be underestimated. With over 13 million RBC units transfused every year in the US, it is projected that more than 300 units of bacterially contaminated RBCs are transfused every year [Brecher and Hay, 2005]. Figure 2.5 highlights key organisms implicated in bacterial infections associated with RBC transfusions.

The reduced risk of bacterial sepsis from transfusion of RBCs compared to PCs is likely due to the refridgerated storage conditions that is known to limit bacterial growth. Gram-negative bacteria are more commonly implicated in RBC transfusion transmitted bacterial infections compared to Gram-positive bacteria [Wagner *et al*, 1994; Hillyer *et al*, 2003; Brecher and Hay, 2005]. Bacteria shown to tolerate and survive in cold temperatures (1-6°C) including *Staphylococcus, Yersiniaceae*, *Serratia* and *Acinetobacter* species are most commonly implicated in RBC-associated TTIs [Maramica, 2019, pp. 409].

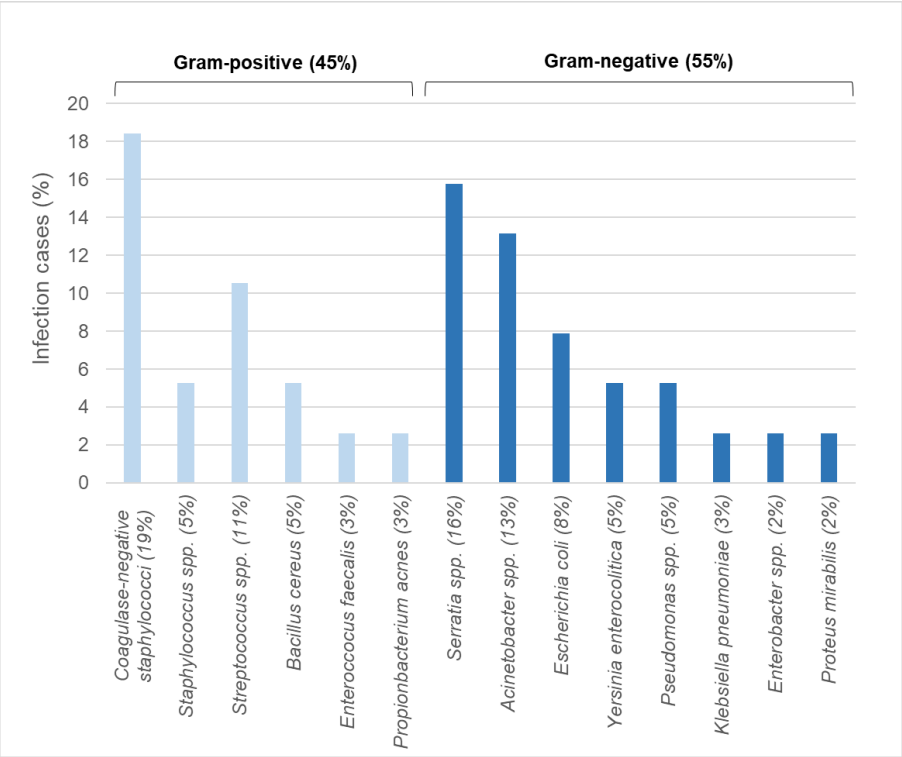

Figure 2.5. Organisms implicated in bacterial infections associated with red blood cell concentrates, reported in the BACTHEM (French), BACON (USA) and SHOT (UK) surveillance studies. Adapted from Brecher and Hay (2005).

2.2.5.4 Bacterial TTIs from Plasma and Plasma Products

Plasma and plasma products are associated with the lowest risk of TTIs. While processes of filtration and freezing have shown to reduce bacterial load, a residual risk of microbial contamination remains [Minno *et al*, 2017]. This is particularly relevant for spore-forming bacteria, specifically Gram-positive *Bacillus* species that can survive adverse conditions such as extreme freezing [Ježková, 1972].

The risk of bacterial contamination remains the greatest concern as viable bacteria continue to be detected in donated plasma-fractions [Damgaard *et al,* 2015; Minno *et al*, 2017]. Damgaard *et al* (2015) conducted a study to identify viable bacteria present in whole-blood donations with focus on plasma-fractions. Bacterial growth was evident in 53% of plasma-fractions, with Gram-positive *Staphylococcus epidermidis* responsible for approximately 40% of contamination cases [Damgaard *et al,* 2015]. This likely stems from the fact that *S. epidermidis* is a common skin commensal, with studies reporting that it is the most common source of infections on indwelling medical devices [Otto, 2009].

As mentioned, bacterial loads at time of donation may be very low, and in the case of plasma, are likely to remain at low levels during freezer storage at -25°C. However, storage at -25°C does not inactivate potential contaminants, instead it inhibits microbial growth, meaning that growth patterns can resume activity during the post-storage processing stages. This includes: (i) the thaw stage, where plasma bags are warmed in a water bath at 37°C [Yazer, 2012], (ii) the inventory period where plasma bags are stored for up to 5-days in hospital fridges [Eder *et al*, 2007], and (iii) the pre-transfusion warming process where plasma bags are warmed to 37°C using a blood warming device [Ghosh and Haldar, 2019]. Each of these processes, provides an opportunity for the revival and growth of organisms. Table 2.1 details key organisms that have been identified in bacterially contaminated plasma and plasma products. Organisms commonly associated with TTIs from RBCs and PCs should also be considered as potential contaminants in plasma.

Table 2.1. Bacterial species identified in plasma and plasma products. Organisms identified in plasma (A) prior to storage [Damgaard *et al*, 2015] and (B) post-storage [Gottlieb, 1993; Brecher and Hay, 2005].

Bacterial species associated with plasma and plasma products*	
(A) Pre-storage contaminants	• ***Staphylococcus* spp.** *(S. aureus, S. epidermidis, S. caprae)* • ***Propionibacterium* spp. (***P. acnes, P. avidum, P. granulosum)* • ***Bacillus* spp.** *(B. pumilus, B. thuringiensis*) • ***Acinetobacter* spp.** • ***Brachybacterium* spp.**
(B) Post-storage contaminants	• ***Pseudomonas* spp.** *(P. aeruginosa and P. cepacia)* • ***Serratia* spp.** • ***Enterobacter* spp.**

*Organisms are listed in order of prevalence.

2.2.6 Transfusion Transmitted Infections – A Global Issue

The WHO urge countries to co-ordinate a blood supply chain at a national level to "promote uniform implementation of standards and consistency in the quality and safety of blood and blood products" [World Health Organization, 2023]. Whilst most developed countries claim to have a nationally coordinated blood transfusion service, the WHO report that only 60% of reporting countries enforce the legislation covering the safety and quality of blood transfusion [World Health Organization, 2023]. This raises concerns, as constant vigilance is required to reduce the risk of established and newly-emerging pathogens entering the blood supply chain – especially in an era of mass global travel.

The residual risk of TTIs is higher in low-income countries as the prevalence of infection in blood donations is significantly higher compared to high-income countries (Table 2.2). This is thought to be due to differences in blood donor eligibility criteria set by the National Health Service. Evidence shows that voluntary unpaid blood donors provide safer blood than paid donors as they are more likely to declare important health information, including lifestyle choices, at the questionnaire stage [World Health Organization, 2023].

Table 2.2. The prevalence of infectious agents (HIV, HBV HCV and *T. pallidum* (the bacteria causing Syphilis)) detected in blood donations by income groups. Adapted from World Health Organization, 2023.

Income countries	HIV	HBV	*HCV*	*T. pallidum*
High-	0.001%	0.01%	0.06%	0.01%
Higher middle-	0.10%	0.29%	0.18%	0.34%
Lower middle-	0.19%	1.96%	0.38%	0.69%
Low-	0.70%	2.81%	1.00%	0.92%

Blood transfusion safety is a major concern in low- and middle-income countries, where the prevalence of transfusion-transmissible infections among blood donors is high and basic risk control measures, such as blood screening, are limited. Low-income countries are the highest risk of TTIs with up to 0.7% and 2.8% of blood donations being infected with HIV and HBV respectively, compared to 0.001% and 0.01% for high-income countries respectively [World Health Organization, 2023]. A

key concern is that low- and middle- income countries do not have access to test kits to implement screening with various countries reporting that they are unable to screen blood donations for 1 or more of the infectious agents as required by their national testing policy.

The contrast in blood transfusion safety between high-income and low-income countries remains a major challenge. It is recognised that new risk-prevention and pathogen reduction techniques must be made accessible and affordable before universal access to safe blood can be achieved.

2.3 I Strategies to Reduce Risk of TTIs from Blood Transfusion

This section will introduce the topic of infection prevention and control in transfusion medicine. Mandatory and recommended screening of blood transfusion products for infectious agents will be covered, and further methods to avoid, detect and actively eliminate potential contamination will be explored.

2.3.1 Protocols to Avoid Contamination

Infection prevention and control strategies, implemented at the time of donation, to minimize the risk of contaminated blood entering the blood supply will be covered in this section.

2.3.1.1 Donor Screening

Donor screening is an essential risk-prevention strategy implemented at the start of the blood supply chain to ensure donor safety and reduce the risk of infection transmission. Before donation, volunteers must complete a health check questionnaire to assess their health-status, lifestyle, travel history and medical history etc, which enables the blood centre to determine if the volunteer is eligible to donate. The donor selection process acts to protect the blood supply by deferring volunteers returning from high-risk areas, including Africa, Western Asia and South America from donation for 28 days, as carriers may be asymptomatic and be unaware that they are infected [JPAC, 2014].

2.3.1.2 Additional Methods to Avoid Contamination

Commensal bacteria found on the donor's skin is a major source of contamination. Whilst skin disinfection reduces bacterial load, residual risk remains, as up to 6% of blood cultures test positive for infectivity even after adequate skin disinfection [Goldman *et al*, 1997; Gibson and Norris, 1998]. Blood diversion, a process in which

the initial sample of donor blood removed, is a common practice to reduce bacterial contamination sourced from the donor's skin or the removal of a skin-core. Studies have shown that diversion of the first 10-40 mL of blood can successfully reduce the residual risk of bacterial infection by up to 50% [DeKorte *et al*, 2002].

The use of apheresis-derived, single-donor products has recently emerged as a preferred alternative to pooled whole-blood-derived products after studies demonstrated a 2-fold reduction in the infectious risk [Vamvakas and Blajchman, 2010; van der Meer, 2013]. At present, it is estimated that 75% of transfused platelets in the US are apheresis-derived [Cotton and McElroy, 2015]. On the contrary, use of apheresis single-donor platelets are limited in the UK due to the rising concerns of the increased risk of transfusion-related acute lung injury (TRALI) associated with single-donor products [JPAC, 2014].

2.3.2 Testing to Detect Contamination

This section will detail the testing methods that are used to detect infectious agents in donated blood. These measures are essential to detect cases of contamination resulting from asymptomatic donors.

The main assays used for blood screening include immunoassays and Nucleic Acid Amplification Testing (NAT) [Kitchen *et al*, 2010]. A sample of donated blood is screened for key infectious markers and in the case of a positive result, all associated blood components suspected as infectious are recalled, discarded and depending on the marker identified, the donor may be contacted [JPAC, 2014].

The WHO states that blood screening should be mandatory for the following infectious markers [Kitchen *et al*, 2010]:

- HIV-1 and HIV-2: screening for HIV antibodies
- HBV: screening for Hepatitis B surface antigen
- HCV: screening for HCV antibodies
- Syphilis: screening for specific *Treponema pallidum* antibodies

In the UK, additional antibody screening is employed for the Human T-cell lymphotropic virus (HTLV-1 and HTLV-II) and as a result, the risk of transfusion transmitted HTLV is 'virtually eliminated' [JPAC, 2014]. Figure 2.6 summaries the mandatory donor and blood screening measures followed in the UK to enhance blood safety.

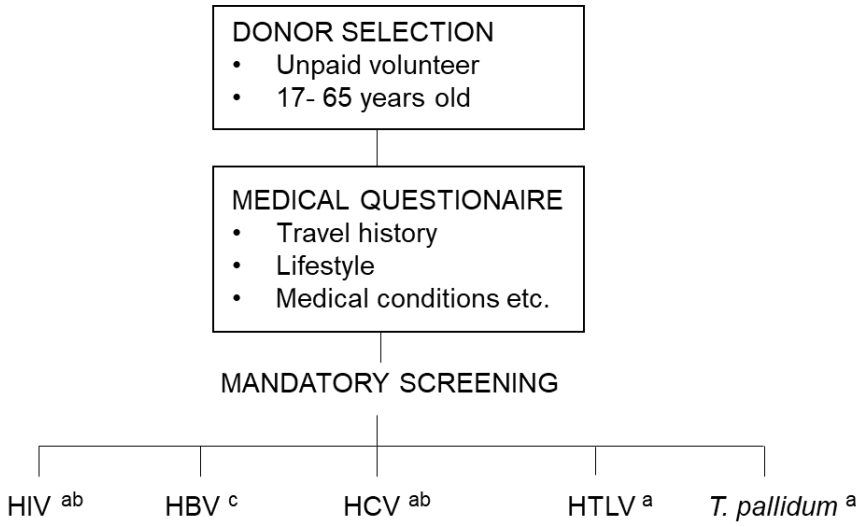

Figure 2.6. Mandatory donor and blood screening tests, conducted in the UK, to minimize the risk of TTIs. Molecular detection assay used to screen for the infectious agents: [a] antibody detection testing, [b] nucleic acid amplification testing and [c] antigen surface testing. Information provided by Blood Transfusion and Tissue Transplantation Services Professional Advisory Committee (2014).

The implementation of blood screening for specific viral agents in blood donations notably reduced the risk of viral TTIs [Burnouf and Radosevich, 2000; Williamson *et al*, 2003]. Nonetheless, there are concerns that the sensitivity of screening tests performed on pooled blood samples is limited, as the dilution process can lead to infectious samples with a low viral load not being detected [Hans and Marwaha, 2014]. In the event of a false negative, a single contaminated blood unit can infect multiple donations which increases the number of recipients potentially exposed to infectious agents. It is more effective to perform NAT on individual blood donations however this is uncommon because of high costs and time restraints [Hans and Marwaha, 2014].

Many bacterial detection methods have been developed to detect and/or monitor the presence of bacteria in a blood product. Manual blood cultures remain the standard detection method for microbial contamination in the UK and Europe. Whilst pooled blood cultures are an effective bacterial detection tool, they introduce various logistical

implications; in the event of a positive result, all associated blood products must be recalled and cultured, which can delay the release of non-infectious blood products to hospitals.

Currently, two automated systems, the BactT/ALERT (Organon Teknika Corp., Durham, USA) and the Pall Bacterial Detection System (*Pall* Corp., East Hills, USA) have been cleared by the FDA for quality control of bacterial culture in PCs [Savini *et al*, 2009]. Additionally, molecular techniques such as the use of non-amplified, chemiluminescence-linked universal bacteria ribonucleic acid (RNA) probes, are used to detect bacterial contamination in blood products. This technology is however limited to detect only four bacterial species (*Staphylococcus epidermidis, Staphylococcus aureus, Pseudomonas aeruginosa* and *Bacillus cereus*) at high population densities [Brecher and Hay, 2005].

Whilst these surveillance systems are efficient detection tools for enhancing blood safety, evidence suggests that the most effective infection prevention strategy is pathogen reduction [Dustan *et al*, 2008; Fournier-Wirth *et al*, 2010; Dodd, 2012], which will be discussed in the next section.

2.3.3 Pathogen Reduction Technologies to Eliminate Contamination

Since the introduction of safety measures including donor screening and NAT for infectious markers, the risk of acquiring TTIs has significantly reduced. Nevertheless, the risk of asymptomatic donors, limited sensitivity of detection testing and newly emerging pathogens continue to compromise the safety of the blood supply. In response to this, PRTs have been developed to further enhance blood safety. This section will detail traditional viral inactivation techniques and also, explore newly developed light-based PRTs for the treatment of blood transfusion products.

2.3.3.1 Standard PRTs for Plasma & Plasma Products

For the last few decades, antiviral techniques have been used to reduce the incidence of viral infectivity through transfusion of plasma and plasma products (Table 2.3). Due to use of chemicals, these traditional antiviral techniques are not compatible for treatment of cellular blood products including PCs and RBCs.

- **Solvent-detergent (SD) Treatment**

Use of SD treatment for viral inactivation of plasma is a technique that has been in use since the early 1990s. The traditional method uses sodium cholate (solvent) and

tri-(N-butyl)-phosphate (detergent) to remove and disrupt lipids from the membranes of viral pathogens. This inactivation mechanism can disrupt the membrane of lipid enveloped viruses, Gram-negative bacteria and protozoa however is ineffective against non-enveloped viruses [Burnouf and Radosevich, 2000]. Since 1992, SD-treated plasma (Octaplas®, Octapharmas AG) has been available for use in Europe. A revised product developed by Octapharma USA (New Jersey, USA) was recently approved for use in the USA in 2013 [Sidonio *et al*, 2022].

- **Methylene Blue (MB) and Visible Light**

A light-based inactivation system using broad-spectrum visible light (fluorescent lamps; 400 – 700 nm) and photosensitive agent methylene-blue (MB) was later manufactured as an antiviral treatment for plasma. Since its development, over 1 million MB-FFP units have been safely transfused throughout Europe. The mechanism of action is triggered by the intercalation of MB into nucleic acid. The excitation of MB by visible light, leads to the formation of singlet oxygen radicals which are found to oxidise guanine bases in nucleic acid strands. This modification prevents RNA transcription and deoxyribonucleic acid (DNA) replication. The mechanism is capable of inactivating various lipid-enveloped viruses and selected Gram-positive bacteria and parasites however inactivation against non-enveloped viruses with tightly interdigitated capsid proteins and Gram-negative bacteria is limited [Seghatchian *et al*, 2011; Pelletier *et al*, 2016].

- **Nanofiltration**

Physical removal of pathogens from plasma can be achieved using nanofiltration. This process, which is effective for removing a broad range of pathogens, including enveloped and non-enveloped viruses, bacteria and yeast, involves filtering plasma through membranes with a small pore size (typically 15-40 nm). Many licensed plasma-derived clotting factors, that are subject to SD treatment, are also nanofiltered [Picker, 2013].

Table 2.3. PRTs applied to plasma and plasma products to reduce the incidence of transmission infectivity. Adapted from Burnouf and Radosevich, 2000 and Williamson *et al*, 2003.

Treatment	Protocol	Mechanism of Action	Chemical Additive	Infectious Agent		
				HIV HBV HCV HTLV	HAV	B19
Solvent-detergent (SD)	Incubation in the presence of SD	Organic solvents remove and disrupt lipids from the membranes of selected enveloped viral agents	✓	✓	✖	✖
Methylene-blue (MB)	Photodynamic procedure using methylene blue and visible light	MB intercalates with nucleic acid → Reactive oxygen species degrade nucleic acid	✓	✓	✖	✓
Pasteurization	Heat treatment at 60°C for 10-hr in liquid state	Destabilization of intermolecular interactions between virus capsid proteins and/or the integrity of the virus envelope	✖	✓	✓	✖
Dry-heat	Heat treatment of a freeze-dried product (100°C for approx. 30 min)		✖	✓	✓	✖
Nanofiltration	Filtration through membranes with very small pore size (typically 15–40 nm)	Physical removal	✖	✓	✓	✓

Whilst these pathogen reduction techniques reduce the risk of blood-borne virus transmission, all, except for nanofiltration, are known to have limited inactivation efficacy against a broad range of bacteria, parasites and protozoa. With regards to product stability, the potential impact on blood quality has been indicated through the loss of protein activity, with studies showing that SD and MB treatments reduce protein functional activity levels (FVIII and fibrinogen) by up to 35%, and more concerningly, are associated with an increased risk of adverse transfusion reaction [Burnouf and Radosevich, 2000; Williamson *et al*, 2003; Karafin and Hillyer, 2013]. Further, since most of these treatments must be carried out before the product is transferred to a

storage bag, there is a risk that pathogen reduced products may get (re-)contaminated during later stages of processing. Nevertheless, the benefits of these treatments outweigh the operational challenges, reduction of product quality and minor risk of associated adverse reaction [Burnouf and Radosevich, 2000; Williamson *et al*, 2003].

Due to the mechanism of action, the PRTs explored in this section are not suitable for cellular components including PCs (stored in plasma), RBCs and whole blood, as they irreversibly damage cellular membranes and function [Picker, 2013]. The next section will cover novel technologies developed to treat both plasma and cellular blood products.

2.3.3.2 PRTs for Plasma & Cellular Blood Products

Continued efforts to improve blood product safety, for cellular blood products as well as plasma, have led to the development of light-based PRTs. These technologies provide a proactive approach to inactivate a broad-spectrum of new- and re-emerging pathogens that continue to compromise patient safety. PRTs have the potential to reduce the rate of TTIs, reduce the wastage of valuable blood products and most importantly, improve overall blood safety. Table 2.4 summaries existing PRTs, their inactivation mechanism and blood product applicability [Marschner & Dimberg, 2019].

The majority of commercialised PRTs use light inactivation mechanisms with or without photosensitisers, to target microbial and viral nucleic acid. Light-based inactivation proves to be more compatible for the treatment of cellular blood products including PCs and whole blood, compared to the conventional chemical-based techniques used for plasma (Section 2.3.3.1). To date, no PRTs for treatment of RBCs are commercially available, however as highlighted in Table 2.4, antimicrobial treatments are under development and currently in Phase 3 clinical trials [Marschner and Dimberg, 2019].

Table 2.4. PRTs for plasma and cellular blood products, their mechanism of action and blood product applicability. The Conformité Européene (CE) mark is required to commercialise the technology in the EU. Information extracted from Marschner and Dimberg (2019).

Technology (Manufacturer)	**Mechanism of Action**	**Plasma**	**Platelets**	**Whole Blood**	**Red Blood Cells**
INTERCEPT (Cerus)	Amotosalen + UVA light	✓ CE marked ✓ FDA approved	✓ CE marked ✓ FDA approved	✖	✖
INTERCEPT- Amustaline (Cerus)	pH driven using Amustaline (S-303)	✖	✖	✖	Phase 3 clinical trials (US, EU)
Mirasol (Terumo BCT)	Riboflavin + UVB light	✓ CE marked	✓ CE marked Pivotal clinical trials (US)	✓ CE marked	Pivotal clinical trials (US)
Theraflex-UV (Macopharma)	UVC light and agitation	✖	✓ CE marked	✖	✖
Theraflex-MB (Macopharma)	Methylene blue + visible light + filtration	✓ CE marked	✖	✖	✖

- **INTERCEPT System**

The INTERCEPT System *(Cerus Corporation, California, USA)* was the first UV-light based technology to receive CE mark approval for use in Europe and to date, is the only FDA approved PRT for use in the USA for treatment of plasma and PCs. The technology makes use of a photosensitiser psoralen, amotosalen *(S-59)* and broad range UVA-light (320–400 nm, 3 Jcm^{-2} delivered over 4–6 minutes) as illustrated in Figure 2.7. Amotosalen targets the helical region of nucleic acid and forms non-covalent bonds (docking phase in Fig 2.7A) between pyramidic bases of DNA or RNA. UVA-light then induces a photodynamic reaction that transforms the non-covalent bond into an irreversible covalent bond that prevents RNA transcription and DNA replication [Schlenke, 2014].

- **INTERCEPT S-303 System**

A pathogen reduction treatment for RBC concentrates, named the INTERCEPT S-303 System (*Cerus Corporation, California, USA*) is currently under development. This system does not use UV-light for pathogen inactivation, instead the inactivation

mechanism is driven by the chemical compound, Amustaline (S-303). Once added to the RBC concentrate, S-303 rapidly penetrates microbial cells and intercalates with nucleic acids. Glutathione (GSH), a natural antioxidant, is used to neutralise non-specific reactions and prevent cellular protein damage. Treatment times can take up to 20-hrs as the non-reactive by-product, acridine (S-300), must be carefully removed to reduce residual toxicity. To date, phase III clinical trials are ongoing to assess the efficacy and safety of INTERCEPT Amustaline treated RBCs [Aubry *et al,* 2018].

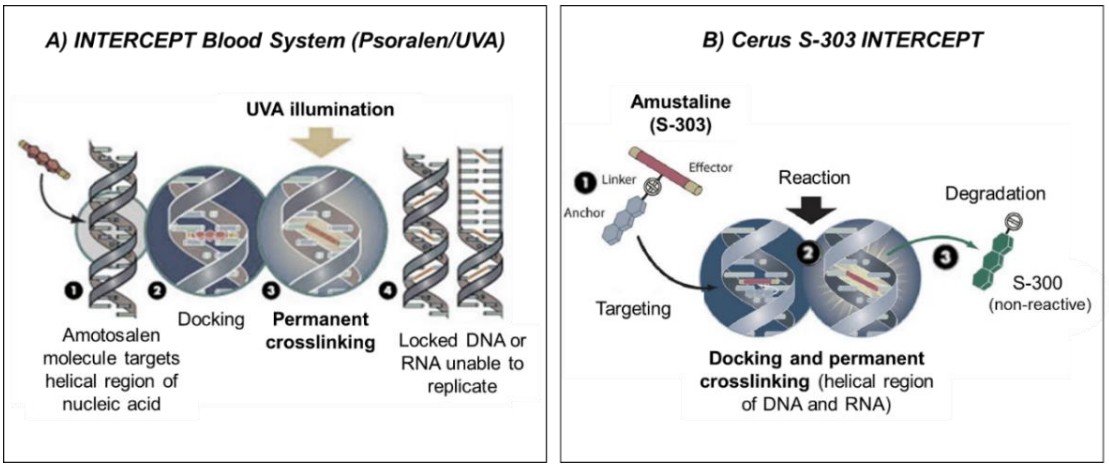

Figure 2.7. The mechanism of action of A) INTERCEPT Blood system for treatment of plasma and PCs and B) INTERCEPT S-303 system (under-development) for treatment of RBC concentrates. Figures adapted from Aubry *et al,* 2018.

- **MIRASOL System**

The MIRASOL system *(Terumo BCT, Colorado, USA)* combines the photosensitization effects of riboflavin and broad-spectrum UVA/B-light (285–365 nm, 5 Jcm^{-2} delivered over 4–6 minutes) to treat plasma and PCs. As detailed in Figure 2.8, following exposure to UV-light, riboflavin binds to nucleic acid bases and mediates oxygen-independent electron transfer resulting in irreversible nucleic acid damage. The permanent modification of nucleic acid bases prevents photo-reactivation associated with shorter-wavelength UV-light exposure [Marschner and Goodrich,

2011]. As riboflavin and its by-product, lumichrome, are considered non-toxic, no removal step is required as part of the treatment.

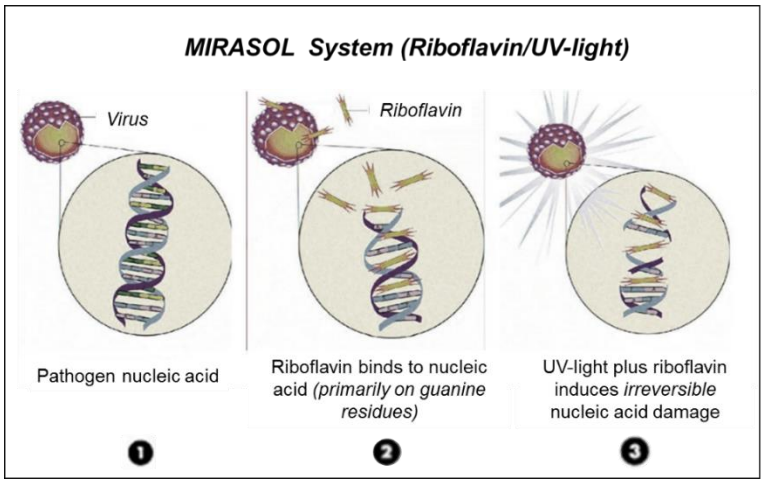

Figure 2.8. The mechanism of action for the MIRASOL system for the treatment of plasma and PCs. Figure adapted from Ito *et al* (1993).

- **Theraflex-UV**

Theraflex-UV technology (Macopharma, Tourcoing, France) uses narrow-bandwidth UVC-light (254 nm, 0.2 Jcm^{-2} delivered in approx. 1-min) to treat PCs. As shown in Figure 2.9, UVC-light targets nucleic acids of microbes and viral particles and induces covalent bond formation between pyrimidine nucleotides. This leads to nucleic acid lesions and the production of photoproducts that block RNA transcription and DNA replication [Seltsam, 2017]. Theraflex-UV technology is currently undergoing clinical efficacy and safety testing in Phase III clinical trials and therefore is not yet available for routine use [Brixner *et al*, 2021].

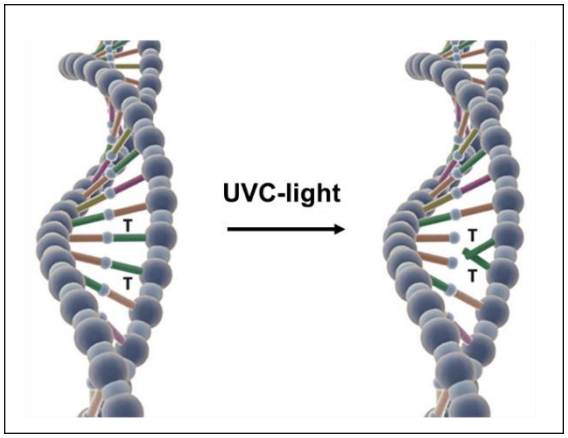

Figure 2.9. The mechanism of action for Theraflex-UV technology for the treatment of PCs. Figure adapted from Gross *et al* (2015).

- **Theraflex-MB**

Methylene Blue (MB) has been widely used as an antiviral treatment for FFP for decades in Europe (Section 2.3.3.1). In 2004, Theraflex-MB (Macopharma, France) was developed to enhance the traditional system that used visible light and MB, by removing residual MB after treatment and reducing the illumination time [Seghatchian *et al*, 2011]. The enhanced Theraflex-MB system can effectively inactivate viruses and has shown potential to reduce bacteria [Ash, 2006; Pelletier, 2006]. Reichenberg *et al* (2015) states that the majority of bacteria are physically removed (through an integrated filtration system) rather than inactivated via the photo-inactivation mechanism [Reichenberg *et al*, 2015].

2.3.3.3 Comparison of PRTs: Inactivation Efficacy

The majority of commercially available PRTs can inactivate a range of microbial agents commonly implicated in TTIs [Schlenke, 2013]. Each technology provides a unique pathogen inactivation profile for a range of viruses, bacteria, yeast, fungi and parasites.

- All technologies are capable of reducing a broad range of Gram-positive and Gram-negative bacteria that are commonly associated with TTIs.
- The INTERCEPT System has a well-established bacterial and viral inactivation profile that includes viral agents that are commonly screened prior to transfusion such as HIV, HBV, HCV, HTLV-1 and HTLV-II.
- MIRASOL and Theraflex-UV technologies demonstrate broad-spectrum antibacterial efficacy and are effective against HBV, HCV and HIV however the degree of inactivation of HTLV-I and HTLV-II has yet to be established.

Each technology does however, have a gap in inactivation efficacy. Firstly, all UV-light based technologies have limited capacity to inactivate bacterial spores. This is concerning as spores can germinate and multiply to a clinically relevant numbers during platelet storage [Seltsam, 2013]. Secondly, UV-light based PRTs are only able to target pathogens that contain nucleic acids and are therefore they are ineffective against prions. Whilst transmission risk is low, there are currently no screening tests that can detect abnormal prions in blood donations, which opens an opportunity for prions to infect the blood supply [Irsch and Lin, 2011 and Schlenke, 2013]. Nonetheless, the broad-spectrum microbial inactivation provided by existing

technologies offer enhanced safety and protection against re- and newly-emerging pathogens.

A summary of the photo-inactivation technologies developed for the treatment of plasma, PCs and/or whole blood, including the wavelength of light used to facilitate microbial inactivation is provided in Figure 2.10.

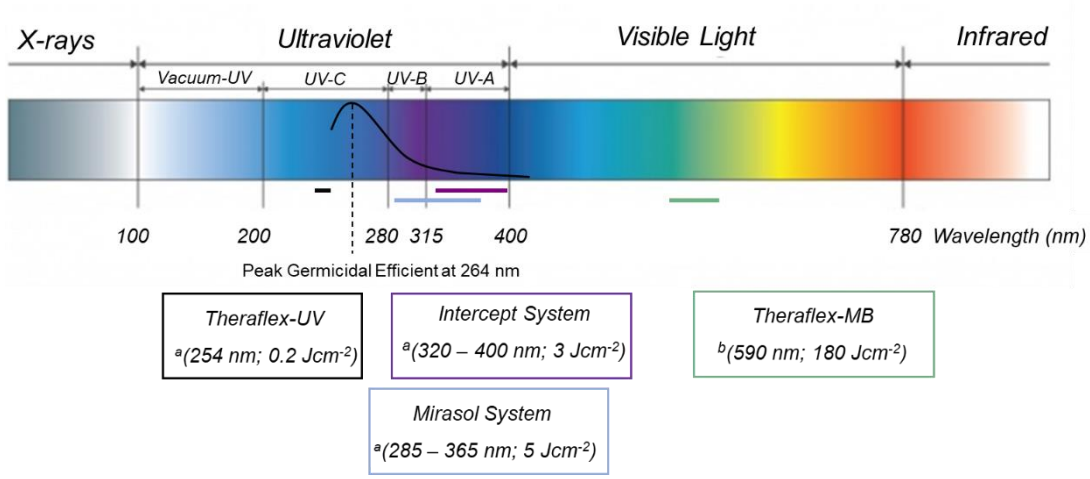

Figure 2.10. Light-based PRTs developed for the treatment of plasma and PCs.
Information extracted from [a]Schlenke *et al* (2014); [b] Seghatchian *et al* (2011).

2.3.3.4 Comparison of PRTs: Product Quality

Ideally, PRTs should not significantly compromise the therapeutic efficacy of the blood product. With respect to plasma, the most clinically important area is the retention of key plasma proteins that support the clotting functionality of blood. For example, as part of the regulatory approval process for a PRT, the Council of Europe state that the treated plasma must retain 60% of the clotting factors (fibrinogen and Factor VIII) compared to FFP [Keitel, 2009]. These parameters are typically tested using clotting assays referred to as the Prothrombin Time Test (PTT) and the Activated Partial Thromboplastin Time Test (APTT) (as covered in Sections 3.5.3 and 3.5.4 respectively). Following guidance by the FDA, protein specific enzyme-linked immunosorbent assays (ELISAs) must also be conducted to quantitatively measure the levels of clinically relevant proteins (including fibrinogen, Protein S, Factor VIII) in treated plasma [Benjamin and McLaughlin, 2009].

Studies show that the majority of light-based technologies lead to significant reductions in overall coagulation activity which overall compromises functional efficacy [Schlenke *et al*, 2014]. For example, a study by Escolar *et al* (2021) reported that patients receiving pathogen reduced blood (via the Intercept or Mirasol System) required more frequent transfusions to patients receiving control non-treated blood, likely due to the reduction in product quality [Escolar *et al*, 2021].

Further, the requirement for photosensitisers can increase processing times and, in rare cases, has been associated with adverse reactions in recipients [Schlenke *et al*, 2014; Piotrowski *et al*, 2018]. As additives are in small quantities and, in most cases, are actively removed from the treated blood product, most available safety data does not highlight significant risks of toxicity, carcinogenicity, mutagenicity, genotoxicity and reproductive toxicity [Seghatchian *et al*, 2011; Drew, 2017; Piotrowski *et al,* 2018]. Clinical safety studies investigating the use of MB, have however reported an increased risk in allergic reactions following transfusion of pathogen inactivated plasma compared to non-treated plasma [Nubret *et al,* 2011; Mertes *et al*, 2012]. This rare but severe adverse effect is most likely due to the sensitisation of the residual additives and/or their photo-products that can induce an immune response. Certain countries, including France and Germany, have discontinued the use of MB-treated plasma following concerns of an increased risk of allergic reaction [Seltsam, 2013].

2.3.4 Summary of Current Infection Prevention and Control Strategies

Infection prevention and control strategies have been introduced to avoid and detect microbial contamination of blood transfusion products. As TTIs remain a concern to patient health, light-based PRTs have been developed to increase the safety margin by actively removing infectious agents. While all demonstrate germicidal efficiency, it is generally accepted that these light-based PRTs have limitations as treatment conditions are shown to compromise blood product quality and stability [Schlenke *et al*, 2014]. Further, the requirement for photosensitizers increases processing times and, in rare cases, has been associated with adverse reactions in recipients depending on the type of photosensitive agent being used [Schlenke *et al*, 2014; Piotrowski *et al*, 2018]. Therefore, there is a need to a develop a safer alternative to the existing antimicrobial technologies that require either UV-light irradiation and/or addition of photosensitizers.

2.4 I Violet-Blue, 405-nm Light as a Pathogen Reduction Technology

Violet-blue 405-nm light has recently shown potential to be developed as a PRT for BTPs. This next section will provide an in-depth review of violet-blue 405-nm light technology, its photoexcitation process, the mechanism of inactivation and antimicrobial efficacy. Finally, this section will highlight recent research that explores the potential use of 405-nm light for the decontamination of BTPs as well as addressing the areas that require further investigation to fully assess its potential as a PRT in transfusion medicine.

2.4.1 Photoexcitation Mechanism

Violet-blue light, in the region of 405-nm, has shown to induce the photoexcitation of endogenous porphyrins within microbial cells, which, through a series of energy transfers, results in the generation of reactive oxygen species (ROS) [Hamblin and Hassan, 2004; Maclean *et al*, 2006, 2008, 2009; Ramakrishnan *et al*, 2016]. These toxic species have shown to cause non-specific, widespread oxidative damage to a vast range of pathogenic organisms (covered in Section 2.4.3).

Porphyrins (the molecules susceptible to photoexcitation by 405-nm light), are a group of naturally occurring macro-cyclic compounds characterised by a tetra-pyrrole structure, with four aromatic pyrrole rings joined by methene bridges. This structural arrangement enables strong absorption of visible light, in region of 400-420 nm, referred to as the Soret band (Figure 2.11). There are several other weaker absorption bands, named Q bands, present between 450–700-nm [Boris, 1981].

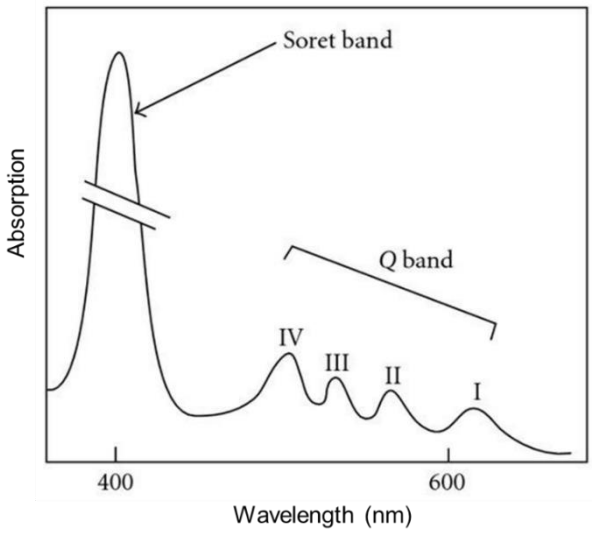

Figure 2.11. Optical absorption spectra of common porphyrins. Adapted from Josefsen and Boyle (2008).

As shown in Figure 2.12, following absorption of photons of these wavelengths, porphyrins are excited to a short-lived, excited singlet state (S_1) before transferring to a high triplet state (S_2) which has an increased lifespan [Maisch, 2009]. Here, the excited porphyrin either returns to the ground state by releasing heat and fluorescence or reacts with ground state molecular oxygen and dissipates its energy through one of two pathways [Yin *et al*, 2013]. The type I pathway involves the electron-transfer to a substrate producing radical ions, that in the presence of oxygen form cytotoxic molecules such as the superoxide anion (O_2- •), hydrogen peroxide (H_2O_2) and hydroxyl radical (•OH). The type II pathway occurs when the excited photosensitiser reacts directly with molecular oxygen resulting in the highly reactive singlet oxygen ($^1O_2$) [Maisch, 2009]. These highly reactive cytotoxic molecules, referred to as reactive oxygen species (ROS), are responsible for the phototoxic effects and drivers for widespread oxidative damage [Hamblin and Hassan, 2004; Maclean *et al*, 2008, 2009, 2016; Lubart *et al*, 2011].

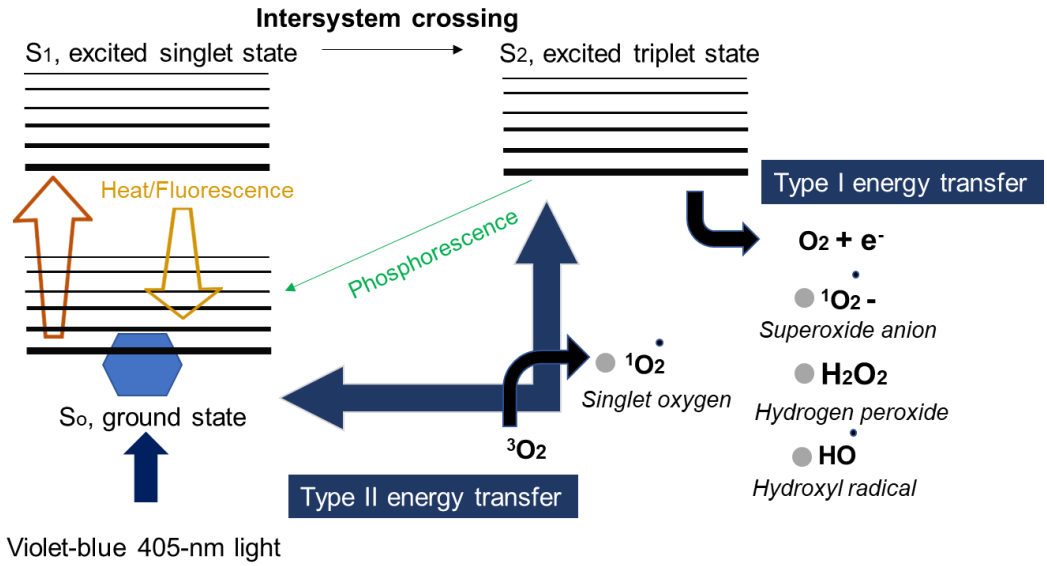

Figure 2.12. Illustration of the photoexcitation process of porphyrins following exposure to violet-blue light. Information extracted from Maisch (2009) and Ramakrishnan *et al* (2016).

2.4.2 Inactivation Mechanism

As described in the previous section, the photoexcitation of endogenous porphyrins present within exposed micro-organisms results in the generation of ROS, which in turn induces widespread oxidative damage. This oxidative damage has been found to impact intracellular molecules such as proteins, lipids and nucleic acids, ultimately

leading to microbial cell death [Maclean *et al,* 2006, 2008, 2009; Enwemeka *et al*, 2008; Kim *et al*, 2016; McKenzie *et al*, 2016; Bumah *et al*, 2017; Kim and Yuk, 2017; Wu *et al*, 2018; Rampon *et al*, 2018].

The loss of membrane integrity has been identified as a major route for 405-nm light microbial inactivation [Kim *et al*, 2015, 2016; McKenzie *et al*, 2016; Wu *et al* 2018]. McKenzie *et al* (2016) observed major changes in the membrane integrity of *S. aureus* and *E. coli* following exposure of violet-blue light, detecting significant nucleic acid leakage in both cases [McKenzie *et al*, 2016]. Many authors report that the membrane damage induced by violet-blue light is a result of a combination of factors, including the oxidation of unsaturated fatty acids and, and denaturation of trans-membrane sodium-potassium protein pumps and lipids which ultimately causes the leakage of intracellular components and cell lysis [Kim *et al*, 2015, 2016; McKenzie *et al*, 2016; Wu *et al,* 2018; Rampon *et al*, 2018].

Degradation of microbial DNA has also been reported, albeit to a lesser extent than membrane damage [Enwemeka *et al*, 2008; Bumah *et al*, 2017; Kim and Yuk 2017]. Enwemeka *et al* (2008) and others hypothesised that damage is likely to occur between pyrimidine bases of DNA which in turn, distorts the shape of the double helix halting its ability to replicate [Enwemeka *et al*, 2008; Kim and Yuk, 2017]. This type of light-induced damage can be reversed in the process called nucleotide excision repair whereby damaged base pairs are removed and resynthesized. However, cell death can occur in cases were the rate of photo-damage exceeds the rate of repair [Enwemeka *et al*, 2008]. Kim and Yuk (2017) support this hypothesis, showing that bacterial DNA is targeted by ROS, with evaluated levels of oxidized guanine bases (8- hydroxydeoxyguanosine) detected in violet-blue light exposed bacterial cells (>2.6 times higher in exposed *versus* non-exposed cells, $P<0.05$).

On the contrary, Kim *et al* (2015, 2016) found no evidence of DNA damage, via comet assay or DNA ladder analysis, in a range of bacteria (including *S. aureus, E. coli* and *B. cereus)* exposed to violet-blue light. The varying methods of dose delivery used by the authors may play a part in understanding the different routes for microbial inactivation identified. However, it is likely that the widespread, non-specific oxidative damage is a result of a combination of factors, with cellular membrane degradation being a key driver. Potential routes of microbial inactivation by violet-blue light are summarised in Figure 2.13.

Tomb *et al* (2017a) found that high doses of 405-nm light could inactivate norovirus surrogate, feline calicivirus (FCV) in non-biological media. As viruses do not contain porphyrins, it was hypothesised that the inactivation was primarily due to the presence of low-level UVA-light (315-400 nm) wavelengths in the spectral output of the 405 nm LED array used in the study, which are known to induce oxidative DNA damage [Girard *et al*, 2011; Tomb *et al*, 2017a]. Interestingly, inactivation of FCV was significantly enhanced when exposures were carried out in organically rich, biological media, with 50–85% less dose required for similar levels of viral inactivation in non-biological media [Tomb *et al,* 2017a]. Under these conditions, it has been hypothesised that porphyrins residing in the biological media are acting as natural exogenous photosensitizers [Tomb *et al*, 2014, 2017a]. Further to this, Rathnasinghe *et al* (2021) found an increased susceptibly to 405-nm light inactivation of lipid-enveloped viruses (Severe Acute Respiratory Syndrome Coronavirus 2 (SARS-CoV-2) and Influenza A) compared to non-enveloped viruses (Encephalomyocarditis virus (EMCV)) and suggested that this may be due to the excitation of photosensitive components present in the lipid envelope [Rathnasinghe *et al*, 2021].

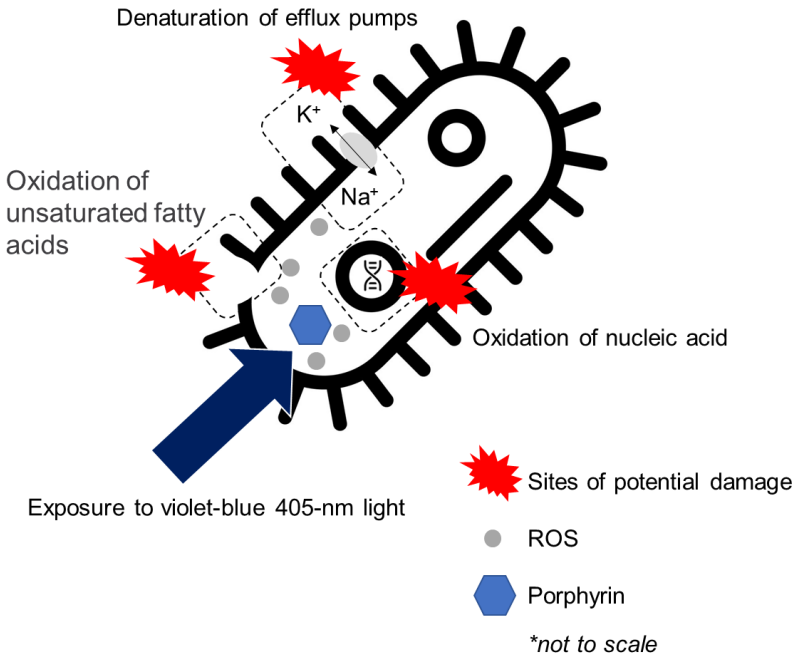

Figure 2.13. Potential microbial inactivation mechanisms of violet-blue 405-nm light. Evidence of loss of membrane integrity by Kim *et al*, 2015, 2016; McKenzie *et al*, 2016; Wu *et al*, 2018; Rampon *et al*, 2018 and DNA damage by Enwemeka *et al* (2008); Bumah *et al* (2017) and Kim and Yuk (2017).

2.4.3 Germicidal Efficacy of Violet-blue, 405-nm Light

A wide range of pathogens, including bacterial (vegetative cells and spores), fungal, yeast and viral agents have shown susceptibility to violet-blue, 405-nm light inactivation in non-biological suspensions [Maclean *et al*, 2006, 2008, 2009, 2013; Murdoch *et al*, 2012, 2013; Moorhead *et al,* 2016. Zhang *et al*, 2016; Tomb *et al,* 2017a; Trzaska *et al*, 2017; Rathnasinghe *et al*, 2021]. Microbial inactivation has been achieved under a range of conditions including in liquid suspensions (organically-rich and minimal media), on surfaces and in aerosols [Maclean *et al*, 2008, 2009, 2013; Murdoch *et al*, 2012, 2013; Dougall *et al*, 2018]. For this reason, violet-blue 405-nm light has shown promise to be developed as an antimicrobial technology across a broad range of applications.

Studies show that the dose levels of 405-nm light required to achieve inactivation vary between organisms. For instance, the increased susceptibility of Gram-positive bacteria compared to Gram-negative bacteria is well-documented [Gupta *et al*, 2015] with authors attributing this trend to differences in cell structure and porphyrin content. Bacterial spores, known to be highly tolerable microbes that show resistance to standard chemical- and heat-based disinfectant treatments, require around 10-fold higher doses of 405-nm light than vegetative cells [Moorhead *et al*, 2016].

405-nm light has also proven to inactivate a selection of viruses in minimal media including SARS-CoV-2, Influenza A, EMCV and FCV, albeit using significantly higher doses than that required for bacterial cells [Tomb *et al*, 2017a; Rathnasinghe *et al*, 2021]. The antifungal efficacy of 405-nm light has also been demonstrated against a range of pathogens known to affect humans, including *Candida albicans*, *Scedosporium apiospermum,* and on dormant and germinating spores of *Aspergillus niger* [Murdoch *et al*, 2013; Trzaska *et al*, 2017].

2.4.4 Unique Benefits of Violet-blue, 405-nm Light

Growing evidence of the antimicrobial efficacy of violet-blue 405-nm light has led to its development as an infection prevention and control strategy across a diverse range of applications. As the peak antimicrobial wavelength lies within the visible light region, 405-nm light is considered a safer alternative to UV-light for certain decontamination applications, with microbial inactivation achieved at exposure levels that are non-detrimental to mammalian cells and safe for human exposure [Barneck *et al*, 2016; Ramakrishnan *et al*, 2016]. As a result, this technology is being developed

for a range of clinical applications including environmental decontamination [Sinclair *et al*, 2023] and wound decontamination [McDonald *et al,* 2012].

Although less germicidal than UV-light, 405-nm light has the advantage that it can provide effective microbial inactivation with improved penetrability and without causing material damage [Irving *et al*, 2016]. A study by Irving *et al* (2016), showed that samples of endoscope material exposed to UVC-light developed surface cracking and blistering whilst 405-nm light exposed samples showed little to no changes. 405-nm light is therefore being explored as a safer alternative to UVC-light for use in medical device storage, with regards to material compatibility.

Additionally, the non-specific oxidative inactivation mechanism exerted on 405-nm light exposed micro-organisms has shown to reduce the opportunity for microbes to develop genetic mutations and acquire resistance [Zhang *et al*, 2014; Tomb *et al*, 2017b; Sułek *et al*, 2020]. Tomb *et al* (2017b) demonstrated that *S. aureus* did not develop resistance against high-intensity 405-nm light after receiving 15 repeated sub-lethal exposures [Tomb *et al*, 2017b]. This is an advantage over antimicrobial treatments such as antibiotics and UV-light, which use specific cellular targets to achieve inactivation [Ramakrishnan *et al*, 2014].

Overall, the ability for 405-nm light to provide broad spectrum pathogen inactivation, without the need for external photosensitizers, using dose levels that are safe for human and material exposure, provides a unique opportunity to develop the technology as a decontamination tool across a diverse range of applications [Maclean *et al*, 2013; Irving *et al*, 2016].

2.4.5 Potential Use of 405-nm Light as a PRT for Blood Transfusion Products

With a peak antimicrobial wavelength in the visible light region, the operational benefits of 405-nm light, including its non-ionizing nature, penetrability, and non-requirement for photosensitizing agents, make it an ideal candidate for investigation as a PRT for BTPs. As a result of collaborative research between The ROLEST research group (University of Strathclyde), and The Office of Blood Research and Review (US FDA), and also work by other research groups, the body of evidence supporting the development of violet-blue 405-nm light as a PRT for BTPs has grown since the start of this research project (2018). In summary, studies have demonstrated the antimicrobial action of violet-blue light for pathogen reduction in both plasma and PCs using selected bacteria, yeast and blood-borne parasites *Trypanosoma cruzi* and

Leishmania donovani [Maclean *et al,* 2016; Maclean *et al,* 2020; Lu *et al*, 2020; Jankowska *et al*, 2020; Kaldhone *et al*, 2024]. The potential for viral inactivation has also been evidenced in plasma [Tomb *et al*, 2017a; Ragupathy *et al*, 2022]. Preliminary research has also shown potential of violet-blue 405-nm light for pathogen reduction of red blood cell products under certain conditions [White *et al*, 2017; Devoy *et al*, 2020]. Table 2.5 overviews the pathogen inactivation data for treatment of blood products using violet-blue, 405-nm light that has been published to date.

The antimicrobial action of violet-blue 405-nm light in blood products was first demonstrated in plasma [Maclean *et al,* 2016]. This proof of concept study showed that 405-nm light was capable of inactivating *S. aureus*, *S. epidermidis* and *E. coli* in low volume plasma samples. Experiments were then scaled up to assess the inactivation efficacy of 405-nm light for plasma whilst in sealed storage bags. 99.9% reduction of low density *S. aureus* contamination ($\leq 10^3$ CFUmL^{-1}), selected to represent a clinically realistic scenario, was achieved using 405-nm light doses of 144 Jcm^{-2} [Maclean *et al*, 2016]. By assessing the inactivation efficacy of different methods of dose delivery (doses applied using irradiances of 5, 16 and 48 mWcm^{-2}), the study found that use of lower irradiances was more efficient, in terms of both optical energy and antimicrobial activity, compared to higher irradiances.

Table 2.5. Pathogen inactivation of plasma and PCs using 405-nm light. Plaque-forming units per millilitre (PFU/mL).

Blood Products	Scale of testing	Pathogen	Contamination level	Reference
Plasma	3 mL	*S. aureus,* *S. epidermidis,* *E. coli*	10^5 CFUmL^{-1}	Maclean *et al,* 2016
	1.5 mL	*FCV*	2×10^5 PFU/mL	Tomb e*t al,* 2017a
	25 mL	*HIV*	10 ng/mL	Ragupathy *et al*, 2022
	6 mL	*T. cruzi*	1×10^8 parasites/mL	Jankowska *et al*, 2020
	30 mL, 300 mL	*S. aureus*	10^1–10^3 CFUmL^{-1}	Maclean *et al,* 2016
PCs	3 mL	*B. cereus,* *S. epidermidis,* *S. pyogenes,* MRSA USA 300, *P. aeruginosa* *C. albicans*	1×10^5 CFUmL^{-1}	Lu *et al*, 2020
	6 mL	*T. cruzi*	1×10^8 parasites/mL	Jankowska *et al*, 2020
	40 mL	*L. donovani*	2×10^7 parasites/mL	Kaldhone *et al,* 2024
	200 mL	*S. aureus*	1×10^2 CFUmL^{-1}	Maclean *et al,* 2020

Previous work also demonstrated the antiviral potential, with successful inactivation (>4 $\log_{10}$ reductions) of a non-enveloped virus, FCV and an enveloped virus, HIV-1 achieved in plasma with a dose of 561 and 270 Jcm^{-2} [Tomb *et al*, 2017a; Ragupathy *et al*, 2022]. Whilst these studies provide evidence of the inactivation efficacy of 405-nm light for plasma using selected pathogens, all authors highlighted the need to expand the microbiological data, using a wide range of organisms at different seeding densities. Further it should be noted that, to date, no compatibility studies investigating the suitability of 405-nm light with the plasma itself in terms of protein integrity have been conducted.

Research has also been conducted to investigate the use of 405-nm light for pathogen reduction of PCs [Lu *et al,* 2020; Maclean *et al,* 2020; Jankowska *et al*, 2020]. Lu *et al* (2020) demonstrated the inactivation efficacy of 405-nm light for treatment of PCs, through exposure of small volume (3 mL) platelet bags seeded with bacteria and a yeast (Gram-positive bacteria: *B. cereus, S. epidermidis, S. pyogenes* and methicillin-resistant *S. aureus*; a Gram-negative bacterium: *P. aeruginosa*; and a yeast: *C. albicans*) [Lu *et al*, 2020]. All microbial contaminants were reduced following exposure to a 405-nm light dose of 75 Jcm^{-2}, with no microbial growth detected in exposed samples after a 5-day storage period. The integrity and stability of 405-nm light exposed PCs was also investigated using a dose of 75 Jcm^{-2}. Initial compatibility tests indicated that this effective antibacterial dose did not have an adverse effect on platelet activation, or aggregation. A proof of concept murine model also demonstrated that *in vivo* platelet survival was unaltered following exposure to 405-nm light after infusion into mice [Lu *et al*, 2020].

Research by Maclean *et al* (2020), evaluated the antimicrobial efficacy, dose efficiency and potential compatibility of 405-nm light for treatment of clinically relevant, 200 mL volumes of prebagged PCs [Maclean *et al*, 2020]. Significant bacterial reductions were achieved in 405-nm light exposed PCs with >99% inactivation achieved using doses in the region of 180 Jcm^{-2}. The use of lower irradiance levels for treatment of PCs were also found to be more germicidally efficient compared to higher irradiance levels, with a significant reduction being achieved with 43.2 Jcm^{-2} using 3 $mWcm^{-2}$ compared to 180 Jcm^{-2} required for 10 $mWcm^{-2}$ [$P = 0.008$, 0.002 respectively]. Again, the potential compatibility of 405-nm light with PCs was demonstrated within a murine model with no significant differences [$P > 0.05$] in

recovery detected between non-exposed PCs and those exposed to antibacterial doses ≤288 Jcm^{-2}.

The antiparasitic efficacy of 405-nm light with plasma and PCs was reported using the blood-borne parasites, Trypanosoma cruzi, that causes Chagas disease and *Leishmania donovani*, that causes Leishmaniasis in humans [Jankowska *et al*, 2020; Kaldhone *et al*, 2024]. Results demonstrated that a 405-nm light dose of 270 Jcm^{-2} was capable of completely inactivating *T. cruzi* in low volume plasma and platelet samples, and *L. donovani* in small platelet bags, with up to 9.0-log reductions achieved. In agreement of findings by Maclean *et al* (2020), these studies found that 405-nm light exposed platelets had similar *in vitro* metabolic and biochemical indices compared to non-exposed control platelets, indicating potential compatibility with effective antiparasitic doses [Maclean *et al*, 2020; Jankowska *et al*, 2020; Kaldhone *et al*, 2024].

To date, no clinically approved PRTs are available for the treatment of RBC components. This is likely due to the opacity and fragility of RBCs which limits the use of light and/or chemical additives to pathogen reduce blood without adversely affecting its functional efficacy. Preliminary research has investigated the potential compatibility of violet-blue 405-nm light with RBCs components without the need for additional photosensitizers. Whilst early stage, 405-nm light has shown the ability to reduce low-level bacterial contamination in bovine red cell suspensions with low treatment doses <90 Jcm^{-2} also indicating potential compatibility [White *et al,* 2017; Devoy *et al*, 2020]. Future work is required to fully evaluate the potential of antimicrobial 405-nm light as a PRT for RBC components.

These proof-of-concept studies clearly demonstrate the potential of violet-blue 405-nm light to enhance blood transfusion safety. However, to fully assess the suitability of this technology for pathogen reduction treatment of BTPs, there are a variety of both antimicrobial and protein compatibility tests, as well as technological challenges, which need to be further investigated.

2.5 Aims of the Study

This thesis will focus on the development of 405-nm light as a PRT for treatment of plasma, an important blood transfusion product, but also the suspending fluid for PCs, and whole blood components. Small-scale studies will be conducted to identify an effective 405-nm light dose the provides broad-spectrum antimicrobial efficacy, while preserving plasma protein integrity. Further, the effects of varying the method of dose delivery on antibacterial efficacy and protein compatibility will be investigated using low, mid and high-intensity 405-nm light treatment regimes. Data from the small-scale studies will be used for the development of a large-scale light unit to enable the treatment of prebagged plasma. A proof-of-concept study will be performed to assess the broad-spectrum antimicrobial efficacy and compatibility of 405-nm light for the treatment of small, 100 mL prebagged plasma. The final stage of this research will see plasma volumes scaled up to 300 mL bags, to reflect a more clinically relevant situation. Results from the antimicrobial efficacy and protein compatibility tests will be examined to identify a 405-nm light dose that is both effective and compatible for the treatment of 300 mL prebagged plasma.

This research project had four key objectives to identify and optimise the operational factors required to ensure the reliable, repeatable, and effective use of 405-nm light technology for decontamination of prebagged plasma:

1. Small-scale testing: Investigate the broad-spectrum antimicrobial efficacy of 405-nm light for treatment of plasma samples, using dose levels that show compatibility with the plasma itself in terms of protein integrity.
2. Small-scale testing: Assess the impact of varying the method of 405-nm light dose delivery on antibacterial efficacy and protein stability of plasma samples.
3. Large-scale technology development using 100 mL prebagged plasma, as a proof-of-concept model: Assess the broad-spectrum antimicrobial efficacy and compatibility of 405-nm light for the treatment of 100 mL prebagged plasma.
4. Large-scale technology development using clinically relevant prebagged plasma: Assess the antimicrobial efficacy and compatibility of 405-nm light for the treatment of clinically-relevant, 300 mL prebagged plasma.

These research outputs will provide novel and important information that will support the future development of violet-blue, 405-nm light as a PRT not only for plasma but for a range of blood transfusion products.

Chapter Three I General Methodology & Materials

3.0 I Overview

This study focused on the development of a PRT for the treatment of plasma, and this chapter outlines the general protocols used for the preparation and handling of biological materials including plasma and microorganisms. General details of the 405-nm light-emitting diode (LED) array sources used within this study are also included, as well as the general protocols used for assessing antimicrobial efficacy and protein compatibility of the light treatments. Specific details relating to the different light treatment methods, and the small-scale and larger-scale LED systems are detailed in the subsequent results chapters.

3.1 I Plasma

This section details the appropriate storage, preparation and handling of plasma used throughout the study. Details of the optical characterisation of plasma are also included.

3.1.1 Storage, Preparation and Handling of Plasma

Plasma was sourced from:

- Scottish National Blood Transfusion Service (SNBTS, UK). Human fresh frozen plasma from a single donor suspended in anticoagulant solution, citrate phosphate dextrose-adenine-1 (CPDA-1), provided in a 300 mL blood bag.
- TCS Biosciences Ltd (UK). Human fresh frozen plasma from a mixed pool suspended in anticoagulant solution, CPDA-1, provided in a 1 L bottle.

The stock of plasma was slowly defrosted, decanted into sterile 50 mL centrifuge tubes and 1.5 mL Eppendorf's for experimental use and stored at -20°C until required (Fig 3.1). Prior to use, appropriate volumes of plasma were thawed at room temperature and mixed using a vortex for 5-10 seconds to ensure plasma proteins were equally dispersed throughout the suspension. All disposable equipment that

came into contact with plasma was treated as potentially hazardous and disposed of via clinical waste.

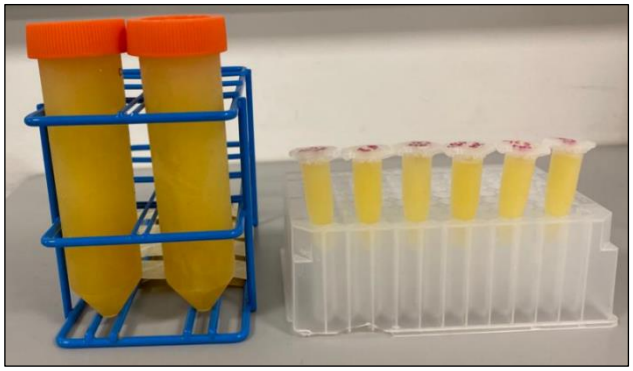

Figure 3.1. Preparation of plasma for experimental use and storage.

The use of human blood products was approved by the University of Strathclyde Ethics Committee (UEC19/45). All SNBTS and TCS Biosciences human blood products were pre-screened for HBV antigens and antibodies to HIV, HCV and syphilis before release for experimental use. All human blood products were treated as potentially hazardous and appropriate safety measures were put in place during experimentation.

3.1.2. Optical Characterisation of Plasma

The transmissibility of plasma from different batches was analysed by UV-Vis spectrophotometry (Biomate 5, Thermo Sectronic). The optical transmissibility of plasma samples (n=8) between 200 and 600 nm (Fig 3.2) was found to be 0.1-3.6 % at 405-nm, demonstrating the natural variation in optical density of plasma.

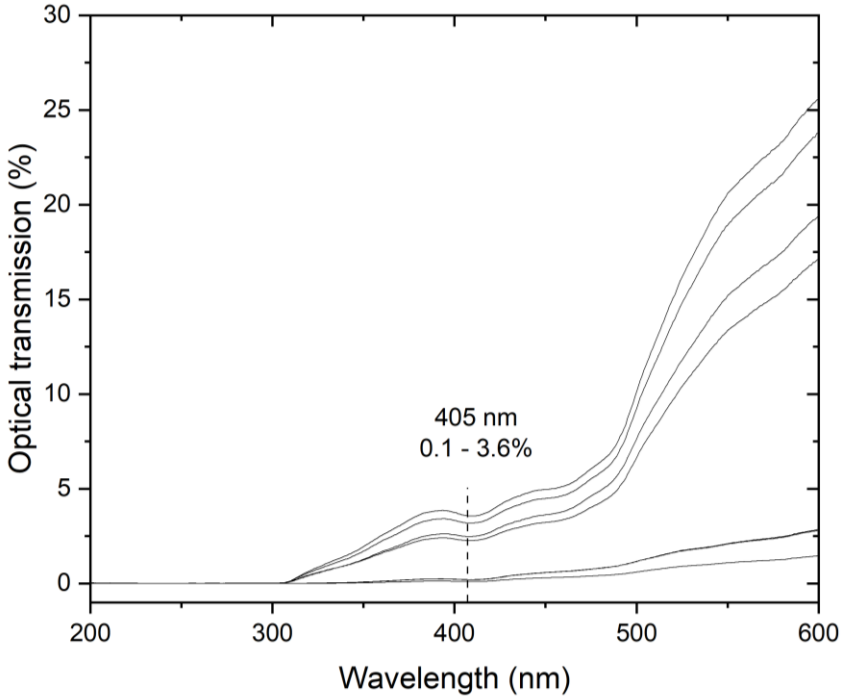

Figure 3.2. Optical characterisation of plasma. Optical characterisation of plasma samples, measured between 200–600 nm, demonstrating natural variation in optical transmission (n=8).

3.2 I Microorganisms

Microbial inactivation studies utilised a range of bacteria commonly associated with TTIs. This section details the procedures for the cultivation and maintenance of microorganisms, artificial seeding of plasma, and microbial enumeration.

3.2.1 Microbial Culture Media

Media was prepared according to the manufacturer's guidelines (Table 3.1) and then sterilised by autoclaving at 121°C for 15-mins. After autoclaving agar media, molten agar was placed in a water bath maintained at 48°C and allowed to cool before pouring into 90 mm single vent Petri dishes. All media listed in Table 3.1. was supplied by Oxoid, UK.

Table 3.1. Growth media and diluents used for microbial cultivation and sample preparation (Media supplied by Oxoid, UK).

Media	Quantity	Product Code
Nutrient Broth (NB)	13 g/L	CM0001
Nutrient Agar (NA)	28 g/L	CM0003
Tryptone Soya Broth (TSB)	30 g/L	CM0876
Tryptone Soya Agar (TSA)	40 g/L	PO0163
Malt Extract Broth (MEB)	20 g/L	CM0057
with 0.1% yeast extract (YE)	0.1 g/100 ml	LP0021
Malt Extract Agar	50 g/L	CM0059
with 0.1% yeast extract (YE)	0.1 g/100 ml	LP0021
Phosphate Buffer Saline (PBS)	1/100mL	BR0014G

3.2.2 Microbial Strains

Bacterial cultures were obtained from the National Collection of Type Cultures (NCTC; Collindale, UK), and the Belgian Coordinated Collections of Microorganisms (BCCM), Laboratorium voor Microbiologie (LMG; Gent, Belgium). Yeast cultures were sourced from the Leibniz Institute DSMZ – German Collection of Microorganisms and Cell Cultures GmbH (Süd, Germany). Details of the microbial strains and the culture media type used for cultivation are listed in Table 3.2.

Table 3.2. Microbial strains and cultivation media used during experimentation. Culture type indicates use for broth and agar media.

Microbial species	Strain	Gram status	Broth/Agar used
Staphylococcus aureus	NCTC 4135	+	NB/NA
Staphylococcus epidermidis	LMG 10273	+	TSB/TSA
Bacillus cereus	NCTC 11143	+	NB/NA
Escherichia coli	NCTC 9001	-	NB/NA
Pseudomonas aeruginosa	NCTC 9009	-	NB/NA
Acinetobacter baumannii	LMG1041	-	NB/NA
Yersinia enterocolitica	LMG07899	-	TSB/TSA
Klebsiella pneumoniae	LMG03081	-	NB/NA
Enterobacter cloacae	LMG02783	-	NB/NA
Candida albicans	DSM 1386	n/a	MEB/MEA+ 0.3% YE
Candida auris	DSM 105988	n/a	MEB/MEA + 0.3% YE

3.2.3 Culturing and Maintaining Microbial Cultures

The pure microbial strain from the culture collection was reconstituted, by inoculation into an appropriate broth (indicated in Table 3.2), and stored on Microbank™ beads (ProLab Diagnostics) at -20°C. To prepare a microbial culture for experimental use, the inoculated bead was removed from the Microbank™ collection and streaked onto an agar plate (medium type specified in Table 3.2). The streaked plate was incubated at 37°C for 24-hrs before being sub-cultured and incubated overnight on an agar slope. This slope 'stock' culture was stored in the laboratory fridge at 4°C for short-term storage and as a source of inoculum for daily experimental work. To ensure purity, cultures were re-streaked every 4 to 6 weeks by streaking onto a fresh agar plate and performing a Gram stain on an isolated colony.

For experimental use, a fresh culture was prepared by extracting a loop of bacteria or yeast from the stock culture and inoculating 100 mL of broth media (type specified in Table 3.2). The inoculated broth was incubated overnight at 37°C under rotary conditions (120 rpm) to provide a population of approximately 10^9 colony forming units per millilitre ($CFUmL^{-1}$), with exception of *B. cereus*, *C. albicans* and *C. auris* which grew to a population density of approximately 10^8 $CFUmL^{-1}$.

3.2.4 Re-Suspension and Serial Dilutions

Following cultivation, the microbial broth was centrifuged at 3939 x g (4300 rpm) for 10-mins at 20°C. The supernatant was discarded and the resultant microbial pellet re-suspended in 100 mL PBS. This working culture was serially diluted (10-fold dilutions; 1 mL microbial suspension into 9 mL PBS) to the microbial population required for experimental use.

3.2.5 Plating and Microbial Enumeration

To examine antimicrobial efficacy of a light treatment, the microbial population density of samples was enumerated pre- and post-exposure to measure the reduction in population size.

To assess microbial counts, samples were plated onto agar and incubated at 37°C for 18 to 24-hrs. Samples were plated using either the spread plate or pour plate method, depending on the expected sample population. For spread plating, 100 µL samples were pipetted onto an agar plate and manually spread using an L-shaped spreader.

For enumeration, colonies counted per plate were scaled to represent $CFUmL^{-1}$ by multiplying by a factor of 10. If the sample population was anticipated to be >300 CFU/plate, samples were serially diluted (10-fold dilutions) prior to spread plating. If the sample population was expected to be low (<30 CFU/plate), the pour plate method was used. For this, 1 mL sample was pipetted into a Petri dish, and ~20 mL molten agar was poured onto the sample, and the plate gently rotated clockwise (×5) and then anticlockwise (×5), to ensure thorough mixing of the suspension. The agar was left to solidify before incubation.

All organisms investigated in this study required incubation at 37°C for 24-hrs. The plate count was recorded in the standard counting unit, $CFUmL^{-1}$, and transferred to an electronic source (Excel and Origin files) for data analysis and storage.

3.3 I 405-nm Light Sources

For this research study, light emitting diode (LED) arrays, with a peak wavelength in the region of 405-nm (see example emission spectrum in Figure 3.3), were used as the light sources for exposure of plasma. Two different light systems were developed for testing:

- A small scale, single array system for small volume (250 µL) sample treatments, (**detailed in Chapters 4 and 5**) - shown in Figure 3.4a, and;
- A larger, scaled up system, for treatment of plasma transfusion bags of 100-300 mL volumes (**detailed in Chapters 6 and 7**) – shown in Figure 3.4b.

Specific details of the 405-nm light treatment systems, optical configurations and sample exposure conditions are described in detail in the relevant experimental chapters.

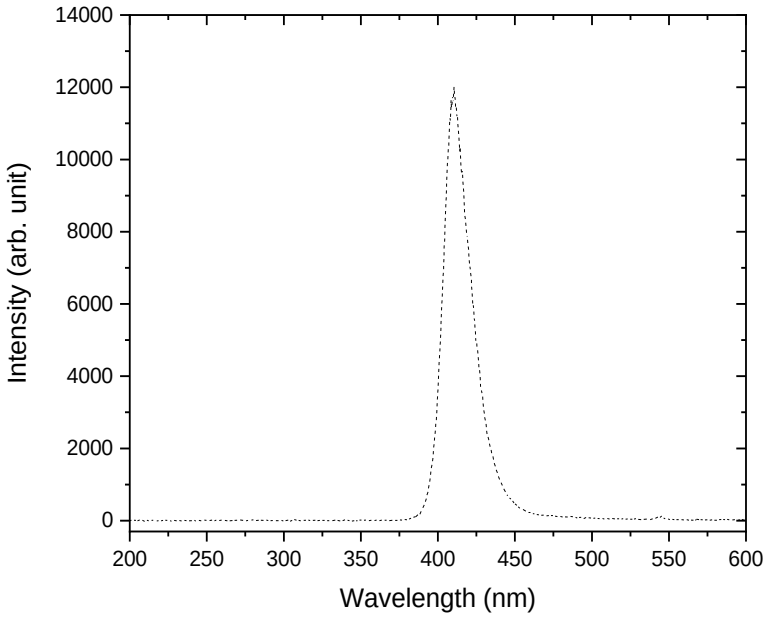

Figure 3.3. Optical emission spectrum of a 405-nm LED array used in this study. Optical data captured using a high-resolution spectrometer (HR4000, Ocean Optics Inc, Germany) and SpectraSuite software (Version 2.0.151).

3.4 I Antimicrobial Efficacy Testing

A key research area in this Thesis focused on the assessment of the antimicrobial efficacy of 405-nm light for pathogen reduction of plasma. This section outlines general methodology used to assess microbial inactivation in exposed plasma. Detailed methodology for each microbial inactivation study will be provided in each results chapter.

3.4.1 Microbial Inactivation of Small Volume Plasma Samples

To prepare 1 mL seeded plasma for experimental use, 10 µL microbial suspension (prepared as detailed in Section 3.2) was seeded into 990 µL plasma (1:100 dilution). For example, to prepare plasma with a microbial population of ~10^3 $CFUmL^{-1}$, 10 µL 10^5 $CFUmL^{-1}$ microbial suspension was added to 990 µL plasma. Seeded plasma was vortexed to ensure uniform dispersal of microbial cells, and samples (250 µL) transferred into a 96-well microplate, covered with ultra-clear adhesive sealing film (Thermo Fisher Scientific, #AB0558), and positioned directly below the light source (full details in Chapter 4), as shown in Figure 3.4A. Zero-hour controls were plated to determine the starting population of the seeded plasma. Equivalent control samples were prepared and held in identical conditions but shielded from light treatment.

Following light treatment, samples were plated and incubated at 37°C overnight, and surviving colonies enumerated.

3.4.2 Microbial Inactivation of Prebagged Plasma

To prepare seeded plasma for the 100 mL bag exposures, 110 mL plasma was prepared: 100 mL to be used for the bag exposure, and 10 mL to be used for a non-exposed control. This 110 mL volume was prepared by seeding 1.1 mL microbial suspension into 108.9 mL plasma (1:100 dilution). 100 mL of the seeded plasma was then transferred to a 150 mL transfer blood bag (Grifols, UK) for exposure. The remaining 10 mL seeded plasma was transferred to a sterile Universal tube, covered in tin-foil to prevent light exposure, and used to represent a non-exposed control.

To prepare seeded plasma for the 300 mL bag exposures, 310 mL plasma was prepared: 300 mL for the bag exposure, and 10 mL for the non-exposed control). This 310 mL volume was prepared by seeding 3.1 mL microbial suspension into 306.9 mL plasma (1:100 dilution). 300 mL of the seeded plasma was transferred to a 450 mL blood bag (Grifols, UK) for exposure, and the remaining 10 mL was transferred to a foil-wrapped Universal and used as the non-exposed control.

During light treatment, plasma bags were held horizontally on a custom built rig, directly under the 405-nm light unit (full details in Chapter 6). Following light treatment, samples were plated and incubated at 37°C overnight, and surviving colonies then enumerated.

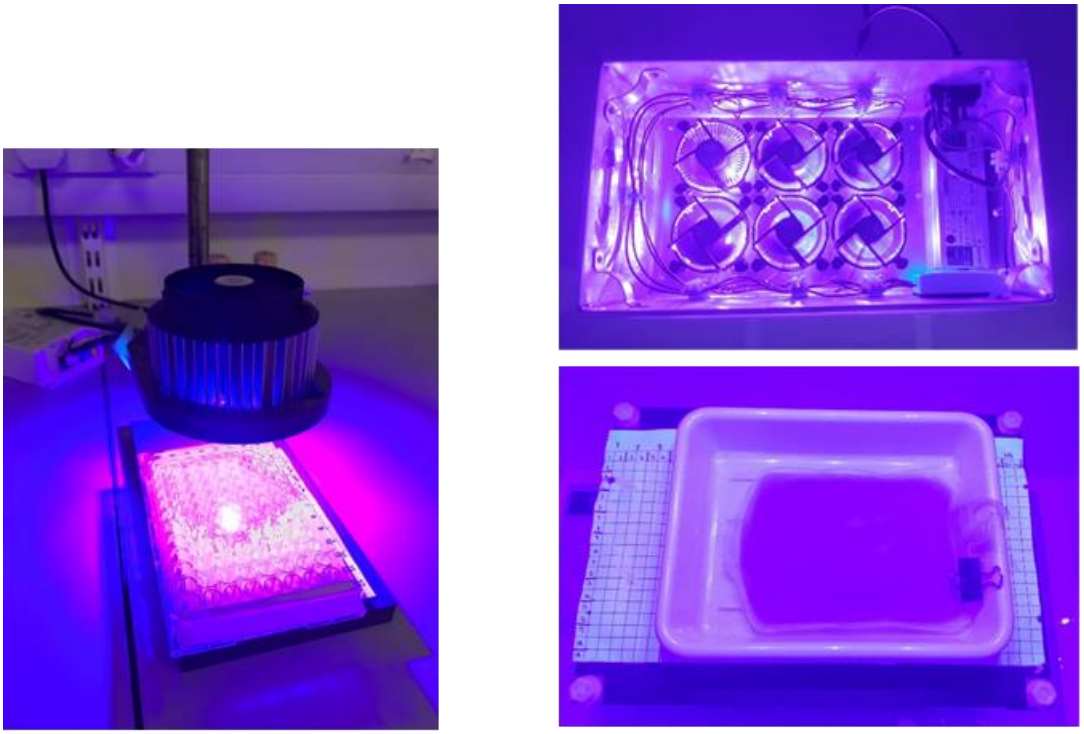

A) B)

Figure 3.4. Experimental set-ups for 405-nm light treatment of blood plasma. Images show A) the small-scale setup for exposing plasma samples in a 96-well microplate and B) the large-scale exposure system developed for treatment of prebagged plasma.

3.5 I Protein Compatibility Testing

Protein stability studies were conducted to assess the compatibility of 405-nm light for the pathogen reduction treatment of plasma. A number of tests were used to assess a range of markers indicative of plasma protein quality and functionality, including:

- Sodium dodecyl-sulfate polyacrylamide gel electrophoresis (SDS-PAGE)*:* used to visually examine general protein integrity following exposure to light treatment (Section 3.5.1).
- Advanced Oxidation Protein Products (AOPP) Assay: used to quantitatively assess the oxidative stress levels in light-treated plasma, using Chloramine-T as a marker of oxidative damage (Section 3.5.2).
- Prothrombin Time (PTT) and Activated Partial Thromboplastin Time (APTT) manual clotting tests: performed to measure and evaluate the stability of clotting factors of the extrinsic and intrinsic coagulation cascade respectively (Sections 3.5.3 and 3.5.4).

- Human Protein S (anticlotting agent) and Fibrinogen (clotting agent) enzyme-linked immunosorbent assays (ELISAs): used to quantitatively measure specific protein content in light-exposed plasma (Sections 3.5.5 and 3.5.6).

This section covers the general methodology for each protein test, however detailed methods are provided in subsequent experimental chapters.

3.5.1 Assessment of General Protein Integrity through SDS-PAGE

Preliminary protein compatibility tests were conducted using sodium dodecyl-sulfate polyacrylamide gel electrophoresis (SDS-PAGE). This analytical technique separates proteins based on their molecular weight (kDa), which enables the integrity of highly abundant proteins in plasma samples to be visually assessed. To compare the integrity of plasma proteins in light-exposed and non-exposed plasma, plasma samples were (1) prepared to their reduced state, (2) separated according to their molecular weight using gel electrophoresis and (3) stained for visual analysis.

3.5.1.1 Preparation of Samples and Controls for SDS-PAGE

The following media was required for sample and control preparation.

- Sample Reducing Agent, 10X Bolt™ #B0009 (Thermo Fisher Scientific, UK)
- Lithium dodecyl sulfate (LDS) Sample Buffer, 4X Bolt™ #B0007 (Thermo Fisher Scientific, UK)
- Tris Buffered Saline (TBS), #T6664 (Sigma-Aldrich, UK)
- Proteinase K, #1.24568 (Sigma-Aldrich, UK)

Plasma samples were diluted (100-fold; 1 µL plasma into 99 µL TBS) to reduce the masking effect of highly abundant proteins and to allow for better resolution of lower abundance proteins. Samples were then prepared as specified in Table 3.3. Sample buffer, containing a range of compounds including LDS, glycerol and tracking dyes Commassie Brilliant Blue and Phenol red, was added to apply a negative charge to proteins to promote the separation of proteins and track the position of the sample during electrophoresis. Sample reducing agent was used during sample preparation to cleave disulfide bond crosslinks within proteins and between protein subunits, causing 3D tertiary structures to unfold into primary linear protein subunits, which typically leads to better separation during electrophoresis. To accelerate the reduction process, samples were heat treated in a thermocycler (Prime Thermal Cycler, Techne, UK) at 70°C for 10-mins. Prepared samples were stored at -20°C until required.

Table 3.3. Preparation of a reduced plasma samples for SDS-PAGE.

Reagent	Volume (µL)
Diluted sample	100
Deionized water	30
LDS sample buffer	50
Sample reducing agent	20

Control samples were prepared for comparative purposes:

- **A positive control,** was prepared to demonstrate complete plasma protein degradation. Proteinase K (100 µL of 0.1 mg/mL) was mixed with a fresh plasma sample (100 µL) and heat treated in a thermocycler at 65°C for 3-hrs. The degraded plasma sample was diluted in TBS (50-fold; 2 µL sample into 98 µL TBS) before reducing the sample following the steps outlined in Table 3.3.
- **A negative control,** representing a sample containing no plasma, was prepared. This control was prepared by substituting the plasma with TBS and proceeding to sample reduction as per Table 3.3.
- **A Standard Protein Ladder** (Invitrogen™ SeeBlue® Plus2 Pre-Stained), which contained a set of known molecular-weight (kDa) protein markers, was used to aid the identification of the protein bands in the plasma samples.

3.5.1.2 Separation of Plasma Proteins by Electrophoresis

The following equipment and media were required for conducting gel electrophoresis.

- Plasma samples and controls, as prepared in Section 3.5.1.1
- Invitrogen™ Mini Gel Tank (Fisher Scientific, UK)
- Gel, Invitrogen™ Bolt 4-12% Bis-Tris Plus, 1.0 mm x 15 well gels
- Running buffer solution, 25 mL NuPAGE MES SDS (20X)) added to 475 mL deionized water
- A protein standard, Invitrogen™ SeeBlue® Plus2 Pre-Stained
- Antioxidant agent, Invitrogen™ Bolt Antioxidant

All electrophoresis media was supplied by Thermo Fisher, UK and stored at -4 °*C* until required.

Methodology

After sample preparation (Section 3.5.1.1), the mini gel tank was assembled (Figure 3.5). The cassette clamp was secured into the chamber with the anode connector aligned to the centre. The chamber was filled with running buffer solution to the level of the metal cathode.

A) B)

Figure 3.5. SDS-PAGE equipment A) Mini gel tank and B) Alignment of cassette clamps in tank chambers.

The gel cassette was removed from its packaging and rinsed gently with tap water. The comb and white tape at the bottom of the cassette were removed. Gel wells were then rinsed with running buffer. The gel cassette was placed into the chamber with the wells facing the front of the tank. 10 µL volumes of protein standard, test and control samples were loaded into the wells of the gel. All samples were vortexed before loading to ensure uniform dispersion of proteins.

The gel cassette was gently lowered to the bottom of the chamber and secured into place with cassette clamps. Running buffer was then added to the level of the fill line. When performing SDS-PAGE under reducing conditions, antioxidant agent (0.4 mL) was added to running buffer to prevent sample re-oxidation.

The lid was secured onto the electrophoresis tank and the power supply was set to provide 200 V at 120 mA. During the separation process, proteins migrated from the cathode to the anode at the bottom of the gel matrix. The power supply was turned off, at approximately 25-mins, when the dye front approached the bottom of the gel matrix. The gel cassette was removed by releasing the cassette clamps. The gel was then stained for visual analysis.

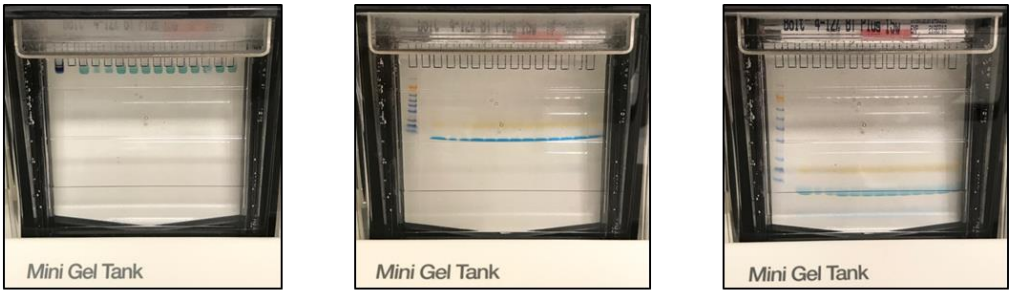

A) B) C)

Figure 3.6. Appearance of samples during SDS-PAGE at A) time zero, B) 15-mins and C) 25-mins.

3.5.1.3 Staining, De-staining and Drying Gel for Visual Analysis

All media was prepared in the fume hood and stored in a flammable cabinet.

- 0.1% Coomassie Blue Stain

Coomassie blue powder (0.125 g; Thermo Fisher) was mixed with methanol (200 mL; Arcos), acetic acid (35 mL; Sigma) and deionized water (265 mL). This reagent was used to fix and stain the protein bands in the gel.

- De-staining Solution

Methanol (50 mL) and acetic acid (50 mL) were mixed with deionized water (400 mL) in a 1:1:8 ratio respectively. This step removed excess dye from the gel matrix background which was crucial in resolving individual protein bands for analysis.

- Drying Solution

Ethanol (105 mL; Thermo Fisher) and glycerol (40 mL; Sigma) were mixed in distilled water (855 mL).

After gel electrophoresis, the gel was removed from the cassette and submerged in 0.1% Coomassie blue stain for 1-hr on an orbital shaker set to 60 rpm. The stained gel was gently rinsed with tap water before being suspended in de-staining solution for approximately 4-hrs under agitation at 60 rpm. Absorbent paper towels were placed in the container to help draw out the stain. Once de-stained, the gel was submerged in drying solution for 5 to 10-mins and gently rinsed with water. Prior to gel analysis, the gel was placed between cellophane sheets and a mini plastic roller was used to remove air bubbles.

3.5.1.4 Analysis of Electrophoretic Gels

To assess general plasma protein integrity, electrophoretic band patterns of the exposed and non-exposed plasma samples were compared noting differences in density, size and sharpness. Electrophoretic gels were photographed with a smartphone, with a 20X Macro Lens (*MPOW Fisheye Lens*) used for magnification in some cases and transferred to a computer (.JPEG) for storage and image processing. To aid visual analysis, semi-quantitative analysis of gels was also performed using ImageJ Image Processing software (http://rsb.info.nih.gov/ij) to establish protein intensity levels as an indicator of protein damage, as per methodology outlined by Alonso Villela *et al* (2020).

In SDS-PAGE analysis, it is common for highly abundant proteins to mask the presence of proteins in low abundance. Therefore, to support analysis, a Standard Plasma Protein Band-pattern Reference Chart – shown in Figure 3.7 – was created to identify highly abundant proteins that, based on relative molecular mass, are likely to reside in specific band regions (Schenk *et al*, 2008; Gautam *et al*, 2013). For the purposes of SDS-PAGE analysis, proteins in the region of 80 to 198 kDa are referred to as high molecule weight proteins (HMWPs).

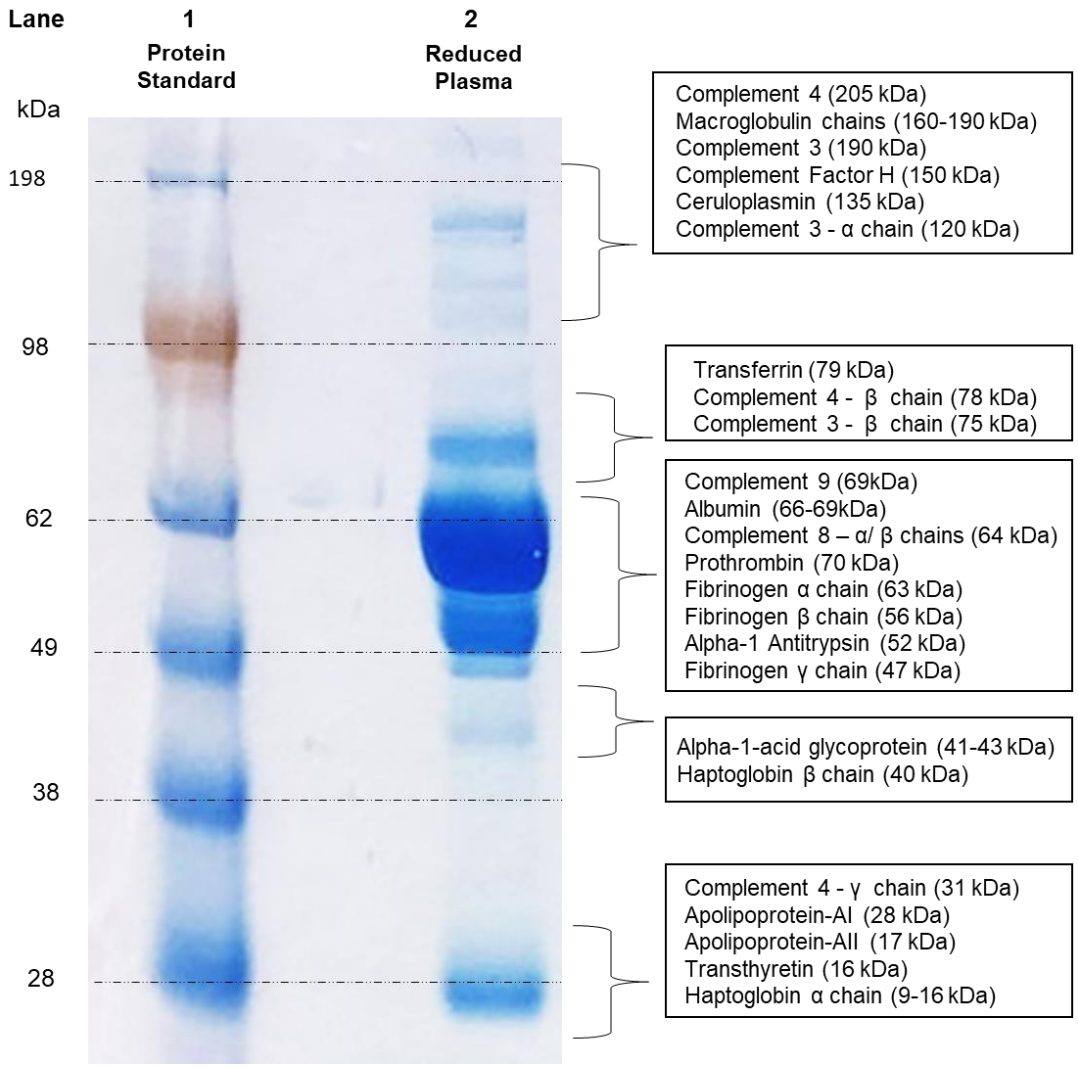

Figure 3.7. Plasma protein band-pattern reference chart for highly abundant plasma proteins. A protein standard ladder (Lane 1) was used to identify the molecular weight of protein bands. SDS-PAGE analysis of non-exposed plasma under reduced conditions (Lane 2). Plasma proteins associated with band regions are highlighted (banding information sourced from Schenk *et al*, 2008; Gautam *et al*, 2013).

Before conducting 405-nm light exposures, it was important to characterise the natural variation of protein in plasma, between different samples and batches, using SDS-PAGE. This pre-work is covered in Appendix A. As highlighted in Figure A, there are minor differences in electrophoretic patterns between non-exposed plasma samples, likely due to natural sample-to-sample and batch-to-batch variation in protein content. This tool was therefore used as an indicator to detect major changes in protein integrity.

3.5.2 Use of an Advanced Oxidation Protein Products Assay to Assess Oxidative Stress Levels

An advanced oxidation protein products (AOPP) assay was used to quantitatively measure the level of oxidative stress in 405-nm light exposed and non-exposed plasma. The AOPP Assay Kit (ab242295; Abcam), which uses Chloramine-T as a marker of oxidative damage, was used in accordance with manufacturer's instructions. A 100 µM Chloramine Stock solution was first prepared by reconstituting 5 µL of Chloramine Standard in 4.995 mL of 1X Assay Diluent. This 100 µM Chloramine Stock solution was then used to prepare a series of chloramine standards by diluting in fixed volumes of 1X Assay diluent, as shown in Table 3.4.

Table 3.4. Chloramine standard preparation for AOPP assay.

Standard #	Chloramine Stock Solution (µL)	1x Assay Diluent (µL)	Chloramine Concentration (µM)
1	500	0	100
2	400	100	80
3	300	200	60
4	200	300	40
5	100	400	20
6	50	450	10
7	25	475	5
8	0	500	0

Chloramine reaction initiator reagent was prepared by dissolving 200 mg in 1 mL distilled water. Exposed and non-exposed plasma samples were diluted in PBS (1:10) prior to testing. 200 µL volumes of diluted plasma samples, and Chloramine-T standards (100 to 0 µM) were transferred to a 96-well plate. 10 µL Chloramine Reaction Initiator was then added to all wells. The plate was agitated for 5-mins (120 rpm at room temperature) and 20 µL Stop Solution was then added. Absorbance at 340-nm was measured using a Multiskan GO Microplate Spectrophotometer (Thermo Fisher, UK). AOPP levels were calculated by reference to the chloramine standard curve and expressed as mean (n=3) ±SD of Chloramine-T equivalents (µM), representative of oxidative stress levels, with values corrected for dilution factor.

3.5.3 Use of the Prothrombin Time Test to Assess Functionality of Blood Clotting Factors in The Extrinsic and Common Coagulation Pathways.

The Prothrombin Time (PTT) assay is a standard *in vitro* screening test used to assess the stability of plasma. PTT reagent (AlphaLabs, UK) was used to provide a source of tissue factor (TF), calcium (Ca^{2+}) and phospholipids (PL) to activate factor VII in the extrinsic coagulation pathway (shown in Figure 3.8). The time to clot indicates the stability of clotting factors in the extrinsic (VII) and common (I, II, V and X) coagulation pathway.

The PTT reagent was used in accordance with manufacturer's instructions. In summary, a vial of PTT reagent was reconstituted into 4 mL distilled water and pre-incubated at 37°C for 30-min. 50 µL volumes of pre-incubated plasma (37°C for 2-min) were pipetted into wells of a 24-well plate. 100 µL volumes of pre-incubated PTT reagent were added to the plasma sample. The time taken for visual clot formation was recorded in seconds using a stopwatch. Data was presented as the mean time to clot ± SD (n=3).

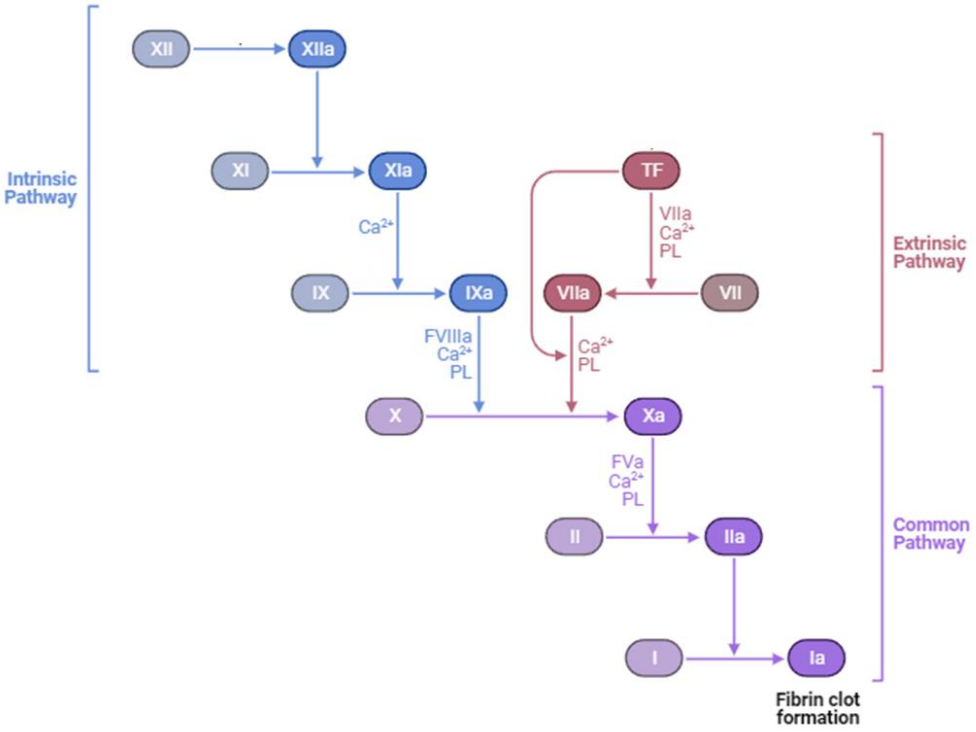

Figure 3.8. Diagram of the clotting cascade. Adapted from BioRender.com.

3.5.4 Use of the Activated Partial Thromboplastin Time Test to Assess Functionality of Blood Clotting Factors in the Intrinsic Coagulation Pathway.

Activated Partial Thromboplastin Time (APTT) testing is a screening technique used to assess the functionality of intrinsic coagulation pathway proteins. It is used for quantitative measurement of intrinsic factors (VIII, IX, XI, and XII) and common pathway factors (I, II, V and X) of coagulation. This assay was used in this study to compare the clotting activity, driven by intrinsic pathway factors, of exposed and non-exposed control plasma. The APPT test kit (Enzyme Research Laboratories, UK) contained Phospholin ES and calcium chloride ($CaCl_2$) reagents that were packaged ready for use.

Prior to use, the vial of $CaCl_2$ was incubated at 37°C for 30-min. 100 µL volumes of plasma and Phospholin ES reagent were pipetted into a 24-well plate (1:1 ratio), and gently mixed. The sample plate was incubated at 37°C for 5-min. 100 µL volumes of pre-incubated $CaCl_2$ were added to samples, and a timer started immediately. The time taken for a clot to be observed was recorded in seconds. Data was presented as the mean time to clot ± SD (n = 3).

3.5.5 Use of a Human Protein S ELISA for the Measurement of Human Protein S in Plasma.

A human Protein S, *in vitro* competitive enzyme-linked immunosorbent assay (ELISA) was used to quantitatively measure the levels of Protein S in plasma. Protein S, is a key anticlotting plasma protein that inactivates clotting factors Va and VIIIa to inhibit clot formation. The Protein S ELISA kit (ab125969; Abcam) was used in accordance with manufacturer's instructions. Protein S standards were prepared in the concentration range of 8 to 0 µg/mL by serially diluting a 8 µg/mL Chloramine Stock solution with 1X Assay Diluent as shown in Table 3.5.

Prior to testing, exposed and non-exposed plasma samples were diluted with 1X Assay diluent (1:10). 25 µL volumes of standards and plasma samples were added to each well of the supplied 96-well plate that was precoated and blocked with Protein S specific antibody. 25 µL of Biotinylated Protein S was added to each well, after which the plate was sealed with tape and incubated at room temperature for 2-hr. The plate was manually washed with 1X Wash Buffer. This process was repeated five times, inverting the plate to decant the contents and completely remove the liquid each time. 50 µL volumes of 1X Streptavidin-Peroxidase Conjugate were added to each well,

before re-sealing the plate and incubating for 30-mins. 50 µL volumes of Chromogen Substrate were then added to each well to visualise the enzymatic reaction that produced a blue colour product. The microplate was incubated for 10-mins, under agitation at 100 rpm, at room temperature. Finally, 50 µL volumes of Stop Solution were added to each well, which resulted in a yellow colour product. The density of yellow colouration was inversely proportional to the concentration of Protein S captured in the plate. Absorbance at 450-nm was immediately measured using a Multiskan GO Microplate Spectrophotometer. Protein S levels were expressed as µg/mL calculated using the Protein S, known concentration, standard curve and presented as mean ± SD (n=2).

Table 3.5. Protein S standard preparation for Protein S ELISA.

Standard #	Chloramine Stock Solution (µL)	1x Assay Diluent (µL)	Chloramine Concentration (µg/mL)
1	2-µG of Protein S in 250-µL of Diluent		8
2	120	120	4
3	120	120	2
4	120	120	1
5	120	120	0.5
6	120	120	0.25
7	-	120	0

3.5.6 Use of Fibrinogen ELISA for the Quantitative Measurement of Fibrinogen in Plasma

Fibrinogen (Factor I) is an essential plasma protein that, when activated to fibrin, binds to platelets and helps to form a stable blood clot. It is therefore important to assess the stability of fibrinogen in plasma following exposure to 405-nm light. The Human Fibrinogen SimpleStep ELISA kit (ab241383, Abcam) was used for the quantitative measurement of fibrinogen in the exposed plasma, and the methodology was followed as per manufacturer's instructions. A 100 pg/mL fibrinogen stock solution was first prepared by reconstituting the contents of the fibrinogen standard vial into 500 µL sample diluent. This 100 pg/mL fibrinogen stock solution was used to prepare a series of fibrinogen standards by diluting in fixed volumes of sample diluent, as shown in Table 3.6. Wash Buffer was prepared by diluting 5 mL Wash Buffer 10X with 45 mL deionized water. Antibody Cocktail was prepared by combining 600 µL 10X Capture

Antibody and 600 µL 10X Detector Antibody with 4.8 mL Antibody Diluent. Exposed and non-exposed plasma samples were serially diluted in Sample Diluent (1:100,000) prior to testing. 50 µL volumes of standard or sample were added to wells of the precoated 96-well plate, with all plasma samples assayed in triplicate. 50 µL volumes of Antibody Cocktail (capture and detector antibody) was then added to each well. The microplate was sealed and incubated under agitation at 400 rpm for 1-hr at room temperature. After the incubation period, all wells were decanted and manually washed with Wash Buffer. After repeating this wash process three times, the microplate was inverted and gently tapped on a paper towel to remove excess liquid.

Table 3.6. Fibrinogen standard preparation for fibrinogen ELISA.

Standard #	Fibrinogen Stock Solution (µL)	1x Sample Diluent (µL)	Fibrinogen Concentration (pg/mL)
1	Fibrinogen standard vial added to 500-µL of Sample Diluent		100,000
2	32	368	8,000
3	150	150	4,000
4	150	150	2,000
5	150	150	1,000
6	150	150	500
7	150	150	250
8	150	150	125
9	0	150	0

100 µL 3,3′,5,5′-Tetramethylbenzidine (TMB) Development Solution was added to each well. The microplate was re-sealed and incubated under agitation at 400 rpm for 10-min, during which the standards and samples produced a blue coloured product. 100 µL Stop Solution was then added to each well, which converted the standards and samples to a yellow coloured product. The density of yellow colouration was proportional to the concentration of fibrinogen captured in the plate. Absorbance at 450-nm was immediately measured using a Multiskan GO Microplate Spectrophotometer. The concentration of fibrinogen in samples were calculated using the fibrinogen standard curve with values corrected for dilution factor. Results were recorded as the mean fibrinogen concentration (mg/mL) ± SD taken from triplicate samples.

Chapter Four I Broad-Spectrum Antimicrobial Efficacy of 405-nm Light for Plasma Treatment: Small-Scale Testing

4.0 I Introduction

As detailed in Section 2.4.5, violet-blue 405-nm light is being considered as an alternative, potentially safer and less damaging antimicrobial approach to pathogen reduction of blood platelets and plasma, compared to existing PRTs that require the use of UV-light and photosensitizers. Preliminary research has demonstrated the antimicrobial efficacy of 405-nm light for treatment of plasma using selected organisms (Maclean *et al*, 2016), however it is important to expand on this existing microbiological data and assess the broad-spectrum antimicrobial efficacy of 405-nm light for treatment of plasma before its potential use as a PRT can be fully assessed. Importantly, there is currently no knowledge on the compatibility of 405-nm light with the plasma itself, therefore gaining an insight into the impact of 405-nm light exposure on essential plasma proteins will also be crucial for the development of the technology as a PRT.

As a proof-of concept, this Chapter aimed to expand the knowledge of the antimicrobial efficacy and compatibility of 405-nm light for plasma using a small-scale exposure system, using a fixed, high-intensity irradiance (100 $mWcm^{-2}$). To identify an effective antimicrobial dose, the inactivation kinetics of two key problematic organisms – *Staphylococcus aureus* and *Escherichia coli* – were first determined. Proteomic testing (using SDS-PAGE and an AOPP assay) was then conducted to assess the compatibility of antimicrobial doses with plasma proteins, and further, to identify upper dose levels beyond which major protein damage could be observed. Small volumes of plasma seeded with a range of organisms at different densities (10^1–10^3, 10^4–10^6, 10^7–10^8 CFU mL^{-1}) were then exposed to a fixed treatment of 360 Jcm^{-2} (a dose which displayed both antimicrobial effects and compatibility with the plasma itself) to assess the broad spectrum antimicrobial efficacy of the 405-nm light treatment at small-scale.

Overall, this chapter had three key objectives:

1. To determine an effective antimicrobial 405-nm light dose for treatment of small volumes (250 µL) of plasma, using selected bacteria – *S. aureus* and *E. coli* - and a fixed irradiance of 100 $mWcm^{-2}$.
2. To investigate the effects of the same antimicrobial doses on the integrity of the plasma proteins, using SDS-PAGE and an AOPP assay, in order to establish compatible dose levels, and also the upper threshold, above which damage to proteins is observed.
3. To demonstrate the broad spectrum antimicrobial efficacy, of a fixed dose of 405-nm light – selected based on the initial antibacterial and compatibility testing (objectives 1 & 2) – against a range of organisms seeded in small volumes of plasma.

4.1 I 405-nm Light Treatment System

This study used a small-scale single-array exposure system, with a fixed light irradiance, for exposure of:

- plasma seeded with bacteria and yeast, to establish the efficacy of the light treatment for inactivation of microbial contaminants; and,
- plasma alone, to establish the impact of the light treatment on the plasma itself, by analysis of the plasma proteins.

This section provides details of the LED array used, and the small-scale treatment system for exposure of the plasma samples.

The light source used was a single LED array (ENFIS PhotonStar UNO 24, PhotonStar Technologies, UK; Figure 4.1A-C), with a peak wavelength in the region of 405-nm and 14-nm full-width half-maximum (FWHM) (Figure 4.1D). The array was powered by a 40 V Philips Xitanium LED Driver (Philips, Netherlands) and bonded to a heat sink and fan for thermal management (Figure 4.1A).

For treatment of small volume plasma samples held in multi-well plates, the light source was housed in a custom-made stand (Figure 4.2), which held the array in a fixed position, 4 cm directly above the sample surface, providing an irradiance of ~100 $mWcm^{-2}$ (measured using a radiant power meter and photodiode detector (LOT-Oriel Ltd)).

The small volume plasma samples were light exposed either seeded with bacterial contamination (Sections 4.2 and 4.5) in order to establish antimicrobial efficacy, or non-seeded, in order to evaluate the effect of the light treatment on the plasma itself (Section 4.3 and 4.4).

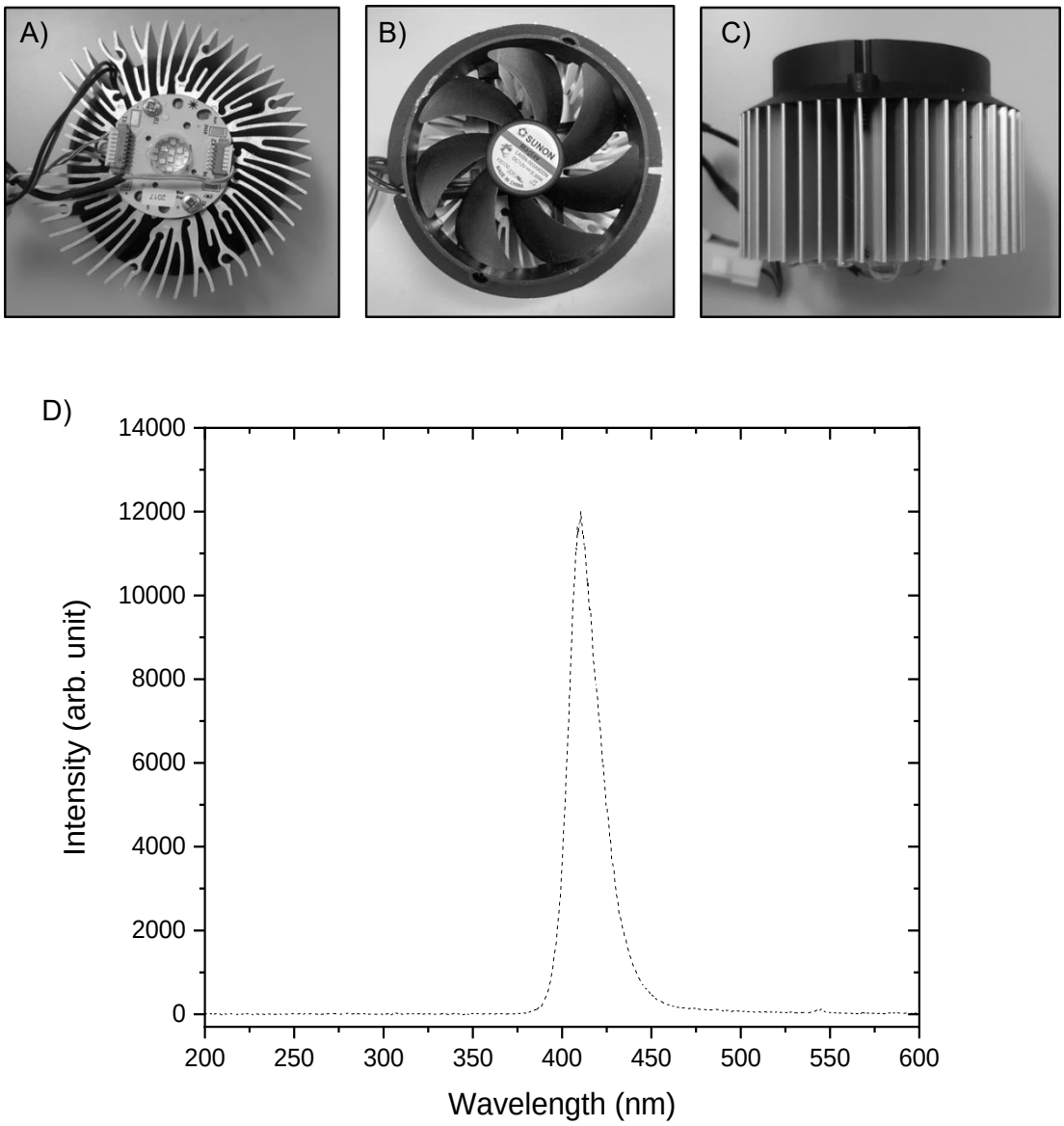

Figure 4.1. 405-nm LED array and optical characterisation. The LED array (A) is attached to a cooling module (fan (B) and heat sink (C)) for thermal management. (D) Optical emission spectrum of the LED array used for the treatment of plasma, captured using a high-resolution spectrometer (HR4000, Ocean Optics Inc, Germany) and SpectraSuite software (Version 2.0.151).

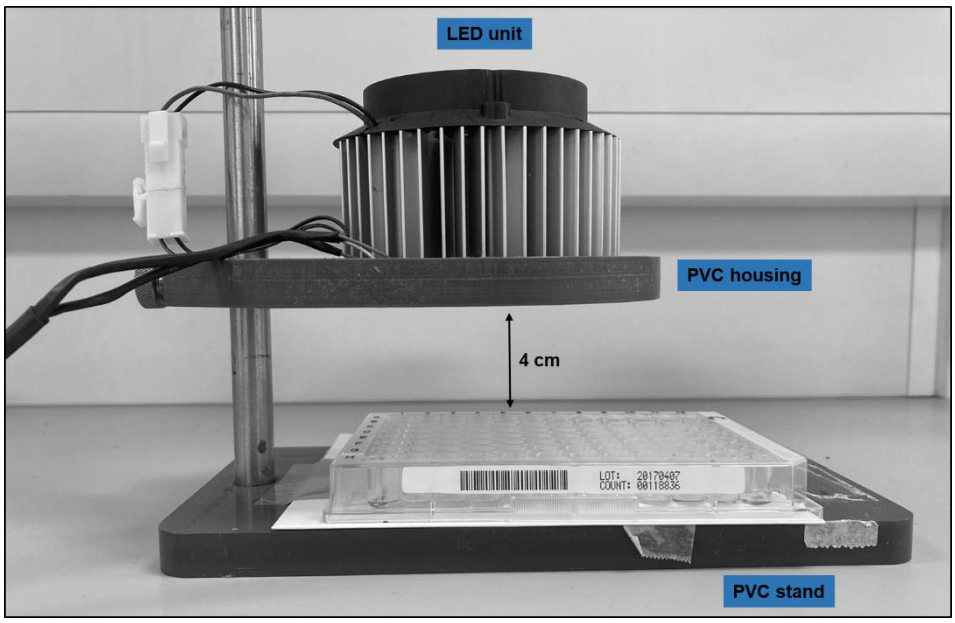

Figure 4.2. Experimental arrangement for the exposure of plasma samples to 100 mWcm^{-2} 405-nm light. The LED array is housed in a custom-made rig. The light source was positioned 4 cm above the sample surface, providing an irradiance of 100 mWcm^{-2}.

4.2 I Determination of an Effective Antimicrobial 405-nm Light Dose

4.2.1 Methods: Inactivation of Selected Bacteria in Plasma Samples

To identify an effective antimicrobial dose, the inactivation kinetics of *S. aureus* and *E. coli* seeded in small volume plasma samples were first established. Bacteria were cultured as detailed in Section 3.2.3, and seeded into plasma samples at a density of ~10^2 CFU mL^{-1}. 250 µL volumes (n=3) of seeded plasma were then transferred into a 96-well plate, covered with ultra-clear adhesive sealing film and positioned below the light array (as shown in Figure 4.2). Seeded plasma was exposed to a fixed irradiance of 100 mWcm^{-2} for increasing treatment times. The applied 405-nm light dose was calculated using *Equation 1:*

$$\text{Dose (Jcm}^{-2}\text{)} = \text{Irradiance (Wcm}^{-2}\text{)} \times \text{Exposure time (seconds)} \quad (1)$$

Equivalent control samples were held in identical conditions but shielded from 405-nm light treatment. Post-exposure, samples were spread plated onto nutrient agar (100µL/plate), incubated at 37°C overnight, and surviving colonies enumerated, with results recorded as mean (n≥3) $\log_{10}$ CFUmL^{-1} ± SD. Antimicrobial data was analysed

[$P \leq 0.05$; 2 sample t test (Minitab v18)] to determine any significant differences in microbial counts between exposed and non-exposed control plasma samples (n≥3).

4.2.2 Results: Inactivation of Selected Bacteria in Plasma Samples

Figure 4.3 illustrates the efficacy of 100 mWcm^{-2} 405-nm light for inactivation of low-level (~10^2 CFU mL^{-1}) *S. aureus* and *E. coli* contamination in plasma samples. A significant 0.8 $\log_{10}$ reduction of *S. aureus* was achieved after exposure to the lowest dose of 72 J cm^{-2} (82% reduction, $P = 0.041$), and a 2.4 $\log_{10}$ reduction was recorded after exposure to 144 Jcm^{-2} (24-min exposure). Reduction of *E. coli* contamination required increased doses (Fig. 4.3B), with a significant 0.3 $\log_{10}$ reduction not observed until exposure to 144 J cm^{-2} [$P = 0.008$]. Inactivation was more gradual, with 0.6 $\log_{10}$ reduction observed by 180 J cm^{-2}, followed by a sharp decrease and 2.4 $\log_{10}$ reduction by 360 J cm^{-2}. Bacterial levels in control samples remained constant over the exposure period.

Inactivation kinetics identified that a 405-nm light dose of 360 J cm^{-2} was an effective antibacterial dose that achieved inactivation of both *S. aureus* and *E. coli* low-level contamination in plasma. This dose was therefore selected as the fixed light treatment for use in subsequent microbial inactivation tests.

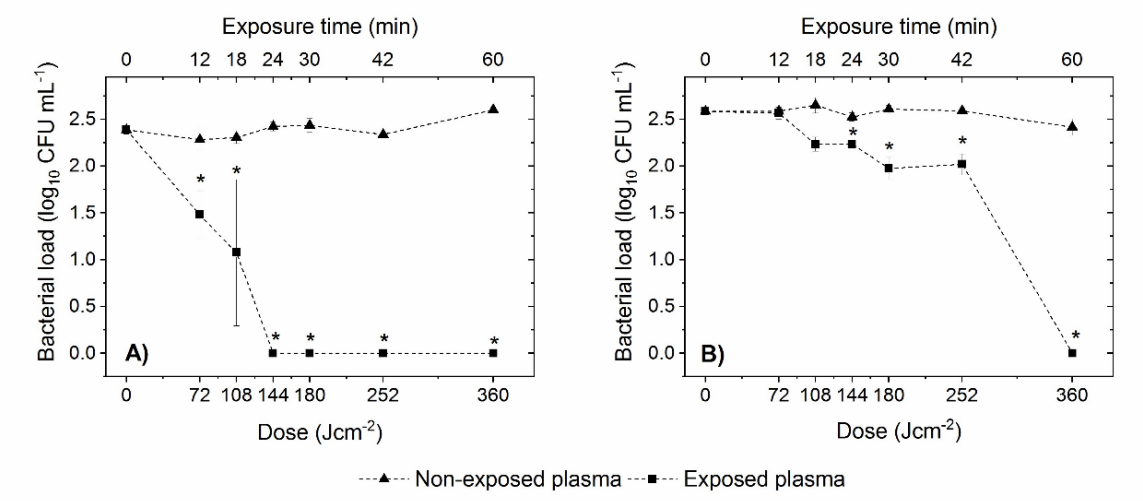

Figure 4.3. Inactivation kinetics for the 405-nm light treatment of plasma samples seeded with low-level bacterial contamination. *S. aureus*, (A) and *E. coli*, (B) were used to seed small volume (250 µL) plasma samples at approx. 10^2 CFUmL^{-1}, and were exposed to 405-nm light at an irradiance of 100 mWcm^{-2}. Data represent mean ($n \geq 3$) ± SD, with asterisks (*) representing a significant decrease in the bacterial load in treated plasma when compared to the equivalent nontreated control [$P \leq 0.05$; 2-sample *t* test (Minitab v18)].

4.3 I Assessment of the Protein Integrity of 405-nm Light Exposed Plasma using SDS-PAGE

4.3.1 Methods: Light Treatment and Analysis of Plasma Proteins Using SDS-PAGE

A key objective of this study was to examine the compatibility of the effective antimicrobial doses with plasma proteins, and also establish the upper threshold energy level at which damage occurs. SDS-PAGE was the first technique used to assess the integrity of the plasma proteins following 405-nm light exposure.

Unseeded plasma samples were exposed under the same conditions as described in Section 4.2.1. 250 µL volumes of unseeded plasma were held in a 96-well plate, covered with ultra-clear adhesive sealing film, and positioned below the light array (Figure 4.2). Plasma samples were exposed to 100 $mWcm^{-2}$ 405-nm light for up to 144-hrs (≤51.84 $kJcm^{-2}$). Non-exposed control samples were held under identical conditions, but shielded from 405-nm light exposure, for the same durations. Post-exposure, exposed and equivalent control samples were prepared for analysis using SDS-PAGE using the methodology details in Section 3.5.1.

4.3.2 Results: Protein Integrity of 405-nm Light Exposed Plasma using SDS-PAGE

4.3.2.1 Results: Establishing a Compatible 405-nm Light Dose for Treatment of Plasma

Initial tests evaluated the compatibility of 405-nm light with plasma using antimicrobial doses from 360 Jcm^{-2} to 1.8$kJcm^{-2}$. This dose range was selected as initial bacterial inactivation tests (Figure 4.3) demonstrated that a dose of 360 Jcm^{-2} was an effective antimicrobial dose for treatment of plasma.

Figure 4.4A is an image of the gel used to assess protein integrity of plasma exposed to 100 $mWcm^{-2}$ 405-nm light for 1 to 5-hr (0.36-1.8 $kJcm^{-2}$). The electrophoretic patterns of plasma exposed to a dose of 360 Jcm^{-2} did not demonstrate visually detectable differences between the exposed and non-exposed plasma samples (Lanes 2 and 3), indicating that the antimicrobial effect can be achieved without visible damage to the plasma proteins.

Early evidence of protein modifications were indicated in the electrophoretic patterns of plasma exposed to an increased dose of 720 Jcm^{-2} (2× the effective antimicrobial

dose), where protein banding appeared to show slight changes in the region of the HMWPs (80-198 kDa). However, as highlighted in Figure 4.4B, the intensity level of the plasma proteins exposed to 720 Jcm^{-2} was similar to that of some of the other non-exposed controls, therefore these changes may be due to sample-to-sample variation (as discussed in Appendix A).

Upon exposure to further increased dose levels, there were clearer indications of protein modification of HMWPs. As shown in Figure 4.4B, the intensity levels of HWMPs in plasma exposed to ≥1.08$kJcm^{-2}$ were considerably higher than their non-exposed paired control. Nevertheless, comparison with the positive control (+ve, Lane 13), showing complete plasma protein degradation, suggests that the degree of modification observed upon exposure to doses ≤1.8$kJcm^{-2}$, should not be regarded as major damage.

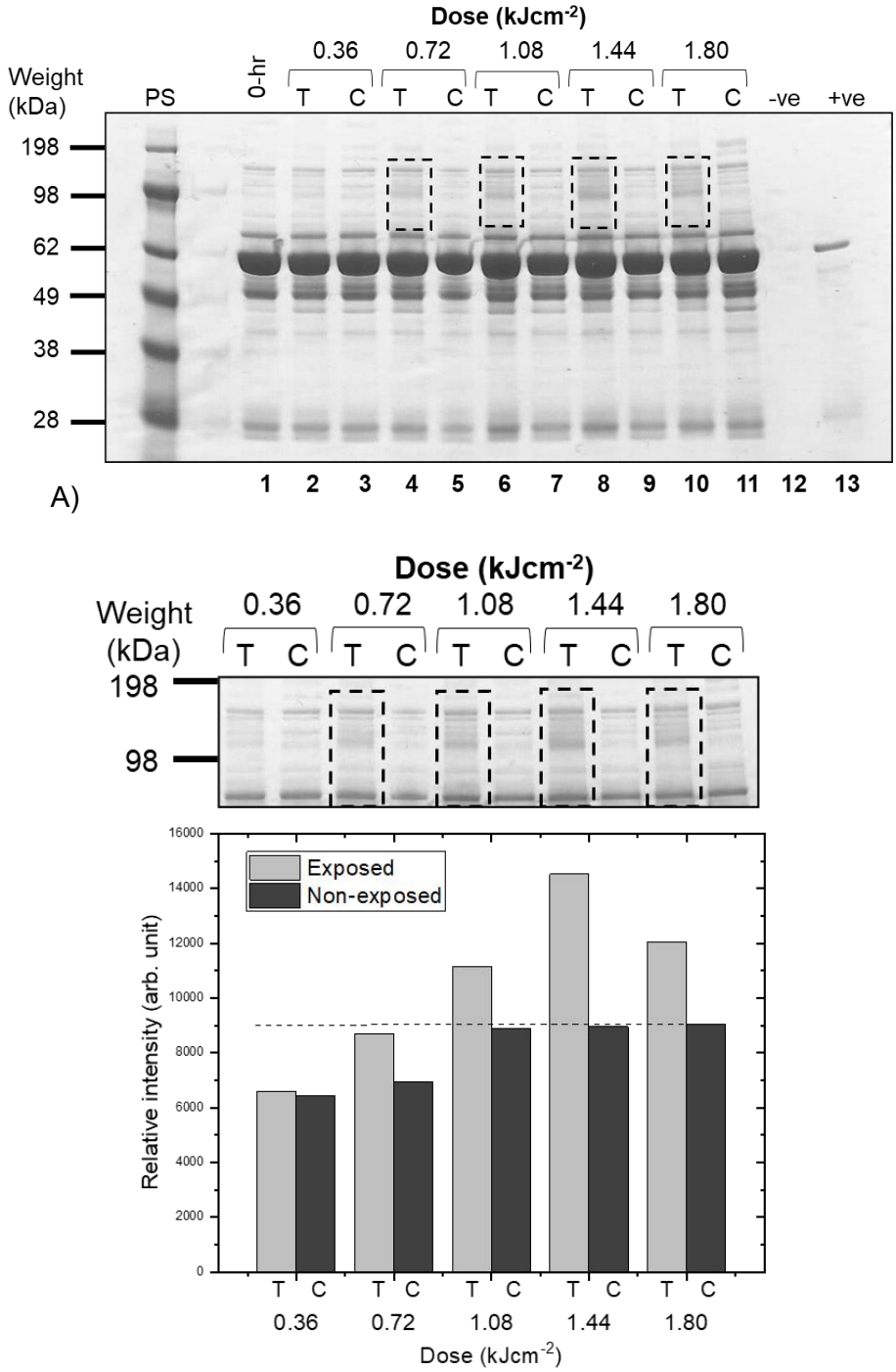

Figure 4.4. Protein integrity of plasma exposed to 405-nm light doses (0.36 – 1.80 kJcm^{-2}), assessed via SDS-PAGE. Images show A) SDS-PAGE analysis of exposed plasma ('T') in even Lanes: *2 (0.36 kJcm^{-2}), 4 (0.72 kJcm^{-2}), 6 (1.08 kJcm^{-2}), 8 (1.44 kJcm^{-2}) and 10 (1.80 kJcm^{-2})* ; and non-exposed control samples ('C'), in odd Lanes *(3, 5, 7, 9 and 11)*. A) protein standard (PS), 0-hr control (*Lane 1*), negative contol (*Lane 12*), and positive control *(Lane 13*) representing complete protein degradation, were included for comparitive purposes. B) Semi-quantiative analysis of protein levels in the HMWP region (Image J software). The dashed line represents the highest intensity level recorded for non-exposed control samples.

4.3.2.2 Results: Determining an Upper Threshold Dose of 405-nm Light for Plasma Compatibility

Doses greater than 1.80 $kJcm^{-2}$ were also investigated to establish the upper threshold dose level which visibly induced major protein damage. This provided an insight to the plasma proteins that show susceptibility to degradation by 405-nm light. Figure 4.5 illustrates the electrophoretic patterns of plasma exposed to 405-nm light doses of up to 25.92 $kJcm^{-2}$ (100 $mWcm^{-2}$ for 1, 5, 24, 48 and 72-hrs, respectively). Results demonstrate that plasma protein damage increased respectively with increased exposure to 405-nm light. The electrophoretic pattern of plasma exposed to a dose of 1.80 $kJcm^{-2}$ (Lane 4) supports the results in Figure 4.4 as it also provides early evidence of modification of HMWPs (80-198 kDa). Changes in HMWPs became more visually detectable after exposure to a dose of 8.64 $kJcm^{-2}$, with major protein modifications visible in plasma exposed to 17.28 and 25.92 $kJcm^{-2}$ (Lanes 6 and 7) thought to be due to cross linking of proteins. As indicated in Figure 4.5B, the level of HMWPs in plasma exposed to ≥17.28 $kJcm^{-2}$ was 5× higher than that detected in plasma exposed to 360 Jcm^{-2}, indicating that protein integrity has been affected.

The loss of protein banding at approx 45 kDa, associated with haptoglobin chains and glycoproteins (see Figure 3.7) was visually detectable in the electrophoretic pattern of plasma exposed to a dose of 25.92 $kJcm^{-2}$ (Figure 4.5A, Lane 7). Despite major protein modifications detected in plasma exposed to 25.92 $kJcm^{-2}$, comparison with the positive control (Figure 4.5A, Lane 8) indicates that excessily high doses do not result in complete plasma protein degradation.

Dose levels were increased further to identify other plasma proteins that show susceptibility to photodegradation following exposure to high doses of 405-nm light. Figure 4.6A is an image of the gel used to assess protein integrity of plasma exposed to doses of up to 51.84 $kJcm^{-2}$. In agreement with previous results, the majority of protein damage occurred in the HMWP region after exposure to 17.28 $kJcm^{-2}$. In this gel analysis, the loss of protein banding, indicative of protein degradation, at approx. 45, 49 and 62 kDa was also observed following exposure to a dose of 17.28 $kJcm^{-2}$, with complete loss of distinct banding after exposure to a dose of 51.84 $kJcm^{-2}$.

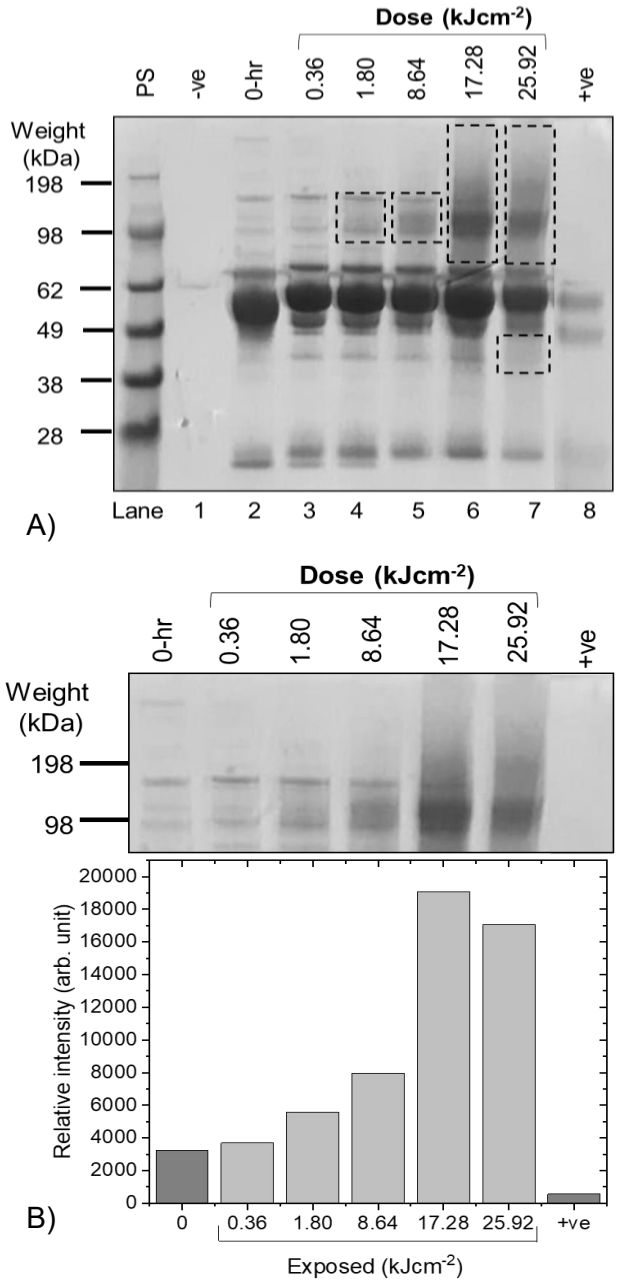

Figure 4.5. Plasma protein damage observed upon exposure to high doses of 405-nm light (≤25.92 kJcm^{-2}), assessed via SDS-PAGE. Image show A) SDS-PAGE analysis of exposed plasma in Lanes: *3 (0.36 kJcm^{-2}, 1-hr), 4 (1.80 kJcm^{-2}, 5-hrs), 5 (8.64 kJcm^{-2}, 24-hrs), 6 (17.28 kJcm^{-2}, 48-hrs) and 7 (25.92 kJcm^{-2}, 72-hrs)*. The protein standard (PS) was included to identify the approximate molecular weight of proteins. Lanes 1, 2 and 8 represent negative (-ve), 0-hr and positive control (+ve), respectively. Image B) represents the semi-quantiative analysis of protein levels in the HMWP region, performed using ImageJ software.

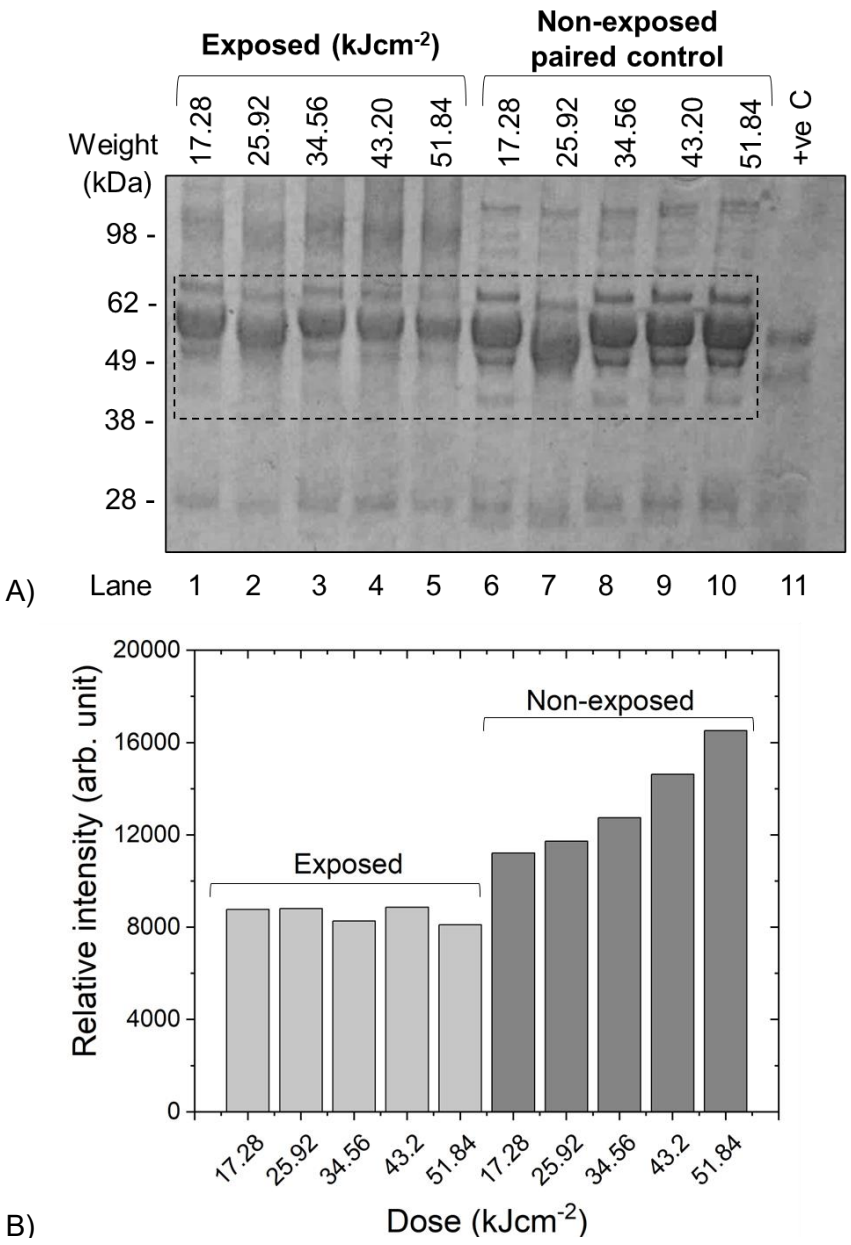

Figure 4.6. Plasma protein damage observed upon exposure to high doses of 405-nm light (≤51.84 kJcm^{-2}), assessed via SDS-PAGE. Image A) shows SDS-PAGE analysis of exposed plasma in Lanes: *1 (17.28 kJcm^{-2}, 48-hrs), 2 (25.92 kJcm^{-2}, 72-hrs), 3 (34.56 kJcm^{-2}, 96-hrs), 4 (43.20 kJcm^{-2}, 120-hrs) and 5 (51.84 kJcm^{-2}, 144-hrs).* Lanes *6-10* represent the equivalent, non-exposed plasma samples. A positive control (*+ve*) (*Lane 11)* representing complete protein degradation was included for comparitive purposes. Image B) represents the semi-quantiative analysis for the segment highlighted in Image A (~45-70 kDa) (ImageJ software).

4.3.2.3 Assessment of 405-nm Light Induced Thermal Effects on Plasma

A supplementary study was conducted to examine the protein integrity of heat-treated plasma, to assess whether the high intensity 405-nm light treatment used in these tests caused any heat-induced protein damage.

To do this, 250 µL volumes of plasma were exposed to 100 $mWcm^{-2}$ light for up to 72-hrs, as detailed in Section 4.3.1, and the sample temperature was measured using a thermocouple (KM340, Comark Instruments, UK) after 1, 5, 24, 48 and 72-hrs (0.36, 1.80, 8.64, 17.80 and 25.92 $kJcm^{-2}$ respectively). As shown in Table 4.1, the temperature of plasma increased from 22℃ (0-hr) to 40°C after 1-hr of light exposure. The temperature of plasma then remained at 40°C for 24-hrs, after which there was an increase to 43°C for the remainder of the exposure period.

Table 4.1. Thermal assessment of plasma during exposure to 100 $mWcm^{-2}$ 405-nm light. The temperature of plasma was measured at set time points using a thermocouple (KM340, Comark Instruments, UK).

Time point (hr)	Equivalent dose ($kJcm^{-2}$)	Temperature recorded (°C)
0	0	22
1	0.36	40
5	1.80	40
24	8.64	40
48	17.80	43
72	25.92	43

To investigate the impact of these temperatures on the plasma, plasma samples were heat treated at the temperatures recorded during light exposure. An Eppendorf containing 250 µL of plasma was placed in a water bath (Grant Water-bath, Scientific Laboratory Supplies, UK), set to match the temperatures recorded during light exposure (40°C from 0-24-hrs, 43°C from 24-72-hrs). At each time point, 1 µL of plasma was removed and diluted in 99 µL of TBS before proceeding to sample preparation for SDS-PAGE analysis (Section 3.5.1). A ‘worst case scenario’ control was also prepared by heat treating plasma at 43°C (the maximum temperature recorded during the light treatment) for the full 72-hr period. Protein integrity of heat-treated plasma was then analysed using SDS-PAGE. Plasma samples exposed to 405-nm light (0.36, 1.80, 8.64, 17.80 and 25.92 $kJcm^{-2}$) were included in the SDS-

PAGE gel to enable a direct comparison (Figure 4.7). No visually differences were detected between the electrophoretic patterns of heat-treated plasma and the non-exposed 0-hr control sample (Lane 1). This confirms that the protein modifications observed in plasma exposed to high doses of 405-nm light (Lanes 4-6) was as a direct result of light exposure and not due to residual heating effects.

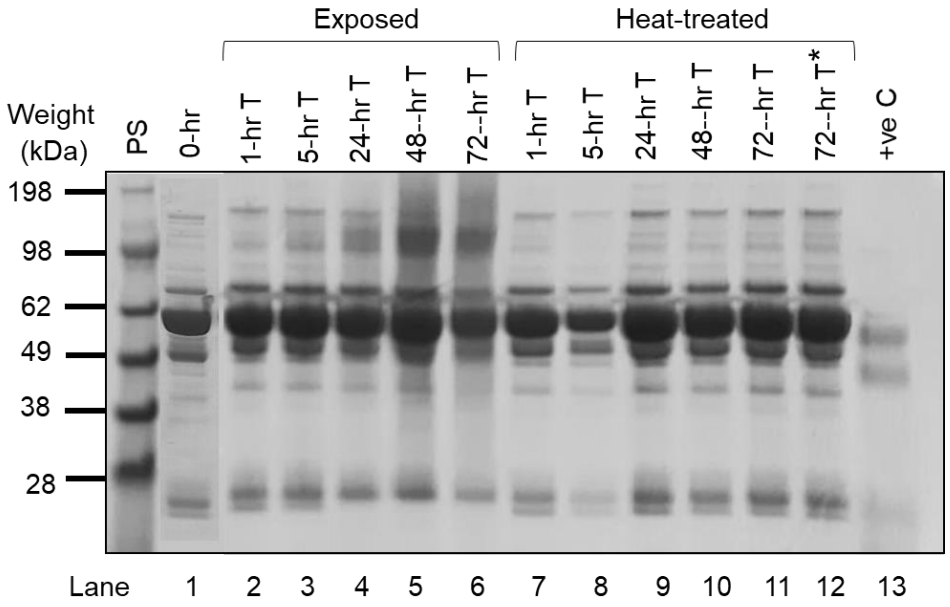

Figure 4.7. Thermal assessment of plasma exposed to 100mWcm^{-2} 405-nm light. Image shows the SDS-PAGE analysis of plasma exposed to 100 mWcm^{-2} 405-nm light in Lanes: *2 (0.36 kJcm^{-2}, 1-hr), 3 (1.80 kJcm^{-2}, 5-hrs), 4 (8.64 kJcm^{-2}, 24-hrs), 5 (17.80 kJcm^{-2}, 48-hrs)* and *6 (25.92 kJcm^{-2}, 72-hrs).* Non-exposed, heat-treated plasma are shown in Lanes: *7 (1-hr), 8 (5-hrs), 9 (24-hrs), 10 (48-hrs)* and *11 (72-hrs).* Lane 12(*) represents the 'worst-case scenario' heat-treated plasma sample (43°C for 72-hrs), representative of the maximum temperature of the plasma samples over extended treatment periods. A 0-hr (Lane 1) and positive control (+ve C, Lane 13) were included for comparitive purposes.

4.4 I Assessment of Plasma Protein Compatibility using an AOPP Assay

This section investigates the oxidative stress levels in 405-nm light exposed and non-exposed plasma using an advanced oxidation protein products (AOPP) assay.

4.4.1 Methods: Measurement of AOPPs in Light Exposed Plasma Samples

An AOPP assay, which uses Chloramine-T as a marker of oxidative damage, was used to quantitatively assess potential protein damage in 405-nm light exposed plasma. The AOPP Assay Kit (ab242295; Abcam) was used in accordance with manufacturer's instructions, as per Section 3.5.2. In brief, plasma was exposed to

100 mWcm^{-2} 405-nm light (0.36, 0.72, 1.08, 1.80, 8.64, 17.28 and 25.92 kJ cm^{-2}) as described in Section 4.3.1. Exposed and non-exposed control plasma samples were diluted in PBS (1:10). 250 µL volumes of the diluted plasma (n=3), and standards of Chloramine-T (0-100 µM), were transferred to a 96-well plate and 10 µL of Chloramine Reaction Initiator was added to all wells. The plate was shaken for 5-min (120 rpm, room temperature) and 20 µL of Stop Solution was then added. Absorbance of samples at 340 nm was then measured, and the AOPP levels expressed as µM of Chloramine-T equivalents, with values corrected for dilution factor. AOPP data was presented as mean (n=3) ± SD. The level of AOPP was used as a marker for the oxidative stress levels in the plasma.

4.4.2 Results: Measurement of AOPPs in Light Exposed Plasma Samples

Figure 4.8 shows the results from the AOPP assay used to quantitatively assess potential oxidative damage in plasma exposed to 100 mWcm^{-2} 405-nm light for doses up to 25.92 kJcm^{-2} (72-hrs). Whilst slight fluctuations were observed, there were no significant differences in the AOPP levels, indicative of oxidative damage, of exposed and non-exposed plasma samples following doses up to 1.44 kJcm^{-2} [$P > 0.05$]. Exposure to a dose of 1.8 kJcm^{-2}, resulted a significant increase in oxidative stress levels, where AOPP levels increased from 18 µM in non-exposed plasma to 21 µM in exposed plasma [$P = 0.011$]. From this point, AOPP levels increased linearly following exposure to 405-nm light (≥8.64 kJ cm^{-2}), with a maximum AOPP level of 53 µM measured after exposure to a dose of 25.95 kJ cm^{-2}; 2× higher than AOPP levels in non-exposed controls [$P < 0.001$]. AOPP levels in non-exposed control samples showed no significant change over the treatment period [$P = 0.134$].

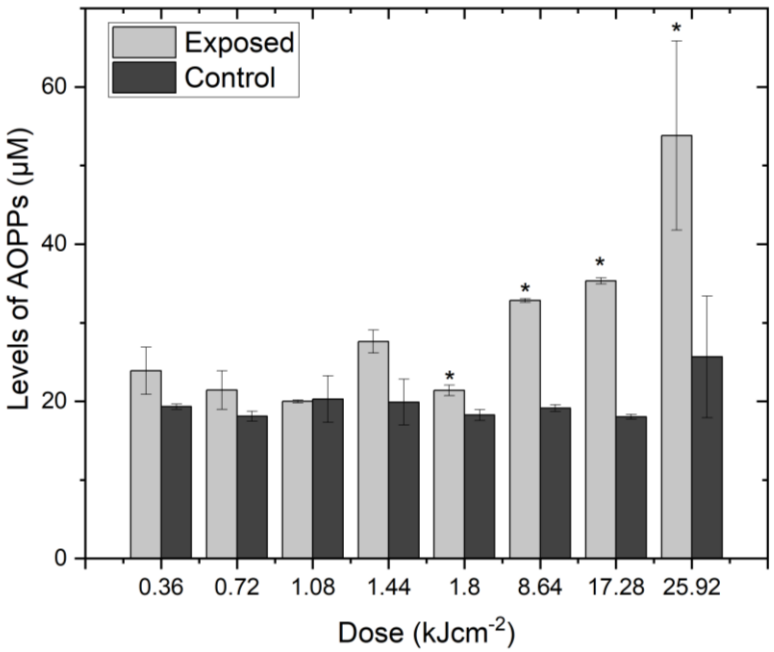

Figure 4.8. Level of AOPPs detected in plasma following exposure to 100 mWcm^{-2} 405-nm light (0.36–25.92 kJcm^{-2}). The concentration of AOPPs is expressed as µM of Chloramine-T equivalents, with values corrected for dilution factor. Data represent mean (n=3)±SD, with asterisks (*) representing a significant increase in AOPP level detected in exposed plasma when compared to the equivalent non-exposed control [$P \leq 0.05$; 2-sample *t* test (Minitab v18)].

4.5 I Broad-Spectrum Antimicrobial Efficacy of a Fixed 405-nm Light Treatment

Results have now determined that a 405-nm light dose of 360 Jcm^{-2} achieved antibacterial efficacy (Figure 4.3) whilst not inducing damage to plasma proteins (Figures 4.4 and 4.5) in small volume samples. This section investigates the antimicrobial efficacy of this fixed dose against a range of organisms at various seeding densities in plasma.

4.5.1 Methods: Broad-Spectrum Antimicrobial Efficacy of 360 Jcm^{-2} 405-nm Light Treatment

Testing was conducted using a panel of bacteria and yeast commonly implicated in TTIs: *S. aureus, S. epidermidis, B. cereus, E. coli, P. aeruginosa, A. baumannii, K. pneumoniae, Y. enterocolitica, C. albicans* and *C. auris*. Organisms were cultured as detailed in Section 3.2.3, and seeded into plasma at 'low' (10^1-10^3 CFUmL^{-1}), 'medium' (10^3-10^6 CFUmL^{-1}) and 'high' (10^6-10^8 CFUmL^{-1}) density levels, in order to

represent a range of contamination levels, from a realistic clinical scenario to a high microbial challenge. 250 µL volumes of seeded plasma (n=3) were transferred into a 96-well plate, covered with ultra-clear adhesive sealing film and exposed to 100 mWcm^{-2} for 1-hr (360 Jcm^{-2}), as described in Section 4.2.1. Control samples were shielded from the light treatment. Post-exposure, samples were spread plated onto the appropriate agar (detailed in Section 3.2.5), incubated at 37°C overnight, and enumerated.

4.5.2 Results: Broad-Spectrum Antimicrobial Efficacy of 360 Jcm^{-2} 405-nm Light Treatment

The antimicrobial efficacy of 405-nm light, at a fixed dose of 360 Jcm^{-2}, against a range of organisms, at low, medium and high contamination levels in plasma, are shown in Figures 4.9 (bacterial contaminants) and 4.10 (yeast contaminants).

Broad-spectrum antibacterial efficacy was observed, with significant bacterial inactivation achieved for all species [$P \leq 0.05$]. 99.0 – 100 % inactivation was achieved across all seeding densities for all organisms except *E. coli*, which achieved 95.1–100.0% inactivation.

Exposure of low-density (10^1-10^3 CFUmL^{-1}) seeded plasma to a dose of 360 Jcm^{-2} reduced the bacterial load by up to 2.6-log$_{10}$ resulting in complete inactivation for *S. aureus*, *S. epidermidis*, *B. cereus*, *E. coli* and *P. aeruginosa* (Figure 4.9, A-E). Although not completely eliminated, *A. baumannii*, *Y. enterocolitica* and *K. pneumoniae* were successfully reduced by 2.55-, 2.35-and 2.41-log$_{10}$ respectively after exposure which resulted in a bacterial load of ≤5 CFUmL^{-1} in exposed plasma samples (≥99.01% reduction). Results for medium-density (10^3-10^6 CFUmL^{-1}) seeded plasma demonstrate that a dose of 360 Jcm^{-2} can significantly reduce all bacterial species, with over 4.5-log$_{10}$ reductions achieved for *Y. enterocolitica* (Figure 4.9G) and *K. pneumoniae* (Figure 4.9H) and over for 5.0-log$_{10}$ reductions for *S. epidermidis* (Figure 4.9B), *P. aeruginosa* (Figure 4.9E) and *A. baumannii* (Figure 4.9F) [$P \leq 0.05$]. Similar results were observed for inactivation of high-density (10^6-10^8 CFUmL^{-1}) seeded plasma with all organisms being significantly reduced in plasma following exposure to a dose of 360 Jcm^{-2} [$P \leq 0.05$]. The level of bacterial inactivation achieved by a dose of 360 Jcm^{-2} varied most between organisms seeded at high population densities. Exposure to a dose of 360 Jcm^{-2} achieved a 7.8-log$_{10}$ reduction for *K. pneumoniae* and *A. baumannii*, whilst a 1.32-log$_{10}$ reduction was

achieved for *E. coli*. It should be noted however that this *E. coli* reduction represents a highly significant 95.05% inactivation [$P = 0.005$].

Data for *P. aeruginosa* and *K. pneumoniae* (Figure 4.9, E and H) show that near complete inactivation (≤5 $CFUmL^{-1}$) was achieved following exposure to the fixed dose when seeded in plasma at all contamination levels. The bacterial load in non-exposed plasma samples remained relatively unchanged throughout the treatment period.

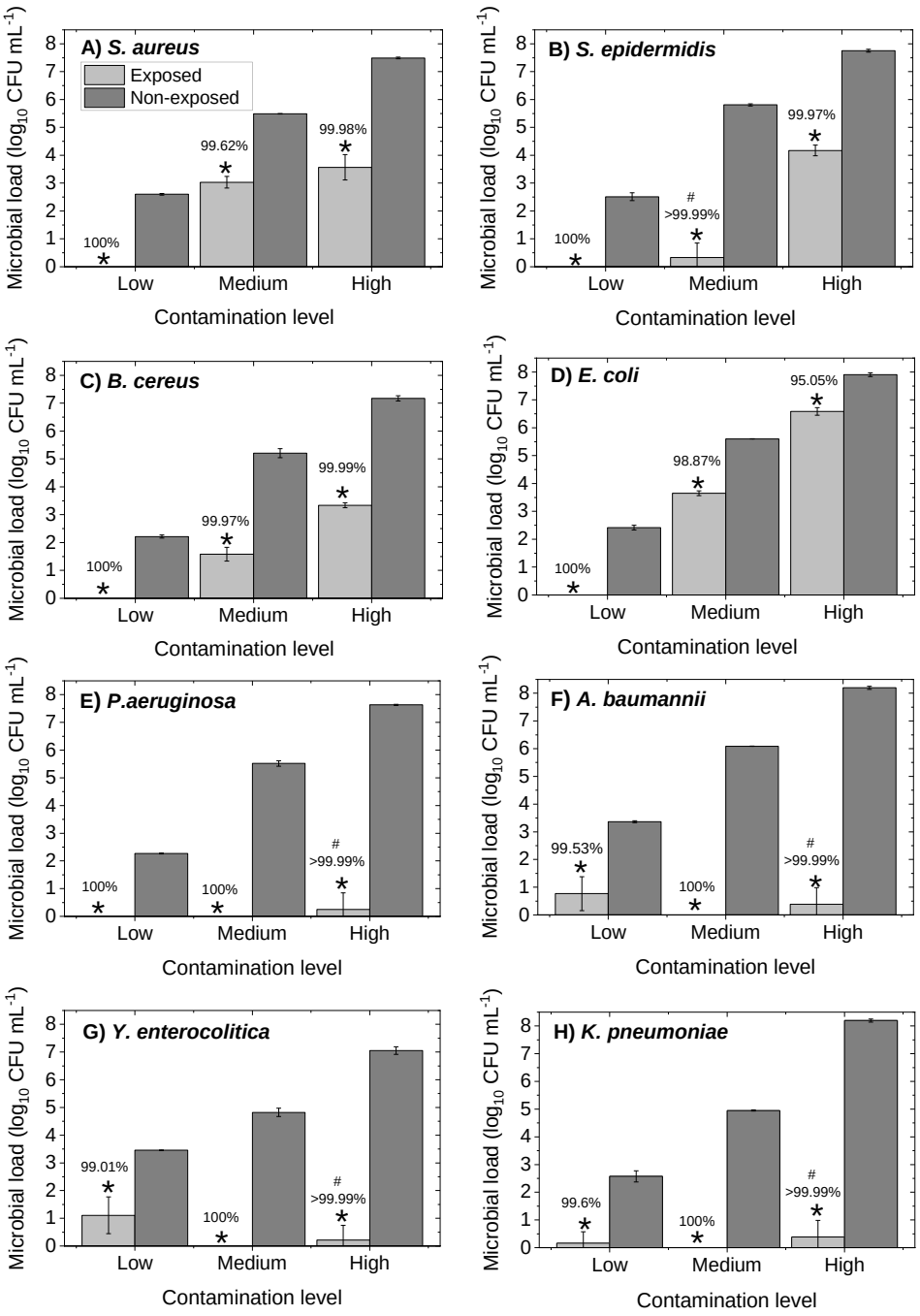

Figure 4.9. Broad-spectrum inactivation of bacteria in plasma samples using a 405-nm light dose of 360 Jcm^{-2}. Plasma seeded with A) *S. aureus*; B) *S. epidermidis*; C) *B. cereus*; D) *E. coli*; E) *P. aeruginosa*; F) *A. baumannii*; G) *Y. enterocolitica*; H) *K. pneumoniae* at low, medium and high-densities exposed to 360 Jcm^{-2} 405-nm light. # Data points representing >99.99% bacterial reductions indicate that near complete inactivation (≤ 10 CFUmL^{-1}) was achieved. Data represents mean log counts±SD (n≥3), with (*) representing significant differences between exposed and non-exposed controls [$P \leq 0.05$; 2-sample t-test (Minitab v18)].

Figure 4.10 shows the inactivation of yeast, *C. albicans* and *C. auris*, at a range of seeding densities following exposure to 360 Jcm^{-2} light. Both species were completely inactivated when seeded in plasma at low seeding densities, using a dose of 360 Jcm^{-2}. Microbial loads in exposed plasma seeded at mid-level were reduced by 3.2-log and 2.4-log for *C. albicans* and *C. auris*, respectively. Results for plasma seeded with yeast at high contamination levels demonstrate that a dose of 360 Jcm^{-2} can significantly reduce microbial load, with up to 2.4-log reductions achieved [$P = 0.006$].

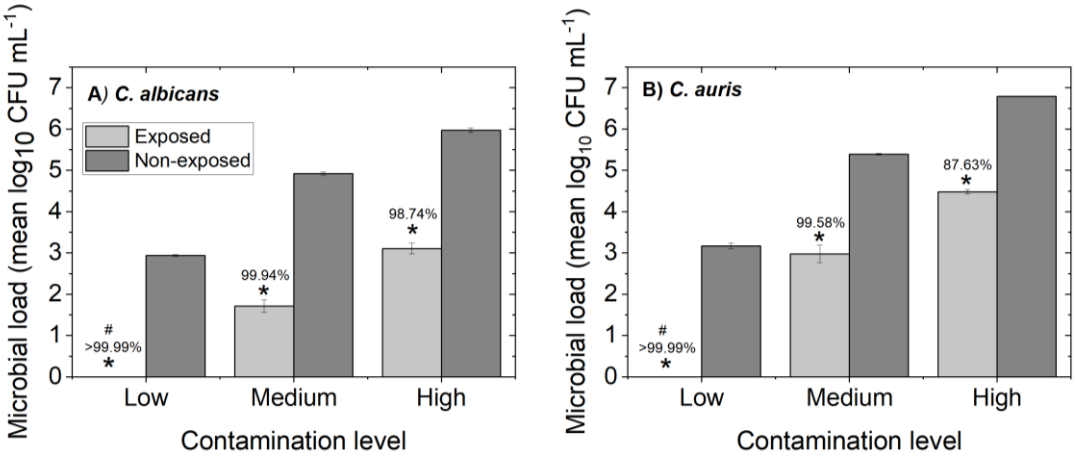

Figure 4.10. Inactivation of yeast in plasma samples using a fixed 405-nm light dose of 360 Jcm^{-2}. Plasma seeded with A) *C. albicans* and B) *C. auris* at low, medium and high-densities was exposed to a 405-nm light dose of 360 Jcm^{-2}. # Data points representing >99.99% microbial reductions indicate that near complete inactivation (≤10 $CFUmL^{-1}$) was achieved. Data represents mean log microbial counts±SD (n≥3), with asterisks (*) representing significant decrease in the microbial load in treated plasma when compared to the equivalent non-treated control [$P \leq 0.05$; 2-sample t-test (Minitab v18)].

Overall, a fixed 405-nm light treatment dose of 360 Jcm^{-2} (100 $mWcm^{-2}$ for 1-hr) demonstrated broad-spectrum microbial inactivation in plasma with significant reductions [$P \leq 0.05$] achieved for all species at low-, medium- and high-density populations.

4.6 I Discussion

The work of this chapter has investigated the broad-spectrum antimicrobial efficacy of 405-nm light for treatment of low volume plasma, at a dose level that shows compatibility with plasma proteins. Initial tests were carried out to identify an antimicrobial dose that was both effective against selected microbes and displayed compatibility with the plasma itself. These tests identified that a fixed 405-nm light

dose of 360 Jcm^{-2} (1-hr at 100 $mWcm^{-2}$) was an effective treatment, which both completely inactivated *S. aureus* and *E. coli* seeded at low-level contamination levels, and displayed compatibility with plasma proteins. As a result, this dose was used to assess the broad-spectrum antimicrobial efficacy of 405-nm light against a panel of organisms commonly associated with TTIs, at a range of contamination levels.

Initial microbial inactivation tests, indicated that *S. aureus* has greater susceptibility to 405-nm light inactivation compared to *E. coli*, with approximately 2.5 times less dose required to achieve significant inactivation of *S. aureus* (72 Jcm^{-2} *versus* 180 Jcm^{-2}). This is consistent with other studies showing that Gram-positive bacteria *(*mainly staphylococci*)* typically have greater susceptibility to 405-nm light inactivation than Gram-negative bacteria in both non-biological and biological media including plasma [Nitzan *et al*, 2004, Maclean *et al*, 2009, 2016; McKenzie *et al*, 2016]. This trend is thought to be due to the differences in cell structures and the endogenous porphyrins expressed by the bacterial cell [Maclean *et al*, 2016].

Proteomic tests were then conducted to assess the compatibility of the effective antimicrobial dose with plasma proteins and further, to determine upper threshold doses where protein damage was visually evident. SDS-PAGE analysis indicated that exposure to an effective antimicrobial dose of 360 Jcm^{-2} did not induce any major plasma protein damage. In fact, the earliest evidence of visible protein modification was detected in the electrophoretic patterns of the high molecular weight proteins (80-198 kDa) after exposure to a dose of 720 Jcm^{-2}; 2× the effective antimicrobial dose.

After exposure to this dose, the level of protein degradation increased relatively with increased exposure to 405-nm light. As shown in Figure 4.5A and 4.6A, major protein modifications were visible after exposure to a dose of 17.28 $kJcm^{-2}$, where protein bands of all molecular weights were affected. In particular, band patterns of plasma exposed to ≥17.28 $kJcm^{-2}$ indicates the loss of protein in the region of 45 kDa suggesting that highly abundant proteins, alpha-1-acid glycoprotein and haptoglobin β chains are susceptible to degradation by 405-nm light [Schenk *et al*, 2008; Gautam *et al*, 2013]. Major visibly detectable differences were evident in the HMWP region. This indicates that HMWPs including complement proteins, macroglobulin chains, ceruloplasmin and transferrin may be susceptible to degradation by 405-nm light [Schenk *et al*, 2008; Gautam *et al*, 2013]. The detection of low abundance but clinically important proteins, such as clotting factors, are limited using SDS-PAGE, as highly abundant proteins dominate the electrophoretic band patterns. Nevertheless, SDS-

PAGE analysis was useful to get an insight to general plasma protein stability following exposure to 405-nm light.

To support this work, an AOPP assay was used to quantitatively measure any potential oxidative damage in exposed plasma (Figure 4.8). Results from the AOPP assay support findings from the SDS-PAGE analysis, indicating that no significant oxidative protein damage occurs in plasma following exposure to a dose of 360 Jcm^{-2}. In fact, AOPP testing indicates that no significant plasma protein oxidation was detected following exposure to doses of up to 1.44 $kJcm^{-2}$; 4×greater than the effective antimicrobial dose. Recent research suggests that the key protein responsible for this oxidation reaction detected via AOPP assay is oxidized fibrinogen, an essential plasma protein involved in coagulation; however, the assay is a useful indicator representative for oxidative damage of all plasma proteins [Selmeci *et al,* 2006].

A supplementary study was conducted to investigate whether the 405-nm light treatment used in this study induced any thermal effects on plasma. Since the electrophoretic pattern of heat treated plasma samples showed no detectable differences with non-exposed plasma, it was confirmed that the protein modifications observed in this study were a direct result of exposure to excessively high doses of 405-nm light.

The exact mechanism of protein damage by 405-nm light is unclear. However, it is thought that 405-nm light may be interacting with light absorbing proteins that naturally reside within organically rich media such as plasma. Plasma naturally contains a range of porphyrin- and flavin-protein complexes (strong absorption band in the region of 400-nm) such as riboflavin (Vitamin B2), bilirubin, carotenoids, hemoglobulin and transferrin and ceruloplasmin that are known to be predisposed to photosensitisation [Lund and Baron, 2010; Pandey and Rizvi, 2010]. In this regard, it's likely that photosensitive components within plasma could act as exogenous photosensitizers and contribute to ROS production. Previous work by Tomb *et al* (2017a) investigating the antiviral efficacy of 405-nm light, reported a similar hypothesis, as it attributed the enhanced susceptibility of Feline Calicivirus (FCV) when suspended in plasma compared to minimal media, to the presence of natural photosensitive proteins.

On review of literature, it appears that interactions between ROS and proteins can result in mild to major oxidative damage, the severity being largely dependent on the type and level of ROS present [O'Flaherty and Matsushita-Fournier, 2017]. ROS-

induced oxidative damage can lead to changes to protein hydrophobicity, conformation and polymerization which can directly affect the overall functionality of proteins [Skibsted *et al*, 2010]. Mild oxidative stress typically leads to thiol oxidation (protein-to-protein cross linking) and S-glutathionylation. These modifications are easily reverted through interaction with antioxidants, such as Vitamin C and E, that have scavenging properties. Strong oxidative stress, associated with high ROS levels, is typically characterised by protein sulfonation which is more difficult to revert as it can cause permanent protein damage which halts protein function [O'Flaherty and Matsushita-Fournier, 2017].

Whilst this Chapter focuses on the photodegradation of plasma proteins, it should be noted that lipids, due to their abundance and rapid rates of reaction with free radicals, may also be susceptible to photodegradation. Products of lipid peroxidation, such as 4-hydroxynonenal (4-HNE), can cause the irreversible formation of protein adducts [Zhong and Yin, 2015]. Figure 4.11 overviews major redox reactions that can result in protein and lipid modification.

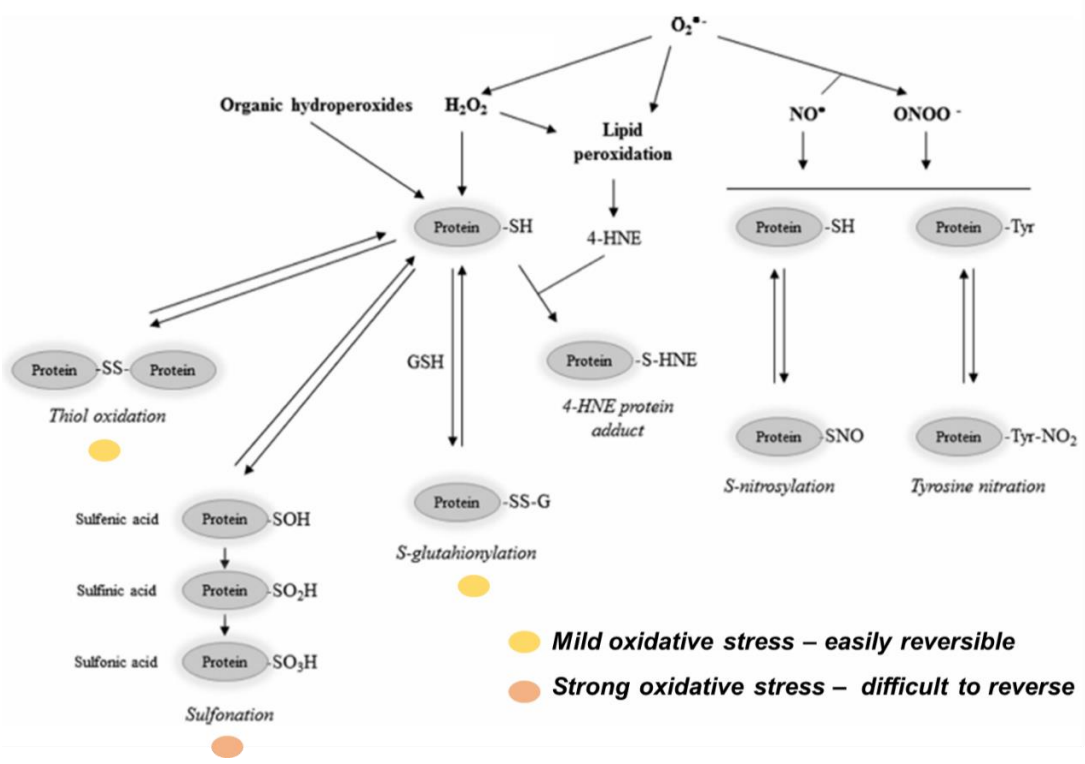

Figure 4.11. Major redox protein and lipid modifications. ROS promote different protein and lipid modifications depending on their abundance and concentration. Adapted from O'Flaherty and Matsushita-Fournier (2017).

Results from this study suggest that photodegradation of proteins by 405-nm light is dominated by protein-to-protein cross linking induced through thiol oxidation. As highlighted in Figure 4.12, the density of proteins in the HMWP region, indicative of increased protein levels, increased respectively with increased exposure to 405-nm light. It can therefore be suggested that the increase in protein levels observed in the HMWP region of the electrophoretic band pattern of exposed plasma may be a result of protein-to-protein cross linking. As mentioned above, this type of ROS-induced protein change is considered a product of mild oxidative stress which can be reversed. With this in mind, future tests should investigate whether the 405-nm light induced protein modifications are reversible, by analysing protein integrity of exposed plasma after a period in storage.

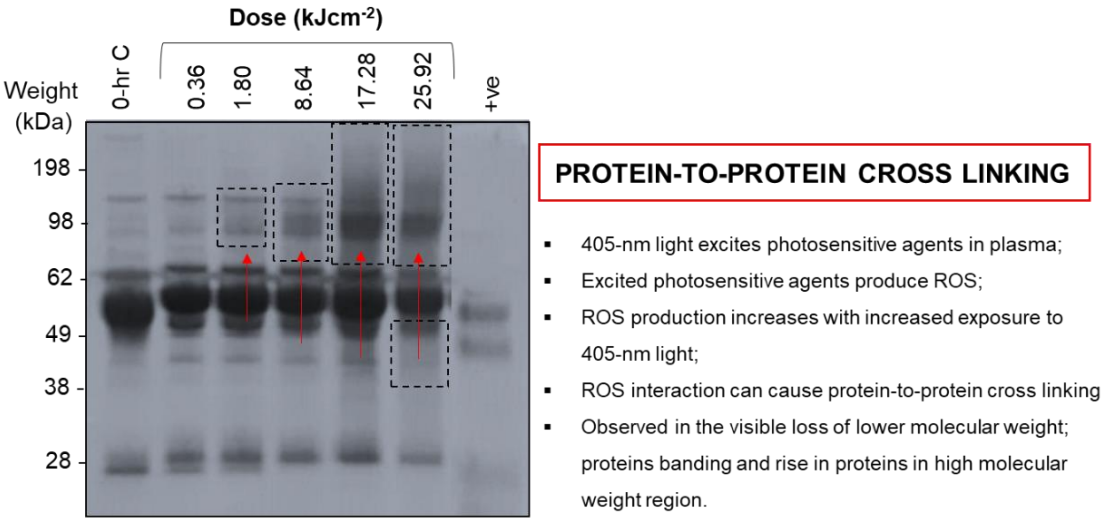

Figure 4.12. Hypothesised degradation mechanism of plasma proteins following exposure to excessively high doses of 405-nm light.

The inactivation data presented in this study has provided the first evidence of the broad-spectrum antimicrobial efficacy of 405-nm light for treatment of plasma. Significant inactivation of a range of microbial species, commonly implicated in transfusion-transmitted infections, was achieved in plasma samples at low, medium and high contamination levels. This study found that microbes, regardless of Gram status, show differences in susceptibility to 405-nm light. This is thought to be due to the fact that each organism has a unique photosensitivity, due to the range of porphyrin types and levels expressed. For instance, the levels of coproporphyrin –the primary porphyrin thought to be responsible for ROS production in bacterial cells- and uroporphyrin vary significantly between Gram-positive organisms [Nitzan *et al*, 2004;

Marschner and Goodrich, 2011]. The porphyrins expressed by the microbial cell, are known to influence susceptibility to 405-nm light as they produce different ROS which are known to vary in toxicity [Ramakrishnan *et al*, 2016].

This helps to explain why *P. aeruginosa* – a Gram-negative rod – demonstrated higher susceptibility to inactivation by 405-nm light compared to other Gram-negative organisms such as *E. coli*. *P. aeruginosa,* unlike other Gram-negative organisms, as it mainly produces coproporphyrin - the same predominant porphyrin produced by the highly susceptible Gram-positive, staphylococcal species [Amin *et al*, 2016]. The high sensitivity of *P. aeruginosa* to 405-nm light inactivation has also been observed in PCs, with approximately 1.5 times less dose required for complete inactivation, compared to *S. epidermidis* and *B. cereus* (50 *versus* 75 Jcm^{-2}) [Lu *et al*, 2020].

Further, it is likely that microorganisms will have differing sensitivities to externally-generated ROS (generated from photosensitive porphyrin- and flavin-protein complexes naturally residing in plasma, as discussed above). This is particularly relevant to Gram-negative bacteria, as there is a possibility that the outer membrane may be more susceptible to externally-generated, ROS induced damage compared to the peptidoglycan layer of Gram-positive bacteria.

Results demonstrated successful reductions of all species, not only at low contamination levels ($<10^3$ CFU mL^{-1}), but at contamination levels as high as 10^8 CFU mL^{-1}. As naturally occurring levels of contamination in blood products are known to be as low as 10-100 cells per unit prior to storage, the low-level seeding densities used in this study are the most clinically representative [Brecher *et al*, 2000]. As shown in Figures 4.9 and 4.10, successful broad-spectrum decontamination of plasma seeded at these levels was achieved, with >99.01–100% inactivation (≤5 CFU mL^{-1} remaining) after exposure to a dose of 360 J cm^{-2}, with minor differences likely due to the slightly varying starting populations between the different species. As these microbial inactivation tests used a fixed 405-nm light treatment, it would be of interest to assess the inactivation kinetics of the panel of organisms at low seeding densities to determine the exact dose required to eliminate ‘naturally occurring’ levels of contamination.

It is worth noting that the work of this study, to establish broad-spectrum antimicrobial efficacy of 405-nm light for pathogens present in plasma, was conducted using low sample volumes and high irradiance light treatments to generate proof-of-concept data. As demonstrated in earlier studies by Maclean *et al*, practical application of the

technology would involve utilizing lower irradiances for whole bag treatment [Maclean *et al,* 2016, 2020]. Subsequent chapters will build on the knowledge gained from the small-scale testing reported here to support the development of a more clinically representative, 405-nm light treatment to treat prebagged plasma.

Overall, this chapter has successfully demonstrated the broad-spectrum antimicrobial efficacy of a 405-nm light dose of 360 Jcm^{-2} (100 $mWcm^{-2}$ for 1-hr) for treatment of plasma, with compatibility also demonstrated with the plasma itself. To determine the optimal method of dose delivery of 405-nm light, it is of interest to investigate different treatment regimes (by varying irradiance and exposure time) and their suitability for safe and effective decontamination of plasma. The following Chapter will explore this by assessing the influence of three different treatment regimes, delivering a fixed dose of 360 Jcm^{-2}, using low-, mid- and high-intensity irradiances, on the antibacterial efficiency and protein compatibility of plasma.

Chapter Five I Assessing the Influence of 405-nm Light Dose Delivery on Antibacterial Efficiency and Protein Compatibility: Small-Scale Testing

5.0 I Introduction

Evidence for the broad-spectrum inactivation efficacy of a fixed 405-nm light dose (360 Jcm^{-2} applied using 100 $mWcm^{-2}$), displaying both antimicrobial effects and compatibility with the plasma itself, for treatment of plasma samples was first reported in Chapter 4. Moving forward, there was a need to investigate whether varying the method of dose delivery, i.e. the use of different irradiances and exposure times, influences the compatibility or the antibacterial efficiency (the dose at which inactivation is achieved) of the 405-nm light treatment. In terms of antibacterial efficiency, identifying the impact of altering the irradiance levels used for treatment is particularly important for practical development of the technology: the 100 $mWcm^{2}$ irradiance used in Chapter 4 is suitable for proof-of-concept testing, but for development of a large-scale treatment system, lower irradiance levels will be required, so determining how lower irradiances – and lower doses – impact antibacterial efficiency, is an important factor in technology development.

Prior research by Maclean *et al* (2016, 2020), covered in Section 2.4.5, indicated that the application of a 405-nm light dose using low irradiances provides greater inactivation efficiency for treatment of plasma and PCs, compared to higher irradiances [Maclean *et al,* 2016, 2020]. This Chapter was designed to expand on these insights by analysing the inactivation kinetics of *S. aureus* and *E. coli* at different contamination levels, using a wider range of 405-nm light irradiances. Further, as there was little to no knowledge on the effects of varying the method of dose delivery with regard to protein compatibility, it was essential to evaluate how different light treatment regimes effect plasma protein integrity and functionality. The results from both the antibacterial efficiency and protein compatibility tests would give an insight to the optimal treatment type of 405-nm light for application with plasma.

In this study, low volume plasma samples were exposed to three different regimes with a fixed dose applied using low (1 $mWcm^{-2}$), mid (10 $mWcm^{-2}$) and high (100 $mWcm^{-2}$) irradiance 405-nm light. The study first assessed the dose delivery effects on antibacterial efficiency by exposing plasma seeded with *S. aureus* and

E. coli, at different population densities, to different treatment regimes of 405-nm light. Protein compatibility tests were then conducted to assess whether varying the method of dose delivery influenced the protein integrity (via SDS-PAGE) and/or functionality (via clotting assays) of plasma.

Overall, this study had two main aims:

- To compare the inactivation efficiency of a low, mid and high intensity 405-nm light treatment against *S. aureus* and *E. coli* (representative of a Gram-positive and Gram-negative bacteria, respectively) seeded in plasma, at contamination levels of 10^2 and 10^5 $CFUmL^{-1}$.
- To assess the protein integrity (via SDS-PAGE) and functionality (via clotting assays) of plasma exposed to low, mid and high intensity 405-nm light treatments, in order to evaluate how the method of dose delivery influences treatment compatibility.

5.1 I Experimental Setup for Varying the 405-nm Light Treatment Regime

This study used the small-scale exposure system (Chapter 4, Figure 4.2) to investigate the antibacterial efficiency and protein compatibility of different regimes using low, mid and high irradiances of 405-nm light for treatment of plasma. The three different light irradiances selected were 1, 10, and 100 $mWcm^{-2}$, and these were used to apply fixed doses in order to enable a direct comparison between treatment types. To keep the total dose constant in each case, the sample exposure time was adjusted according to the *Equation 1* (see Section 4.2.1).

Table 5.1 details the 405-nm light treatment regimes using the different irradiances to deliver fixed doses of up to 360 Jcm^{-2}. As shown in Figure 5.1, the distance between the LED array and sample microplate was adjusted and fixed at 32 cm, 15 cm and 4 cm to provide irradiances of 1, 10 and 100 $mWcm^{-2}$ at the sample surface, respectively (measured using a radiant power meter and photodiode detector).

Table 5.1. 405-nm light treatment regimes. Fixed doses of 405-nm light were delivered using 1, 10 and 100 mWcm^{-2} irradiances for low, mid and high intensity treatments respectively. Exposure times were calculated using *Equation 1.*

	Irradiance		
Dose (Jcm^{-2})	**1 mWcm^{-2}(-hr)**	**10 mWcm^{-2}(-hr)**	**100 mWcm^{-2}(-min)**
72	20	2	12
108	30	3	18
144	40	4	24
180	50	5	30
252	70	7	42
360	100	10	60

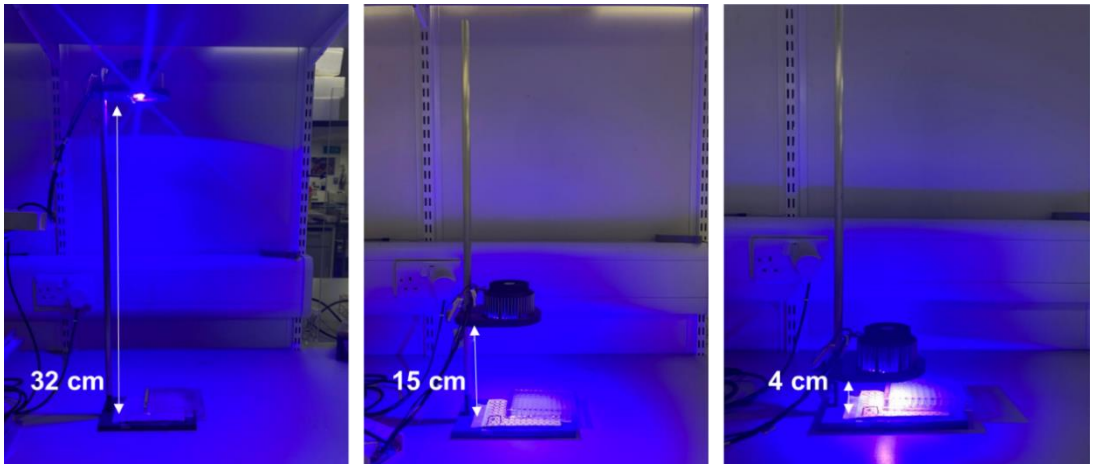

A) B) C)

Figure 5.1. Experimental set-up for different 405-nm light treatment regimes. Fixed doses of 405-nm light were applied via low (1 mWcm^{-2}), mid (10 mWcm^{-2}) and high (100 mWcm^{-2}) intensity treatments by positioning the LED array A) 32 cm, B) 15 cm and C) 4 cm from the sample surface respectively (measured using a radiant power meter and photodiode detector (LOT-Oriel Ltd)).

5.2 | Impact of Different Treatment Regimes on Antibacterial Efficacy

This section describes the inactivation of *S. aureus* and *E. coli*, observed in plasma when seeded at population densities of 10^2 and 10^5 CFUmL^{-1}, following exposure to 405-nm light using different treatment regimes.

5.2.1 Methods: Exposure of Bacteria to Varying Treatment Regimes

Dose delivery experiments were conducted using a small-scale exposure system to investigate if inactivation of bacteria in plasma was dose dependent. To investigate and compare the antibacterial efficiency of different treatment regimes, 250-µL volumes (n=3) of plasma seeded with *S. aureus* and *E. coli* at cell densities of 10^2 and 10^5 CFUmL^{-1} (as per Section 4.2.1), were transferred into a 96-well plate, covered with ultra-clear adhesive sealing film and positioned below the light array. Seeded plasma was exposed to 405-nm light at 1, 10 and 100 mWcm^{-2} irradiances using the treatment regimes outlined in Table 5.1. These treatment regimes ensured that samples were exposed to fixed doses using the different irradiances, and that inactivation kinetics could be directly compared. Control samples were held in identical conditions but shielded from the 405-nm light. Post-exposure, samples were plated onto nutrient agar, incubated at 37°C overnight and enumerated.

5.2.2 Results: Inactivation of S. aureus in Plasma using Varying 405-nm Light Treatment Regimes

Figure 5.2 demonstrates the efficacy of 405-nm light for decontamination of plasma seeded with *S. aureus* at ~10^2 CFUmL^{-1} with fixed doses applied using A) 1, B) 10 and C) 100 mWcm^{-2} irradiances. Starting bacterial populations of plasma (~10^2 CFUmL^{-1}) were similar for each 405-nm light exposure [P = 0.62]. Generally, a steady downward trend in contamination was observed after exposure to doses in the region of 72 – 144 Jcm^{-2} when applied using any of the three irradiances. Bacterial loads in non-exposed control samples remained relatively constant over the treatment period when doses were applied with irradiances of 10 (10-hrs) and 100 mWcm^{-2} (1-hr) [P = 0.09, 0.58 respectively]. Contamination levels of non-exposed controls rose by >1-log$_{10}$ over the 100-hr period for the low intensity, 1 mWcm^{-2} treatment regime [P = 0.001].

To compare the full antibacterial efficacy of different treatment regimes, taking account of the bacterial growth observed in non-exposed controls, the bacterial survival of exposed and equivalent non-exposed controls was calculated as a percentage (%).

Figure 5.2D demonstrates the % bacterial survival following exposure to different 405-nm light treatment regimes. An initial dose of 72 Jcm^{-2} applied using an irradiance of 1 $mWcm^{-2}$ achieved the greatest level of inactivation compared to other irradiances, with a 92% reduction observed. Use of 100 $mWcm^{-2}$ irradiances achieved similar inactivation, with 72 Jcm^{-2} achieving an 82% reduction in contamination. A significantly lower bacterial reduction of 33% was achieved with a dose of 72 Jcm^{-2} using an irradiance of 10 $mWcm^{-2}$. After this point, the bacterial loads in exposed plasma were similar regardless of the dose delivery regime, with a dose of 108 Jcm^{-2} resulting in >99% bacterial reductions.

Figure 5.3 demonstrates the inactivation efficacy of 405-nm light against *S. aureus* seeded in plasma at $\sim 10^5$ $CFUmL^{-1}$ with fixed doses applied using A) 1, B) 10 and C) 100 $mWcm^{-2}$ irradiances. 405-nm light significantly reduced contamination in plasma using an initial dose of 72 Jcm^{-2} when applied using any of the three light intensity treatments [$P > 0.05$]. As shown in Figure 5.3A, doses applied using 1 $mWcm^{-2}$ irradiances resulted in a steady downward trend in contamination following exposure to 252 Jcm^{-2} (70-hrs) with bacterial loads reduced by 3.26-log_{10}. After this point, the rate of inactivation slowed, with a final 3.93-log_{10} reduction achieved after exposure to 360 Jcm^{-2} [$P = 0.02$]. In the low intensity treatment regime, bacterial levels in non-exposed controls significantly rose from 5.8-log_{10} to 6.7-log_{10} over the 100-hr treatment period [$P = 0.00$].

As shown in Figure 5.3B, using 10 $mWcm^{-2}$ irradiances, the majority of inactivation was achieved between exposure to 180 and 252 Jcm^{-2} whereby bacterial loads decreased from 4.1-log_{10} to 2.1-log_{10}. After this point, bacterial levels remained relatively constant over the exposure period. The inactivation kinetics shown in Figure 5.3D, demonstrates a gradual reduction in bacterial load following exposure to 100 $mWcm^{-2}$ irradiances, with a 1.5-log_{10} reduction achieved after 360 Jcm^{-2} (1-hr).

These results show that use of lower irradiances are more efficient for the inactivation of *S. aureus* in plasma compared to higher irradiances. Comparison of exposure to an initial dose of 72 Jcm^{-2} highlights this difference in efficiency with a 89% reduction achieved after exposure to 1 $mWcm^{-2}$, a 77% reduction after exposure to 10 $mWcm^{-2}$ and a 52% reduction after exposure to 100 $mWcm^{-2}$. This trend, whereby use of lower irradiances resulted in significantly greater bacterial inactivation compared to higher irradiances, was observed at all dose levels applied.

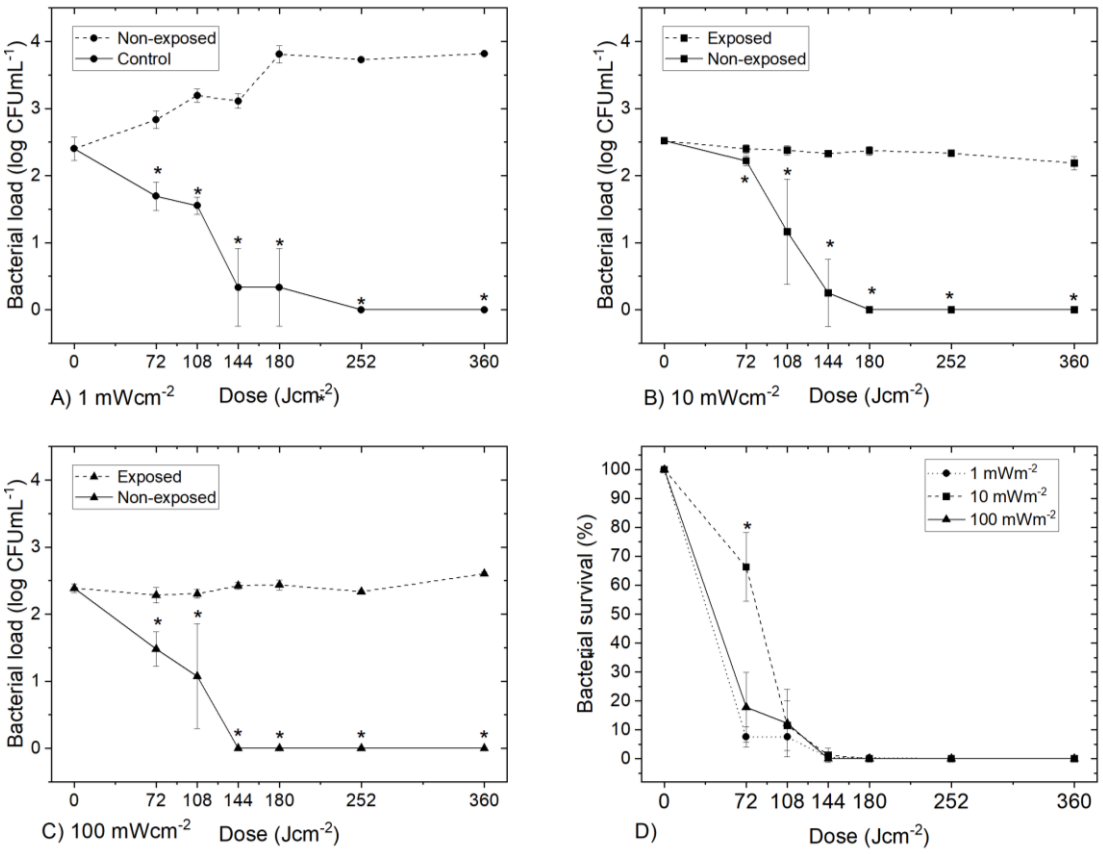

Figure 5.2. 405-nm light inactivation of *S. aureus* seeded in plasma at 10^2 CFUmL^{-1} using fixed doses applied with irradiances of A) 1 mWcm^{-2}, B) 10 mWcm^{-2} and C) 100 mWcm^{-2}. Data in Images A-C show mean $\log_{10}$ (CFUmL^{-1})±SD (n=3) with asterisks (*) representing a significant difference between bacterial counts in exposed and equivalent non-exposed samples [$P \leq 0.05$; 2-sample t-test (Minitab v18)]. Image D) represents the % bacterial survival between exposed and non-exposed plasma samples, where (*) represent significantly different bacterial reductions compared to other irradiances applying the same dose [$P < 0.05$; one-way ANOVA with Tukey *post-hoc* test (Minitab v18)].

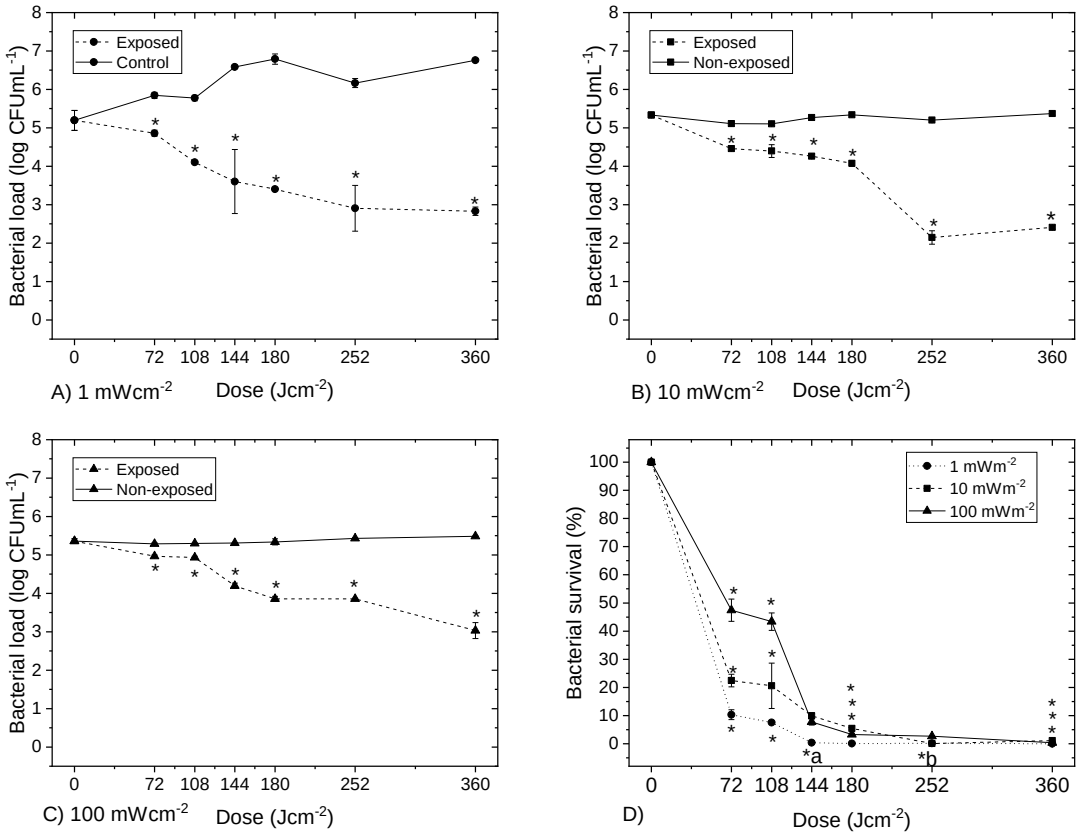

Figure 5.3. 405-nm light inactivation of *S. aureus* seeded in plasma at ~10^5 $CFUmL^{-1}$ using fixed doses applied with irradiances of A) 1, B) 10 and C) 100 $mWcm^{-2}$. Data in Images A-C show mean log_{10} ($CFUmL^{-1}$)±SD (n=3) with asterisks (*) representing a significant difference between bacterial counts in exposed and equivalent non-exposed samples [$P \leq 0.05$; 2-sample t-test (Minitab v18)]. Image D) represents the % bacterial survival between exposed and non-exposed plasma samples, where (*) represent significantly to all other irradiances; (*a) 1 $mWcm^{-2}$ significantly different to 10 and 100 $mWcm^{-2}$; (*b) 1 and 10 $mWcm^{-2}$ significantly different to 100 $mWcm^{-2}$ [$P < 0.05$; one-way ANOVA with Tukey *post-hoc* test (Minitab v18)].

5.2.3 Results: Inactivation of E. coli in Plasma using Varying 405-nm Light Treatment Regimes

Results in Figure 5.4 demonstrate the inactivation efficacy of 405-nm light against *E. coli* seeded in plasma at ~10^2 CFUmL^{-1} with fixed doses applied using A) 1, B) 10 and C) 100 mWcm^{-2} irradiances. All 405-nm light treatment regimes, successfully reduced *E. coli* contamination in plasma, with complete inactivation achieved after exposure to a dose of 360 Jcm^{-2}.

Figure 5.4A shows that use of 1 mWcm^{-2} 405-nm light irradiances completely reduced bacterial contamination in plasma using an initial dose of 72 Jcm^{-2} [P = 0.00]. Thereafter, bacterial loads remained at undetectable levels over the 100-hr exposure period. Contamination levels in non-exposed controls rose significantly by approx. 6–log$_{10}$ over the course of the 100-hr treatment period [P = 0.00]. Inactivation of *E. coli* using 10 mWcm^{-2} occurred at a slower rate, with an increased dose of 252 Jcm^{-2} required to achieve complete inactivation (Figure 5.4B). Use of 100 mWcm^{-2} irradiances, again required increased doses compared to lower irradiances, with a dose of 144 Jcm^{-2} required to achieve significant bacterial reductions [P = 0.01] (Figure 5.4C). In this case, the majority of inactivation occurred following exposure to 360 Jcm^{-2}, with a 2.4-log$_{10}$ reduction achieved. Contamination levels in non-exposed controls were constant over the course of the experiments using 10 and 100 mWcm^{-2} (P > 0.05).

As shown in Figure 5.4D, use of lower irradiances is more efficient for the inactivation of *E. coli* seeded in plasma at ~10^2 CFUmL^{-1} compared to higher irradiances. The difference in inactivation efficiency is highlighted upon comparison of exposure to an initial dose of 72 Jcm^{-2}, where use of 1 mWcm^{-2} achieved a 100% reduction, 10 mWcm^{-2} achieved an 89% reduction and 100 mWcm^{-2} achieved a 7% reduction [P = 0.00]. The inactivation efficiency of doses >72 Jcm^{-2} were, generally, similar when applied using 1 and 10 mWcm^{-2} irradiances, with use of 100 mWcm^{-2} irradiances requiring markedly increased doses to achieve comparable reductions.

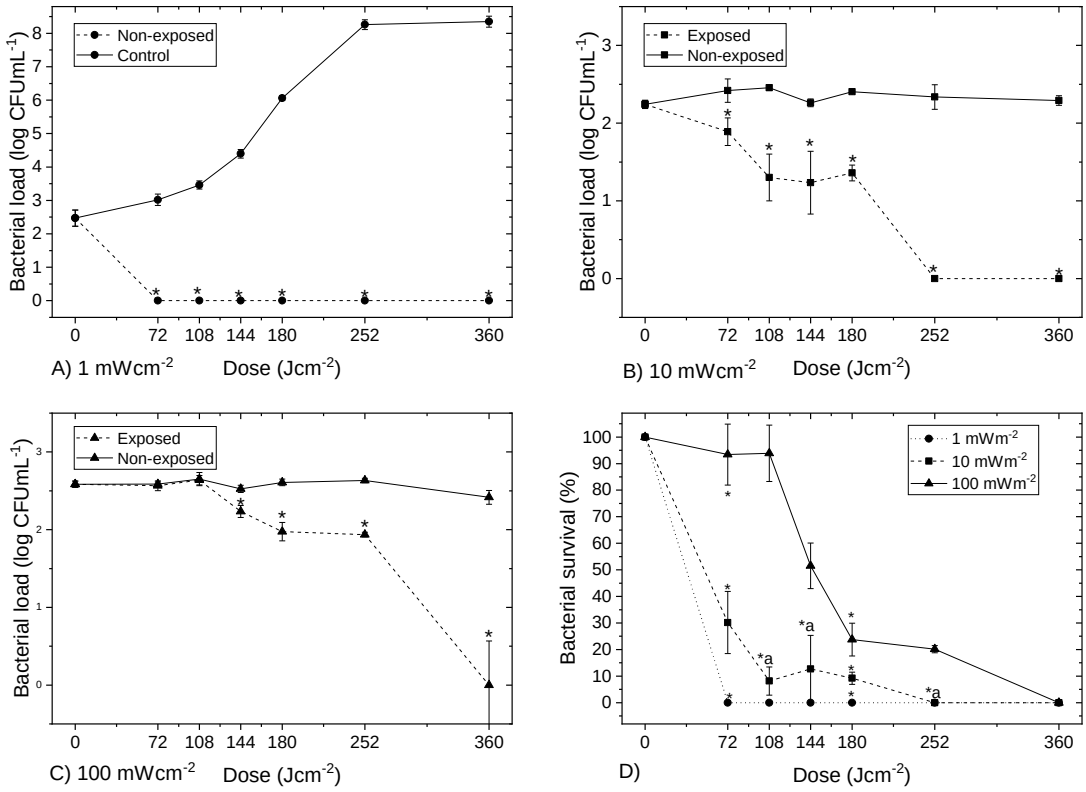

Figure 5.4. 405-nm light inactivation of *E. coli* seeded in plasma at 10^2 CFUmL^{-1} using fixed doses applied with irradiances of A) 1, B) 10 and C) 100 mWcm^{-2}. Data in Images A - C show mean $\log_{10}$ (CFUmL^{-1})±SD (n=3) with asterisks (*) representing a significant difference between bacterial counts in exposed and equivalent non-exposed samples [$P \leq 0.05$; 2-sample t-test (Minitab v18)]. Image D) represents the % bacterial survival between exposed and non-exposed plasma samples, where (*) represent significantly to all other irradiances and (*a) 1 and 10 mWcm^{-2} significantly different to 100 mWcm^{-2} [$P < 0.05$; one-way ANOVA with Tukey *post-hoc* test (Minitab v18)].

Results in Figure 5.5 demonstrate the inactivation efficacy of 405-nm light against *E. coli* seeded in plasma at ~10^5 CFUmL^{-1} with fixed doses applied using A) 1, B) 10 and C) 100 mWcm^{-2} irradiances. All 405-nm light treatment regimes achieved significant bacterial reductions with applied doses of 108 Jcm^{-2} ($P < 0.05$). Steady downward trends in contamination are observed following exposure to all 405-nm light treatment regimes (Fig 5.5A-C).

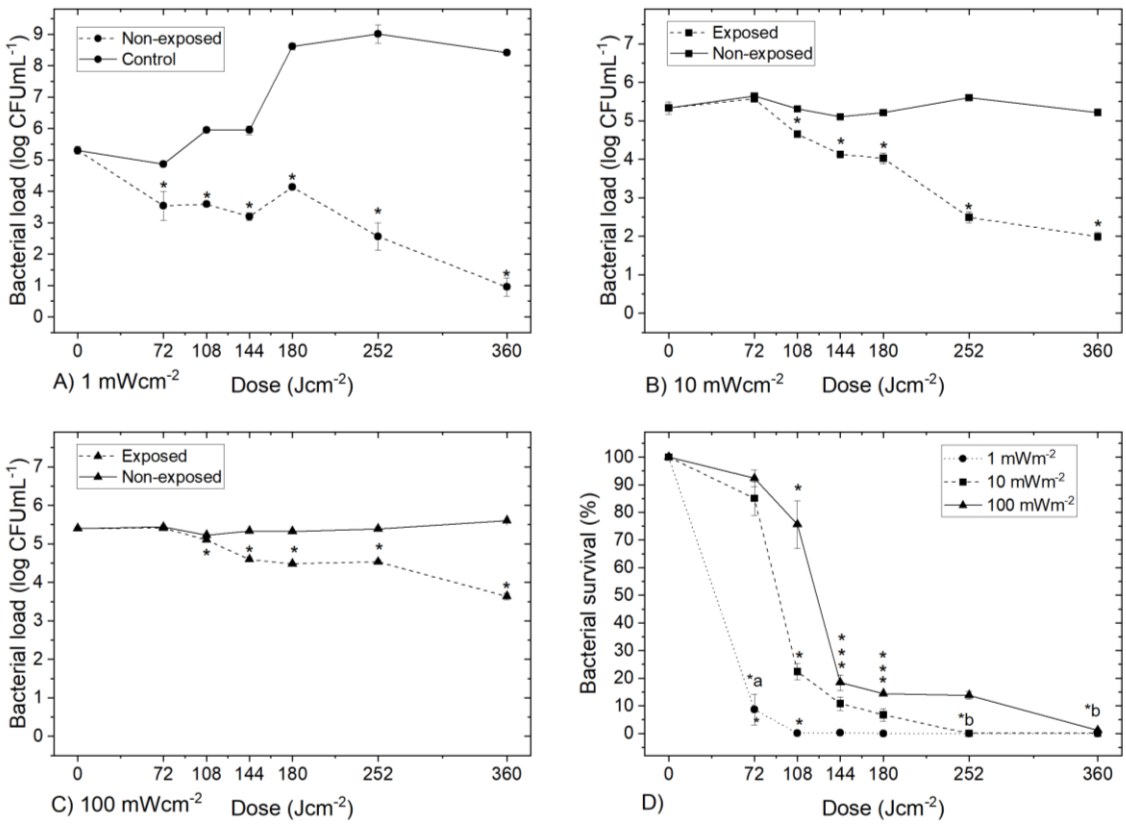

Figure 5.5. 405-nm light inactivation of *E. coli* seeded in plasma at 10^5 $CFUmL^{-1}$ using fixed doses applied with irradiances of A) 1, B) 10 and C) 100 $mWcm^{-2}$. Data in Images A - C show mean log_{10} ($CFUmL^{-1}$)±SD (n = 3) with asterisks (*) representing a significant difference between bacterial counts in exposed and equivalent non-exposed samples [$P \leq 0.05$; 2-sample t-test (Minitab v18)]. Image D) represents the % bacterial survival between exposed and non-exposed plasma samples, where (*) represent significantly to all other irradiances; (*a) 1 $mWcm^{-2}$ significantly different to 10 and 100 $mWcm^{-2}$ and (*b) 1 and 10 $mWcm^{-2}$ significantly different to 100 $mWcm^{-2}$ [$P < 0.05$; one-way ANOVA with Tukey *post-hoc* test (Minitab v18)].

Use of 1 $mWcm^{-2}$ irradiances achieved the highest level of inactivation with a bacterial population of 0.95-log_{10} remaining in plasma exposed 360 Jcm^{-2}, compared to 1.99- and 3.65-log_{10} when the dose was applied using 10 and 100 $mWcm^{-2}$ irradiances respectively. Bacterial loads in non-exposed control plasma remained stable over the treatment period for 10 and 100 $mWcm^{-2}$ exposures, whereas the bacterial load increased by >3-log_{10} over the 100-hr treatment period for the 1 $mWcm^{-2}$ exposure.

5.2.4 Results: Dose Requirement for a 1-log$_{10}$ Reduction of Bacteria using Different Treatment Regimes

Table 5.2 outlines the dose required to achieve a 1-log$_{10}$ reduction of *S. aureus* and *E. coli* seeded in plasma at 10^2 and 10^5 CFUmL^{-1}, using the three different treatment regimes. A 1-log$_{10}$ reduction of both *S. aureus* and *E. coli* was achieved using the lowest dose when applied using the lowest irradiance of 1 mWcm^{-2}. For *S. aureus* seeded at 10^2 CFUmL^{-1}, a 1-log$_{10}$ reduction was achieved using a dose of 72 Jcm^{-2} applied using 1 mWcm^{-2} irradiance 405-nm light. A slightly higher dose of 108 Jcm^{-2} was required to achieve a 1-log$_{10}$ reduction when using 10 and 100 mWcm^{-2} irradiances. A similar trend was observed for *S. aureus* seeded at 10^5 CFUmL^{-1} where use of 1 mWcm^{-2} 405-nm light achieved a 1-log$_{10}$ reduction with a dose of 108 Jcm^{-2}, compared to 10 and 100 mWcm^{-2} which required higher dose levels of 144 Jcm^{-2} to achieve similar levels in activation.

For *E. coli,* the dose required to achieve a 1-log$_{10}$ reduction increased with the use of increased irradiance levels. Use of 1 mWcm^{-2} irradiances achieved a 1-log$_{10}$ reduction of *E. coli* with a dose of 72 Jcm^{-2}, when seeded in plasma at 10^2 and 10^5 CFUmL^{-1}. Inactivation by 10 mWcm^{-2} irradiances required doses in the region of 108–180 Jcm^{-2} to achieve a 1-log$_{10}$ reduction, with doses required increasing with increased level of contamination. Use of 100 mWcm^{-2} irradiances required the highest dose of 360 Jcm^{-2} to achieve a 1-log$_{10}$ reduction of *E. coli* when seeded at 10^2 and 10^5 CFUmL^{-1}.

In summary, the use of low, 1 mWcm^{-2} irradiances consistently achieved 1-log$_{10}$ reductions of bacteria (*S. aureus* and *E. coli* at both 10^2 and 10^5 CFUmL^{-1}) using the lowest dose, compared to 10 and 100 mWcm^{-2}.

Table 5.2. Dose requirements to achieve a 1-log_{10} reduction of bacteria seeded in plasma using three fixed irradiances of 1, 10 and 100 $mWcm^{-2}$. As highlighted, the lowest irradiance (1 $mWcm^{-2}$) was the most efficient for bacterial inactivation in all cases.

Bacteria	Contamination level (~$CFUmL^{-1}$)	Irradiance ($mWcm^{-2}$)	Dose (Jcm^{-2}) required for 1-log_{10} reduction
S. aureus	**10^2**	**1**	**72**
		10	108
		100	108
	10^5	**1**	**108**
		10	144
		100	144
E. coli	**10^2**	**1**	**72**
		10	108
		100	360
	10^5	**1**	**72**
		10	180
		100	360

5.3 I Impact of Different Treatment Regimes on Plasma Compatibility

This section investigates the compatibility of different 405-nm light treatment regimes with plasma proteins. Protein integrity and clotting functionality of exposed and non-exposed plasma was assessed using SDS-PAGE and clotting assays, respectively.

5.3.1 Methods: Impact of Varying Treatment Regime on Plasma Compatibility

To assess the impact of varying the method of dose delivery on protein compatibility, triplicate samples (250 µL) of non-seeded plasma were transferred to a 96-well plate, covered with ultra-clear adhesive sealing film and positioned below the light array for exposure. Plasma samples were exposed to 405-nm light at 1, 10 and 100 $mWcm^{-2}$ using the treatment regimes outlined in Table 5.1. Control samples were held in identical conditions but shielded from the 405-nm light. Post-exposure, the integrity of proteins was analysed using SDS-PAGE (see Section 3.5.1) and clotting functionality quantified using PTT and APTT assays (see Sections 3.5.3 and 3.5.4, respectively).

5.3.2 Results: Impact of Varying Treatment Regime on Plasma Compatibility Assessed using SDS-PAGE

Figure 5.6 is an image of an SDS-PAGE gel used to compare the electrophoretic patterns of plasma exposed to varying 405-nm light treatment regimes, with doses up to 360 Jcm^{-2} applied using low, mid and high intensity irradiances (1, 10 and 100 $mWcm^{-2}$ respectively). The electrophoretic patterns of plasma exposed to doses up to 144 Jcm^{-2} delivered using low, mid and high intensity treatments did not demonstrate visually detectable differences, indicating that the method of dose delivery does not affect protein integrity observed in this dose region. Whilst no obvious damage was observed upon exposure to 180 Jcm^{-2}, analysis of HMWPs, typically associated with clotting factors such as fibrinogen, was difficult to determine.

When exposed to an increased dose of 252 Jcm^{-2}, there were clearer indications of protein modifications of HMWPs. Changes in HMWP banding were visible in plasma exposed to doses ≥252 Jcm^{-2}, when applied using all three irradiances. In these cases, it is difficult to visually determine the degree of change between the varying treatment regimes. As highlighted in Figure 5.6B, a loss of protein banding at approximately 45 kDa was detected in plasma exposed to 360 Jcm^{-2} applied using high, 100 $mWcm^{-2}$ irradiances (Lane 19). Nevertheless, comparison with a positive control (Section 4.3.2.1, Figure 4.4A, Lane 13) representing complete plasma protein degradation, suggests that the degree of change observed in any of samples analysed in this gel should not be regarded as major damage.

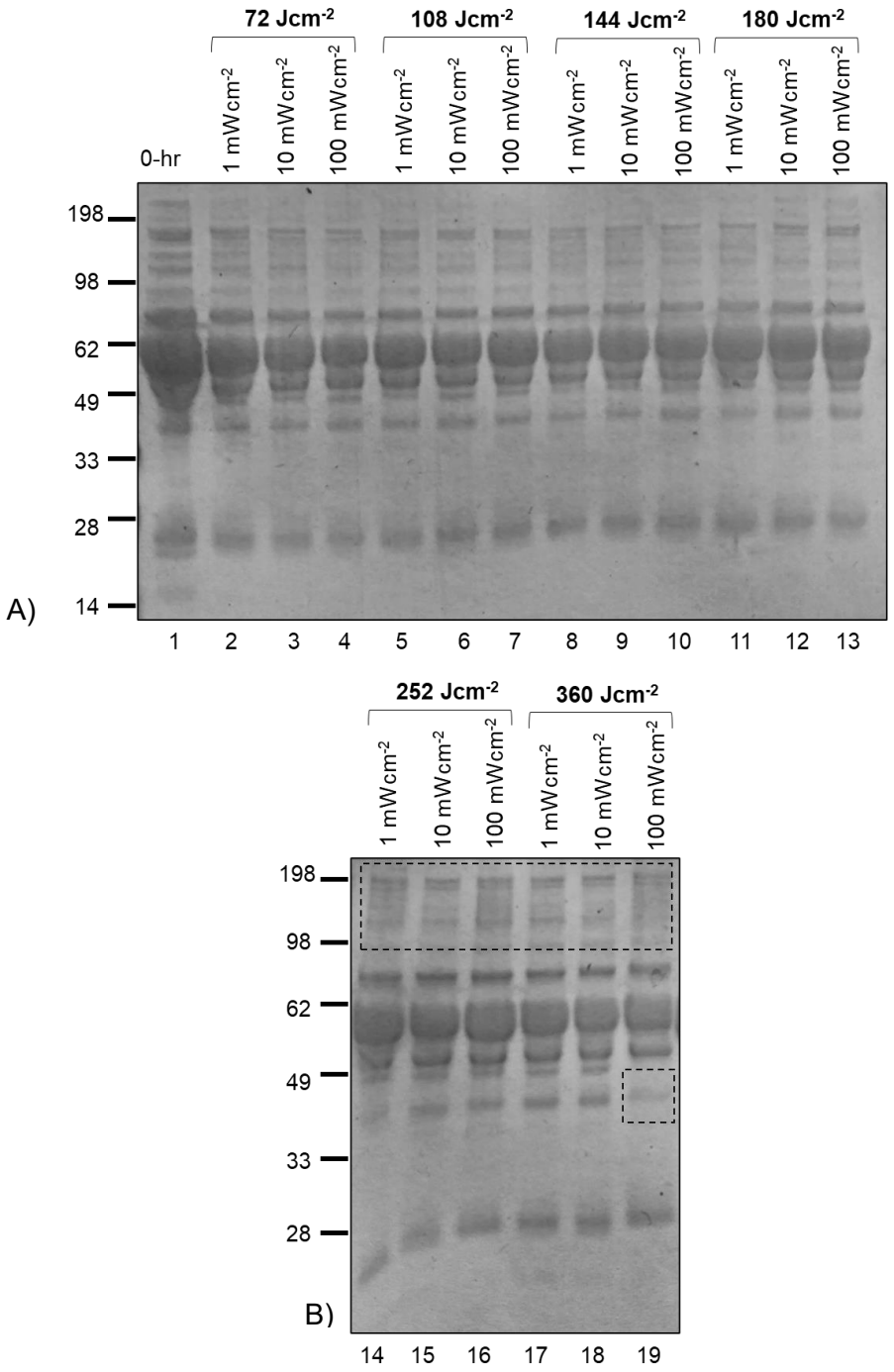

Figure 5.6. Analysis of protein integrity of plasma exposed to varying treatment regimes of 405-nm light. SDS-PAGE analysis of plasma exposed to 72–180 Jcm^{-2} is shown in Image A) and 252–360 Jcm^{-2} shown in Image B). Doses have been applied using 1 (*Lanes 2, 5, 8, 11, 14 and 17*), 10 (*Lanes 3, 6, 9, 12, 15, 18*) and 100 mWcm^{-2} (*Lanes 4, 7, 10, 13, 16 and 19*) irradiances. A zero-hr control (*0-hr; Lane 1*) was included for comparison purposes.

5.3.3 Results: Impact of Varying Treatment Regime on Plasma Compatibility Assessed using Clotting Assays

Clotting assays, commonly used to measure the stability of essential clotting factors in plasma, were used to gain a deeper understanding of the interactions of 405-nm light and plasma proteins when varying the method of dose delivery. Figure 5.7 shows the PTT values, representing the time to clot via extrinsic and common coagulation pathways, for plasma following exposure to varying 405-nm light treatment regimes.

As shown in Figure 5.7A, the time to clot for plasma exposed to doses ≤180 Jcm^{-2}, applied using 1 $mWcm^{-2}$ irradiances remained relatively stable [$P > 0.05$]. A significant increase in time to clot was observed after exposure to 252 Jcm^{-2}, with the time to clot for exposed and non-exposed plasma at 48 s and 44 s, respectively [$P = 0.001$]. As shown in Figure 5.7B, using 10 $mWcm^{-2}$ irradiances, the time to clot increased slightly after exposure to 108 Jcm^{-2}, with the time to clot for exposed and non-exposed plasma at 33 s and 29 s, respectively [$P = 0.01$]. After this point, the time to clot remained relatively stable following exposure to doses up to 180 Jcm^{-2}, with clotting times fluctuating between 32–34 s. Exposure to 360 Jcm^{-2} increased the time to clot from 33 s to 46 s, for non-exposed and exposed samples respectively. Figure 5.7C shows the time to clot for plasma exposed to 405-nm light using 100 $mWcm^{-2}$ irradiances. The time to clot for plasma exposed to doses between 72 and 144 Jcm^{-2}, remained stable in the region of 25 s. After this point, clotting times increased in a constant upward trend, with the time to clot after 360 Jcm^{-2} for exposed and non-exposed plasma at 37 s and 23 s, respectively [$P = 0.00$].

For treatment regimes using 1 and 10 $mWcm^{-2}$ irradiances, the time to clot for non-exposed controls increased linearly over the 100-hr treatment period (17% increase) and the 10-hr treatment period (12% increase) respectively [$P = 0.00, 0.01$]. The time to clot for non-exposed controls, in the treatment regime using 100 $mWcm^{-2}$ irradiances, remained relatively stable over the 1-hr treatment period [$P = 0.56$]. As the time to clot in non-exposed controls increased over the treatment period when using 1 and 10 $mWcm^{-2}$ irradiances, it was of interest to assess the percentage change in clotting time, between exposed and non-exposed plasma samples. As shown in Fig 5.7D, all treatment regimes resulted in an increased time to clot upon exposure to increasing treatment. Results indicate that the higher the irradiance used

to apply the dose, the greater the change in PTT clotting time. This is evident at all dose intervals, with the treatment regime using the lowest irradiance of 1 mWcm^{-2} resulting in the smallest change in PTT values.

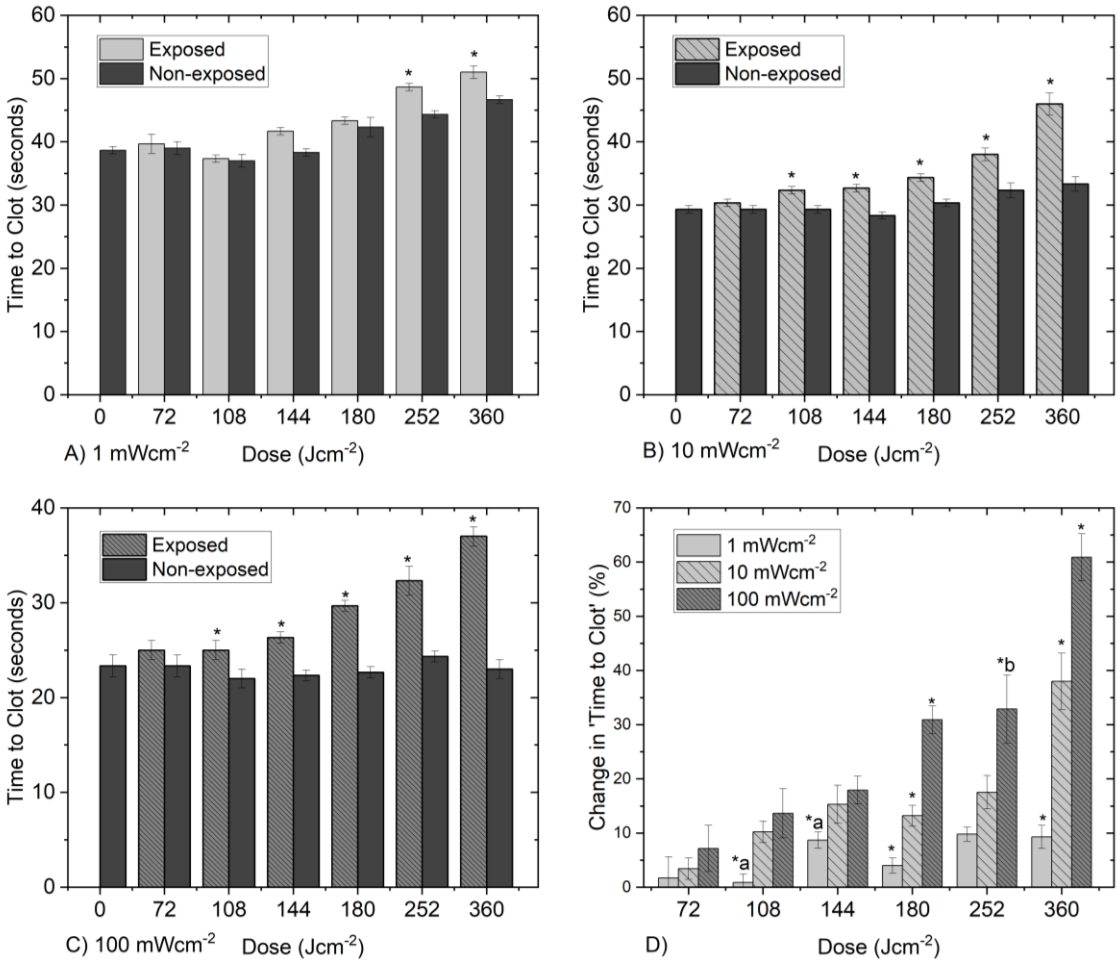

Figure 5.7. Comparison of the PTT values of plasma exposed to varying 405-nm light treatment regimes using A) 1, B) 10 and C) 100 mWcm^{-2} irradiances. Data in Images A - C show mean time to clot in seconds ± SD (n=3) with asterisks (*) representing a significant difference between clot times of exposed and equivalent non-exposed samples [$P \leq 0.05$; 2-sample t-test (Minitab v18)]. Image D) represents the % change in time to clot between exposed and non-exposed plasma samples, where (*) represent significantly to all other irradiances; (*a) significantly different to 10 and 100 mWcm^{-2} and (*b) significantly different to 1 and 10 mWcm^{-2} [$P < 0.05$; one-way ANOVA with Tukey *post-hoc* test (Minitab v18)].

Figure 5.8 shows the APTT values, representing the time to clot via intrinsic and common coagulation pathways, for plasma following exposure to varying 405-nm light treatment regimes. As shown in Fig 5.8A, APTT values for plasma exposed to doses

up to 144 Jcm^{-2} remained stable using 1 $mWcm^{-2}$ irradiances [$P > 0.05$]. An increase in time to clot was observed in the region of 252 Jcm^{-2}, with APTT values of exposed and non-exposed plasma measured at 47 s and 44 s, respectively [$P = 0.04$]. The impact on APTT values, was more apparent in treatment regimes using 10 and 100 $mWcm^{-2}$ irradiances. As shown in Fig 5.8B and C, APTT values increased in a constant linear trend following increased exposure to 405-nm light. Using 10 $mWcm^{-2}$, APTT values slightly increased following doses of up to 180 Jcm^{-2}, after which a notable change was observed with the time to clot for exposed and non-exposed plasma at 51 s and 45 s, respectively [$P = 0.01$]. Using 100 $mWcm^{-2}$, APTT values increased significantly from 42 s to 47 s following exposure to 108 Jcm^{-2} [$P = 0.04$], with the time to clot increasing linearly thereafter.

As shown in Fig 5.8D, the higher the irradiance used to apply the dose, the greater the change in APTT clotting time. Comparison of exposure to a dose of 360 Jcm^{-2} highlights the difference between treatment regimes, with the time to clot increasing by 8% after exposure to 1 $mWcm^{-2}$, 14% after exposure to 10 $mWcm^{-2}$ and 29% after exposure to 100 $mWcm^{-2}$. This trend was observed with all applied doses in the region of 108 – 360 Jcm^{-2}.

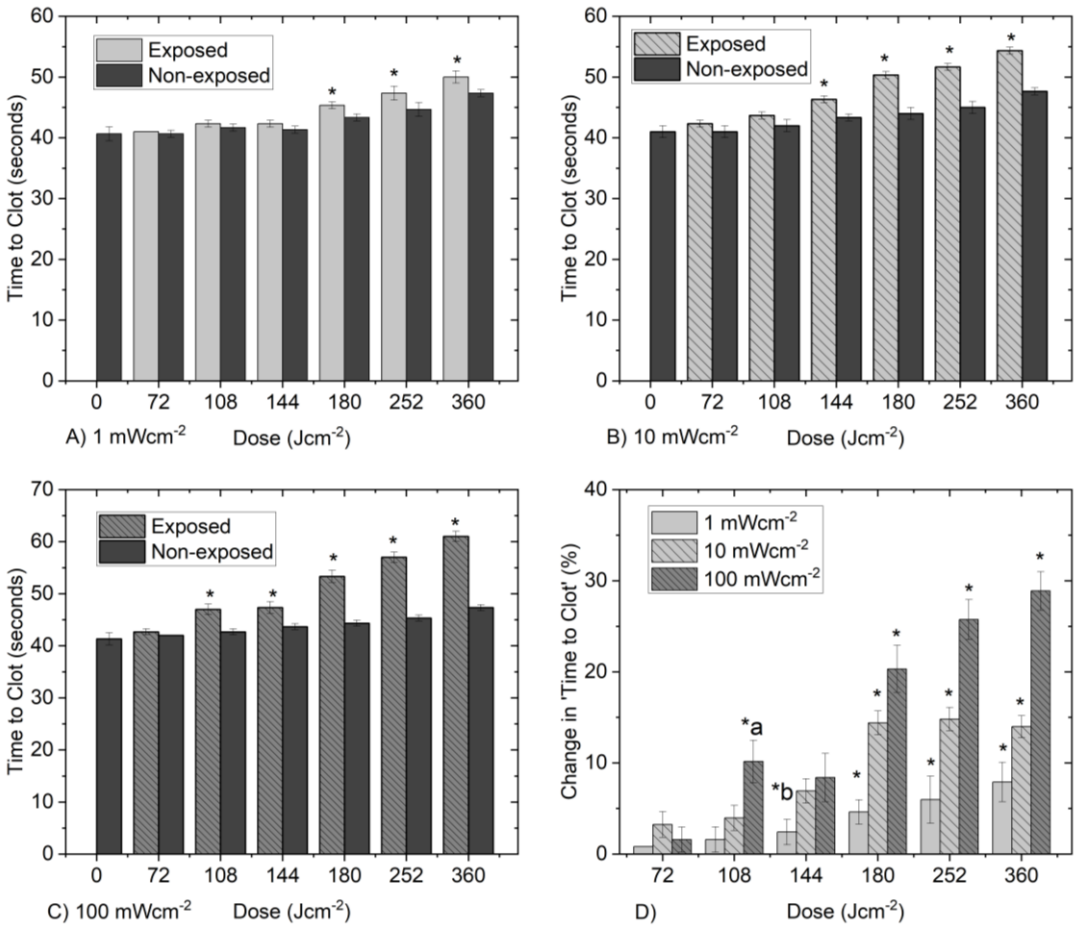

Figure 5.8. Comparison of the APTT values of plasma exposed to varying 405-nm light treatment regimes, using A) 1, B) 10 and C) 100 mWcm^{-2} irradiances. Data in Images A - C show mean time to clot in seconds ± SD (n=3) with asterisks (*) representing a significant difference between clot times of exposed and equivalent non-exposed samples [$P \leq 0.05$; 2-sample t-test (Minitab v18)]. Image D) represents the % change in time to clot between exposed and non-exposed plasma samples, where (*) represent significantly to all other irradiances; (*a) significantly different to 1 and 10 mWcm^{-2} and (*b) significantly different to 10 and 100 mWcm^{-2} [$P < 0.05$; one-way ANOVA with Tukey *post-hoc* test (Minitab v18)].

5.4 I Discussion

The work of this Chapter has provided an insight to the influence of varying the 405-nm light treatment regime on both antibacterial efficiency and protein compatibility. The results in this Chapter demonstrate for the first time that the use of lower irradiances provide both greater antibacterial efficiency and treatment compatibility compared to higher irradiances when applying a fixed 405-nm light dose. This section

will discuss both the inactivation efficiency and protein compatibility of the different methods of dose delivery of 405-nm light for the treatment of plasma.

With regards to antibacterial efficiency, comparison of the dose requirements for 1-log_{10} reductions of *E. coli* highlights the difference in inactivation efficiency, with 5× the dose required by a high intensity treatment compared to a low intensity treatment; 72 Jcm^{-2} required for 1 $mWcm^{-2}$, 108 -180 Jcm^{-2} required for 10 $mWcm^{-2}$ and 360 Jcm^{-2} required for 100 $mWcm^{-2}$. Similar findings have been reported in larger-scale studies investigating the antibacterial efficiency of different 405-nm light regimes for treatment of prebagged plasma and platelets [Maclean *et al* 2016, 2020]. It is thought that there is a critical level of photons that can be involved in the photoexcitation process of porphyrins, and above such an irradiance level it is likely that excess photons are unable to be absorbed and therefore, cannot contribute to the inactivation mechanism. This theory has been linked to the limit on the free porphyrin-to-photon ratio [Maclean *et al*, 2016, 2020]. As higher irradiances potentially lead to the provision of excess photon energy, it is likely that use of lower irradiances is more efficient with regards to both antibacterial activity and optical energy, including power consumption, compared to higher irradiances.

In contrast, some published studies have found the inactivation of bacteria by 405-nm light to be less influenced by the method of dose delivery [Murdoch *et al*, 2012; Endarko *et al,* 2012]. Murdoch *et al* (2012), demonstrated that applying a fixed dose using different irradiance levels (10, 20 and 30 $mWcm^{-2}$), had no influence on the rate of inactivation of a Gram-positive bacterium, *Listeria monocytogenes* [Murdoch *et al*, 2012]. Similarly, Endarko *et al* (2012) showed that the inactivation rate of *L. monocytogenes* was similar when varying the 405-nm light treatment using four different light irradiances (8.6, 44.7, 66.1 and 85.6 $mWcm^{-2}$) to deliver a fixed dose. The difference between these findings and the findings reported in this Thesis, may be, in part, due to the different suspension mediums used to assess bacterial inactivation. The difference in inactivation efficiency between methods of dose delivery, suggests that photo-sensitive agents present in biological media, such as plasma and platelets, may be able to interact with 405-nm light and potentially, enhance bacterial inactivation when doses are applied using low intensity irradiances over longer exposure times. Further, as this research study investigated the dose delivery effects using a wider range of irradiances between 1 and 100 $mWcm^{-2}$ (increased by a factor of 100, compared to a factor of 3 and 10 for Murdoch *et al*,

2012, and Endarko *et al*, 2012 respectively), it is possible that the range of irradiances used in the other studies are too limited to detect any significant differences between treatment regimes.

Using a high intensity rapid treatment, the expected inactivation trend was observed whereby lower doses of 405-nm light were required to inactivate *S. aureus* compared to *E. coli*. This trend was less pronounced when using low intensity prolonged treatments, with similar levels of inactivation achieved with a fixed dose for both *S. aureus* and *E. coli*. In this regard, it is likely that longer exposure periods are required for the inactivation of Gram-negative bacteria, such as *E. coli*, that typically show resilience to rapid 405-nm light treatments. This may be partly due to the fact that continuous exposure to low intensity light is more effective at disrupting the double layered outer membrane (bilayers) present in Gram-negative bacteria, which is thought to be a key driver for 405-nm light inactivation.

When assessing the viability of a PRT, it is essential to consider i) the treatment time required to achieve antimicrobial effects, and ii) the stage at which the treatment should be implemented, i.e. pre- or post-storage. Focusing on treatment time, it is clear that high irradiances can deliver effective antimicrobial doses over a much shorter exposure period compared to low irradiances. In the case of *E. coli*, even though dose requirements were 5× higher using a high irradiance treatment compared to the low intensity treatment (360 *versus* 72 Jcm^{-2}, respectively), the treatment time was significantly shorter at 1-hr for a high intensity treatment *versus* 10-hrs for a low intensity treatment. This factor must be considered in the practical implementation of the technology, as long exposure periods may not be suitable in a clinical setting. Whilst this study was designed to determine the optimal treatment regime, it has shown that all treatment regimes using low, mid and high intensity 405-nm light can successfully reduce bacterial contamination in plasma. This provides an opportunity to have a flexible approach whereby the treatment regime could be tailored depending on the clinical application i.e. utilise low irradiances for continuous exposure during blood bag storage or high irradiances for rapid exposures pre- or post-storage.

Results from this study highlight the issue of bacterial growth that can occur in nutrient-rich media, at room temperature, over an extended period. This is highlighted in Fig 5.4A, where *E. coli* contamination in non-exposed controls rose by >6-log_{10} over a 100-hr period. In this case, continuous exposure to low irradiance 405-nm light

demonstrated both a bactericidal and bacteriostatic effect, with light treatment not only reducing bacterial contamination but preventing bacterial growth throughout the treatment period. This has particular clinical relevance for the storage of thawed plasma in hospital inventories, whereby liquid plasma is stored at *2 to 6°C*, for up to 5 days [Eder *et al*, 2007]. Whilst refrigerated conditions typically inhibit microbial growth, certain organisms classified as psychrophiles [Tribelli and López, 2018], have optimum growth temperatures in cold environments and, can therefore re-establish growth patterns during storage in the fridge inventories.

Further, the thaw- and pre-transfusion warming processes, whereby prebagged plasma is subject to temperatures in the region of 37°C, introduces an opportunity for the revival and growth of microbes that demonstrate optimal growth at human body temperatures [Ghosh and Haldar, 2019]. The ability to apply antimicrobial doses of 405-nm light through continuous, low intensity exposure provides an opportunity to develop a treatment for *in situ* storage applications. This would not only reduce microbial load but also prevent the opportunity for organisms to re-establish growth patterns during extended periods in storage.

As the majority of commercially available PRTs employ UV-light disinfection, it was of interest to investigate whether UV-light demonstrated a similar relationship when varying the method of dose delivery. There is a significant amount of evidence demonstrating that UV-light inactivation is a dose-dependent process, however research investigating dose-delivery effects is limited. Recently, a study demonstrated that UVC-light inactivation is not influenced by the method of dose delivery i.e. no change in dose requirements for inactivation when using different irradiance levels [Li *et al*, 2022; Kitagawa *et al*, 2021]. Kitagawa *et al* (2021) demonstrated that there were no significant differences in the reduction of Severe Acute Respiratory Syndrome Coronavirus-2 (SARS-CoV-2) when fixed doses were applied using three different irradiances of 222 nm, far UVC-light [Kitagawa *et al,* 2021]. This limits the flexibility of UV-light based PRTs. To the best of the authors' knowledge, all commercially available PRTs use fixed treatments to treat plasma at the blood centre or hospital blood bank, and do not offer the opportunity to be integrated into an *in situ* storage application in a hospital setting.

A key focus of this Chapter assessed whether treatment compatibility is influenced by the method of dose delivery. SDS-PAGE analysis, used to assess the integrity of highly abundant plasma proteins, did not identify any major differences when varying the method of dose delivery. Results from clotting assays, used to assess the stability and functionality of clotting factors, did however indicate clear differences in the compatibility of different treatment regimes.

Analysis of clotting assays demonstrated that use of lower irradiances are significantly more compatible with protein clotting factors compared to use of higher irradiances when applying a fixed antibacterial dose. The impact on clotting activity increased with an increased irradiance level used to deliver the dose. A potential explanation for this trend links back to the 'limit on the free porphyrin-to-photon ratio' theory. It is likely that use of higher irradiances leads to the provision of excess photon energy that, whilst not being involved in the photoexcitation process, can interact with photo-sensitive agents in the plasma capable of generating ROS. In short, the higher levels of excess photon energy; the higher levels of interaction with photo-sensitive agents; the higher levels of ROS produced. Consequences of protein oxidation through involvement of ROS are discussed in Section 4.6 (Figure 4.12), however the key routes of oxidation include, the formation of protein-protein cross bridges, oxidation of the protein backbone resulting in protein and amino acid side chain modification [Lund and Baron, 2010]. These findings are supported by Harutyunyan *et al* (2017), whose work demonstrated that higher levels of ROS in plasma are directly related to a reduction in clotting activity [Harutyunyan *et al*, 2017].

Results in this study show that 405-nm light exposure has more of an effect on the clotting proteins involved in the extrinsic coagulation pathway, measured via PTT assay, compared to clotting activity of intrinsic coagulation pathway, measured via the APTT assay. This indicates that the clotting Factor VII (Proconvertin), key factor of the extrinsic coagulation pathway, may be more sensitive to degradation by 405-nm light compared to Factors VIII, IX, XI and XII, that are involved in the intrinsic coagulation pathway (details of coagulation cascade provided in Section 3.5.3, Figure 3.8). Nevertheless, work by Harutyunyan *et al* (2017), demonstrated that plasma coagulation is predominantly influenced by the stability of the Factors involved in the common coagulation pathway (Factors I, II, V and X, respectively). Harutyunyan *et al* (2017) showed that changes in Prothrombin (Factor II) stability had the most

significant effect on overall clotting functionality. With this in mind, future work should investigate the stability and retention of Prothrombin directly via an ELISA assay, in addition to performing PTT and APTT clotting assays.

As described above, this Chapter expanded on the protein compatibility testing previously covered in Chapter 4, by introducing clotting assays to assess the functionality of clotting factors. These clotting assays provided more information on the compatibility of a dose of 360 Jcm^{-2} (100 $mWcm^{-2}$ for 1-hr) with plasma proteins. Results from this study, indicated that delivering the fixed dose using high irradiances affected the stability of plasma clotting factors. The clinical relevance of the clotting assays, whilst at this scale of testing, is unknown, as exposures have been performed in a static, small-scale system using microlitre volume samples. Results from clotting assays will be more clinically-relevant in subsequent Chapters investigating application with large volumes of prebagged plasma. Nevertheless, at this stage, the clotting assays provide a useful insight to the interactions of 405-nm light with plasma proteins, when low volume samples are exposed to different treatment regimes.

It should be noted that clotting times recorded for non-exposed control plasma were approximately 10-seconds longer than standard clotting times set by the blood bank laboratories [NHS South Tees Hospital, 2021]. This is likely due to the fact that standard laboratory testing is performed on fresh plasma within 8-hrs of collection, whereas this study used post-storage thawed plasma which had undergone, unavoidable freeze-thaw processes. Further, clotting times for non-exposed control plasma generally increased in a linear trend over the treatment period. This was expected as research shows that, for most clotting factors, there is a continual decline in activity during storage [Cardigan and Green, 2015]. As a result, the time to clot for exposed and an equivalent non-exposed, control was used for comparison purposes.

In summary, the results from this study demonstrated that applying a dose using lower irradiance light is both more efficient and compatible for treatment of plasma compared to higher irradiances. Nevertheless, various practical factors including treatment times, must be considered before the viability of the technology can be fully assessed. This Chapter has shown that 405-nm light can provide a flexible approach to pathogen reduction whereby the method of dose delivery can be altered depending on the application i.e. higher irradiances for rapid pre/post-storage treatments or lower

irradiances for continuous *in situ* storage treatment. This study was performed using a static, small-scale system to expose microlitre volume plasma samples and therefore can only provide an insight to how the method of dose delivery effects antibacterial efficiency and protein compatibility on this scale. Further tests are required to scale-up exposures and assess the efficacy and compatibility of 405-nm light with large volume, plasma bags to represent a clinical scenario. The next Chapter will address this by developing a large-scale 405-nm light unit for the exposure of prebagged plasma.

Chapter Six I Broad-Spectrum Antimicrobial Efficacy and Compatibility of 405-nm Light for Treatment of 100 mL Prebagged Plasma

6.0 I Introduction

The ideal PRT would provide an optimal balance of antimicrobial activity and blood product compatibility, whilst being relatively inexpensive and simple to implement. This Thesis focuses on the development of a novel, alternative PRT for the treatment of prebagged plasma using visible, violet-blue 405-nm light. As a proof-of-concept, Chapter 4 used a small-scale exposure system to demonstrate the broad antimicrobial action of a fixed 405-nm light treatment for plasma samples, using dose levels that showed compatibility with the plasma itself. Using the same small-scale exposure system, Chapter 5 provided an insight to the antibacterial efficiency and protein compatibility of three different 405-nm light dose delivery regimes for treatment of plasma.

Moving forward, it was essential to scale-up experiments to determine the 405-nm light dose requirements for an effective and compatible treatment of prebagged plasma. Existing knowledge on the use of 405-nm light for treatment of prebagged plasma is limited. To date, only one organism (*S. aureus*) has been investigated in prebagged plasma [Maclean *et al*, 2016], and to the best of the authors knowledge, no research has been conducted to assess the compatibility of 405-nm light with prebagged plasma. This Chapter will investigate the broad-spectrum antimicrobial efficacy and protein compatibility of 405-nm light for treatment of 100 mL prebagged plasma – a significant scale up in volume compared to the 250 µL sample volumes used in Chapters 4 and 5. The use of 100 mL prebagged plasma was an intermediate step before scaling up to clinically-relevant 300 mL plasma bags (which will be the focus of Chapter 7).

To do this, a large-scale, violet-blue 405-nm light unit was designed and developed for the treatment of prebagged plasma. The broad-spectrum antimicrobial efficacy of 405-nm light was then investigated using five common bacterial contaminants and a yeast (*S. aureus*, *S. epidermidis*, *E. coli*, *P. aeruginosa*, *A. baumannii* and *C. albicans)*. This involved exposing artificially contaminated 100 mL plasma bags to increasing doses of 405-nm light (16 $mWcm^{-2}$; ≤403 Jcm^{-2}) using the large-scale light

unit, and assessing post-exposure microbial loads. Post-exposure plasma protein integrity was then investigated using SDS-PAGE, an AOPP assay, clotting assays and human Protein S and fibrinogen ELISAs.

Overall, this study had three key objectives:

1. To design, develop, and characterise a large-scale 405-nm light unit for treatment of prebagged plasma.
2. To investigate the microbial inactivation efficacy of 405-nm light (16mWcm^{-2}; ≤403 Jcm^{-2}) against a range of bacteria and a yeast seeded at ~10^{3}CFUmL^{-1} in 100 mL prebagged plasma using the large-scale light unit.
3. To investigate the compatibility of effective antimicrobial doses of 405-nm light (16mWcm^{-2}; ≤403 Jcm^{-2}) for the treatment of 100 mL prebagged plasma, using a range of proteomic techniques (SDS-PAGE, an AOPP assay, clotting assays, and human fibrinogen and Protein S ELISAs).

6.1 I Design, Development & Characterisation of a Large-Scale 405-nm Light Unit for Treatment of Prebagged Plasma

This section will cover the design, development and characterisation of a large-scale 405-nm light unit for treatment of prebagged plasma. Exact experimental setups, including 405-nm light treatment conditions and blood bag volumes, are detailed in methodology sections.

6.1.1 Design and Development of the 405-nm Light Unit

A prototype light unit was developed to evaluate the use of 405-nm light as a PRT for prebagged plasma. The light source used in the large scale system was a 4-LED array (LZ4-00UB00-U7, Osram LED Engin, USA; Figure 6.1), with a centre wavelength in the region of 405-nm, and a bandwidth of approximately 17 nm at full-width-half-maximum (FWHM). The light unit was composed of six 4-LED arrays, arranged in a 2 × 3 configuration, powered by a 75 W, 15 V 5A dimmable LED driver (Model HLG-80H-15, Type Ab, Mean Well, Netherlands). For thermal management, a heat sink and fan module (Novatech, UK) was bonded to each LED array to prevent heat transfer to test samples (Figure 6.1). The fan modules were powered in parallel by a 12 V driver (Digi-Key, UK). The optical emission spectrum of each LED array, measured using a spectrometer (Model HR4000, Ocean Optics) and SpectraSuite version 2.0.151, are shown in Figure 6.2.

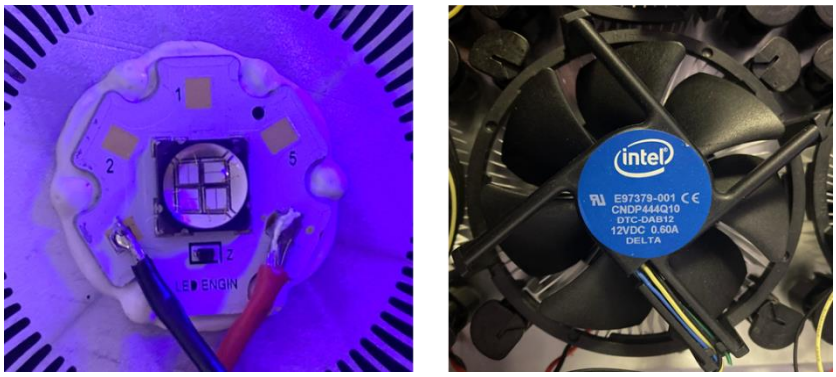

A) B)

Figure 6.1. The 405-nm light source and thermal heat management. Appearance of: A) 4-LED array (Osram LED Engin (USA)) and B) heat sink and fan module.

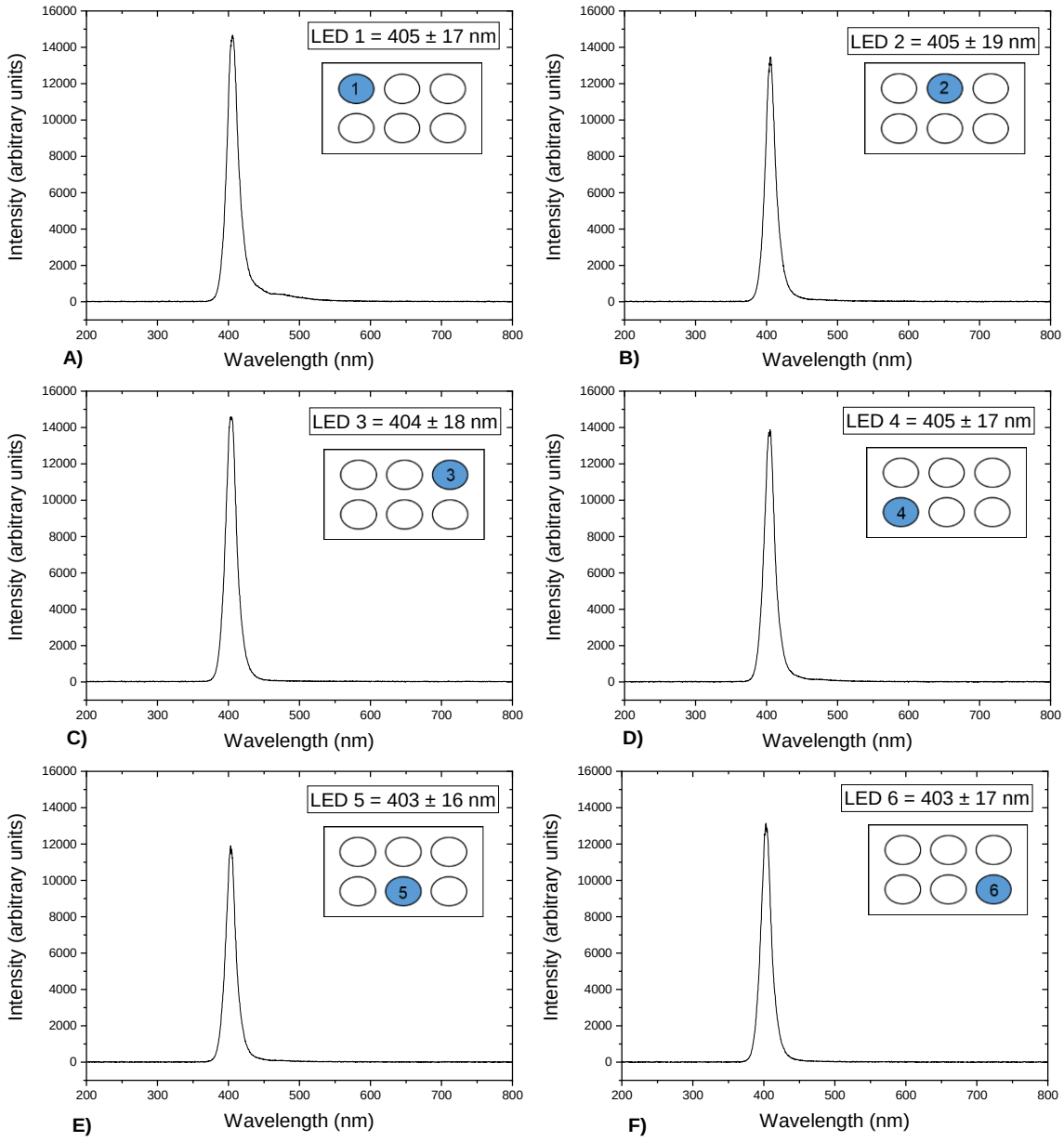

Figure 6.2. Optical emission spectrum of LED arrays used in the large-scale violet-blue light unit for treatment of prebagged plasma. Images show the optical emission spectra for each light source measured using a HR4000 spectrometer (Ocean Optics, Germany) and Spectra Suite software version 2.0.151.

The component list and electrical circuit for the 405-nm light system are provided in Table 6.1 and Figure 6.3, respectively. The LED arrays and fan driver circuits were connected in parallel to the mains supply. The switch was connected to provide dual control of both circuits, to ensure that the LED arrays and fan modules would turn on simultaneously. All electrical components were housed in a metal case (435×240×150 mm). During operation, the large-scale 405-nm light unit was placed on the glass panel of a floor-standing incubator lid to illuminate prebagged plasma (Figure 6.4D). The plasma bag was held inside the incubator (New Brunswick Scientific C25KC, USA), set at 22°C with agitation at 84 rpm, on a custom-built PVC test rig (Figure 6.4E) with an exposure plate approximately 12 cm from the light unit.

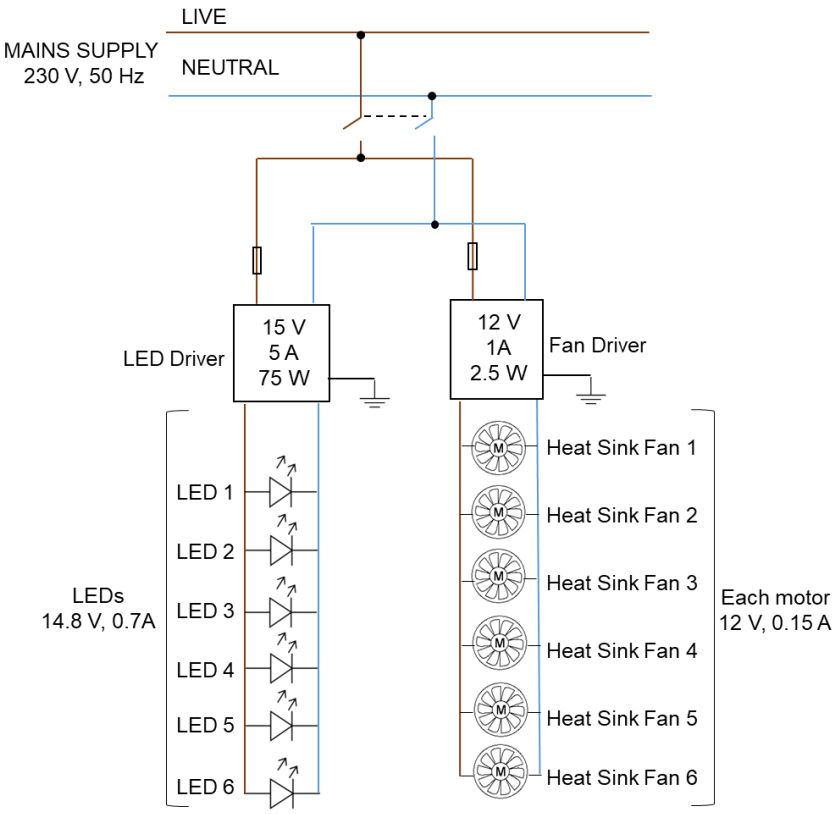

Figure 6.3. Electrical circuit for the large-scale 405-nm light unit. LED arrays were powered in parallel with a 15 V LED driver. A heat sink and fan module, powered in parallel with a 12 V driver, was attached to each LED array to prevent heat transfer.

Table 6.1. Electrical component list for the large-scale 405-nm light unit.

Component	Type	Manufacturer	Manufacturer Number
4-LED array (n=6)	385-410nm Violet LED Emitter	OSRAM LED Engin	LZ4-40UB00-00U7
LED driver (n=1)	Dimmable LED Driver PS TYPE AB, 15V 5A	Mean Well	HLG80H-15A
Heat sink and fan module (n=6)	Intel Socket Aluminium Heat Sink & Fan	Novatech	E97379-001
Fan driver (n=1)	Driver CV AC/DC 12V 1A	Digi-Key	APV-12-12
Switch panel mount (n=1)	Bulgin C14 Snap-In IEC Connector Male, 250v 10A	RS	BZH01/Z0000/02
Power cable & plug (n=1)	Schurter 2m Power Cable, C13, IEC-UK Plug, 250V 10 A	RS	6051.2008

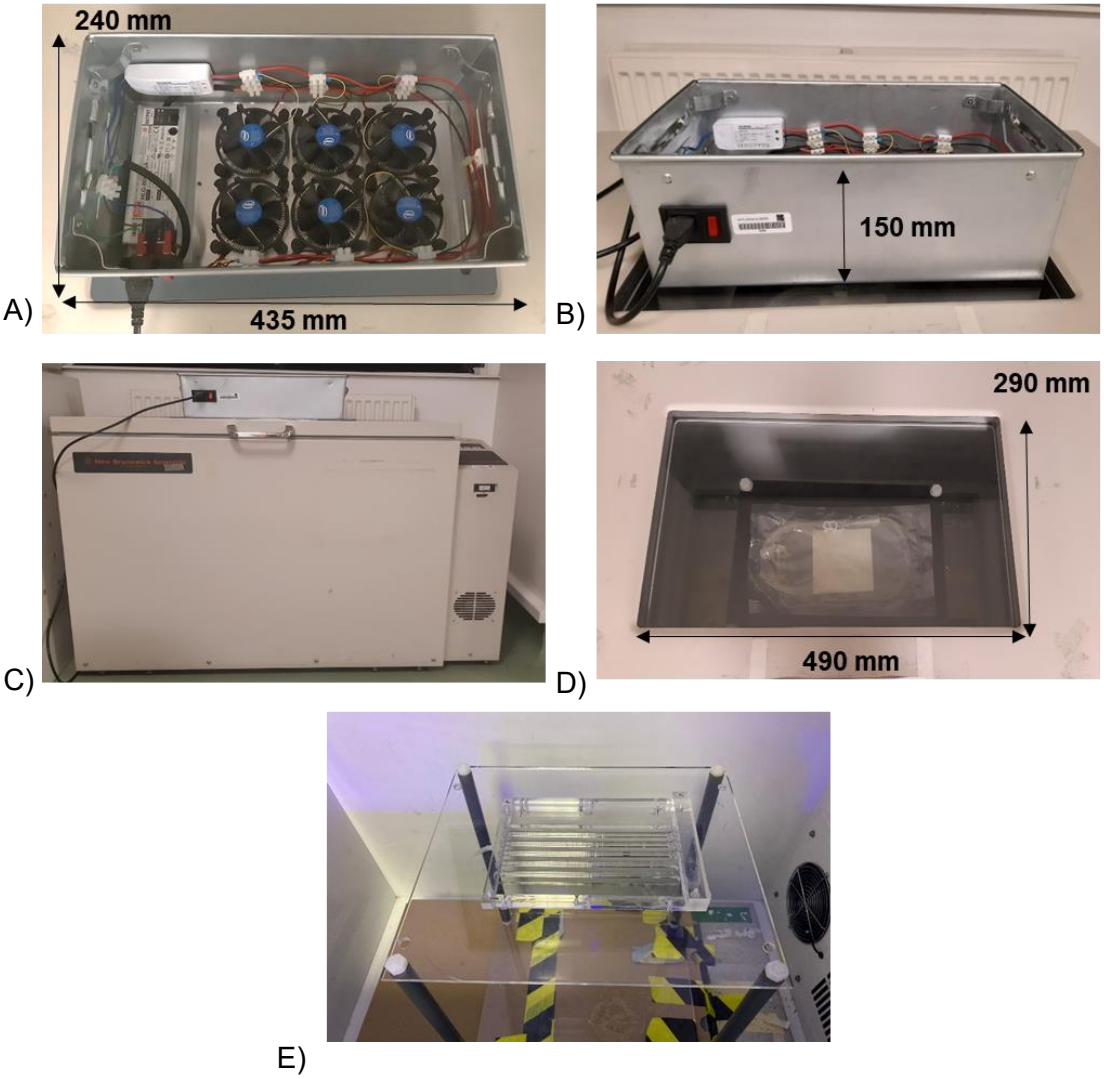

Figure 6.4. The large-scale 405-nm light exposure system for treatment of prebagged plasma. Appearance of: A) electrical components of the light unit, B) metal container, C) standing incubator (New Brunswick Scientific C25KC, USA) D) glass panel on standing incubator lid and E) custom-made PVC test rig with shaker plate.

6.1.2 Characterisation of the Large-scale 405-nm Light Unit

Before conducting experiments, the 405-nm light unit was characterised to establish critical elements including (i) the irradiance profile across the bag surface and (ii) thermal assessment during treatment to ensure no thermal effects on the plasma.

6.1.2.1 Irradiance Profile for the 100 mL Bag Exposure

The 405-nm light unit was held in a fixed position, 12 cm above the base of the shaker plate, where the plasma bags were horizontally positioned. The optical profile of the light distribution across the blood bag (15×13 cm), used for the 100 mL plasma exposure, was measured using a radiant power meter and photodiode detector (LOT-Oriel Ltd, USA). The optical data was mapped using a Contour Colour Map (OriginPro2018 Software), as shown in Figure 6.5. An average irradiance of ~16 mWcm^{-2} was measured across the bag surface, taking account of a 26% reduction in irradiance as the light transmits through the blood bag material and into the plasma.

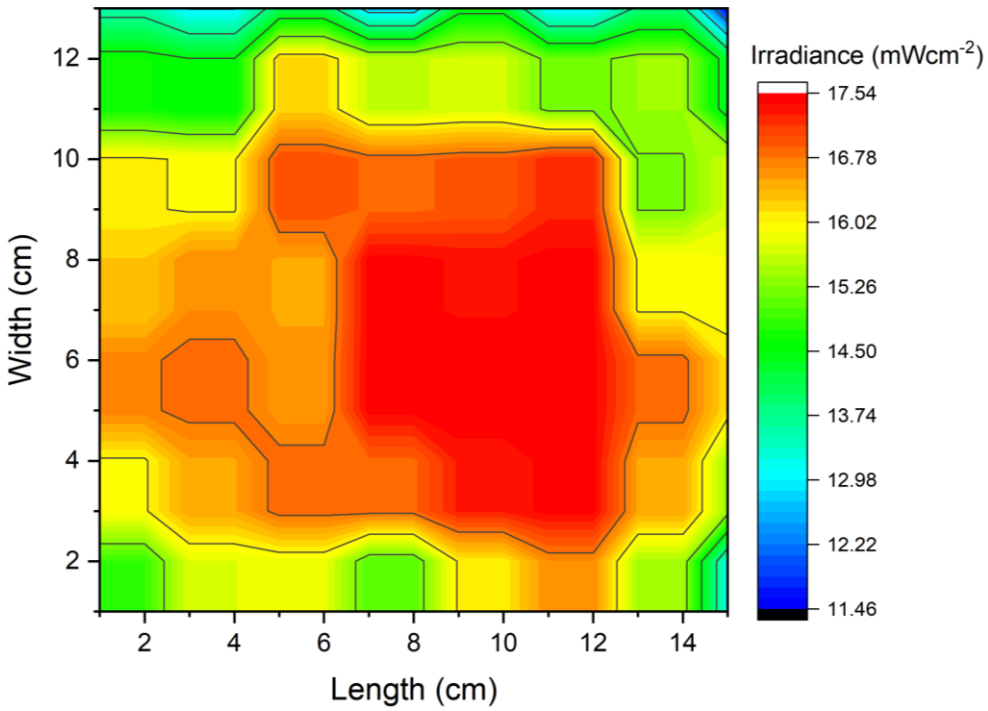

Figure 6.5. Model showing the irradiance profile across the surface area of a 100 mL blood bag. Irradiance profile across the blood bag surface with an average irradiance of ~16 mWcm^{-2} measured, taking account of the loss of light transmission through the PVC blood bag material (plotted using OriginPro 2018 software).

6.1.2.2 Thermal Assessment of the 405-nm Light Exposure System

During light treatment, the blood bag was held inside of an incubator, set at a temperature of 22°C, with the light source positioned on top of the window panel of the incubator. Prior to experimentation using biological material, a test was conducted using 100 mL prebagged PBS to ensure that the temperature of the fluid remained relatively stable during exposures. A 100 mL bag of PBS was held in test conditions (16mWcm^{-2}; ≤403 Jcm^{-2}) with the temperature of the fluid monitored throughout the exposure period using a thermoprobe (KM480, Comark Instruments, UK). As shown in Figure 6.6, the temperature of the PBS did not exceed 22°C throughout the exposure period (~16 mWcm^{-2}; ≤403 Jcm^{-2}), thereby confirming that the 405-nm light treatment did not induce thermal effects.

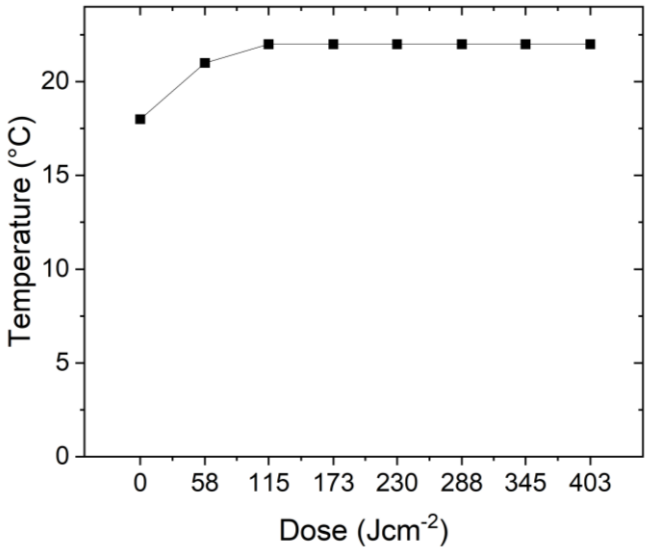

Figure 6.6. Thermal assessment of 100 mL prebagged PBS during 405-nm light treatment (~16 mWcm^{-2}; ≤403 Jcm^{-2}). Image shows the temperature of the PBS measured using a thermoprobe (KM480, Comark Instruments, UK), whilst held in a standing incubator (New Brunswick Scientific C25KC, USA) set at 22°C, during exposure to 405-nm light.

6.2 I Antimicrobial Efficacy of a 405-nm Light Exposure for the Treatment of 100 mL Prebagged Plasma

This section investigates the antimicrobial efficacy of 405-nm light for the treatment of 100 mL prebagged plasma.

6.2.1 Methods: Microbial Inactivation of 100 mL Prebagged Plasma using 405-nm Light

The broad-spectrum antimicrobial efficacy of a fixed 405-nm light exposure for treatment of 100 mL prebagged plasma was investigated. The organisms used in this study: *S. aureus, S. epidermidis* (Gram-positive bacteria)*, E. coli, P. aeruginosa, A. baumannii* (Gram-negative bacteria) and *C. albicans* (yeast). All organisms were cultured as per Section 3.2.3. To prepare organisms for seeding into the plasma, the microbial stock solution was serially diluted *(10-fold dilution; 1 mL microbial suspension into 9 mL PBS)* to a population of ~10^5 $CFUmL^{-1}$. Prior to experimentation, 110 mL frozen plasma (TCS Biosciences Ltd, UK) was thawed at room temperature. To seed the 110 mL plasma at a microbial density of ~10^3 $CFUmL^{-1}$, 1.1 mL plasma was substituted with 1.1 mL 10^5 $CFUmL^{-1}$ microbial suspension. The seeded plasma was mixed thoroughly to ensure the microbial sample was equally dispersed throughout the media. 100 mL seeded plasma was transferred to a 150 mL blood bag (Grifols, UK) for exposure and 10 mL was transferred to a foil-covered Universal to act as a non-exposed control.

As shown in Figure 6.7, 100 mL prebagged plasma *was* exposed to ~16 $mWcm^{-2}$ 405-nm light for up to 7-hrs (≤403 Jcm^{-2}), under agitation (84 rpm). The temperature of plasma was monitored throughout the exposure period using a thermoprobe, to ensure plasma remained at 22°*C* during treatment. Post-exposure, plasma samples were spread-plated (100 µL) or pour-plated (1 mL), depending on the expected population density, on nutrient agar for bacteria, except for *S. epidermidis* and *C. albicans* which were plated on tryptone soya agar, and malt extract broth with 0.1% yeast extract (Oxoid Ltd., UK), respectively. Plates were incubated at 37°C for 24-hrs. Surviving microorganisms were enumerated with results recorded as mean microbial load ($CFUmL^{-1}$, n≥3±SD).

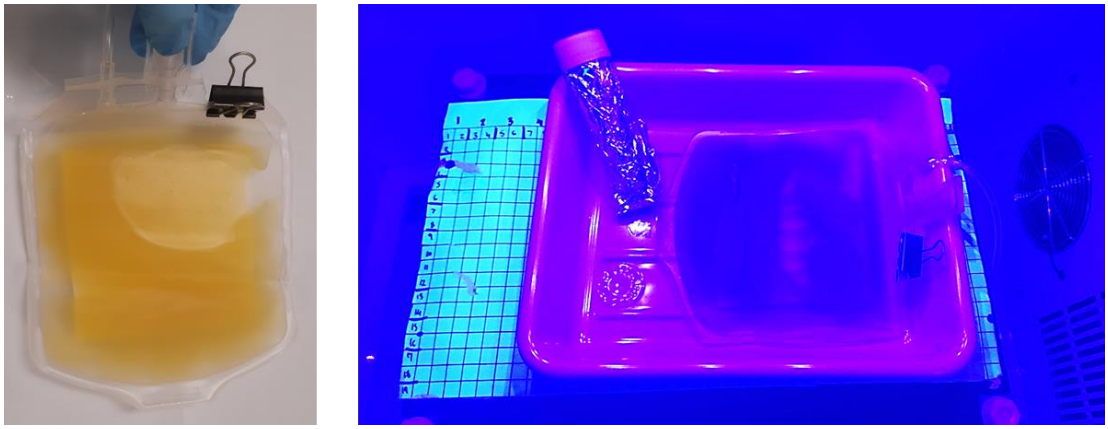

A) B)

Figure 6.7. Experimental arrangement for 405-nm light exposure of 100 mL prebagged plasma. Appearance of (A) 100 mL prebagged plasma and B) configuration of exposed and non-exposed (foil-covered Universal) plasma during light treatment.

6.2.2 Results: Antimicrobial Efficacy of 405-nm Light for Treatment of 100 mL Prebagged Plasma

Figure 6.8 illustrates the efficacy of 16 $mWcm^{-2}$ 405-nm light for inactivation of A) *S. aureus*, B) *S. epidermidis*, C) *E. coli*, D) *P. aeruginosa*, E) *A. baumannii* and F) *C. albicans* seeded at approximately 10^3 $CFUmL^{-1}$ in 100 mL prebagged plasma. All organisms were significantly reduced [$P < 0.05$] after exposure to an initial dose of 58 Jcm^{-2} (1-hr). Inactivation kinetics of *S. aureus, S. epidermidis, P. aeruginosa, A. baumannii* and *C. albicans* were similar, with most of the inactivation (>97%) achieved after exposure to 115 Jcm^{-2} (2-hr) [P = 0.032, 0.036, 0.035, 0.010 and 0.00, respectively]. Contamination levels continued to decrease for the remainder of the exposure period with near-complete inactivation (≤10 $CFUmL^{-1}$) observed following exposure to 288 Jcm^{-2} (5-hr). The reduction of *E. coli* followed a similar trend but required slightly increased doses, with >95% inactivation by 173 Jcm^{-2}. Microbial contamination in non-exposed control samples showed no significant decrease over the treatment period [$P > 0.05$] (contamination levels of *P. aeruginosa* in non-exposed plasma actually rose by >20% over the treatment period [$P = 0.001$]).

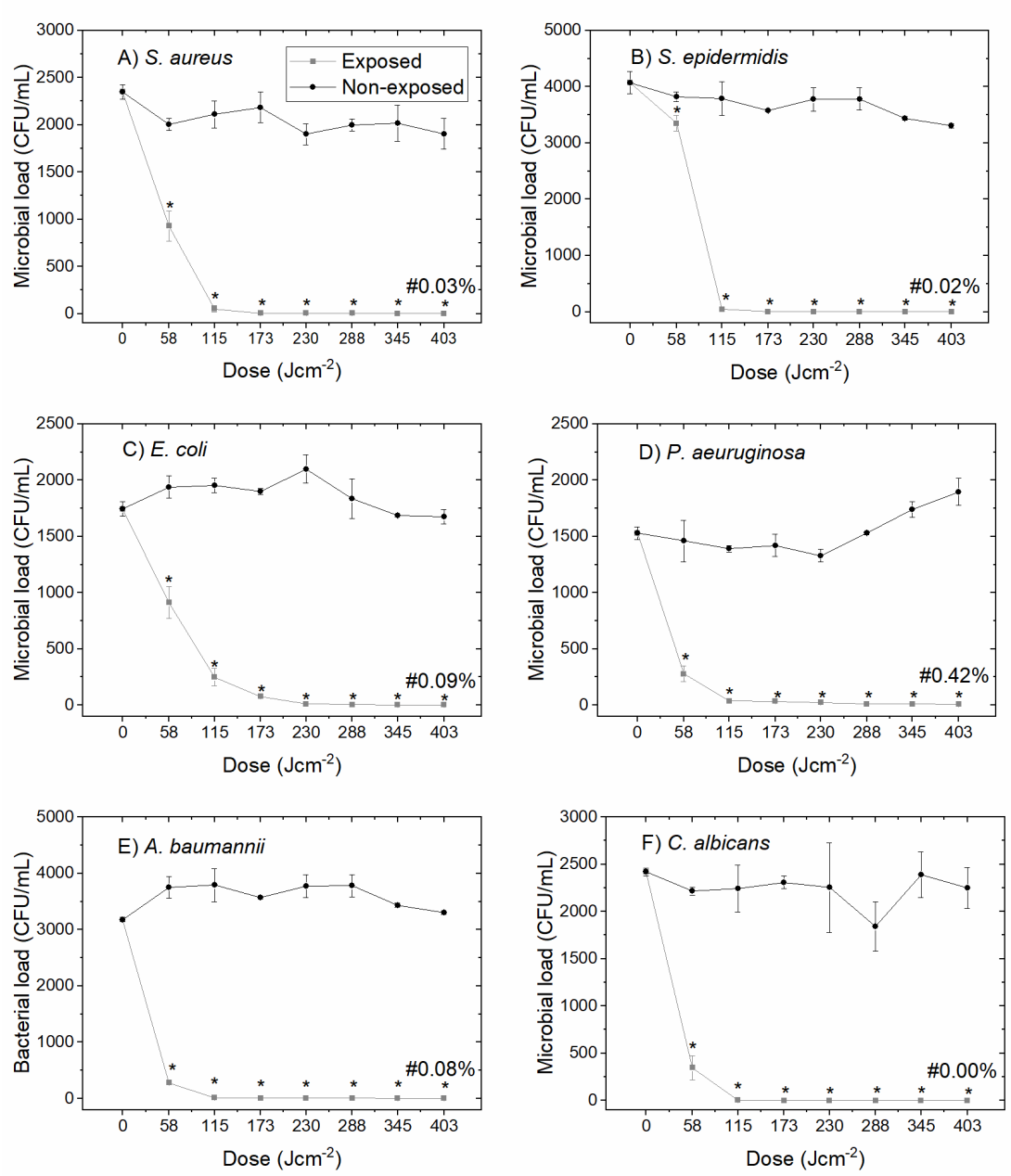

Figure 6.8. Broad-spectrum microbial reduction of 100 mL prebagged plasma using 405-nm light, as a function of dose. 100 mL prebagged plasma, seeded with microbes at ~10^3 CFUmL^{-1} (A, *S. aureus*; B**,** *S. epidermidis*; C, *E. coli*; D, *P. aeruginosa*; E, *A. baumannii* and *F, C. albicans*), was exposed with 16 mWcm^{-2} 405-nm light, under agitation (84 rpm; 22°C), Data represents mean microbial load in CFUmL^{-1} (n=3±SD) with (*) representing a significant decrease in the microbial load in exposed plasma when compared to the equivalent non-exposed control [$P \leq 0.05$; 2-sample t-test (Minitab v18)]. (#) represents the % survival after exposure to 403 Jcm^{-2}.

6.3 I Analysis of the Protein Compatibility of 405-nm Light with 100 mL Prebagged Plasma

To assess whether the fixed 405-nm light treatment was compatible with the prebagged plasma itself, a range of protein assays were used to examine post-exposure protein integrity and clotting activity. 100 mL prebagged plasma was exposed to 405-nm light (~16 $mWcm^{-2}$; ≤403 Jcm^{-2}), with 1 mL volumes of exposed and non-exposed plasma collected every hour over a 7-hr treatment (dose equivalents of 58, 115, 173, 230, 345 and 403 Jcm^{-2}). Sample were transferred to Eppendorfs for storage at -20°C until required for protein analysis. The following sections will cover the range of protein assay used to assess the compatibility of 405-nm light with 100 mL prebagged plasma:

- General protein integrity via SDS-PAGE;
- General oxidative stress levels in plasma via an AOPP assay;
- Stability of proteins involved in the extrinsic coagulation pathway via PTT assays;
- Stability of proteins involved in the intrinsic coagulation pathway via APTT assays;
- Integrity of essential clotting and anti-clotting proteins, fibrinogen, and Protein S respectively, using enzyme-linked immunosorbent assays.

6.3.1 Assessment of General Protein Integrity of 405-nm Light Exposed 100 mL Prebagged Plasma using SDS-PAGE

SDS-PAGE was used as an indicator tool to assess general protein integrity of exposed and non-exposed plasma through visual comparison of protein band patterns. General methodology is provided in Section 3.5.1.

Figure 6.9A is an image of the master gel used to assess plasma protein integrity and compare protein band patterns of plasma exposed to 16 $mWcm^{-2}$ 405-nm light (≤403 Jcm^{-2}). The electrophoretic band patterns of plasma exposed to doses up to 403 Jcm^{-2} show no major differences compared to equivalent non-exposed control samples. Minimal differences were observed in band patterns at 45–80 kDa (Section highlighted in Figure 6.9B) between exposed and non-exposed plasma up to 345 Jcm^{-2}. This change may be partly due to sample-to-sample variation, shown in Appendix A, as the intensity level of plasma proteins exposed to 403 Jcm^{-2} are similar to that of other non-exposed controls.

There were clearer indications of protein modification of HMWPs (80–198 kDa) following exposure to 405-nm light. Visually detectable differences were observed between exposed and non-exposed controls following exposure to doses ≥173 Jcm^{-2} (lane 5 *versus* 6), with the loss and blurring of band patterns more apparent as the applied dose increases. Nevertheless, comparison with the positive control (+ve), representing complete plasma protein degradation, suggests that the degree of modification observed in plasma exposed to doses ≤173 Jcm^{-2}, should not be regarded as major damage.

Whilst SDS-PAGE analysis provided an insight to general protein compatibility, more-in-depth proteomic tests were conducted to examine key functional proteins and clotting factors that are known to reside in the HMWP region of gels.

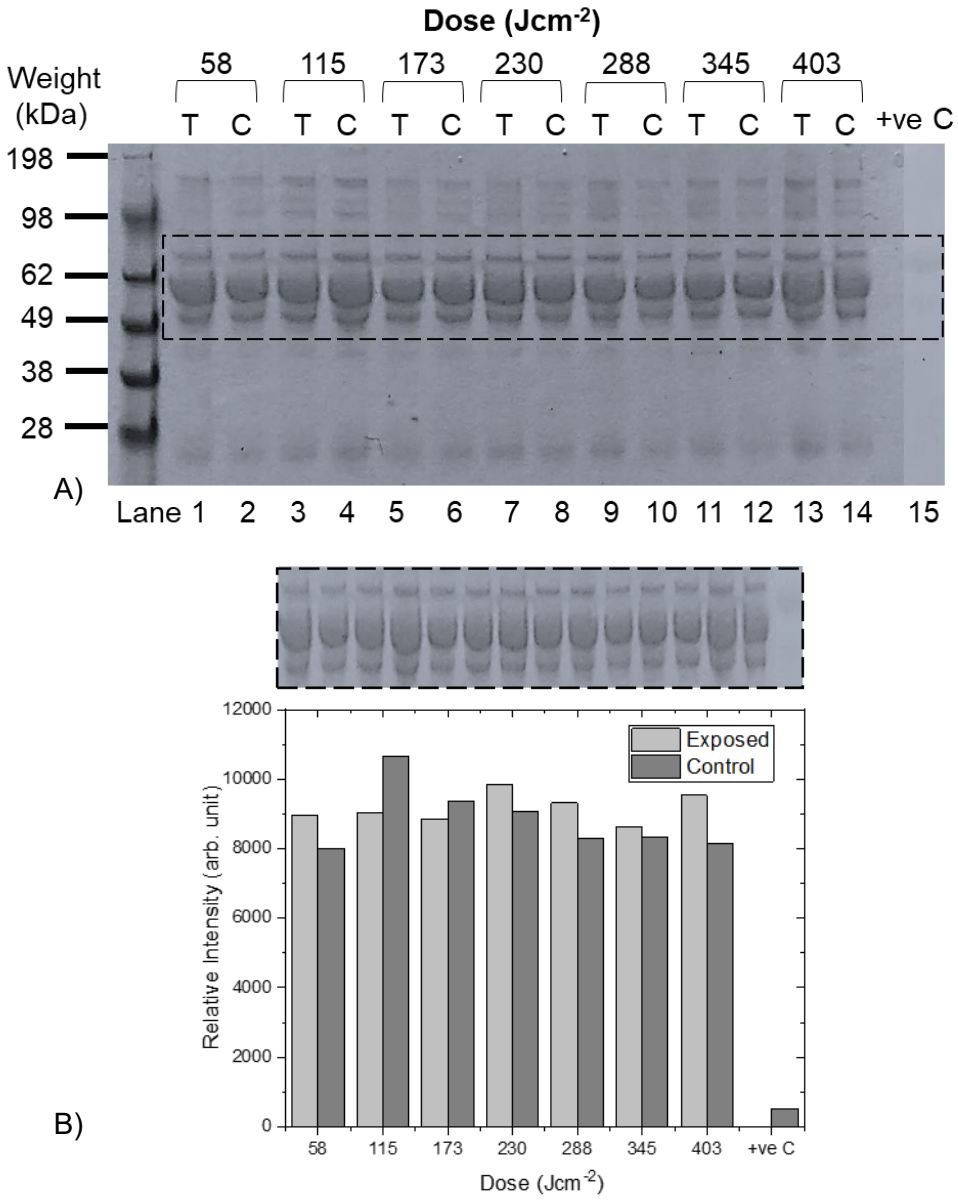

Figure 6.9. Assessement of the compatability of 405-nm light with 100 mL prebagged plasma using SDS-PAGE. Plasma exposed to 16mWcm^{-2} 405-nm light (≤403 Jcm^{-2}), and their paired non-exposed control samples were analysed. A: SDS-PAGE master gel. The protein profiles show plasma samples which had been exposed in odd lanes: *1 (58 Jcm^{-2}), 3 (115 Jcm^{-2}), 5 (173 Jcm^{-2}), 7 (230 Jcm^{-2}), 9 (288Jcm^{-2}), 11 (345 Jcm^{-2})* and *13 (403 Jcm^{-2})* labelled 'T' for test, and equivalent non-exposed control samples posiitoned in even lanes (*2, 4, 6, 8, 10, 12, 14*), labelled 'C' for control. A positive control (*+ve*) representing complete protein degradation was included for comparitive purposes. B: Semi-quantiative analysis of protein levels within 45-80 kDa region (Image J software).

6.3.2 Assessment of Post-Exposure Oxidative Stress Levels in 100 mL Prebagged Plasma using an AOPP Assay

An AOPP assay was used to quantitatively measure the level of oxidative stress in 405-nm light exposed 100 mL prebagged plasma compared to non-exposed plasma. General methodology for the AOPP assay is provided in Section 3.5.2. The level of AOPPs, indicative of oxidative damage, in plasma exposed to 405-nm light for up to 7-hr (16 mWcm^{-2}, ≤403 Jcm^{-2}) and paired non-exposed control samples were assessed.

As shown in Figure 6.10, no differences in AOPP levels, representative of oxidative damage, were observed between exposed and non-exposed plasma samples [$P > 0.05$] throughout the 405-nm light treatment (≤403 Jcm^{-2}). AOPP levels in non-exposed control samples showed no significant change [$P = 0.153$, 2-sample t test]. The slight fluctuations in AOPP levels observed in exposed and non-exposed controls, detected between 18.4–24.0 µM over the treatment period, are likely due to natural variances in fibrinogen, which is thought to be the key plasma protein responsible for AOPP production.

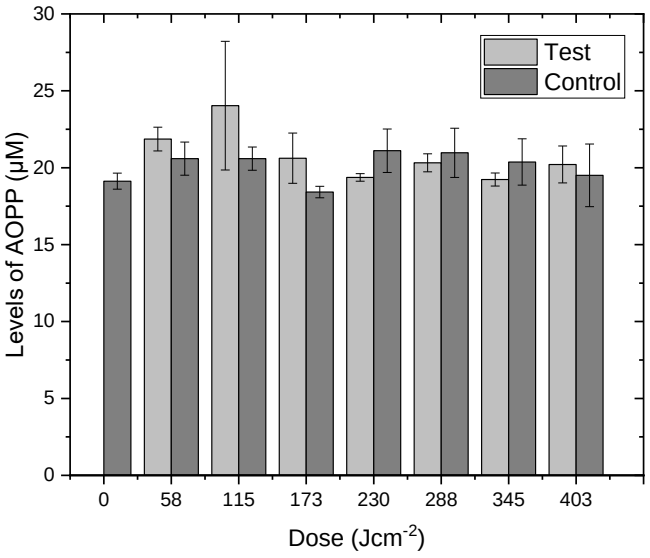

Figure 6.10. Levels of AOPPs detected in 100 mL prebagged plasma following exposure to 16 mWcm^{-2} 405-nm light (≤403 Jcm^{-2}). The concentration of AOPPs is expressed as µM of Chloramine-T equivalents, marker of oxidative damage, with values corrected for dilution factor. Data represent mean (n=3)±SD. No significant changes in AOPP levels were detected in exposed plasma when compared to the equivalent non-exposed control [$P > 0.05$; 2-sample *t* test (Minitab v18)].

6.3.3 Assessment of Post-Exposed Clotting Activity of 100 mL Prebagged Plasma Using a PTT Assay

To examine whether 405-nm light affects the coagulation function of plasma, the prothrombin time (PTT) assay was performed to assess the stability of extrinsic-common pathways. Methodology was followed as per Section 3.5.3. The PTT assay was conducted on two separate 100 mL plasma bags, with data presented separately (Figure 6.11A and 6.11B) due to batch-to-batch variation in clotting times. The clotting times of plasma exposed to doses up to 115 Jcm^{-2} (2-hr) were similar to paired non-exposed controls [$P > 0.05$]. This was the case for both 100 mL prebagged plasma exposures (Figure 6.11A and 6.11B). After this point, PTT values increased steadily with increased exposure to 405-nm light.

As shown in Figure 6.11A, a significant increase in PTT values was detected in plasma exposed to doses ≥173 Jcm^{-2}, with clotting times prolonged by up to 9% compared to non-exposed controls [$P = 0.013$]. Following exposure to a dose of 403 Jcm^{-2}, clotting times of exposed plasma increased by 51%, from a mean value of 23 to 35 s. Similar results were observed in Figure 6.11B. The time to clot in plasma exposed to a dose of 173 Jcm^{-2} increased from a mean value of 32 to 37 s representing an increase of 13% [$P = 0.007$]. PTT values increased linearly upon exposure to increasing dose levels, with PTT values increasing from 33 s in non-exposed controls, to a mean of 48 s after exposure to 403 Jcm^{-2} [$P = 0.00$, 46% increase]. PTT values for non-exposed controls, in both experiments (Figure 6.11A and B) were stable over the 7-hr treatment period [$P > 0.05$].

Table 6.2 details the percentage increase in PTT of plasma exposed to 405-nm light doses up to 403 Jcm^{-2} compared to equivalent non-exposed controls. The average percentage increase in PTT for exposed plasma was calculated using sets of data from two separate 100 mL plasma bag exposures (Figure 6.11A and B). The average time to clot for plasma slightly increased following exposure to 405-nm light doses of 58, 115 and 173 Jcm^{-2} by 3, 10 and 11% respectively. The maximum PTT value was recorded following exposure to a dose of 403 Jcm^{-2}, with clotting times increasing by 49%.

Overall, these results indicate that doses up to 115 Jcm^{-2} applied to 100 mL prebagged plasma, did not significantly effect the functionality of clotting proteins tested through the PPT assay.

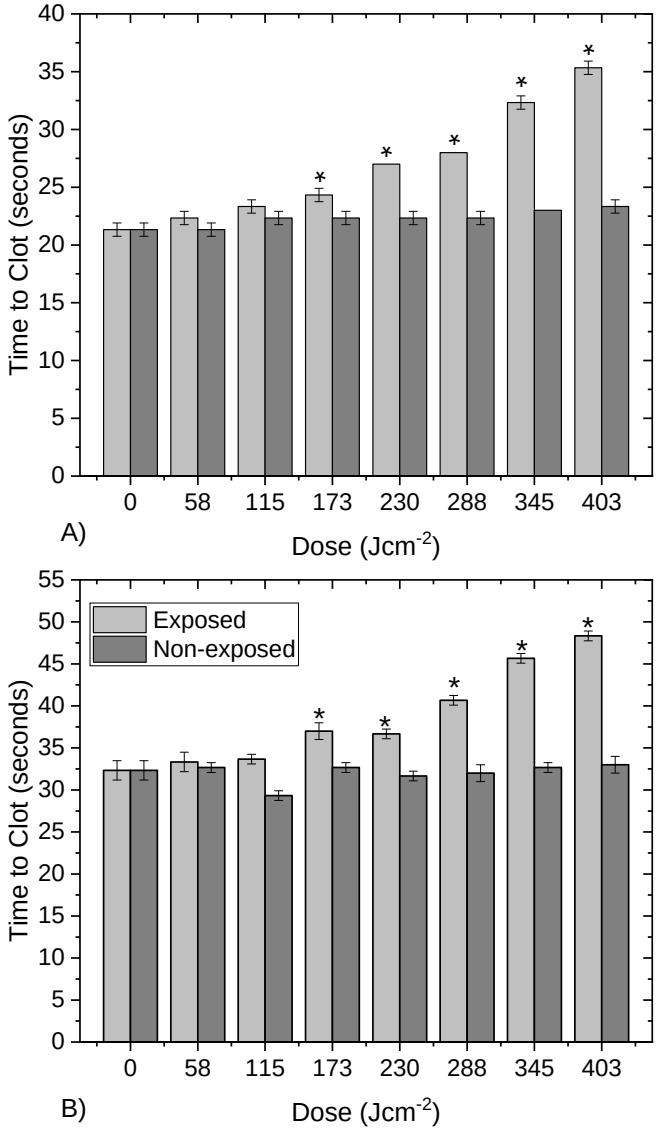

Figure 6.11. Assessement of the PTT clotting activity of 100 mL prebagged plasma exposed to 405-nm light (16 mWcm^{-2}; ≤403 Jcm^{-2}). Figure shows the time to clot (extrinsic and common factors) for plasma exposed to 16 mWcm^{-2} 405-nm light for 1–7-hrs (58, 115, 173, 230, 345 and 403 Jcm^{-2}) and paired non-exposed controls. PTT test assay was conducted on two separate 100 mL plasma bags (A and B). Data represents mean clotting times (n≥3±SD) with asterisks (*) representing significant increase in the time to clot in exposed plasma compared to the paired non-exposed control [P ≤ 0.05; 2-sample t-test (Minitab v18)].

Table 6.2. Change in clotting times (via PTT) of 100 mL prebagged plasma following exposure to 405-nm light (16 mWcm^{-2}; ≤403 Jcm^{-2}). The change in clotting time is recorded as percentage increase (%), between exposed and non-exposed plasma.

Dose (Jcm^{-2})	Test A Mean (% increase)	Test B Mean (% increase)	Mean of Tests (% increase)
58	4.6	2.0	**3.3**
115	4.4	12.5	**9.5**
173	8.9	13.2	**11.0**
230	20.8	15.7	**18.2**
288	25.3	27.0	**26.1**
345	40.5	39.8	**40.1**
403	51.4	46.4	**48.9**

6.3.4 Assessment of Post-Exposed Clotting Functionality of 100 mL Prebagged Plasma Using APTT Assays

The APTT assay was used to assess the stability of clotting factors in the intrinsic (VIII, IX, XI, and XII) and common (I, II, V and X) coagulation pathway, of 405-nm light exposed plasma. General methodology for the APTT assay is provided in Section 3.5.4. An APTT assay was conducted on two separate 100 mL prebagged plasma exposures (Figure 6.12A and B). APTT values for plasma exposed to 16 mWcm^{-2} 405-nm light for 1–7-hr (58, 115, 173, 230, 345 and 403 Jcm^{-2}), and paired non-exposed control samples were recorded manualy using a stopwatch.

As shown in Figure 6.12A, there was no difference in the time to clot between plasma exposed to doses ≤115 Jcm^{-2} and paired non-exposed controls [$P > 0.05$]. An initial increase in APTT values was observed following exposure to a dose of 173 Jcm^{-2} with clot formation detected at 123 s and 100 s for exposed and non-exposed plasma respectively, representing a 18% increase in time to clot [$P = 0.001$]. After this point, a linear and upward trend in clotting time was observed with exposure to increased 405-nm light doses up to 403 Jcm^{-2}.

For the second 100 mL plasma bag exposure, the APTT values of plasma exposed to ≤230 Jcm^{-2} were slightly higher than compared their paired non-exposed controls, with a maximum 8% increase observed over the initial exposure period. A stark increase in clotting time was observed following exposure to a dose of 288 Jcm^{-2}, where APTT values increased from 105 s in non-exposed control plasma to 156 s in

exposed plasma, representing a 32% increase in time to clot. APTT values continued to increase following exposure to 405-nm light with a 41% increase in clotting time recorded in plasma exposed 403 Jcm^{-2}. Clotting times in non-exposed controls, in Figure 6.12A and B, showed no significant change over the 7-hr treatment period [$P > 0.05$].

Table 6.3 details the percentage increase in APTT of plasma exposed to 405-nm light doses up to 403 Jcm^{-2} compared to equivalent non-exposed controls. Considering the effect on clotting times from both plasma bag exposures, a dose of 115 Jcm^{-2} would be considered the safe upper threshold at which 405-nm light had a minimal effect (5% increase in clotting time) on the functionality of clotting proteins tested through the APPT assay. However it should be highlighted that the threshold dose levels are notably different when the bag exposures are analysed independently. A dose of 230 Jcm^{-2} had minimal effect on the clotting activity of the plasma in the second bag exposure (Figure 6.12B), whereas this dose level reduced the clotting function of the plasma from the first bag exposure to a much greatter extent (Figure 6.12A) (7.9% versus 28.8% increase in time to clot respectively).

The results from the APTT clotting assays therefore highlight the batch-to-batch variation in plasma. To mitigate this, the number of clotting tests should be increased to improve the realibiltiy of the results.

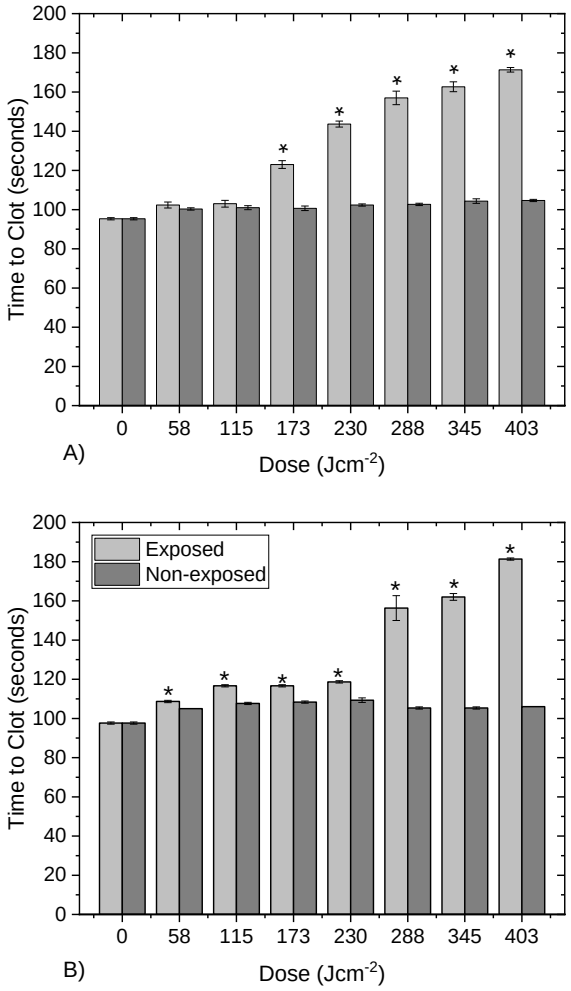

Figure 6.12. Assessement of the APTT clotting activity of 100 mL prebagged plasma exposed to 405-nm light (16 mWcm^{-2}; ≤403 Jcm^{-2}). Time taken for clot formation (intrinsic and common factors) for plasma exposed to 16 mWcm^{-2} 405-nm light for 1–7-hrs (58, 115, 173, 230, 345 and 403 Jcm^{-2}) and paired non-exposed controls. An APTT assay was conducted on two separate 100 mL plasma bags (A and B). Data represents mean clotting times (n≥3±SD) with asterisks (*) representing significant increase in the time to clot in exposed plasma compared to the paired non-exposed control [$P \leq 0.05$; 2-sample t-test (Minitab v18)].

Table 6.3. Change in clotting times (via APTT) of 100 mL prebagged plasma following exposure to 405-nm light (16 mWcm^{-2}; ≤403 Jcm^{-2}). The change in clotting time is recorded as percentage increase (%), between exposed and non-exposed plasma.

Dose (Jcm^{-2})	Test A Mean (% increase)	Test B Mean (% increase)	Mean of Tests (% increase)
58	2.0	3.4	**2.7**
115	1.9	7.7	**4.8**
173	18.2	7.1	**12.7**
230	28.8	7.9	**18.3**
288	34.6	32.6	**33.6**
345	35.9	35.0	**35.4**
403	38.9	41.5	**40.2**

6.3.5 Determination of Fibrinogen and Protein S levels in 405-nm Light Exposed 100 mL Prebagged Plasma

To assess whether 405-nm light affects the integrity of essential clotting and anti-clotting proteins in the 100 mL prebagged plasma, the Human Protein S and Fibrinogen enzyme-linked immunosorbent assays (ELISAs) were used as per the methods in Sections 3.5.5 and 3.5.6, respectively.

Results from the fibrinogen and Protein S assay, conducted on 405-nm light exposed 100 mL prebagged plasma are shown in Figure 6.13A and 6.13B, respectively. Minimal reductions were observed throughout the exposure period, with a maximum reduction of 1.7% for fibrinogen, after 58 Jcm^{-2} [P = 0.59], and 2.0% for Protein S, after 403 Jcm^{-2} [P = 0.47]. Fibrinogen levels were relatively stable throughout the treatment period, with slight variations in the region of 0.68–0.69 mgmL^{-1} for both exposed and non-exposed plasma. Protein S content slightly varied between 5.76–6.29 µgmL^{-1} and 5.36–5.88 µgmL^{-1} for exposed and non-exposed human plasma throughout the exposure period, respectively.

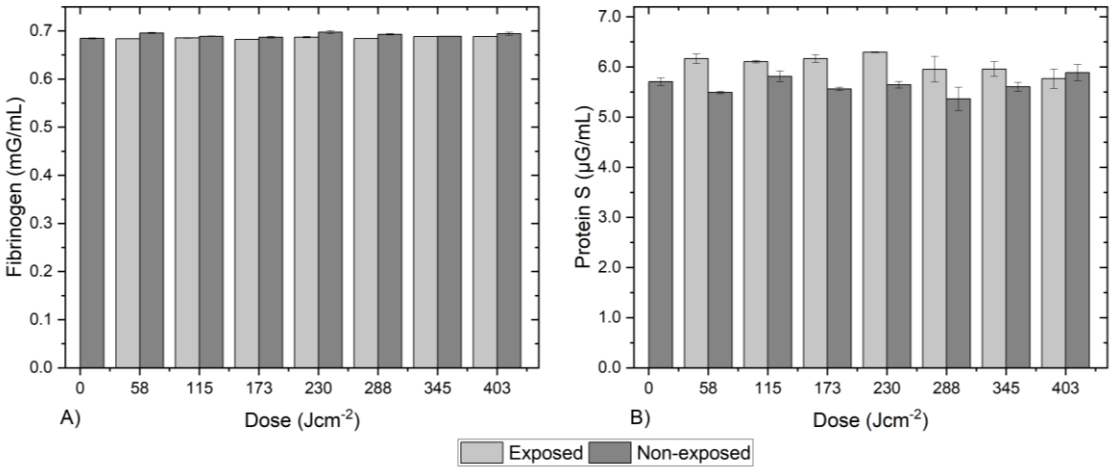

Figure 6.13. Fibrinogen (A) and Protein S (B) levels in 405-nm light exposed 100 mL prebagged plasma (16 mWcm$^{-2,}$ ≤403 Jcm^{-2}). Data represents the mean concentration of fibrinogen in plasma (n = 2 ± SD). No significant reductions in protein content were detected between exposed and non-exposed controls [*P* > 0.05; 2-sample *t* test (Minitab v18)].

6.4 I Discussion

This Chapter demonstrates the broad-spectrum antimicrobial efficacy and protein compatibility potential of 405-nm light for treatment of prebagged plasma, using 100 mL volumes. Exposure of small 100 mL prebagged plasma, was used as a proof-of-concept to demonstrate that 405-nm light can inactivate a range of microbial contaminants seeded in plasma whilst held within sealed blood bags. A range of protein assays were then used to investigate the compatibility of effective antimicrobial doses with 405-nm light exposed, 100 mL prebagged plasma.

Inactivation kinetics for all organisms were similar with the majority of inactivation achieved by 2-hrs (115 Jcm^{-2}), except for *E. coli,* a Gram-negative bacterium, that required 4-hrs (230 Jcm^{-2}) to achieve comparable activation. As expressed in previous chapters, the increased tolerance of *E. coli* to 405-nm light has been frequently reported in both non-biological and biological media including plasma [Nitzan *et al*, 2004, Maclean *et al*, 2009, 2016; McKenzie *et al*, 2016]. Violet-blue light and broader photodynamic studies show that Gram-positive bacteria tend to have greater susceptibility to 405-nm light than Gram-negative when suspended in non-biological media which is thought to be due to differences in the intracellular porphyrins expressed by the microbe, the key drivers for 405-nm light inactivation, and/or differences in cell structure.

In the work of this Chapter however, Gram-negative bacteria *P. aeruginosa* and *A. baummannii*, show similar susceptibility to inactivation compared to Gram-positive staphylococci (similar trend reported in Chapter 4 using small-scale testing), which strengthens the hypothesis that the photosensitisation of agents within plasma, including flavins and chromophores, have the potential to enhance the antimicrobial effects of 405-nm light caused by extracellular oxidative damage to the outer membrane of Gram-negative organisms. Enhanced inactivation of Gram-negative bacteria in plasma, is clinically beneficial as Gram-negative infections are responsible for the majority of transfusion-associated bacterial sepsis fatalities [Brecher and Hay, 2005].

During this study, it became apparent that some bacterial species were unstable whilst suspended in larger volumes of plasma. Microbial inactivation tests were conducted using *Bacillus cereus, Klebsiella pneumonia, Yersinia Enterobacter* and *Enterobacter cloacae* however microbial counts were undetectable in exposed and non-exposed control plasma throughout the 7-hr period. As the inactivation efficacy of 405-nm light could not be measured, the microbial data was excluded from this study. As these microbes were successfully investigated in small-scale studies (Chapter 4), it is thought that these microbes may be interacting with processing agents in plasma when suspended in large volumes. Future work should therefore, repeat these microbial tests using different batches of plasma, or sourcing bacterial strains cultured from blood.

Comparison of the dose requirements for bacterial inactivation in low volume samples *versus* larger volume suspensions (250 µL samples *versus* 100 mL bags), shows that approximately 70% less dose is required to achieve comparable reductions in 100 mL bags compared to 250 µL samples (115 Jcm^{-2} compared to 360 Jcm^{-2}). As the sample depth in both cases was 1 cm, the reduced dose requirement is likely due to the fact that different treatment regimes were used to apply the antimicrobial dose, and that the bag exposure were performed under which increases the likelihood of 405-nm light interacting with microbes at the surface level of the bag. The need for agitation during the light treatment, will be even more important when scaling-up to larger, more clinically-relevant bag volumes.

This Chapter also investigated the protein compatibility potential of 405-nm light for treatment of prebagged plasma for the first time. Table 6.4 compares the threshold dose at which significant changes in protein integrity and/or functionality were

observed in 405-nm light exposed 100 mL prebagged plasma using a range of protein assays. As shown, no signs of general oxidative protein damage (measured via AOPP assay) nor changes in the levels of fibrinogen or Protein S were observed following exposure to doses up to 403 Jcm^{-2}. However, a notable increase in time to clot was observed following exposure to a dose of 173 Jcm^{-2}, with PTT and APTT clotting times increasing by 11% and 13% respectively. Similar findings were reported in Chapter 5, where PTT and APTT clotting times in small volume samples exposed to a similar dose level (10 $mWcm^{-2}$, 180 Jcm^{-2}) increased by 13% and 14% respectively.

At this dose, the degradation of HMWPs was also observed in SDS-PAGE analysis. This indicates that plasma proteins (80 – 198 kDa) including complement proteins (C3, C4 and Factor H), macroglobulins and ceruloplasmin, show susceptibility to degradation following exposure to 405-nm light doses of ≥173 Jcm^{-2}, in 100 mL prebagged plasma. The earliest signs of 405-nm light induced protein damage in small-scale plasma exposures in Chapter 4, were also observed in the HMWP region (Figure 4.4). The loss of complement proteins may not be considered clinically important, as they are in fact associated with post-transfusion haemolytic reactions, and can trigger an inflammatory response and increase tissue damage [Roumenina *et al,* 2019]. However, the retention of macroglobulins, a broad-spectrum protease inhibitor, and ceruloplasmin, an essential copper-carrying protein, are clinically important, therefore future work should include specific ELISAs to quantify protein levels to ensure post-treatment levels are above normal threshold levels for transfusion.

Table 6.4. Comparison of the threshold dose at which significant changes in protein integrity and/or functionality observed in 100 mL prebagged plasma exposed to 405-nm light (16 $mWcm^{-2}$; ≤ 403 Jcm^{-2}).

Proteomic test	Dose level at which changes were detected (Jcm^{-2})	Protein showing susceptibility
SDS-PAGE	≥173	High molecular weight proteins; complement proteins (C3, C4 and Factor H), macroglobulins and ceruloplasmin.
AOPP	No significant change	No change in AOPP levels after exposure to doses ≤403 Jcm^{-2}
PTT	≥173	Coagulation factors VII (extrinsic) and I, II, V, X (common)
APTT	≥173	Coagulation factors VIII, IX, XI, and XII (intrinsic) and I, II, V, X (common)
Human Protein S ELISA	No significant change	Little to no change in Protein S levels after exposure to doses ≤403 Jcm^{-2} – 2% loss
Human Fibrinogen ELISA	No significant change	No change in fibrinogen levels after exposure to doses ≤403 Jcm^{-2} – 1.7% loss

Within the context of this Chapter, a dose of 115 Jcm^{-2} 405-nm light was identified as an effective and compatible treatment, capable of broad-spectrum microbial inactivation in 100 mL prebagged plasma, without visible degradation of proteins. The protein compatibility results obtained in this study have highlighted that clotting factors, measured via PTT and APTT assay, may be the most sensitive to 405-nm light degradation. This indicates that, of all protein assays employed in this research, the use of clotting assays may be the most sensitive tool to accurately measure the compatibility of 405-nm light with plasma proteins.

Whilst 100 mL bags are smaller than those used in a clinical setting, the use of lower volumes was important to generate proof-of-concept microbial inactivation and protein compatibility data whilst minimizing the use, wastage and cost of biological media. The next Chapter will scale up experiments to assess the pathogen reduction efficacy and potential compatibility of 405-nm light for the treatment of 300 mL prebagged plasma, to reflect a more clinically relevant scenario.

Chapter Seven I 405-nm Light as a PRT for the Treatment of 300 mL Prebagged Plasma

7.0 I Introduction

The final stage of the experimental work of this Thesis, aimed to scale up the prebagged plasma treatments, from the 100 mL volumes used in Chapter 6, to a more clinically representative volume of 300 mL. As demonstrated in Chapter 6, 405-nm light is capable of broad-spectrum microbial inactivation (Gram-positive and Gram-negative bacteria and yeast) for treatment of 100 mL prebagged plasma using dose levels (115 Jcm^{-2}) that preserve plasma protein integrity and functionality. To underpin the operational requirements for a safe and effective 405-nm light treatment for clinical application, this chapter scaled up experiments to assess the antimicrobial efficacy and compatibility of 405-nm light for the treatment of larger volume, 300 mL prebagged plasma.

The large-scale 405-nm light unit (detailed in Section 6.1.1 and 6.1.2) was also employed in this chapter for the treatment of 300 mL plasma bags. Microbial inactivation tests were first conducted, whereby large volumes of prebagged plasma artificially contaminated with three key problematic organisms (*S. aureus*, *E. coli and C. albicans*, representative of a Gram-positive bacterium, a Gram-negative bacterium, and a yeast, respectively*)*, were exposed to a fixed 405-nm light treatment (16 $mWcm^{-2}$; ≤403 Jcm^{-2}). A range of proteomic tests were then performed to assess post-exposure protein integrity and coagulation function of 300 mL prebagged plasma to evaluate the compatibility of effective antimicrobial doses of 405-nm light with plasma.

This study had two key objectives:

1. To assess the microbial inactivation efficacy of 405-nm light against key problematic organisms commonly associated with TTIs (*S. aureus, E. coli* and *C. albicans*), in 300 mL prebagged plasma using a large-scale light unit.
2. To assess the compatibility of antimicrobial doses of 405-nm light with plasma proteins for the treatment of 300 mL prebagged plasma, using a range of proteomic techniques (SDS-PAGE, AOPP assay, clotting assays, and human fibrinogen and Protein S ELISAs).

7.1 I Antimicrobial Efficacy of a 405-nm Light Exposure for the Treatment of 300 mL Prebagged Plasma

This section will cover the test regime used to assess the antimicrobial efficacy of 405-nm light for the treatment of 300 mL prebagged plasma.

7.1.1 *Methods: Pathogen Reduction of 300 mL Prebagged Plasma using 405-nm Light*

The optical profile of the light distribution across the blood bag (18×13 cm), used for the 300 mL plasma exposure, is shown in Figure 7.1. An average irradiance of ~16 mWcm^{-2} was measured across the bag surface, taking account of a 26% reduction in irradiance as the light transmits through the blood bag material and into the plasma.

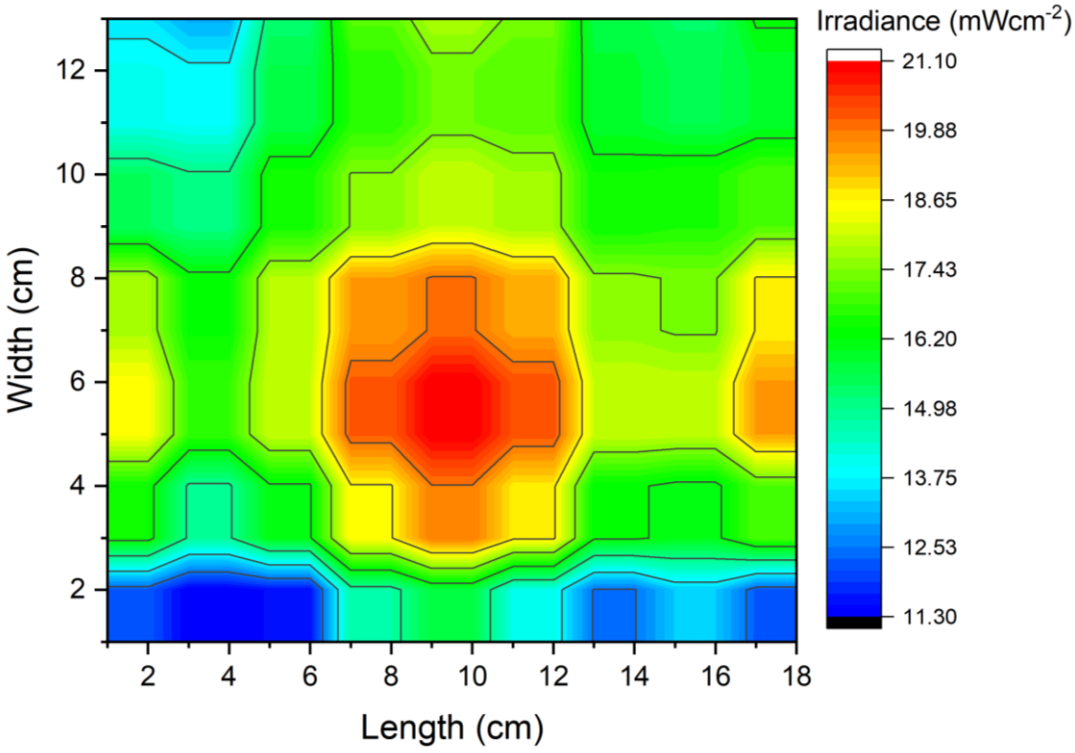

Figure 7.1. Model showing the irradiance profile across the surface area of a 300 mL blood bag. Irradiance profile across the blood bag surface with an average irradiance of ~16 mWcm^{-2} measured, taking account of the loss of light transmission through the PVC blood bag material (plotted using OriginPro 2018 software).

The methodology developed in Chapter 6, used to assess the antimicrobial efficacy in 100 mL plasma bags (Section 6.2.1) was applied in this section of work, however volumes were scaled appropriately for the treatment of 300 mL plasma bags. The

organisms used in this study were *S. aureus*, *E. coli* and *C. albicans* as a representative of a Gram-positive bacterium, a Gram-negative bacterium, and a yeast, respectively. All organisms were cultured as per Section 3.2.3. Microbial suspensions were used to spike the plasma to achieve a contamination level of ~10^3 $CFUmL^{-1}$.

In each case, 300 mL seeded plasma (transferred to a 450 mL blood bag (Grifols, UK)) was treated with ~16 $mWcm^{-2}$ 405-nm light for up to 7-hr (≤403 Jcm^{-2}) under agitation at 84 rpm, with 10 mL plasma held in identical conditions but foil-covered to act as a dark control (Figure 7.2). The plasma bag had a depth of 3 cm. The temperature of plasma was monitored throughout the exposure period using a thermocouple, to ensure plasma remained at *22°C* during treatment. Post-exposure, plasma samples were spread-plated (100 µL) or pour-plated (1 mL), depending on the expected population density, on nutrient agar for bacteria, or malt extract agar with 0.1% yeast extract (Oxoid Ltd., UK) for *C. albicans.* Plates were incubated at 37°C for 24-hr. Surviving microorganisms were enumerated with results recorded as mean microbial load ($CFUmL^{-1}$, n≥4±SD).

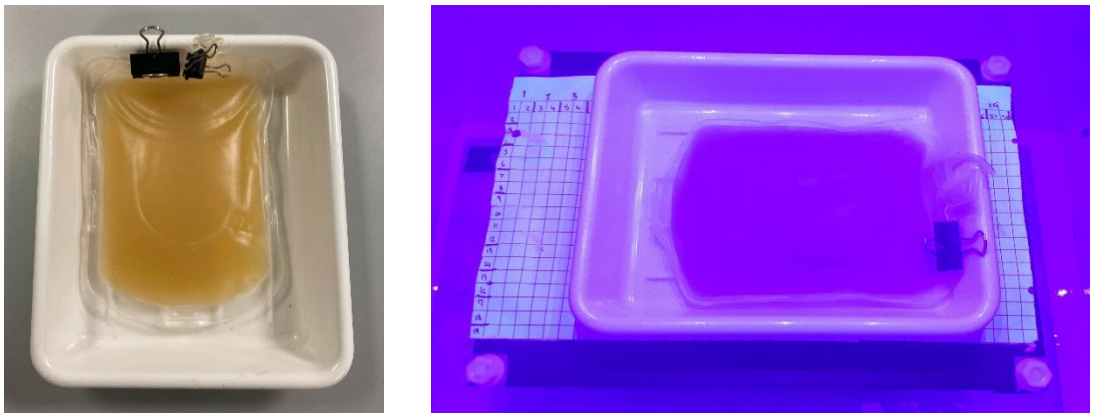

A) B)

Figure 7.2. Experimental arrangement for 405-nm light exposure of 300 mL prebagged plasma. Appearance of (A) 300 mL prebagged plasma and B) setup during light treatment.

7.1.2 Results: Pathogen Reduction of 300 mL prebagged Plasma using 405-nm Light

Results from the exposure of 300 mL prebagged plasma seeded with A) *S. aureus*, B) *E. coli* and C) *C. albicans* (approx. 10^3 CFUmL^{-1}) to 16 mWcm^{-2} 405-nm light are presented in Figure 7.3. A 405-nm light dose of 115 Jcm^{-2} (2-hr) significantly reduced all organisms under investigation [$P < 0.05$]. Of the organisms tested, *C. albicans* was the most susceptible to inactivation with 99.4% reduction achieved by 173 Jcm^{-2} (3-hr) [$P = 0.035$]. Inactivation kinetics for bacteria showed *S. aureus* to be reduced by 99.1% with 230 Jcm^{-2} (4-hr) and 96.2% reduction of *E. coli* by 288 Jcm^{-2} (5-hr) [$P = 0.012$ and 0.018 respectively].

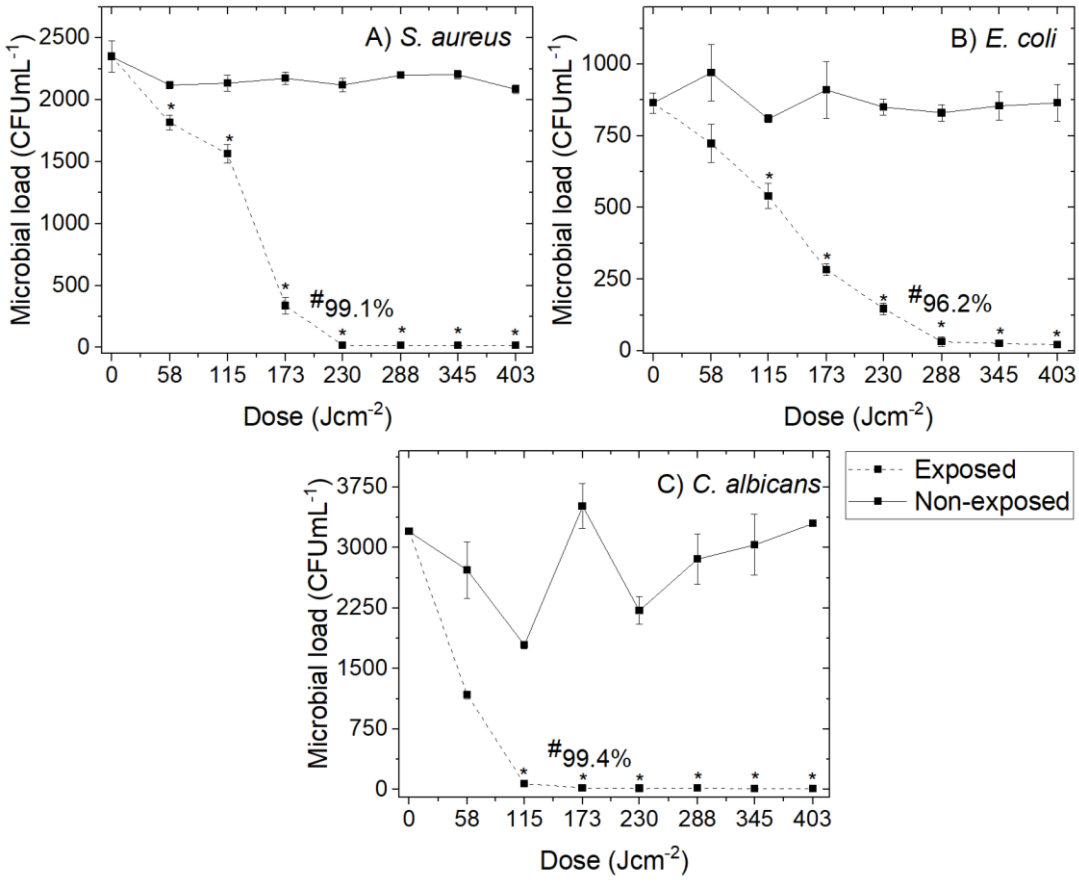

Figure 7.3. Pathogen reduction of 300 mL prebagged plasma using 405-nm light treatment, as a function of dose. Plasma bags were spiked with A) *S. aureus*, B) *E. coli* and C) *C. albicans* at approx. 10^3 CFUmL^{-1} and exposed to 16 mWcm^{-2} under constant agitation (84 rpm; 22°C). Data represents mean CFUmL^{-1} (n≥4 ±SD), with (*) representing significant differences between treated and non-treated samples [$P < 0.05$; paired t-test (Minitab v18)]. (#) notes the % reduction achieved by A) 230 Jcm^{-2}, B) 288 Jcm^{-2} and C) 173 Jcm^{-2}.

7.2 I Analysis of the Protein Compatibility of 405-nm Light with 300 mL Prebagged Plasma

A similar methodology was applied as per Chapter 6 (Section 6.3), whereby 300 mL prebagged plasma was exposed to 405-nm light (~16 $mWcm^{-2}$; ≤403 Jcm^{-2}), with 1-mL volumes of exposed and non-exposed plasma collected every hour over a 7-hr treatment (dose equivalents of 58, 115, 173, 230, 345 and 403 Jcm^{-2}). These plasma samples were then analysed using a range of proteomic testing to assess post-exposure plasma protein integrity.

7.2.1 Assessment of Protein Integrity of 405-nm Light Exposed 300 mL Prebagged Plasma using SDS-PAGE

Light-exposed plasma samples were analysed using SDS-PAGE, as detailed in Section 3.5.1. Figure 7.4 is an image of the master gel used to compare the electrophoretic band patterns of 300 mL prebagged plasma exposed to 16 $mWcm^{-2}$ 405-nm light (≤403 Jcm^{-2}). Whilst the intensity of the electrophoretic patterns for the non-exposed controls are visibly higher than exposed plasma samples (likely due to overloading the sample at the pipetting stage), it's important to note that no major changes in band patterns of exposed plasma are observed following exposure to 405-nm light. The earliest evidence of protein modification is observed in plasma exposed to 58 Jcm^{-2}, where there is a slight loss of protein banding in the region of 45 kDa. Upon exposure to increased doses, the intensity level of this protein band decreases, with complete loss detected after 345 Jcm^{-2} (as highlighted in Figure 7.4, Lane 11). However, as the protein banding is visibly detectable in plasma exposed 403 Jcm^{-2} (Lane 13) it is likely that these minimal changes are a result of sample-to-sample variation. Further, there is a visible loss of protein banding at approximately 198 kDa in all exposed plasma samples, however it is difficult to measure the accuracy of this as the intensity level varies between the non-exposed controls. Again, comparison with a positive control (shown in Figure 4.4A), showing complete plasma protein degradation, suggests that the degree of modification described above, should not be regarded as major damage.

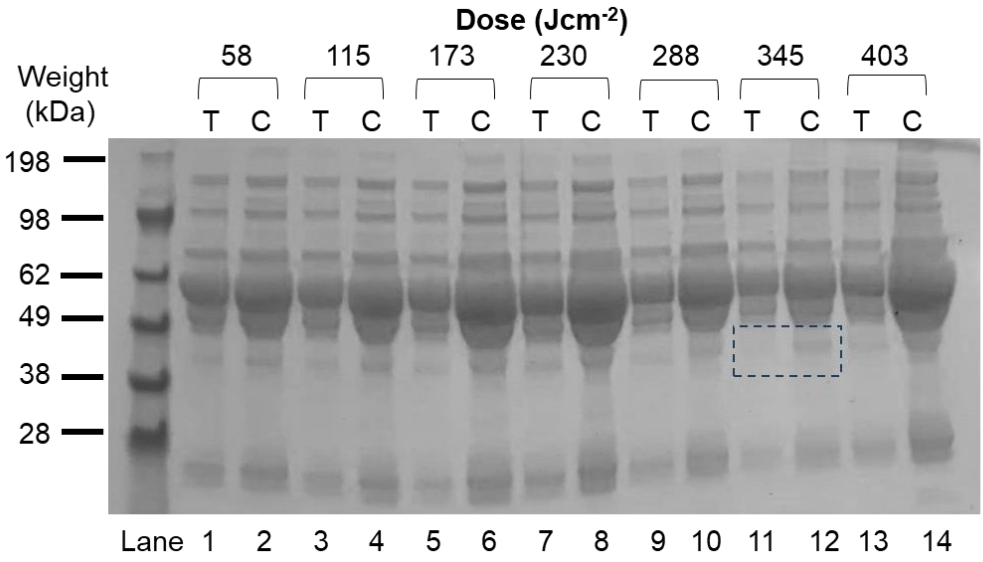

Figure 7.4. Assessement of the compatability of 405-nm light with 300 mL prebagged plasma using SDS-PAGE. Plasma exposed to 16 mWcm^{-2} 405-nm light (≤403 Jcm^{-2}), and their paired non-exposed control samples were analysed. The protein profiles show plasma samples which had been exposed in odd lanes: *1 (58 Jcm^{-2}), 3 (115 Jcm^{-2}), 5 (173 Jcm^{-2}), 7 (230 Jcm^{-2}), 9 (288 Jcm^{-2}), 11 (345 Jcm^{-2}) and 13 (403 Jcm^{-2})* labelled 'T' for test, and equivalent non-exposed control samples posiitoned in even lanes *(2, 4, 6, 8, 10, 12* and *14)*, labelled 'C' for control. Dashed box highlights the loss of protein banding at 45 kDa for plasma exposed to 345 Jcm^{-2}.

7.2.2 Assessment of Post-Exposure Oxidative Stress Levels in 300 mL Prebagged Plasma using an AOPP Assay

To quantitatively assess potential oxidative damage in the treated 300 mL volumes of prebagged plasma, an AOPP assay was conducted (as per Section 3.5.2). Results in Figure 7.5 show that there was no significant difference in the AOPP levels, indicative of general oxidative stress, between treated and non-treated plasma samples following exposure to the maximum applied dose of 403 Jcm^{-2} [$P > 0.05$]. The levels of AOPP of treated and non-treated samples fluctuated within the region of 25.5 - 29.2 µM, likely due to natural sample-to-sample variation in fibrinogen content, over the treatment period. AOPP levels in non-treated control plasma remained relatively constant [$P = 0.371$]. These results suggest that 405-nm light doses up to 403 Jcm^{-2} do not induce oxidative protein damage in treated plasma.

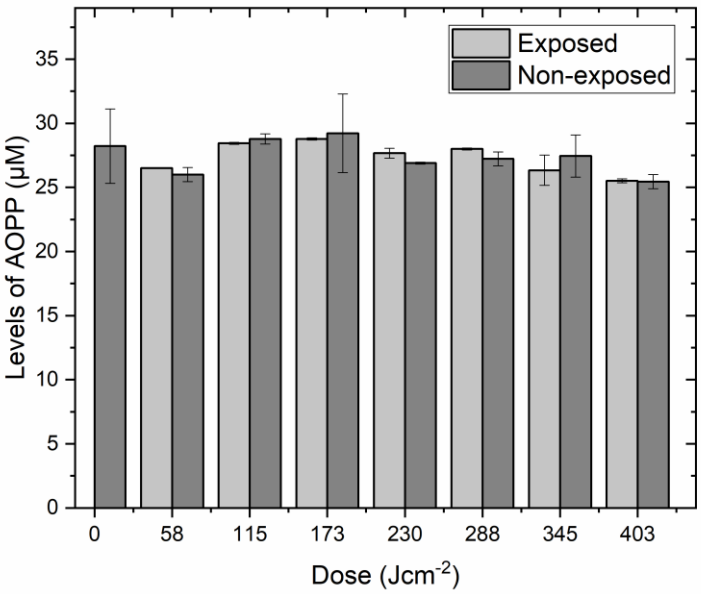

Figure 7.5. Levels of advanced oxidation protein products (AOPPs) detected in 300 mL prebagged plasma following exposure to 16 mWcm^{-2} 405-nm light (≤ 403 Jcm^{-2}). The concentration of AOPPs is expressed as μM of Chloramine-T equivalents, marker of oxidative damage, with values corrected for dilution factor. Data represent mean (n=3 ± SD). No significant changes in AOPP levels were detected in treated plasma when compared to the equivalent non-treated control [$P > 0.05$; 2-sample *t* test (Minitab v18)].

7.2.3 Assessment of Post-Exposure Clotting Activity of 300 mL Prebagged Plasma Using Clotting Assays

To examine whether 405-nm light affects the coagulation function of plasma, prothrombin time (PTT) and activated partial thromboplastin time (APTT) assays were performed to assess the stability of extrinsic-common and intrinsic-common coagulation pathways, respectively, following the methodology detailed in Sections 3.5.3 and 3.5.4. Figure 7.6A shows that there was no significant difference in PTT values between 300 mL prebagged plasma treated with doses up to 403 Jcm^{-2} and non-treated controls [$P > 0.05$]. Results from the APTT assay (Figure 7.6B), demonstrate that clotting times for 300 mL prebagged plasma treated with doses up to 288 Jcm^{-2} are similar to non-treated controls, with APTT values remaining relatively stable between 84 s – 90 s [$P > 0.05$]. A slight increase in APTT values was detected in plasma treated to doses ≥345 Jcm^{-2}, with clotting times prolonged by a maximum of 4.3% compared to non-treated controls [$P = 0.022, 0.028$]. These results suggest that exposure to 405-nm light doses up to 403 Jcm^{-2} have little to no effect on the

coagulation properties of prebagged plasma. In general, trends from clotting assays showed slight increases in clotting times over the 7-hr treatment period in both treated and non-treated samples, however the change was insignificant in both cases [$P > 0.05$].

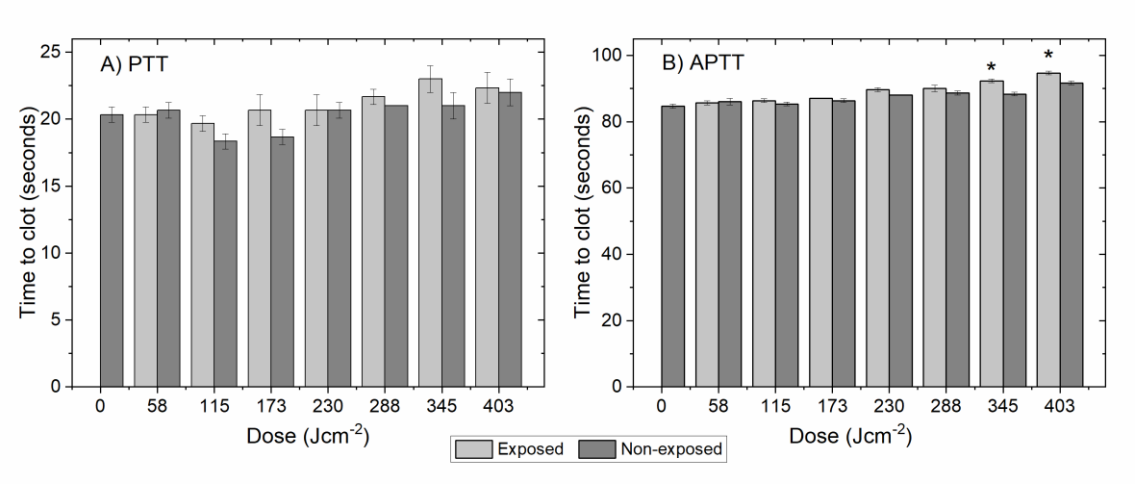

Figure 7.6. Assessment of the clotting functionality of 300 mL prebagged plasma treated with 405-nm light using A) PTT and B) APTT assays. Time to clot for plasma treated with 16 $mWcm^{-2}$ 405-nm light for doses up to 403 Jcm^{-2} (7-hr) compared to non-treated controls. Data represents mean time to clot (n=3 ± SD) with (*) representing significant increase in clotting times between treated and non-treated plasma [$P \leq 0.05$; 2-sample t-test (Minitab v18)].

7.2.4 Determination of Fibrinogen and Protein S levels in 405-nm Light Exposed 300 mL Prebagged Plasma

Light-exposed plasma samples were analysed using ELISAs to investigate changes in levels human Protein S and fibrinogen, as detailed in Sections 3.5.5. and 3.5.6. Results from assays, conducted on 405-nm light treated 300 mL prebagged plasma are shown in Figure 7.7A and 7.7B, respectively. Minimal reductions were observed throughout the exposure period, with a maximum reduction of 6.5% for fibrinogen, after 288 Jcm^{-2} [$P = 0.306$], and 5.7% for Protein S, after 403 Jcm^{-2} [$P = 0.326$]. Nevertheless, no change in fibrinogen or Protein S content was found to be significant at any point throughout the exposure period [$P > 0.05$]. Fibrinogen content was relatively stable throughout the treatment period, with slight variations in the region of 0.63 – 0.67 $mgmL^{-1}$ and 0.65 – 0.71 $mgmL^{-1}$ for treated and non-treated plasma, respectively. Protein S content slightly varied between 5.84 – 6.17 μgmL^{-1} and 5.85 – 6.46 μgmL^{-1} for treated and non-treated plasma throughout the exposure period, respectively.

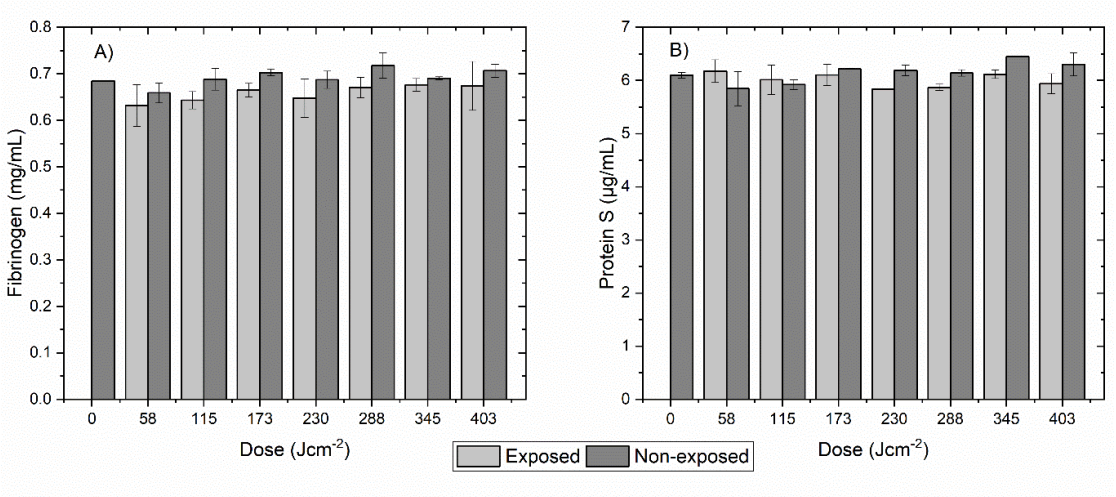

Figure 7.7. Fibrinogen (A) and Protein S (B) levels in 405-nm light treated 300 mL prebagged plasma (≤403 Jcm^{-2}). Data represents the mean concentration of fibrinogen in plasma (n=3 ± SD). No significant differences were detected between treated and non-treated controls [*P* > 0.05; 2-sample *t* test (Minitab v18)].

7.3 I Discussion

Overall, this study demonstrates the antimicrobial efficacy and potential compatibility of violet-blue, 405-nm light for treatment of *ex vivo* stored 300 mL plasma bags. This research expanded on the findings of Chapter 6, which demonstrated the broad-spectrum antimicrobial efficacy of 405-nm light for treatment of 100 mL plasma bags. The work of this chapter saw the samples scaled up to a clinically realistic volume of 300 mL, with *S. aureus* (Gram-positive bacteria), the more resilient *E. coli* (Gram-negative bacteria), and a yeast, *C. albicans*, selected for assessing antimicrobial efficacy. Following this, to assess the compatibility of effective antimicrobial doses with 300 mL prebagged plasma, various proteomics tests were conducted to assess the stability and functionality of 405-nm light treated plasma.

Results show that 405-nm light can effectively reduce microbial contamination in large volume plasma bags, with the pathogens under investigation all reduced by >96%, using doses (288 Jcm^{-2}) that demonstrated a high compatibility potential, with no significant changes in AOPP levels, clotting activity, or fibrinogen and Protein S, detected in treated plasma. Whilst doses in the region of 288 Jcm^{-2} are relatively high compared to existing UV-light and photosensitizer based technologies (typically delivering doses in the region of 3 Jcm^{-2}), treatment by 405-nm light eliminates the need for application of photosensitive agents, which are associated with lengthy

processing times (up to 24-hr in some cases) and can also increase the risk of adverse reaction in recipients [Irsch and Lin, 2011].

Of all organisms investigated, *C. albicans* was the most susceptible to 405-nm light inactivation. This finding is interesting as fungi are generally considered to be more difficult to inactivate than bacteria by antimicrobial treatments [Donnelly *et al*, 2008; Garcia-Rubio *et al*, 2020]. Donnelly *et al* (2008) attributes the increased resistance of fungi to the complexity and thickness of the outer cell wall, which contains components such as chitin, mannan, glucan and lipids. Additionally, the plasma membrane that separates the outer cell wall with the periplasmic space is thought to reduce the diffusion of photosensitizing agents, used in photodynamic inactivation, into the cell thereby limiting cell damage [Donnelly *et al*, 2008]. This finding therefore supports the hypothesis described in Section 6.4, whereby photosensitive agents naturally residing in plasma (flavins, cytochromes and chromophores etc) are thought to induce extracellular oxidative damage to cell wall structure of organisms, which provides as additional route for 405-nm light inactivation. The ability for 405-nm light to inactivate *C. albicans* (a species of *Candida,* a yeast responsible for up to 10% of all bloodstream infections recorded within hospitals [Kotthoff-Burrell *et al*, 2019], is of particular clinical interest as it has become more resistant to common antifungal therapies in recent years [Kotthoff-Burrell *et al*, 2019]. The findings from this research project, along with other publications that assess the antifungal efficacy of 405-nm light in non-biological media [Murdoch *et al*, 2013; Imada *et al*, 2014], support the use of 405-nm light as an alternative antimicrobial tool capable of reducing fungal contamination.

Comparison of dose requirements for microbial inactivation in different volume plasma bags, shows that approximately 2.5 times the dose is required to achieve comparable reductions in 300 mL bags compared to 100 mL bags (288 Jcm^{-2} compared to 115 Jcm^{-2}). The increased dose requirement is likely due to the difference in the bag depths – approximately 1 cm for 100 mL and 3 cm for 300 mL volumes, respectively – since light transmission will be reduced at increased depths. This stresses the importance to continuously agitate the bags during light treatment to ensure uniform mixing of potential contaminants to maximise the antimicrobial effects of 405-nm light. Recent studies by the collaborating research team have also demonstrated the antiviral and antiparasitic efficacy of 405-nm light in plasma, with >4-log_{10} reductions achieved using 270 Jcm^{-2} (similar to the effective antimicrobial dose identified in this

Chapter) [Jankowska *et al*, 2020; Ragupathy *et al*, 2022]. Microbial inactivation data for the treatment of PCs using 405-nm light has also become available in recent years [Maclean *et al*, 2020; Jankowska *et al*, 2020; Lu *et al*, 2020; Kaldhone *et al*, 2024]. These proof-of-concept studies demonstrate the ability of 405-nm light to inactivate a range of bacteria, a yeast, and two key problematic parasites in PCs. Since the transmissibility of 405-nm light in PCs is in the same region as – if not slightly lower than – plasma (0.1–0.3% compared to 0.08–3.6%, respectively) it would be expected that similar pathogen reduction would be observed in plasma using similar treatment levels (Maclean *et al*, 2020). Nevertheless, future work is required to expand the inactivation profile in plasma for a range of pathogens associated with TTIs including bacterial spores, as well as a range of viruses and protozoa [Brecher and Hay, 2005; Klein, 2005].

It is essential that a pathogen reduction treatment does not significantly impact the safety, quality, or effectiveness of the treated blood product. Preliminary compatibility studies covered in Chapter 4, indicated that low volume (250 µL) plasma samples treated with an effective antimicrobial dose of 360 Jcm^{-2} (100 $mWcm^{-2}$ for 1-hr) showed no major signs of protein degradation via SDS-PAGE analysis and AOPP assay. For 100 mL prebagged plasma, the upper threshold dose where protein damage was observed was slightly lower at approximately 115 Jcm^{-2}, potentially due to the fact that more in-depth proteomic tests, measuring different types of protein changes, were performed at this stage of the research project (clotting assays, and human Protein S and fibrinogen ELISAs were also used as part of the compatibility study in Chapter 6, in addition to SDS-PAGE and an AOPP assay employed in Chapter 4). The work of Chapter 7 demonstrates that effective antimicrobial doses up to 403 Jcm^{-2}, have little to no effect on the stability and functionality of 300 mL prebagged plasma. The only indication of protein change following 405-nm light treatment of 300 mL bags was observed in the clotting assays, where clotting times slightly increased following exposure to doses ≥345 Jcm^{-2}. The following sections will focus on the results of the compatibility studies for the treatment prebagged plasma using 405-nm light.

There were no signs of oxidative protein damage detected via the AOPP assay in 300 mL volumes of plasma treated with antimicrobial doses up to 403 Jcm^{-2}. It was expected that post-treatment fibrinogen levels would be unaffected since AOPP levels

are a strong indicator for the stability of fibrinogen [Selmeci *et al*, 2006]. Results from the fibrinogen ELISA confirmed this, with no significant changes in fibrinogen levels detected following exposure to doses up to 403 Jcm^{-2}. From this, it appears that visible 405-nm light has a less adverse effect on the integrity of fibrinogen compared to UV-light, even when over 65× the dose is applied (403 Jcm^{-2} 405-nm light *versus* 6 Jcm^{-2} UV-light), with reports stating that UV-light based PRTs can potentially reduce fibrinogen in plasma by up to 21% [Hornsey *et al*, 2009]. The level of Protein S, an essential anti-clotting agent, was minimally effected following exposure to antimicrobial 405-nm light doses up to 403 Jcm^{-2}, which at >94% retention, is similar to levels retained in UV-light inactivated plasma [Hornsey *et al*, 2009; Bubinski *et al*, 2021].

In order to treat or prevent bleeding in patients, it is important to ensure that an antimicrobial treatment of blood transfusion products has little to no effect on the stability and functionality of clotting factors. PTT and APTT tests were used to assess potential changes in coagulation activity in 405-nm light treated plasma. Analysis of PTT results (Figure 7.6A) indicates that 405-nm light has minimal effect on clotting factors involved in the extrinsic (factor VII) and common coagulation (factors I, II, V and X), with no significant differences in time to clot detected between treated and non-treated plasma following exposure to doses up to 403 Jcm^{-2} [$P > 0.05$]. The time to clot, measured via the APTT assay (Figure 7.6B), increased slightly in plasma treated with 405-nm light doses ≥ 345 Jcm^{-2} (6-hr), suggesting that intrinsic clotting factors (factors VIII, IX, XI, and XII) may be more photo-sensitive compared to the extrinsic clotting factor VII. Nevertheless, the overall impact on clotting activity, with a maximum prolongation of 4.3% over the treatment period, is relatively low in comparison to clinically approved, UV-light based PRTs that have shown to prolong clotting times by up to 24% [Hornsey *et al*, 2009; Bubinski *et al*, 2021]. Table 7.1 summaries the effect of an effective antimicrobial 405-nm light treatment (based on results from 300 mL prebagged plasma, following exposure to 403 Jcm^{-2}) on key plasma protein markers, in comparison to commercially available PRTs.

Table 7.1. The impact of commercially available PRTs on key plasma proteins, compared to an antimicrobial 405-nm light dose of 403 Jcm^{-2}. Reductions in fibrinogen and Protein S levels, and changes in time to clot (via PTT and APTT assays) are compared to the proteomic results reported in this Chapter, for the 300 mL prebagged plasma exposure. Asterisks (*) indicate significant difference between treated and non-treated control plasma [$P < 0.05$]. [[1]Bubinski *et al*, 2021; [2]Backholer *et al*, 2016; [3]Hornsey *et al*, 2009].

PRT *(Manufacturer)*	**General Inactivation Mechanism**	**Fibrinogen** *(% loss)*	**Protein S** *(% loss)*	**PTT** *(% increase in time to clot)*	**APTT** *(% increase in time to clot)*
Violet-blue 405-nm Light, 403 Jcm^{-2}	**General oxidative damage through excitation of endogenous porphyrins**	**6%**	**5%**	**3%**	**4%**
Intercept[1] (*Cerus*)	Amotosalen and UVA light	21%*	5%*	5%*	14%*
Theraflex-MB[2] (*Macopharma*)	Methylene-blue photosensitizer and visible light	34%*	5%*	6%*	14%*
Mirasol[3] (*Terumo BCT*)	Riboflavin photosensitizer and UVB-light	21%*	4%*	17%*	24%*

Comparison of the threshold dose between 100 mL and 300 mL plasma bags, where protein damage by 405-nm light is evident, shows that larger volume plasma bags can be treated with significantly higher antimicrobial doses (3× higher; 115 *versus* 288 Jcm^{-2} for 100 and 300 mL volumes, respectively) without any evidence of protein damage. This is likely due to the fact that the same level of light energy is being applied to and distributed throughout a larger volume of plasma at greater depth (as described above regarding the increased dose requirements for microbial inactivation), reducing the proportion of plasma proteins interacting with 405-nm light. The level of mixing occurring in the different plasma bags may also contribute to the differences in dose efficiency and compatibility. In both cases, the bags were agitated

at 84 rpm, however it is difficult to measure and therefore difficult to compare the actual level of mixing of the fluid inside the blood bag (300 mL plasma in a 450 mL bag *versus* 100 mL plasma in 150 mL bag). It would be interest in future work to assess the influence of agitation rate, both with regards to the antimicrobial efficacy and protein compatibility of 405-nm light for treatment of larger volume plasma bags. 405-nm light has also shown potential compatibility with human platelets stored in plasma, a more sensitive cellular blood product, using antimicrobial doses up to 288 Jcm^{-2}, with the recovery of treated and non-treated platelets shown to be statically similar in a murine model [$P > 0.05$] [Maclean *et al*, 2020; Lu *et al*, 2020; Jana *et al*, 2023]. This study, together with previous results, provides further evidence supporting the potential compatibility of antimicrobial doses of 405-nm light for treatment of plasma and platelets stored in plasma.

It should be noted that the 100 and 300 mL bags used in this project were provided by the same manufacturer (Grifols, UK) and in both cases were composed of polyvinyl chloride (PVC) and a plasticizer (Tris (2-Ethylhexyl) Trimellitate (TOTM)), with a bag thickness of 0.39 mm. In terms of transmissibility, a 26% reduction in irradiance was measured for both the small and large volume bags, as the light transmits through the bag material into the plasma. Within the scope of this project, experiments could only be carried out using blood bags from one manufacturer, however from review there are several manufacturers that provide blood bags to hospitals around the world, including Demophorius Healthcare, Fresenius Kabi, Baxter, Macopharma, Neomedic Limited and Terumo BCT. If given the opportunity, future research should investigate the effects of varying the type of blood bag on the efficacy of the 405-nm light treatment. It would be of interest to explore how different types of blood bags, with varying wall thicknesses (typically ranging from 0.14-0.41 mm) and plasticizer composition effects the transmissibility of 405-nm light through the material to treat the plasma [Hmel *et al*, 2002]. This work would help identify whether the 405-nm light treatment conditions would need to be adjusted (i.e. an increased or decreased irradiance of 405-nm light) on a bag-to-bag basis, to ensure that the intended antimicrobial dose is applied to the plasma.

Plasticized PVC has been the preferred choice of material for blood bags since it was introduced in the 1950s [Carmen, 1993]. This is largely due the fact that PVC provides the optimal permeability of oxygen (more relevant to the storage of platelets to ensure sufficient oxygen to maintain aerobic respiration), is durable (to withstand tear on

handling and transportation) and translucent (to allow clinicians to visually monitor the stability of blood products) and is generally cost efficient [Carmen, 1993]. Whilst PVC is the standard base material for blood bags, manufacturers employ different plasticizers, to improve the bags flexibility and resistance to heat (to ensure stability during steam sterilisation) [Larsson *et al*, 2020]. Citrate, di-2-ethylhexylphthalate (DEHP) was the first plasticizer to be used in combination with PVC for blood bags [Larsson *et al*, 2021]. However in the late 1960s, reports concerning the presence of DEHP in stored blood products emerged, as Guess *et al* (1967) confirmed that DEHP was leaching from the plasticized PVC blood bag into plasma. These reports led to a series of investigations into the leachability of DEHP and its physiochemical and toxicological behaviour [Guess *et al*, 1967]. In light of this, blood bag manufacturers started to develop new plasticizers as safer alternatives. Due to the ongoing concerns over the increased risk of cancer and reproductive toxicity associated with the exposure to DEHP, as of May 2025, the European Union officially banned the use of DEHP in storage blood bags [Larrson *et al,* 2022].

A review of existing literature highlights trioctyl-trimellitate (TOTM), n-butyryl-tri-n-hexyl citrate (BTHC), and 1,2-cyclohexane-dicarboxylic acid diisononyl ester (DINCH) as the most studied, plasticizer replacements for a PVC DEHP-free blood bag [Braun *et al*, 2013; Bicalho *et al*, 2016]. As highlighted, the blood bags used in this project were composed of PVC and TOTM. In alignment with the recent plasticizer ban, it is essential that future work examines the susceptibility of different plasticizers to leach from the blood bag into the plasma following 405-nm light irradiation. This can be investigated using high-performance liquid chromatography (HPLC), a technique used to separate, identify and quantify the individual compounds in a chemical mixture [Identification of TOTM as per Radaniel *et al*, 2014].

In this section of work, microbial inactivation and compatibility studies were conducted using a fixed 405-nm light treatment using an irradiance of 16 $mWcm^{-2}$, however the work of Chapter 5 demonstrated antimicrobial efficacy in plasma using low, mid and high of irradiances (1, 10, 100 $mWcm^{-2}$) of 405-nm light. As covered in Section 5.4, research has shown that use of lower irradiances are more germicidally energy efficient compared to higher irradiances for pathogen reduction of plasma and platelets stored in plasma, which is likely due to the free porphyrin-to-photon ratio. Whilst an important consideration, the method of dose delivery must be selected in line with the application type, as the irradiance level directly influences the exposure

time required to apply an effective antimicrobial dose. It is envisioned that the method of dose delivery may be adjusted to suit the practical application i.e. utilising higher irradiances for rapid decontamination pre or post-storage, or lower irradiances to continuously irradiate prebagged plasma or platelets stored in plasma during the inventory period in hospitals.

Overall, this chapter successfully demonstrates the antimicrobial efficacy and compatibility of 405-nm light for the scaled-up treatment of 300 mL prebagged plasma using doses up to 403 Jcm^{-2}. A dose of 288 Jcm^{-2} (5-hr) was identified to be sufficient to reduce pathogens while not harming the quality of the treated prebagged plasma. Given the performance efficacy shown in this Chapter, as well as the review of the safety benefits and decreased toxicity in comparison to commercially available PRTs, the data confirms that there is potential for the development and commercialization of 405-nm light as an alternative PRT for plasma and plasma-based products.

Chapter Eight I Conclusions & Future Work

8.0 I Overview

This research project was conducted to assess the development of violet-blue 405-nm light as an effective and safe PRT for treatment of plasma, and plasma-based blood transfusion products. Initial studies were performed using low volume plasma samples to gain an insight into the dose requirements for microbial inactivation and also to identify the upper threshold doses, to ensure the effective antimicrobial doses were in fact compatible with the plasma itself. The broad-spectrum antimicrobial efficacy of a fixed 405-nm light dose, which displayed both antimicrobial effects and compatibility with the plasma, was then evaluated against a range of organisms commonly associated with TTIs in low volume plasma samples. The small-scale exposure system was then used to investigate the influence of 405-nm light dose delivery, on the antibacterial efficiency and protein compatibility, using different treatment regimes with varying light intensity. Insights from these small-scale exposures, supported the design and development of a large-scale violet-blue 405-nm light unit for treatment of prebagged plasma. Microbial inactivation and protein compatibility tests were first conducted using 100 mL plasma bags, as an intermediate step, before scaling up to more clinically-relevant 300 mL plasma bags.

This Chapter will summarise the main findings from each section of work and discuss ideas for future work, which will further support the development of this antimicrobial light technology within the field of transfusion medicine.

8.1 I Conclusions

8.1.1 Broad Spectrum Antimicrobial Efficacy of 405-nm Light for Plasma Treatment: Small-Scale Testing

Initial microbial inactivation tests determined that a 405-nm light dose of 360 J cm^{-2} (1-hr at 100 $mWcm^{-2}$) was required for complete inactivation of both *S. aureus* and *E. coli* seeded at low contamination levels in plasma samples. Preliminary protein analysis by SDS-PAGE (Figures 4.4 and 4.5) indicated that exposure to an effective antimicrobial dose of 360 Jcm^{-2} did not induce any major plasma protein damage. The earliest sign of protein modification was detected in HMWPs (80-198 kDa; associated with complement proteins, macroglobulin chains, ceruloplasmin and transferrin [Schenk *et al*, 2008; Gautam *et al*, 2013]) following exposure to a dose of 720 Jcm^{-2}:

2× greater than the effective antimicrobial dose. This was supported by the results from an AOPP assay (Figure 4.8), a protein biomarker used to assess oxidative stress, which detected no significant plasma protein oxidation following exposure to doses of up to 1.44 kJcm^{-2}; 4× greater than the effective antimicrobial dose.

This section of work also hypothesised the potential routes of plasma protein damage induced by excessively high doses of 405-nm light. It is thought that porphyrin- and flavin-protein complexes, naturally residing in plasma (such as riboflavin, bilirubin, hemoglobulin etc) may be acting as exogenous photosensitizers, generating ROS which are inducing oxidative damage. Results from this study also suggest that photodegradation of proteins by 405-nm light is dominated by protein-to-protein cross linking induced through thiol oxidation (protein-to-protein cross linking) [O'Flaherty and Matsushita-Fournier, 2017].

On the basis of initial inactivation kinetics and protein analysis, a dose of 360 Jcm^{-2} (1-hr at 100 mWcm^{-2}) was selected for assessing broad-spectrum inactivation efficacy in low volume plasma seeded with a range of bacteria and yeast, at 'low' (10^1-10^3 CFUmL^{-1}), 'medium' (10^4-10^6 CFUmL^{-1}) and 'high' (10^7-10^8 CFU mL^{-1}) density levels, to represent realistic clinical contamination, and medium and high microbial challenges, respectively. Broad-spectrum antimicrobial efficacy was observed with a fixed treatment of 360 J cm^{-2}, with 98.9–100% inactivation achieved across all seeding densities for all organisms, except *E. coli*, which achieved 95.1–100% inactivation. The study found that organisms, regardless of Gram status, presented different susceptibilities to inactivation by 405-nm light, and attributed this to the range of different types and levels of porphyrins expressed by organisms, as well as differing sensitivities to externally-generated ROS (thought to be produced by photosensitive porphyrin- and flavin-protein complexes in the plasma).

8.1.2 Assessing the Influence of 405-nm Light Dose Delivery on Antibacterial Efficiency and Protein Compatibility

After determining that a fixed 405-nm light dose of 360 Jcm^{-2} (100 mWcm^{-2} for 1-hr), was capable of broad-spectrum antimicrobial efficacy in plasma, it was of interest in Chapter 5 to investigate how the method of dose delivery influenced the efficiency and compatibility of the light treatment. Bacterial inactivation and protein compatibility tests were conducted on low volume plasma samples exposed to three different regimes with a fixed dose, applied using low (1 mWcm^{-2}), mid (10 mWcm^{-2}) and high (100 mWcm^{-2}) irradiance 405-nm light.

Bacterial inactivation tests demonstrated that applying a fixed dose with a low irradiance of 1 $mWcm^{-2}$ is more efficient for the inactivation of *S. aureus and E. coli* (at 10^2 and 10^5 $CFUmL^{-2}$) in plasma compared to the higher irradiances tested (Table 5.2). The comparison of dose requirements for 1-log_{10} reductions highlights this trend: for *S. aureus*, 2× a higher dose was required when applied using 100 $mWcm^{-2}$ compared to 1 $mWcm^{-2}$ irradiances; 72-108 Jcm^{-2} required for 1 $mWcm^{-2}$, 108-144 Jcm^{-2} required for 10 $mWcm^{-2}$ and 108-144 Jcm^{-2} required for 100 $mWcm^{-2}$. For a 1-log_{10} reduction of *E. coli*, 5× a higher dose was required when applied using 100 $mWcm^{-2}$ compared to 1 $mWcm^{-2}$ irradiances; 72 Jcm^{-2} required for 1 $mWcm^{-2}$, 108-180 Jcm^{-2} required for 10 $mWcm^{-2}$ and 360 Jcm^{-2} required for 100 $mWcm^{-2}$. This dose delivery effect was thought to be due to a limit on the free porphyrin-to-photon ratio, whereby there is a critical level of photons that can be involved in the photoexcitation process, and above such an irradiance level it is likely that excess photons are unable to be absorbed and therefore, cannot contribute to the inactivation mechanism [Maclean *et al*, 2016, 2020].

With regards to treatment compatibility, initial results gained from SDS-PAGE analysis did not identify any major differences in the integrity of plasma proteins when varying the method of dose delivery. It was through the introduction of clotting assays (PTT and APTT) that assessed the stability of essential clotting factors in plasma, that a distinct difference in the compatibility of the different treatment regimes was observed. The clotting assays demonstrated that use of 1 and 10 $mWcm^{-2}$ irradiances were significantly more compatible with protein clotting factors compared to use of 100 $mWcm^{-2}$ when applying a fixed antibacterial dose (Figures 5.7 and 5.8). This trend is again thought to relate back to the limit on the free porphyrin-to-photon ratio theory, as it is likely that use of higher irradiances leads to the provision of excess photon energy that, whilst not being involved in the photoexcitation process, can interact with photo-sensitive agents in the plasma capable of generating ROS, a key driver for protein oxidation.

Whilst the lowest irradiance of 1 $mWcm^{-2}$ proved to be the most efficient and compatible compared to 10 and 100 $mWcm^{-2}$ irradiances for treatment of plasma samples, the difference in treatment times required to apply an antimicrobial dose (for 72 Jcm^{-2}: 20-hr for 1 $mWcm^{-2}$ *versus* 2-hr for 10 $mWcm^{-2}$ *versus* 12-min for 100 $mWcm^{-2}$) was highlighted. This is an important consideration when evaluating the practical implementation of the technology in a clinical setting. Most importantly, this

Chapter demonstrated that all treatment regimes, using low, mid and high irradiance 405-nm light, could successfully reduce bacterial contamination in plasma, which opens up an opportunity to develop a flexible antimicrobial treatment whereby the treatment regime could be tailored depending on the clinical application.

8.1.3 Broad-Spectrum Antimicrobial Efficacy and Compatibility of 405-nm Light for Treatment of 100 mL Prebagged Plasma

Findings from the small-scale exposure tests of Chapter 4 and 5, provided key information that assisted the development of a large-scale 405 nm light exposure system to treat prebagged plasma. The work of this Chapter used 100 mL plasma bags, as an intermediate to clinically-relevant 300 mL plasma bags, to investigate the broad-spectrum antimicrobial efficacy and protein compatibility of 405-nm light using doses up to 403 Jcm^{-2} (16 $mWcm^{-2}$ for 7-hr). As shown in Figure 6.8, a 405-nm light dose of 115 Jcm^{-2} (2-hr) achieved near complete inactivation for all organisms investigated (*S. aureus*, *S. epidermidis*, *E. coli*, *P. aeruginosa*, *A. baumannii* and the yeast, *C. albicans)*, except for *E. coli*, that required 230 Jcm^{-2} (4-hr) to achieve comparable inactivation.

With prior 405-nm light and broader photoinactivation research reporting that Gram-positive bacteria tend to have greater susceptibility to 405-nm light than Gram-negative when suspended in non-biological media, it was interesting to note that Gram-negative bacteria *P. aeruginosa* and *A. baummannii*, showed similar susceptibility to inactivation compared to Gram-positive staphylococci, when suspended in plasma. This supported the concept that photosensitive agents naturally residing in plasma, including flavins and chromophores, have the potential to enhance the antimicrobial effects of 405-nm light imparting oxidative damage to the outer membrane of some Gram-negative organisms.

This Chapter also found that approximately 70% less dose was required to achieve comparable reductions in 100 mL bags compared to 250 µL samples used in Chapter 4 (115 Jcm^{-2} compared to 360 Jcm^{-2}), even when the depth of the plasma was the same (1 cm). This is attributed to the fact that different treatment regimes were used to apply the antimicrobial doses (100 $mWcm^{-2}$ in Chapter 4 compared to 16 $mWcm^{-2}$ in Chapter 6), as well as the fact that the plasma bags were agitated during treatment. This finding therefore emphasized the importance of bag agitation during the 405-nm light treatment.

A range of proteomic tests were conducted to assess the compatibility of the 405-nm light treatment with 100 mL prebagged plasma. No significant signs of general oxidative protein damage (measured via AOPP assay) nor changes in the levels of fibrinogen or Protein S were observed following exposure to doses up to 403 Jcm^{-2}. Results from SDS-PAGE analysis (Figure 6.9) and clotting assays (Figures 6.11 and 6.12) did however detect changes to the stability of proteins in plasma exposed to doses of 173 Jcm^{-2}.

Taking both the antimicrobial efficacy and compatibility results into consideration, a dose of 115 Jcm^{-2} (2-hr) 405-nm light was identified as an effective and compatible treatment, capable of broad-spectrum microbial inactivation in 100 mL prebagged plasma.

8.1.4 405-nm Light as a PRT for the Treatment of 300 mL Prebagged Plasma

The final stage of this research project scaled up experiments to assess the pathogen reduction efficacy and compatibility of 405-nm light for the treatment of 300 mL prebagged plasma, to reflect a more clinically relevant scenario.

Microbial inactivation tests (Figure 7.3) demonstrated that a 405-nm light dose of 115 Jcm^{-2} (16 $mWcm^{-2}$ for 2-hr) was capable of reducing three key organisms commonly associated with TTIs (*S. aureus*, *E. coli* and *C. albicans* at 10^3 $CFUmL^{-1}$) in 300 mL prebagged plasma. High level inactivation (>99.1%) of *S. aureus* and *C. albicans* was achieved using a 405-nm light dose of 230 Jcm^{-2} (4-hr). Following the trend observed in previous Chapters, *E. coli* demonstrated the highest resistance to inactivation with a 96.2% reduction achieved with a dose of 288 Jcm^{-2} (5-hr). This study found that approximately 2.5× greater dose was required to achieve comparable reductions in 300 mL bags compared to 100 mL bags (288 Jcm^{-2} compared to 115 Jcm^{-2}). The difference in the depth of the plasma bags (1 cm for 100 mL *versus* 3 cm for 300 mL) was thought to be the key reason for the increased dose requirements.

In parallel, a range of proteomic tests (SDS-PAGE, an AOPP assay, clotting assays, and a human fibrinogen and Protein S ELISA) were performed to assess the compatibility of antimicrobial doses of 405-nm light with plasma proteins for the treatment of 300 mL prebagged plasma. Results from the panel of compatibility tests demonstrated that effective antimicrobial doses up to 403 Jcm^{-2}, had little to no effect on the stability and functionality of 300 mL prebagged plasma. The only significant

indication of protein change was detected via clotting assays (Figure 7.6), where a maximum prolongation of 4.3% in time to clot was observed over the treatment period (≤403 Jcm^{-2}). The clinical impact of this protein change is expected to be minimal, as clinically approved, UV-light based PRTs that have shown to prolong clotting times by up to 24% [Hornsey *et al*, 2009; Bubinski *et al*, 2021].

With this in mind, a 405-nm light dose of 288 Jcm^{-2} (16 $mWcm^{-2}$ for 5-hr) was identified to be sufficient treatment to reduce pathogens in 300 mL prebagged plasma whilst preserving plasma stability and functionality. The operational parameters identified in this study will be essential for the next phase of technology development and clinical adoption of violet-blue, 405-nm light as a decontamination tool for prebagged plasma.

8.2 I Future Work

In this Thesis, visible violet-blue 405-nm light presents itself as an alternative, potentially less damaging antimicrobial approach for pathogen reduction of plasma compared to existing technologies which require the use of UV-light and/or photosensitive agents. Future work should continue to expand on the microbiological and protein compatibility data of 405-nm light for plasma decontamination, whilst considering the optimal treatment regime for use in a clinical setting.

8.2.1 Expand on the 405-nm Light Pathogen Reduction Profile for Plasma

This Thesis demonstrated the broad-spectrum antimicrobial efficacy of 405-nm light for treatment of plasma in low volume samples and 100 mL bags. Due to limited resource, three organisms commonly associated with TTIs – a Gram-positive and Gram-negative bacteria and a yeast – were selected for antimicrobial testing using the most clinically relevant, 300 mL, bag volumes. Future work should expand on this research to assess the inactivation of a range of pathogens associated with TTIs in large-volume plasma bags, including a panel of different bacterial species and strains, bacterial spores, viruses and protozoa, that are recommended by the World Health Organization (WHO).

Whilst the work of Chapter 4 demonstrated that 405-nm light can reduce microbial loads at a range of contamination levels (10^2-10^8 $CFUmL^{-1}$) in low volume samples, further work is required to scale-up and repeat these tests in whole bag volumes. This would involve building on the work of Chapter 7, by repeating the microbial inactivation tests at a range of seeding densities to determine if the dose requirements change depending on the level of contamination. This is essential as the level of

contamination at the time of treatment would be unknown. Therefore, the applied treatment dose must be effective against a range of seeding densities, from a low contamination level ($\leq 10^3$ CFUmL^{-1}) typically detected at time of donation to a high microbial challenge ($>10^6$ CFUmL^{-1}) that can develop during time in storage [Brecher *et al*, 2000].

Within this study, the methods used to assess microbial inactivation in plasma followed international best practices, however additional research methods should be used to reflect the physiological conditions in plasma (including the use of microaerophilic environmental conditions, i.e. a controlled atmosphere at 1% oxygen, during the incubation phase), as this may affect the recovery and enumeration of microbial contaminants in clinical scenarios.

8.2.2 Further Compatibility Studies

Various proteomic tests were employed during the course of this research to evaluate the compatibility of antimicrobial doses of 405-nm light with the plasma proteins. Of all the proteomic analysis techniques used in this study, the clotting assays (PTT and APTT) appeared to be the most sensitive tool capable of detecting changes in plasma protein stability, and should therefore be viewed as a benchmark analysis tool in future work. As the proteomic test results varied from bag-to-bag, future work must increase the sample size to increase the reliability of the results and also to reduce the impact of natural protein variation that is observed between different plasma samples and batches (see Appendix A).

Additionally, Chapter 4 highlighted the lack of knowledge on the exact mechanism of 405-nm light induced plasma protein damage. The compatibility results from this study suggest that the photodegradation of proteins by 405-nm light is dominated by protein-to-protein cross linking induced through thiol oxidation. As this is considered a mild, potentially reversible form of oxidative damage, it would be of interest to assess if the protein modifications observed during light treatment are in fact recovered after a period in storage.

As part of the approval process for PRTs in Europe, the treated blood product must meet the guidelines set by the Council of Europe (CoE), that outlines acceptable levels of key plasma proteins for clinical transfusion [Keitel, 2009]. As a reference, it states that pathogen reduced plasma must retain 60% of the clotting factors (fibrinogen and Factor VIII as a minimum) compared to fresh frozen plasma, to be

accepted. This study employed a fibrinogen ELISA for the 300 mL plasma bag exposure, and noted a maximum reduction of 6% - an acceptable level by CoE standards – following exposure to an effective antimicrobial 405-nm light treatment (288 Jcm^{-2}). Whilst the APTT clotting assay used in this study predominantly assessed the functionality of Factor VIII, as per the requirements of the CoE, future protein compatibility tests should directly measure the level of Factor VIII in treated plasma through use of the Human Factor VIII ELISA kit.

To strengthen the case for a clinical evaluation, a vast range of *in vitro* characteristics and coagulation function tests must be performed to demonstrate that safe and acceptable plasma protein levels are retained following light treatment. In line with the minimal requirements enforced by the FDA for approval of a novel plasma components [Benjamin and McLaughlin, 2009], the following *in vitro* characteristics and coagulation function tests will need to be conducted as part of future work (FDA does not define acceptable outcomes for each variable):

- Prothrombin Time Test *(covered in this Thesis)*
- APTT *(covered in this Thesis)*
- Fibrinogen *(covered in this Thesis)*
- Protein S *(covered in this Thesis)*
- Factor V, VIIa, VIII:C and XI
- von Willebrand factor (VWF)
- Antithrombin-III
- Protein C

As part of the route to market, the compatibility of 405-mn light with plasma would need to be demonstrated within a murine model [as per Keil *et al*, 2015], and then through a series of randomised clinical trials to assess if there are any differences in the laboratory or clinical outcomes between individuals receiving pathogen-reduced plasma or non-treated plasma [as detailed in Marschner and Goodrich, 2011; Irsch and Lin, 2011].

The compatibility of 405-nm light with PVC blood bags is another area that must be investigated further. This is most important from a safety point of view, to ensure that the 405-nm light treatment does not compromise material integrity through cracking or blistering, as this would result in a biohazard (leakage of biological fluids) and potentially introduce an opportunity for re-contamination. During this study, no visible, physical damage of the bag material was observed following exposure to 405-nm

light, however further investigation is required to monitor the integrity of the material using a range of laboratory techniques including Fourier Transform Infrared Spectroscopy (FTIR) and Atomic Force Microscopy (AFM) (similar study performed by Irving *et al*, 2016). Additionally, the need to monitor plasticizer stability in the PVC blood bag during treatment is high priority for future work. As highlighted in Section 7.3, HPLC can be used to detect plasticizer leakage from the PVC bag material into the plasma during light treatment [as per Radaniel *et al*, 2014].

In this study, all plasma exposures were conducted using blood bags from the same manufacturer (Grifols, UK). Future research should explore how varying the type of blood bag, with different wall thickness and plasticizer composition, impacts the efficacy of the 405-nm light treatment. This is of clinical interest, as it would help determine whether the 405-nm light treatment would need to be adjusted on a bag-to-bag basis, to ensure that the required antimicrobial dose is applied to the plasma.

8.2.3 Opportunities to Optimise the 405-nm Light Treatment and Expand Treatment Applicability

There are many opportunities that can be explored in an attempt to optimise the 405-nm light treatment for prebagged plasma. The role that agitation plays in enhancing the overall efficiency of the light treatment should be explored. It would be of interest to assess whether increasing the rate of agitation of the plasma bag, from the level used in this study (>84 rpm), enhances the antimicrobial effects and potentially improves the compatibility of the 405-nm light treatment. Another operational consideration that should be explored is the opportunity to develop a bi-directional treatment whereby 405-nm light is delivered to either side of the bag. By doing so, the treatment time required to deliver an antimicrobial dose could be drastically reduced. However, it should be highlighted that it is commonplace for blood transfusion bags to have a large label that outlines important clinical details (blood type, storage conditions, expiry date etc) on one side of the bag, therefore preventing any light transmissibility. To enable a bi-directional treatment, the contents could be transferred to a non-labelled PVC blood bag, however this would eliminate a major competitive advantage of being able to pathogen reduce the prebagged plasma *in situ*, without the requirement for bag transfers or extensive processing, that 405-nm light offers against the commercially available PRTs.

As discussed in Section 2.4.5, violet-blue 405-nm light is also being investigated for the *in situ* pathogen reduction treatment of *ex vivo* stored platelets and RBC

concentrates [Platelets: Jankowska *et al*, 2020; Lu *et al*, 2020; Maclean *et al*, 2020; Kaldhone *et al*, 2024, and RBCs: White *et al,* 2017; Devoy *et al*, 2020]. The work of this research project not only supports the continued development of this technology for treatment of plasma and plasma-based products, but also provides valuable knowledge that will support its expansion to a broader range of blood transfusion products.

8.2.4 Adoption of 405-nm Light as a PRT in the Transfusion Medicine Industry

The findings of this Thesis support the development of antimicrobial 405-nm light as a PRT for use in transfusion medicine. Most importantly, the work of this study has identified the operational requirements for a safe and effective 405-nm light treatment that should inform future technology development.

In terms of the clinical adoption of 405-nm light technology for plasma decontamination, it is envisioned that the decontamination treatment will be applied as an additional safety measure, employed as close to the time of transfusion as possible. This provides protection against contamination that may have occurred following release from the blood bank, as well as reducing the risk against newly emerging or re-emerging infectious agents that were undetected during the mandatory screening tests. The use of 405-nm light during storage of *ex vivo* blood products is also of clinical interest, more so with the treatment of prebagged platelets, as there is an opportunity to extend the shelf life through low irradiance continuous exposure throughout the storage period. Moreover, the non-requirement for bag transfers or photo-sensitive agents significantly simplifies the technology's usage and implementation. This approach removes the need for highly skilled personnel, rendering it accessible and cost-effective within the heathcare sector.

As part of the regulatory approval process, an appropriate ISO standard must be developed to ensure the safe adoption of this technology into the healthcare industry [Rem-Siekmann, 2021]. This will include engaging with key stakeholders (regulatory bodies, technology developers, blood banks and hospitals) to ensure a comprehensive perspective. During this process, factors such as performance criteria, testing methods, safety requirements, quality control measures, and documentation procedures will need to be formalised, and agreed upon by technical experts. A pilot test will need to be conducted to assess the feasibility, practicality, and effectiveness of 405-nm light for treatment of *ex vivo* stored plasma. Based on the feedback from this testing phase, the relevant ISO standard would be revised,

finalised and approved by the technical committee and relevant stakeholders. Developing an ISO standard will play a key role in the adoption of 405-nm light as a PRT in the healthcare industry by ensuring quality, safety regulatory compliance, market access and continuous improvement.

8.3 I Overall Summary

The work of this project has significantly contributed to the development of violet-blue 405-nm light as a novel, PRT for treatment of blood transfusion products, to improve blood safety and reduce the risk of TTIs. Through a series of low volume and more clinically relevant, large volume prebagged plasma exposures, this study showed that 405-nm light can provide broad-spectrum microbial inactivation in plasma, using dose levels that demonstrate a high compatibility potential. Most importantly, this study identified the operational parameters (*288 Jcm^{-2}; 16 $mWcm^{-2}$ for 5-hr*) required for effective antimicrobial 405-nm light treatment of *ex vivo* stored plasma, while preserving plasma protein integrity and functionality. The benefits of antimicrobial 405-nm light, including the superior protein compatibility compared to commercially available PRTs as highlighted in this study, in combination with the non-ionizing nature of 405-nm light, and the non-requirement for photosensitizing agents or bag transfers, present 405-nm light as an ideal candidate for further development as a PRT for use in transfusion medicine.

References

Ackfeld, T., Schmutz, T., Guechi, Y. and Terrier, L.C. (2022) Blood transfusion reactions-a comprehensive review of the literature including a Swiss perspective. *Journal of Clinical Medicine*. May. 11(10), 2859

Adam, E.H. and Fischer, D. (2020) Plasma transfusion practice in adult surgical patients: systematic review of the literature. *Transfusion Medicine Hemotherapy*. 47, 347-360

Alonso Villela, S. M., Kraïem, H., Bouhaouala-Zahar, B., Bideaux, C., Aceves Lara, C. A., and Fillaudeau, L. (2020) A protocol for recombinant protein quantification by densitometry. *Microbiologyopen*. 9(6), 1175-1182

American Red Cross. (2023) *US Blood Supply Facts.* American Red Cross Blood Service. Available from: https://www.redcrossblood.org/donate-blood/how-to-donate/how-blood-donations-help/blood-needs-blood-supply.html [Accessed: June 15, 2023]

American Red Cross. (2022) *More People Now Eligible to Give Blood with the Red Cross.* American Red Cross Blood Service. Available from: https://www.redcross.org/about-us/news-and-events/news/2022/more-people-now-eligible-to-give-blood-with-the-red-cross.html [Accessed: December 2, 2023]

Amin, R.M., Bhayana, B., Hamblin, M.R. and Dai, T. (2016) Antimicrobial blue light inactivation of *Pseudomonas aeruginosa* by photo-excitation of endogenous porphyrins: *In vitro* and *in vivo* studies. *Lasers in Surgery and Medicine*. *48*(5), 562–568

Aubry, M., Laughhunn, A., Maria, S.F., Lanteri, M.C and Stassinopoulos. A. (2018) Amustaline (S-303) treatment inactivates high levels of Chikungunya virus in red-blood-cell components. *Vox Sanguinis*. 113 (3), 232-241

Backholer, L., Wiltshire, M., Proffitt, S., Cookson, P. and Cardigan, R. (2016) Paired comparison of methylene blue- and amotosalen-treated plasma and cryoprecipitate. *Vox Sanguinis.* 110, 352-361

Barneck, M.D., Rhodes, N.L.R., de la Presa, M., Allen, J P., Poursaid, A E., Nourian, M.M., Firpo, M.A. and Langell, J.T. (2016) Violet 405-nm light: a novel therapeutic

agent against common pathogenic bacteria. *Journal of Surgical Research*. 206(2), 316-324

Barton, C. and Bierman, J. (2018) *Factor Products* (2018 ed.). The American College of Clinical Pharmacy

Basu, D. and Kulkarni, R. (2014) Overview of blood components and their preparation. *Indian Journal of Anaesthesia*. 58(5), 529-537

Bicalho, B., Serrano, K., Dos Santos Pereira, A., Devine, D. V. and Acker, J. P. (2016) Blood bag plasticizers influence red blood cell vesiculation rate without altering the lipid composition of the vesicles. *Transfusion Medicine and Hemotherapy*. 43(1), 19-26

Boris, K. and Kim, S. (1981) *Spectroscopy of porphyrins* (3rd ed.). Applied Physics Laboratory, pp. 153–156

Braun, J. M., Sathyanarayana, S. and Hauser, R. (2013) Phthalate exposure and children's health. *Current Opinion in Pediatrics*. 25, 247–254

Brecher, M.E. and Hay, S.N. (2005) Bacterial contamination of blood components. *Clinical Microbiology.* 18, 195–204

Brecher, M.E., Holland, P.V., Pineda, A.A., Tegtmeier, G.E. and Yomtovian, R. (2000) Growth of bacteria inoculated platelets: implications for bacteria detection and the extension of platelet storage. *Transfusion*. 40(11), 1308-1312

Brixner, V., Bug, G., Pohler, P., Krämer, D., Metzner, B., Voß, A., Casper, J., Ritter, U., Klein, S., Alakel, N., Peceny, R., Derigs, H.G., Stegelmann, F., Wolf, M., Schrezenmeier, H., Thiele, T., Seifried, E., Kapels, H.H., Döscher, A., Petershofen, E.K., Müller, T.H. and Seltsam, A. (2021) Efficacy of UVC-treated, pathogen-reduced platelets versus untreated platelets: a randomized controlled non-inferiority trial. *Haematologica.* 106(4), 1086-1096

Bubinski, M., Gronowska, A., Szykula, P., Kluska, K., Kuleta, I., Ciesielska, E., Picard-Maureau, M. and Lachert, E. (2021) Plasma pooling in combination with amotosalen/UVA pathogen inactivation to increase standardisation and safety of therapeutic plasma units. *Transfusion Medicine*. 31, 136–141

Bumah, V.V., Aboualizadeh, E., Masson-Meyers, D.S., Eells, J.T., Enwemeka, C.S. and Hirschmugl, C.J. (2017) Spectrally resolved infrared microscopy and

chemometric tools to reveal the interaction between blue light (470nm) and methicillin-resistant *Staphylococcus aureus*. *Journal of Photochemistry and Photobiology B: Biology.* 167, 150-157

Burghi, G., Ortiz, G.and Bagnulo, H. (2011) Blood transfusions: an independent risk factor for the development of *Candida* infections in critically ill surgical patients. *Critical Care*. 15, 237

Burnouf, T. and Radosevich, M. (2000) Reducing the risk of infection from plasma products: specific preventative strategies. *Blood Reviews*. 14(2), 94-110

Cardigan, R. and Green, L. (2015) Thawed and liquid plasma – what do we know? *Vox Sanguinis*. 109, 1-10

Carmen, R. (1993) The selection of plastic materials for blood bags. *Transfusion Medicine Reviews.* 7(1), 1-10

Chargé, S. and Hodgkinson, K. (2022) Blood: The Basics. *Professional Education*. Available from:https://professionaleducation.blood.ca/en/transfusion/publications/blood-basics [Accessed: March 1, 2022]

Cotton, B.A. and McElroy, L.A. (2015). *Encyclopedia of Trauma Care* (ed.). Springer.

Damgaard, C., Magnussen, K., Enevold, C., Nilsson, M., Tolker-Nielsen, T., Holmstrup, P. and Nielsen, C.K. (2015) Viable bacteria associated with red blood cells and plasma in freshly drawn blood donations. *PLoS One*. 10(3), e0120826

Dean, C.L., Wade, J. and Roback, J.D. (2018) Transfusion-transmitted infections: an update on product screening, diagnostic techniques, and the path ahead. *Journal of Clinical Microbiology*. 56(7):e00352-18

DeKorte, D., Marcelis, J. H., Verhoeven, A. J. and Soeterboek, A. M. (2002) Diversion of first blood volume results in a reduction of bacterial contamination for whole-blood collections. *Vox Sanguinis.* 83**,** 13-16

Devoy, R., MacGregor, S., Atreya, C.D. and Maclean, M. (2020) Assessing compatibility of antimicrobial violet-blue light for pathogen reduction of red blood cell concentrates. *Experimental Hematology.* 88, S57-S86

Di Minno, G., Navarro, D., Perno, C. F., Canaro, M., Gürtler, L., Ironside, J. W., Eichler, H., & Tiede, A. (2017) Pathogen reduction/inactivation of products for the treatment of

bleeding disorders: what are the processes and what should we say to patients? *Annals of Hematology*. 96(8), 1253–1270

Dodd, R.Y. (2012) Emerging pathogens and their implications for the blood supply and transfusion transmitted infections. *British Journal of Haematology*. 159(2), 135-142

Domanović, D.; Cassini, A.; Bekeredjian-Ding, I.; Bokhorst, A.; Bouwknegt, M.; Facco, G.; Galea, G.; Grossi, P.; Jashari, R. and Jungbauer, C. (2017) Prioritizing of bacterial infections transmitted through substances of human origin in Europe*. Transfusion*. 2017(57), 1311–1317

Donnelly, R.F., McCarron, P.A. and Tunney, M.M. (2008) Antifungal photodynamic therapy. *Microbiological Research*. 163(1), 1-12

Dougall, L.R., Anderson, J.G., Timoshkin, I.V., MacGregor, S.J. and Maclean, M. (2018) Efficacy of antimicrobial 405 nm blue-light for inactivation of airborne bacteria. *Proceedings of SPIE*. 10479(1G)

Dunstan, R.A., Seed, C.R. and Keller, A.J. (2008) Emerging viral threats to the Australian blood supply. *Australian and New Zealand Journal of Public Health.* 32, 354-360

Eder, A.F. and Sebok, M.A. (2007) Plasma components: FFP, FP24, and thawed plasma. *Immunohematology.* 23(4), 150–157

Endarko, E., Maclean, M., Timoshkin, I.V., MacGregor, S.J. and Anderson, J.G. (2012) High intensity 405nm light inactivation of *Listeria monocytogenes*. *Photochemistry and Photobiology*. 88(5), 1280-1286

Enwemeka, Chukuka S., Williams, D., Hollosi, S., Yens, D. and Enwemeka, S. K. (2008). Visible 405 nm LSD light photo-destroys methicillin-resistant *Staphylococcus aureus* (MRSA) *in vitro*. *Lasers in Surgery and Medicine*. 40(10), 734–737

Escolar, G., Diaz-Ricart, M., and McCullough, J. (2022) Impact of different pathogen reduction technologies on the biochemistry, function, and clinical effectiveness of platelet concentrates: An updated view during a pandemic. Transfusio*n*. 62, 227–246

Estcourt, L.J., Birchall, J., Allard, S., Bassey, S.J., Hersey, P., Kerr, J.P., Mumford, A.D., Stanworth, S.J. and Tinegate, H. (2017) Guidelines for the use of platelet transfusions. *British Journal of Haematology.* 176, 365-394

FDA Center for Biologics Evaluation and Research. (2018) Fatalities reported to FDA following blood collection and transfusion: annual summary for fiscal year 2018. Available from: https://www.fda.gov/vaccines-blood-biologics/report-problem-center-biologics-evaluation-research/transfusiondonation-fatalities [Accessed: May 10, 2024]

FDA Center for Biologics Evaluation and Research. (2022) Recommendations to reduce the possible risk of transmission of Creutzfeldt-Jakob Disease and variant Creutzfeldt-Jakob Disease by blood and blood components: Guidance for industry. *fda guidance*. Available from: https://www.fda.gov/regulatory-information/search-fda-guidance-documents/recommendations-reduce-possible-risk-transmission-creutzfeldt-jakob-disease-and-variant-creutzfeldt [Accessed: December 2, 2023]

Fournier-Wirth, C., Jaffrezic-Renault, N. and Coste, J. (2010) Detection of blood-transmissible agents: can screening be miniaturized? *Transfusion*. 50(9), 2032-2045

Fred, H.L., Thangam, M. and Aisenberg, G.M. (2018) Pathogens transmitted in red blood cell transfusions: an up-to-date table. *Baylor University Medical Center Proceedings.* 2018(31), 307–309

Garcia-Rubio, R., Oliveira, H.G., Rivera, J. and Trevijano-Contador, N. (2020) The fungal cell wall: *Candida, Cryptococcus,* and *Aspergillus* species. *Frontiers in Microbiology*. 10(2993), 1-12

Gautam, P., Nair, S.C., Ramamoorthy, K., Swamy, C.V. and Nagaraj, R. (2013) Analysis of human blood plasma proteome from ten healthy volunteers from Indian population. *PLoS One*. 8(8), e72584

Gehrie, E.A., Rutter, S.J. and Snyder, E.L. (2019) Pathogen reduction: the state of the science in 2019. *Hematology/Oncology Clinics of North America.* 33(5), 749-766

Ghosh, I. and Haldar, R. (2019) Blood warming in trauma related transfusions-precepts and practices. *Journal of Cardiovascular Medicine and Cardiology*. 6(4), 94-97

Ghosh, K. (2016) Management of haemophilia in developing countries: challenges and options. *Indian Journal of Hematology and Blood Transfusion*. 32(3), 347-55

Gibson, T. and W. Norris. (1998) Skin fragments removed by injection needles. *Lancet*. 2, 983-985

Girard, P. M., Francesconi, S., Pozzebon, M., Graindorge, D., Rochette, P., Drouin, R. and Sage, E. (2011) UVA-induced damage to DNA and proteins: direct versus indirect photochemical processes. *Journal of Physics: Conference Series*. 261, 012002

Goldman, M.G., Roy, N., Frechette, F., Decary, L., Massicotte, L. and Delage, G. (1997) Evaluation of donor skin disinfection methods. *Transfusion*. 37, 309-312

Gottlieb, S. (1999) FDA bans blood donation by people who have lived in UK. *British Medical Journal*. 319(7209), 533-535

Gottlieb, T. (1993) Hazards of bacterial contamination of blood products. *Anaesthesia and Intensive Care.* 21(1), 20-23

Grayson, C.A. (2007) *Blood flows not just through our veins but through our minds. How has the global politics of blood impacted on the UK haemophilia community?* Ph.D. Thesis. University of Sutherland, United Kingdom. Available from: https://haemophilia.org.uk/wp-content/uploads/2021/07 [Accessed: December 18, 2023]

Gross, A., Stangl, K.H., Hoenes, M. and Hessling, M. (2015) Improved drinking water disinfection with UVC-LEDs for *Escherichia coli* and *Bacillus subtilis* utilizing quartz tubes as light guide. *Water*. 7(12), 4605–4621

Grubyte, S., Urboniene, J., Nedzinskiene, L. and Jancoriene, L. (2021) The epidemiological patterns of Hepatitis C in Lithuania: changes in surveillance from 2005 to 2018. *Medicina (Kaunas)*. 57(10), 1120

Guess, W.L., Austin, J. and Jacob, J. (1967) A study of polyvinyl chloride blood bag assemblies, i: alteration or contamination of ACD solutions. *Annals of Pharmacotherapy*. 1, 120–127

Hamblin, M.R. and Hassan T. (2004) Photodynamic therapy: a new antimicrobial approach to infectious disease? *Photochemistry and Photobiology Science*. 3, 436–350

Hans, R. and Marwaha, N. (2014) Nucleic acid testing-benefits and constraints. *Asian Journal of Transfusion Science*. 8(1), 2-3

Harrison, E., Stalhberger, T., Whelan, R., Sugrue, M., Wingard, J.R., Alexander, B.D., Follett, S.A., Bowyer, P. and Denning, D.W. (2010) Denning for the *Aspergillus*

technology consortium (AsTeC): Aspergillus DNA contamination in blood collection tubes. *Diagnostic Microbiology* and *Infectious Disease.* 67(4), 392-394

Harutyunyan, H.A. (2017) Prothrombin and fibrinogen carbonylation: how that can affect the blood clotting. *Redox Report*. 22(4), 160-165

Hillyer, C.D., Josephson, C.A., Blajchman, M.A., Vostal, J.G., Epstein, J.S. and Goodman, J.L. (2003) Bacterial contamination of blood components: risks, strategies, and regulation. *The Hematology ASH Education Program*. 2003(1), 575–589

Hirano, R., Yuichi, S., Kumiko, K. and Motoki, O. (2015) Retrospective analysis of mortality and *Candida* isolates of 75 patients with candidemia: a single hospital experience. *Infection and Drug Resistance*. 8, 199–205

Hmel, P.J., Kennedy, A., Quiles, J.G., Gorogias, M., Seelbaugh, J.P., Morrissette, C.R., Van Ness, K. and Reid, T.J. (2002) Physical and thermal properties of blood storage bags: implications for shipping frozen components on dry ice. *Transfusion*. 42(7), 836-846

Hornsey, V.S., Drummond, O., Morrison, A., McMillan, L., MacGregor, I.R. and Prowse, C.V. (2009) Pathogen reduction of fresh plasma using riboflavin and ultraviolet light: effects on plasma coagulation proteins. *Transfusion*. 49(10), 2167-2172

Imada, K., Tanaka, S., Ibaraki, Y., Yoshimura, K. and Ito, S. (2014) Antifungal effect of 405-nm light on *Botrytis cinerea*. *Letters in Applied Microbiology*. 59(6), 670–676

Irsch, J. and Lin, L. (2011) Pathogen inactivation of platelet and plasma blood components for transfusion using the Intercept blood system™. *Transfusion Medicine and Hemotherapy*. 38(1), 19-31

Irving, D., Lamprou, D.A., Maclean, M., MacGregor, S.J., Anderson, J.G. and Grant, M.H. (2016) A comparison study of the degradative effects and safety implications of UVC and 405 nm germicidal light sources for endoscope storage. *Polymer Degradation and Stability*. 133, 249–254

Ito, K., Inoue, S., Yamamoto, K. and Kawanishi, S. (1993) 8-Hydroxydeoxyguanosine formation at the *5'* site of *5'-gg-3'* sequences in double-stranded DNA by UV radiation with riboflavin. *The Journal of Biological Chemistry.* 268(18), 13221-13227

Jana, S., Heaven, M.R., Dahiya, N., Stewart, C.F., Anderson, J., MacGregor, S., Maclean, M., Alayash, A.I. and Atreya, C. (2023) Antimicrobial 405 nm violet-blue light treatment of *ex vivo* human platelets leads to mitochondrial metabolic reprogramming and potential alteration of Phospho-Proteome. *Journal of Photochemistry and Photobiology B: Biology.* 241, 112672

Jankowska, K.I., Nagarkatti, R., Acharyya, N., Dahiya, N., Stewart, C.F., Macpherson, R.W., Wilson, M.P., Maclean, M., Anderson, J.G., MacGregor, S.J. and Atreya, C.D. Complete inactivation of blood borne pathogen *Trypanosoma cruzi* in stored human platelet concentrates and plasma treated with 405 nm violet-blue light. *Frontiers in Medicine.* 7(617373)

Ježková, Z. (1972) Frozen human plasma and bacterial contamination. *Annals of Hematology.* 25, 249–254

Jia, J., Zhang, M., Ma, Y. and Zhang, Y. (2019) Human parvovirus B19 research concerning the safety of blood and plasma derivatives in China. *Annals of Blood*. 4, 1-9

Joint United Kingdom Blood Transfusion and Tissue Transplantation Services Professional Advisory Committee (JPAC). (2014*) Transfusion Guidelines: Infectious hazards of transfusion*. Available from: https://www.transfusionguidelines.org/transfusion-handbook/5-adverse-effects-of-transfusion/5-3-infectious-hazards-of-transfusion [Accessed: April 1, 2023]

Josefsen, L.B. and Boyle, R.W. (2008) Photodynamic therapy and the development of metal-based photosensitisers. *Metal-Based Drugs*. 2008(276109), 1-23

Kaldhone, P.R., Azodi, N., Markle, H.L., Dahiya, N., Stewart, C., Anderson, J., MacGregor, S., Maclean, M., Nakhasi, H.L. and Gannavaram, S. (2024) The preclinical validation of 405 nm light parasiticidal efficacy on *Leishmania donovani* in *ex vivo* platelets in a Rag2−/− mouse model. *Microorganisms*. 2024(12), 280

Karafin, M.S. and Hillyer, C.D. (2013) Plasma products. *Transfusion Medicine and Hemostasis*. 209–218

Keitel, S. (2009). *Guide to the Preparation, Use and Quality Assurance of Blood Components* (ed.). Council of Europe, pp. 256-258

Kim, M.J. and Yuk, H.G. (2017) Antibacterial mechanism of 405-nanometer light-emitting diode against *Salmonella* at refrigeration temperature. *Applied and Environmental Microbiology.* 83(5), e02582–e02616

Kim, M.J., Mikš-Krajnik, M., Kumar, A., Ghate, V. and Yuk, H.G. (2015) Antibacterial effect and mechanism of high-intensity 405 ± 5 nm light-emitting diode on *Bacillus cereus, Listeria monocytogenes*, and *Staphylococcus aureus* under refrigerated conditions. *Journal of Photochemistry and Photobiology B: Biology*. 153, 33–39

Kim, M.J., Miks-Krjnik, M., Kumar, A. and Yuk, H.G. (2016) Inactivation by 405 nm ± 5 nm light emitting diode on *Escherichia coli, Salmonella Typhimurium,* and *Shigella sonnei* under refrigerated condition might be due to the loss of membrane integrity. *Food Control*. 59, 99-107

Kitagawa, H., Nomura, T., Nazmul, T., Kawano, R., Omori, K., Shigemoto, N., Sakaguchi, T. and Ohge, H. (2021) Effect of intermittent irradiation and fluence-response of 222 nm ultraviolet light on SARS-CoV-2 contamination. *Photodiagnosis and Photodynamic Therapy*. 33, 102184

Kitchen, D.P., Kitchen, S., Jennings, I., Woods, T. and Walker, I. (2010) Quality assurance and quality control of thrombelastography and rotational thromboelastometry: the UK NEQAS for blood coagulation experience. *Seminars in Thrombosis and Hemostasis*. 36(7), 757-763

Klein, H.G. (2005) Pathogen inactivation technology: cleansing the blood supply. *Journal of Internal Medicine*. 257, 224-237

Klein, H.G. and Bryant, B.J. (2009) Pathogen-reduction methods: advantages and limits. *ISBT Science Series.* 4: 154-160

Kotthoff-Burrell E. (2019) Candidemia (blood infection) and other *Candida* infections. *American Journal of Respiratory and Critical Care Medicine*. 200, 9-10

Larsson, L., Ohlsson, S., Derving, J., Diedrich, B., Sandgren, P., Larsson, S. and Uhlin, M. (2022) DEHT is a suitable plasticizer option for phthalate-free storage of irradiated red blood cells. *Vox Sanguinis.* 117(2), 193-200

Larsson, L., Sandgren, P., Ohlsson, S., Derving, J., Friis-Christensen, T., Daggert, F., Frizi, N., Reichenberg, S., Chatellier, S., Diedrich, B., Antovic, J., Larsson, S. and

Uhlin, M. (2021) Non-phthalate plasticizer DEHT preserves adequate blood component quality during storage in PVC blood bags. *Vox Sanguinis.* 116(1), 60-70

Li, M., Zhao, B., Han, L. and Wang, Z. (2022) Study on the inactivation effect and damage on bacteria of ultraviolet light with multi irradiance by UV-LED. *Research Square*

Lu, M., Dai, T.H. and Hu, S.S. (2020). Antimicrobial blue light for decontamination of platelets during storage. *Journal of Biophotonics.* 13, e201960021

Lu, M., Dai, T.H. and Hu, S.S. (2020) Antimicrobial blue light for decontamination of platelets during storage. *Journal of Biophotonics*. 13(e201960021)

Lubart, R., Lipovski, A., Nitzan, Y., & Friedmann, H. (2011). A possible mechanism for the bactericidal effect of visible light. *Laser Therapy.* 20(1), 17-22

Lund, M. and Baron, C. (2010) *Chemical Deterioration and Physical Instability of Food and Beverages* (1st ed.). Woodhead Publishing, pp. 33-69

Maclean, M. (2006) *An investigation into the light inactivation of medically important microorganisms.* Ph.D. thesis. University of Strathclyde, Glasgow, Scotland, United Kingdom

Maclean, M., Anderson, J.G., MacGregor, S.J., White, T. and Atreya, C.D. (2016) A new proof of concept in bacterial reduction: antimicrobial action of violet-blue light (405 nm) in *ex vivo* stored plasma. *Journal of Blood Transfusion*. 1-11

Maclean, M., Gelderman, M.P., Kulkarni, S., Tomb, R.M., Stewart, C.F., Anderson, J.G., MacGregor, S.J. and Atreya, C.D. (2020) Non-ionizing 405 nm light as a potential bactericidal technology for platelet safety: evaluation of *in vitro* bacterial inactivation and *in vivo* platelet recovery in severe combined immunodeficient mice. *Frontiers of Medicine*. 6(331), 1-8

Maclean, M., MacGregor, S.J., Anderson, J.G. and Woolsey, G. (2008) High-intensity narrow-spectrum light inactivation and wavelength sensitivity of *Staphylococcus aureus*. *FEMS Microbiology Letters 285*. 2, 227–232

Maclean, M., MacGregor, S.J., Anderson, J.G. and Woolsey, G. (2009). Inactivation of bacterial pathogens following exposure to light from a 405-nanometer light-emitting diode array. *Applied and Environmental Microbiology*. 75(7), 1932-1937

Maisch, T. (2009) A new strategy to destroy antibiotic resistant microorganisms: antimicrobial photodynamic treatment. *Mini Reviews in Medicinal Chemistry*. 9 (8), 974-983

Maramica, I. (2019) *Transfusion Medicine and Hemostasis* (3rd ed.). Elsevier, pp. 409-411

Marschner, S. and Dimberg, L.Y. (2019) Pathogen reduction technologies. *Transfusion Medicine and Hemostasis*. 48, 289–293

Marschner, S. and Goodrich, R. (2011) Pathogen reduction technology treatment of platelets, plasma and whole blood using riboflavin and UV light. *Transfusion Medicine and Hemotherapy*. 38(1), 8-18

Marwaha, N. (2013) Transfusion related complications in hemophilia. *Asian Journal of Transfusion Science*. 7(1), 6-7

McDonald, R., Macgregor, S.J., Anderson, J.G., Maclean, M. and Grant, M.H. (2011) Effect of 405-nm high-intensity narrow-spectrum light on fibroblast-populated collagen lattices: an *in vitro* model of wound healing. *Journal of Biomedical Optics*. 16(4), 48003

McKenzie, K., Maclean, M., Grant, M.H., Ramakrishnan, P., MacGregor, S.J., and Anderson, J.G. (2016) The effects of 405 nm light on bacterial membrane integrity determined by salt and bile tolerance assays, leakage of UV-absorbing material, and SYTOX green labelling. *Microbiology*. 162(9), 1680-1688

Meißner, A. and Schlenke, P. (2012) Massive bleeding and massive transfusion. *Transfusion Medicine Hemotherapy*. 39(2), 73-84

Mertes, P., Demoly, P., Alperovitch, A., Bazin, A., Bienvenu, J. and Caldani, C. (2012) Methylene blue–treated plasma: An increased allergy risk?. *Journal of Allergy and Clinical Immunology*. *130*(3), 808-812

Moorhead, S., Maclean, M., Coia, J.E., MacGregor, S.J. and Anderson, J.G. (2016) Synergistic efficacy of 405 nm light and chlorinated disinfectants for enhanced decontamination of *Clostridium difficile* spores. *Anaerobe*. 37, 72–77

Murdoch, L.E., Maclean, M., Endarko, E., MacGregor, S.J. and Anderson, J.G. (2012) Bactericidal effects of 405 nm light exposure demonstrated by inactivation of *Escherichia, Salmonella, Shigella, Listeria*, and *Mycobacterium* species in liquid

suspensions and on exposed surfaces. *The Scientific World Journal*. 2012(137805), 1-8

Murdoch, L.E., McKenzie, K., Maclean, M., MacGregor, S.J. and Anderson, J.G. (2013) Lethal effects of high intensity violet 405-nm light on *Saccharomyces cerevisiae, Candida albicans* and on dormant and germinating spores of *Aspergillus niger*. *Fungal Biology.* 117(7-8), 519–527

NHS (a). (2021) *Prevention Creutzfeldt-Jakob disease*. Available from: https://www.nhs.uk/conditions/creutzfeldt-jakob-disease-cjd/prevention [Accessed: August 23, 2023]

NHS Blood and Transplant (a). (2022) *Blood Plasma: making all the difference to patients.* Available from: https://www.blood.co.uk/news-and-campaigns/the-donor/latest-stories/blood-plasma-making-all-the-difference-topatients [Accessed: June 15, 2022]

NHS Blood and Transplant (b). (2022) *How Plasma Helps*. Available from: https://www.blood.co.uk/why-give-blood/how-blood-is-used/bloodcomponents/ [Accessed: May 15, 2022]

NHS Blood and Transplant (c). (2022) *Ban lifted on use of UK plasma to manufacture life-saving albumin treatments.* Available from: https://www.nhsbt.nhs.uk/news/ban-lifted-on-use-of-uk-plasma-to-manufacture-life-saving-albumin-treatments/ [Accessed: May 15, 2022]

NHS Blood and Transplant (d). (2022) *The plasma for medicine programme.* Available from: https://www.nhsbt.nhs.uk/what-we-do/blood-services/plasma-donation/the-plasma-for-medicines-programme/ [Accessed: May 15, 2022]

NHS South Tees Hospital. (2021) *Coagulation Screens*. Available from: https://www.southtees.nhs.uk/services/pathology/tests/coagulation-screens [Accessed: July 17, 2022]

NHS. (2020) *Haemophilia Health A-Z*. Available from: https://www.nhs.uk/conditions/haemophilia/#:~:text=Haemophilia%20is%20a%20rare%20condition,sticky%20and%20form%20a%20clot [Accessed: January 29, 2024]

Nitzan, Y., Salmon-Divon, M., Shporen, E. and Malik, Z. (2004) ALA induced photodynamic effects on Gram-positive and negative bacteria. *Photochemical & Photobiological Sciences*. 3(5), 430-435

Nubret, K., Delhoume, M., Orsel, I., Laudy, J.S., Sellami, M. and Nathan, N. (2011) Anaphylactic shock to fresh-frozen plasma inactivated with methylene blue. *Transfusion*. 51, 125-128

O'Flaherty, C. and Matsushita-Fournier, D. (2017) Reactive oxygen species and protein modifications in spermatozoa. *Biology Of Reproduction*. 97(4), 577-585

Otto, M. (2009) *Staphylococcus epidermidis*--the 'accidental' pathogen. *Nature Reviews Microbiology.* 7(8), 555-567

Pandey, K.B. and Rizvi, S.I. (2010) Markers of oxidative stress in erythrocytes and plasma during aging in humans. *Oxidative Medicine and Cellular Longevity*. 3(1), 2-12

Patel, R.M. and Josephson, C.D. (2018) *Avery's Diseases of the Newborn* (10th ed). Elsevier Saunders, pp. 1180–1186

Pelletier, J.P., Transue, S. and Snyder, E.L. (2016) Pathogen inactivation techniques. *Best Practice and Research Clinical Haematology.* 19(1), 205-242

Picker, S.M. (2013) Current methods for the reduction of blood-borne pathogens: a comprehensive literature review. *Blood Transfusion*. 11(3), 343-348

Piotrowski, D., Przybylska-Baluta, Z. and Jimenez-Marco, T. (2018) Passive haemovigilance of blood components treated with a riboflavin-based pathogen reduction technology. *Blood Transfusion.* 16(4), 348-351

Radaniel, T., Genay, S., Simon, N., Feutry, F., Quagliozzi, F., Barthélémy, C., Lecoeur, M., Sautou, V., Décaudin, B. and Odou, P. (2014) Quantification of five plasticizers used in PVC tubing through high-performance liquid chromatographic-UV detection. *Journal of Chromatography B*. 965, 158-163

Ragupathy, V., Haleyurgirisetty, M., Dahiya, N., Stewart, C.F., Anderson, J.G., MacGregor S.J., Maclean, M., Hewlett, I. and Atreya, C.D. (2022) Visible 405-nm violet-blue light successfully inactivates HIV-1 in human plasma. *Pathogens*. 11(7), 778

Ramakrishnan, P., Maclean, M., MacGregor, S.J., Anderson, J.G. and Grant, M.H. (2016) Cytotoxic responses to 405 nm light exposure in mammalian and bacterial cells: involvement of reactive species. *Toxicology in Vitro*. 33, 54-62

Rampon, C., Volovitch, M., Joliot, A. and Vriz, S. (2018) Hydrogen peroxide and redox regulation of developments. *Antioxidants*. 7(11), 159

Rathnasinghe, R., Jangra, S., Miorin, L., Schotsaert, M., Yahnke, C. and García-Sastre, A. (2021) The virucidal effects of 405 nm visible light on SARS-CoV-2 and Influenza A virus. *Scientific Reports*. 11, 19470

Rem-Siekmann, R. (2021) Quick Guide to Medical Device Standards: ISO standards and beyond, RQM+. Available from: https://www.rqmplus.com/blog/quick-guide-to-medical-device-standards-iso-standards-and-beyond [Accessed: May 10, 2024]

Rumbaut, R.E. and Thiagarajan, P. (2010) *Integrated Systems Physiology: From Molecule to Function to Disease* (ed.). Morgan & Claypool Life Sciences

Salyer, S.W. (2007) *Essential Emergency Medicine* (ed.). Saunders, pp. 555-574

Savini, V., Balbinot, A., Giancola, R., Quaglietta, A., Accorsi, P., D'Antonio, D. and Iacone, A. (2009) Comparison between the BACTEC 9240 and the Pall eBDS system for detection of bacterial platelet concentrate contamination. *Transfusion*. 49(6), 1217-1223

Schenk, S., Schoenhals, G.J., de Souza, G. and Matthias, M. (2008) A high confidence, manually validated human blood plasma protein reference set. *BMC Medical Genomics*. 1(41), 12-15.

Schlenke, P. (2014) Pathogen inactivation technologies for cellular blood components: an update*. Transfusion Medicine and Hemotherapy.* 41(4), 309-325

Scott, S.R. and Wu, Z. (2019) Risks and challenges of HIV infection transmitted via blood transfusion. *Biosafety and Health*. 1(3), 124-128

Seghatchian, J., Struff, W.G. and Reichenberg, S. (2011) Main properties of the Theraflex MB-plasma system for pathogen reduction. *Transfusion medicine and hemotherapy: offizielles Organ der Deutschen Gesellschaft fur Transfusionsmedizin und Immunhamatologie*. *38*(1), 55–64

Selmeci, L., Székely, M., Soós, P., Seres, L., Klinga, N., Geiger, A. and Acsády, G. (2006) Human blood plasma advanced oxidation protein products (AOPP) correlates with fibrinogen levels. *Free Radical Research*. 40(9), 952-958

Seltsam, A. (2017) Pathogen inactivation of cellular blood products—an additional safety layer in transfusion medicine. *Frontiers in Medicine*. 4(219), 1-6

Seltsam, A. and Müller, T.H. (2013) Update on the use of pathogen-reduced human plasma and platelet concentrates. *British Journal of Haematology*. 162, 442-454

Sidonio, R.F., Boban, A., Dubey, L., Inati, A., Csongor, K., Lissitchkov, T., Novik, D., Peteva, E., Taher, A.T., Timofeeva, M.A., Vilchevska, K.V., Vdovin, V., Werner, S., Knaub, S. and Khayat, C. (2022) Efficacy and safety of prophylaxis with a plasma-derived von Willebrand Factor/Factor viii concentrate in previously treated patients with von Willebrand disease. *Blood*. 140 (Supplement 1), 8438–8439

Sinclair, L.G., Dougall, L.R., Ilieva, Z., McKenzie, K., Anderson, J.G., MacGregor, S.J. and Maclean, M. (2023) Laboratory evaluation of the broad-spectrum antibacterial efficacy of a low-irradiance visible 405-nm light system for surface-simulated decontamination. *Health Technology.* 13, 615–629

Singh, G. and Sehgal, R. (2010) Transfusion-transmitted parasitic infections. *Asian Journal of Transfusion Science*. 4(2), 73-77

Skibsted, L. H. (2011) Nitric oxide and quality and safety of muscle based foods. *Nitric Oxide*. 24, 176–183

Solheim, B. G. and Seghatchian, J. (2006) Update on pathogen reduction technology for therapeutic plasma: an overview. *Transfusion and Apheresis Science*. 35(1), 83–90

Stigum, H., Magnus, P. and Samdal, H.H. (2000) Human T-cell lymphotropic virus testing of blood donors in Norway: a cost-effect model. *International Journal of Epidemiological Association*. 29(6), 1076-84

Sułek, A., Pucelik, B., Kobielusz, M., Barzowska, A. and Dąbrowski J.M. (2020) Photodynamic inactivation of bacteria with porphyrin derivatives: effect of charge, lipophilicity, ROS generation, and cellular uptake on their biological activity *in vitro. International Journal of Molecular Sciences*. 21(22), 1-33

The Food and Drug Administration. (2009) Guidance for industry use in medical product development to support labelling claims guidance for industry. *Federal Register*. 1-39, 65132-65133

The Hepatitis C Trust. (2020) *The Infected Blood Inquiry*. Available from: https://www.hepctrust.org.uk/find-support/infected-blood-and-blood-products/infected-blood-inquiry/ [Accessed: August 4, 2023]

The National CJD Research & Surveillance Unit. (2020) *Creutzfeldt-Jakob Disease Surveillance in The UK*, 29th Annual Report, 1-33. Available from: https://www.cjd.ed.ac.uk/sites/default/files/report29.pdf [Accessed: August 24,2023]

Tomb, R.M., Maclean, M., Coia, J. E., Graham, E., McDonald, M., Atreya, C.D., MacGregor, S.J., & Anderson, J.G. (2017a) New proof-of-concept in viral inactivation: virucidal efficacy of 405 nm light against feline calicivirus as a model for norovirus decontamination. *Food and Environmental Virology.* 9(2), 159-167

Tomb, R.M., Maclean, M., Coia, J.E., MacGregor, S.J., & Anderson, J.G. (2017b) Assessment of the potential for resistance to antimicrobial violet-blue light in *Staphylococcus aureus*. *Antimicrobial Resistance and Infection Control.* 6, 100

Tribelli, P.M. and López, N.I. (2018) Reporting Key Features in Cold-Adapted Bacteria. *Life (Basel).* 13;8(1):8

Trzaska, W.J., Wrigley, H.E., Thwaite, J.E. and May, R.C. (2017) Species-specific antifungal activity of blue light. *Scientific Reports.* 7, 4605

Vamvakas, E. C. and Blajchman, M. A. (2010) Blood still kills: six strategies to further reduce allogeneic blood transfusion-related mortality. *Transfusion Medicine Reviews*. *24*(2), 77–124

Van der Meer, P.F. (2013) Platelet concentrates, from whole blood or collected by apheresis? *Transfusion* and *Apheresis Science*. 48(2), 129-131

Wagner, S.J., Friedman, L.I. and Dodd, R.Y. (1994) Transfusion-associated bacterial sepsis. *Clinical Microbial Reviews*. 7(3), 290-302

White, T., Maclean, M., Watson, H., Tomb, R., Anderson, J., MacGregor, S. and Atreya, C. (2017) Physiological effects of pathogen reduction of red blood cell products using antimicrobial blue light. *Experimental Hematology*. 53, S58

Williamson, L.M., Cardigan, R. and Prowse, C.V. (2003) Methylene blue-treated fresh-frozen plasma: what is its contribution to blood safety? *Transfusion*. 43(9), 1322-1329

Winters, J.L. (2017) Plasma exchange in thrombotic microangiopathies (TMAs) other than thrombotic thrombocytopenic purpura (TTP). *Hematology-American Society of Hematology Education Program*. 2017(1), 632-638

World Health Organization. (2023) *Blood safety and availability.* World Health Organization News Room. Available from: https://www.who.int/news-room/fact-sheets/detail/blood-safety-and-availability [Accessed: June 3, 2023]

Wu, J., Chu, Z., Ruan, Z., Wang, X., Dai, T. and Hu, X. (2018) Changes of intracellular porphyrin, reactive oxygen species, and fatty acids profiles during inactivation of methicillin-resistant *Staphylococcus aureus* by antimicrobial blue light. *Frontiers of Physiology.* 28(9), 1658

Yazer, M.H. (2012) A primer on evidence-based plasma therapy. International Society of Blood Transfusion *Science Series.* 7(1), 220–225

Yin, R., Dai, T., Avci, P., Jorge, A.E S., de Melo, W.C.M.A., Vecchio, D., Huang, Y-Y., Gupta, A. and Hamblin, M.R. (2013) Light based anti-infectives: ultraviolet C irradiation, photodynamic therapy, blue light, and beyond. *Current Opinion in Pharmacology*. 13(5), 731–762

Zhang, Y., Zhu, Y., Chen, J., Wang, Y., Sherwood, M.E., Murray, C.K., Vrahas, M.S., Hooper, D.C., Hamblin, M.R. and Dai, T. (2016) Antimicrobial blue light inactivation of *Candida albicans*: *In vitro* and i*n vivo* studies. *Virulence*. 7(5), 536–545

Zhong, H. and Yin, H. (2015) Role of lipid peroxidation derived 4-hydroxynonenal (4-HNE) in cancer: focusing on mitochondria. *Redox Biology*. 4, 193-199

Appendix A I

Characterisation of Plasma using SDS-PAGE

Before conducting 405-nm light exposures, it was important to characterise the natural variation of protein in plasma, between different samples and batches, using SDS-PAGE. Figure A is an image of the gel used to compare the electrophoretic band patterns of different plasma samples from the same batch. As highlighted in Figure A(A1), the electrophoretic patterns of non-exposed plasma samples (Lanes 1-5) show variation, particularly in the high molecular weight region (70-198 kDa). This is reflected in Figure A(A2), where the intensity level of high molecular weight proteins (HMWPs) in lane 1 is *2x* higher than the protein levels observed in Lane 4. The minor differences in electrophoretic patterns of plasma samples shown in Lanes 1–5 is likely due to natural sample-to-sample variation.

A similar test was performed to evaluate the variability of proteins in plasma from batch-to-batch. Figures A(B1) is an image of the gel used to compare electrophoretic patterns of plasma from different batches. Visible differences in the electrophoretic patterns of plasma samples from different batches can be observed. Semi-quantative analysis of electrophoretic bands of HMWPs, shown in Figure A(B2), highlights the differences in protein levels between batches, with the sample in lane 6 shown to have notably lower protein levels compared to all other plasma batches (Lanes 1–5). Batch-to-batch variation is likely due to natural differences in plasma proteome (influenced by genetics, general health, diet and lifestyle) between individuals as well as the method of blood processing. Due to the nature of plasma, it is difficult to confirm whether minor changes in electrophoretic patterns are due to natural variances in plasma or degradative effects of light treatment. Therefore, SDS-PAGE was predominantly used as an indicator for major protein damage only.

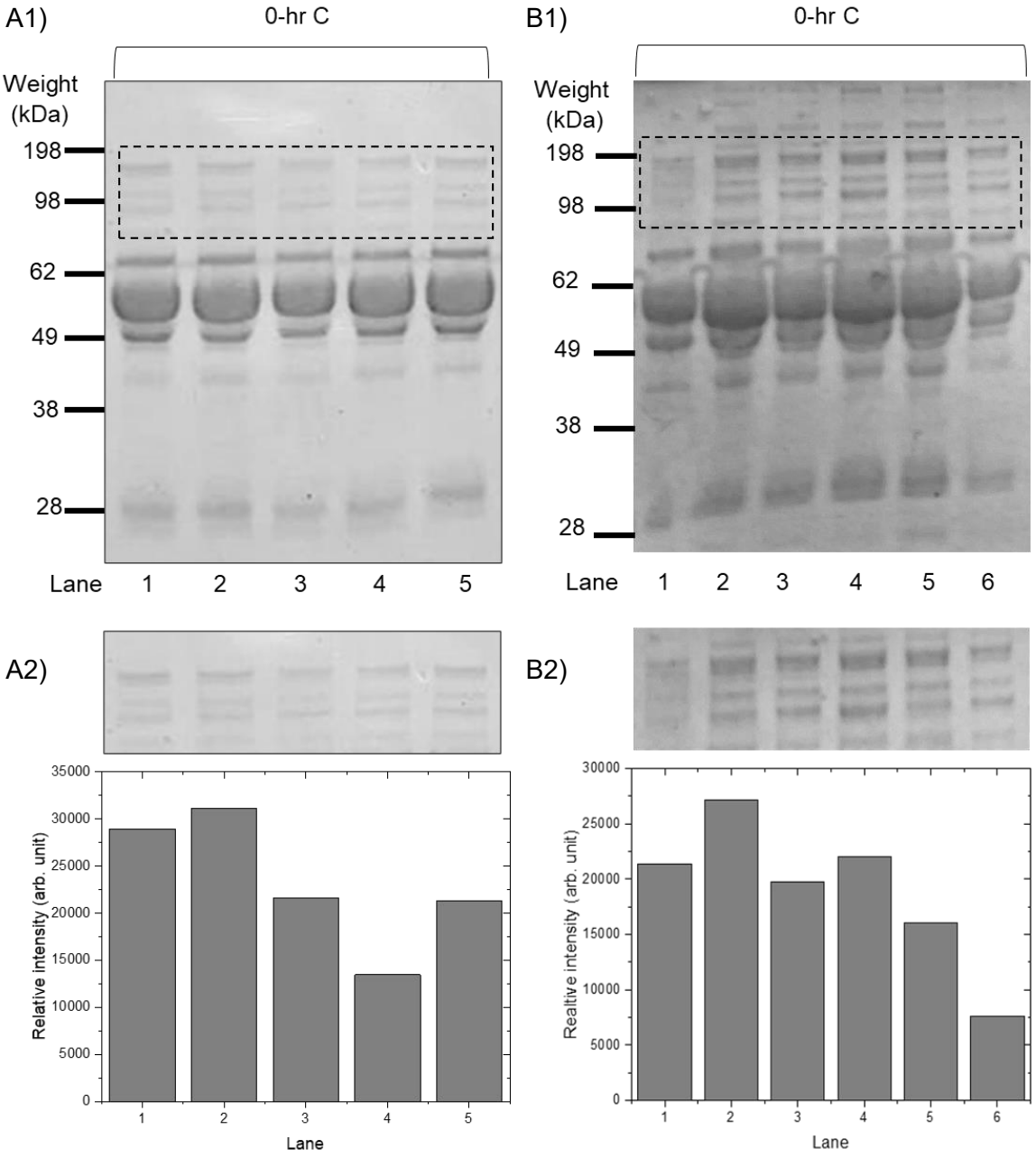

Figure A. Assessing natural protein variation in plasma from A) sample-to-sample and B) batch-to-batch using SDS-PAGE. Images A1 and B1 show the SDS-PAGE analysis of protein profiles of non-exposed plasma from different samples and batches and Images A2 and B2 show the semi-quantitative analysis of protein levels of high molecular weight proteins obtained using ImageJ Software http://rsb.info.nih.gov/ij).

Appendix B I Publications

First Author Peer Reviewed Journal Publications:

- **Stewart, C.F**., Tomb, R.M., Ralston, H.J., Armstrong, J., Anderson, J.G., MacGregor, S.J., Atreya, C.D. and Maclean, M. (2022) Violet-blue 405-nm light-based photoinactivation for pathogen reduction of human plasma provides broad antibacterial efficacy without visible degradation of plasma proteins. *Photochemistry and Photobiology*. 98(2), 504-512
- Microbial Reduction of Prebagged Human Plasma using 405nm Light and its effects on Coagulation Factors. **Stewart, C.F**., McGoldrick, P., Anderson, J.G., MacGregor, S.J., Atreya, C.D. and Maclean, M. *Accepted for Submission to AMB Express*

Co-Author Peer Reviewed Journal Publications:

- Maclean, M., Gelderman, M.P., Kulkarni, S., Tomb, R.M., **Stewart, C.F**., Anderson, J.G., MacGregor, S.J. and Atreya, C.D. (2020) Non-ionizing 405 nm light as a potential bactericidal technology for platelet safety: evaluation of *in vitro* bacterial inactivation and *in vivo* platelet recovery in severe combined immunodeficient mice. *Frontiers of Medicine*. 6(331), 1-8
- Jankowska, K.I., Nagarkatti, R., Acharyya, N., Dahiya, N., **Stewart, C.F**., Macpherson, R.W., Wilson, M.P., Maclean, M., Anderson, J.G., MacGregor, S.J. and Atreya, C.D. (2020) Complete inactivation of blood borne pathogen *Trypanosoma cruzi* in stored human platelet concentrates and plasma treated with 405 nm violet-blue light. *Frontiers in Medicine.* 7(617373)
- Ragupathy, V., Haleyurgirisetty, M., Dahiya, N., **Stewart, C.F.,** Anderson, J.G., MacGregor S.J., Maclean, M., Hewlett, I. and Atreya, C.D. (2022) Visible 405-nm violet-blue light successfully inactivates HIV-1 in human plasma. *Pathogens*. 11(7), 778
- Jana, S., Heaven, M.R., Dahiya, N., **Stewart, C.F.,** Anderson, J., MacGregor, S., Maclean, M., Alayash, A.I. and Atreya, C. (2023) Antimicrobial 405 nm violet-blue light treatment of *ex vivo* human platelets leads to mitochondrial metabolic reprogramming and potential alteration of Phospho-Proteome. *Journal of Photochemistry and Photobiology B: Biology.* 241, 112672
- Kaldhone, P.R., Azodi, N., Markle, H.L., Dahiya, N., **Stewart, C.F**, Anderson, J., MacGregor, S., Maclean, M., Nakhasi, H.L. and Gannavaram, S. (2024) The

preclinical validation of 405 nm light parasiticidal efficacy on *Leishmania donovani* in *ex vivo* platelets in a Rag2−/− mouse model. *Microorganisms*. 2024(12), 28

Grants:

- EPSRC National Productivity Investment Fund (NPIF) Grant awarded to support an Innovation Placement at the collaborative research facility at the Office of Blood Research and Review, Center for Biologics Evaluation and Research (U.S. FDA), under the guidance of Dr CD Atreya (Associate Director for Research), (£3657)
- Microbiology Society Travel Grant awarded to attend the Federation of Infection Societies (FIS) Conference 2019, (£300)

Conference Poster Publications:

- Stewart, C.F., Tomb, R.M., Sinclair, L.G., Cobbett, H.R.J., Hartness, G., MacGregor, S.J., Maclean, M., & Atreya, C.D. (2019, September 5-6). Preliminary Investigation of the Compatibility of Violet-Blue light for Decontamination of Blood Plasma. *BioMedEng19*, Imperial College London
- Stewart, C.F., Sinclair, L., Maclean, M., MacGregor, S.J., & Atreya, C.D. (2019, November 11-14). 405-nm Light for Bacterial Reduction in Blood Plasma: Preliminary investigations into antimicrobial efficacy and plasma protein integrity. *Federation of Infection Societies Conference* (FIS 19), Edinburgh
- Stewart, C.F., MacGregor, S.J., Atreya, C.D., & Maclean, M. (2020, December 12-16). 405-nm Light for Bacterial Reduction in Blood Plasma: The impact of varying the method of dose delivery on antimicrobial efficacy and blood product quality. *The International Society of Blood Transfusion* (Virtual Congress)
- Stewart, C.F., Ralston, H., Armstrong, J., Tomb, R.M., MacGregor, S.J., Atreya, C.D., & Maclean, M. (2020, November 19-21). Visible Violet-Blue Light for Pathogen Reduction of Blood Plasma: Assessment of Broad Spectrum Antibacterial Efficacy and Preliminary Compatibility Studies. *The International Society for Experimental Hematology* (Virtual Congress)
- Stewart, C.F., Ralston, H., MacPherson, R.W., Wilson, M.P., MacGregor, S.J., Atreya, C.D., & Maclean, M. (2021, April 26-29). Antibacterial Action of Visible 405 nm Light for Bacterial Reduction in Blood Plasma. *Microbiology Society* (Virtual Congress)
- Stewart, C.F., Tomb, R.M., MacGregor, S.J., Atreya, C.D., & Maclean, M. (2021, November 8-11). Antimicrobial Violet-blue light for Decontamination of Prebagged

Blood Plasma: Evaluation of Antibacterial Action and Plasma Compatibility Studies. *Federation of Infection Societies Conference* (Virtual Congress)

- Stewart, C.F., MacGregor, S.J., Atreya, C.D., & Maclean, M. (2022, September 13-15). Bacterial Reduction of Pre-bagged Human Plasma using 405 nm Violet-blue Light. *British Blood Transfusion Society (BBTS) Annual Conference* (Virtual Congress)